
**CHARACTERISATION OF THE DOLOMITIC
AQUIFER IN THE COPPERBELT PROVINCE,
NORTHERN ZAMBIA.**

Prepared by:

Martiens Prinsloo
1997574148

Thesis submitted in the fulfillment of the requirements for the degree of

MASTER OF SCIENCE

In the Faculty of Natural and Agricultural Sciences,
Department of Hydrogeology
University of the Free State
Bloemfontein, South Africa

February 2005

Supervisor: P.D. Vermeulen

ACKNOWLEDGEMENTS

1. Firstly, I would like to thank the Mpongwe Development Company (MDC) for allowing me to make use of their data for this study. Special thanks goes to Nick Wilkinson, Colin Huddy and Karl Ullrich, as without their consent and willing contribution, this paper would not have seen the light of day.
2. Secondly, I would like to thank my employer, GCS, and my colleagues for encouraging my personal development and allowing me to make use of one of my work projects as the subject of this study.
3. Special thanks go to the University of the Free State, and in particular the Institute for Groundwater Studies and its staff for acting as study leaders and for guiding me through the process.

TERMINOLOGY

Acid Rain: The acidification of rainfall due to industrialisation.

Aquifer: A saturated permeable geological unit that is sufficiently permeable to yield economic quantities of water to boreholes.

Aquifer Sustainable Yield: The volume of water that can be abstracted from the aquifer during a set time period without dewatering the aquifer.

Aquifer Test: A pumping test performed on a borehole where water is abstracted at a specific volume during a set time period and the drawdown in water level is measured. Following the pumping phase of the test, the recovery of the water level to its natural state is recorded.

Borehole Sustainable Yield: The volume of water that can be abstracted from the borehole, without drawing the water level within the borehole to pump intake level and causing localised dewatering of the aquifer.

Chloride Method: Methodology used to determine initial values for recharge percentage, based on the relative chloride concentrations in rainfall and groundwater that occur in an area.

Coordinate System Used: Where possible all coordinate data has been converted to WGS84 format. The majority of the data was originally supplied in UTM or an unexplained local grid system. Data from the UTM format was easily transformed, while data presented in the local grid system could only be transformed if a detail map with the coordinate system and points of which the coordinates in either the UTM or WGS84 system are shown.

CRD Method: A method used to determine the recharge percentage. The CRD method is based on the argument that equilibrium exists between average annual rainfall and the hydrological response in terms of run-off, recharge, evaporation, plant growth, etc.

Dambo: A small wetland, typically with a diameter of less than 200m. The dambo areas are fed from shallow groundwater.

Dolomite: Forms by the replacement of limestone (magnesium for calcite). The textures and features of the limestone can be lost or retained.

Dolomitic Aquifer: An aquifer consisting of dolomitic rock. The main water movement occurs along solution cavities caused by dissolution of the host rock by slightly acidic water.

Eastern Aquifer: The aquifer underlying the Mpongwe irrigation area, Zambia. Lake Nampamba is located within this aquifer.

Equal Volume Method: This method forms part of the SVF recharge calculation methodology. It applies to situations where the change in groundwater storage over a selected period of time is zero.

Field Capacity Of Soil: The volume of water retained after free drainage (seepage due to gravitational pull) has taken place.

Folding: Bending or buckling of any existing structure in a rock as a result of deformation or tectonics.

Foliation: A continuous or discontinuous layer structure in metamorphic rocks formed by the segregation of different minerals in streaks or lenticels, or by the alteration of bands of different textures.

Hydraulic Conductivity: The volume of water that will move through a porous medium in unit time under a unit hydraulic gradient through a unit area measured at right angles to the direction of flow. It is measured in Length / Time (m/day).

Hydrogeology: A study of the water occurring below the earth's surface. The main concern is flow mechanics through rock.

Jointing: Surface fracturing of a rock without displacement. A joint set consists of a group of approximately parallel joints. A joint system consists of two or more joint sets with a characteristic pattern.

Karstification: The formation of solution cavities caused by dissolution of the dolomitic rock by slightly acidic water.

Kriging: The estimation procedure used in geostatistics using known values and a semi-variogram to determine unknown values.

Lake Nampamba: A sinkhole in the dolomite and limestone of the eastern aquifer. MDC abstracts water from the sinkhole for irrigation purposes.

Lake Kashiba: A sinkhole in the dolomitic aquifer approximately 20km from MDC and Lake Nampamba. It has been suggested that Lake Nampamba and Lake Kashiba are interconnected.

Limestone: A sedimentary rock composed almost entirely of calcium carbonate. Limestones occurring in the study area are chemically precipitated and formed in a shallow sea environment. Chemically precipitated limestone can be classified as oolitic and pisolitic and the (dolomitic) limestones of evaporate sequences.

m/d: Metres per day.

m²/day: Metres squared per day.

mamsl: Metres above mean sea level.

MDC: The Mpongwe Development Company.

mg/l: milligrams per litre.

mS/m: milliSiemens per metre.

Rainfall Stationarity: A condition of no systematical change in the mean and no systematical change in the variance. In hydrological terms, stationarity means that except for cyclic or seasonal fluctuation there is no permanent change in the record over time.

Recharge: The volume of water that percolates through the overlying soil to the aquifer. This can originate from rainfall, a river, a dam, or other similar external sources.

SAWQG: South African Water Quality Guidelines as determined by the South African Department of Water Affairs and Forestry (Vol. 1, 2nd Edition, 1996). In this paper reference is made to the guidelines for Domestic Use purposes.

Storativity: The volume of water released from an aquifer with a thickness (D) from storage per unit surface area of the aquifer per unit decline in the component of hydraulic head normal to that surface. In a vertical column of unit area extending through the confined aquifer, the storativity (S) equals the volume of water released from the aquifer when the piezometric surface drops over a unit distance. It is a dimensionless quantity.

Saturated Volume Fluctuation (SVF) Method: A method used to determine the recharge percentage. It incorporates a lumped parameter approach whereby the status of the aquifer, based on the water level fluctuations of the monitoring boreholes, is integrated and its variation with time analysed.

Transmissivity: The product of the average hydraulic conductivity (K) and the saturated thickness of the aquifer (D). It is the rate of flow under a unit hydraulic gradient through a cross section of unit width over the whole saturated thickness of the aquifer. Transmissivity is measured as Length²/Time (m²/day).

Western Aquifer: The aquifer underlying the Munkumpu irrigation area. Ipumbu Dam is fed from this aquifer through dambo areas.

Wilting point: The soil moisture at which the capillary and surface adhesion forces are greater than the soil suction forces exerted by the plant roots. Wilting point is determined as the water remaining in the soil at a suction pressure of 15 atmospheres.

TABLE OF CONTENTS

Chapter 1 : Background Information.....	1
Chapter 2 : General Site Conditions.....	5
Chapter 2.1 : General Information.....	5
Chapter 2.2 : Topography.....	11
Chapter 2.3 : Rainfall.....	20
Chapter 2.4 : Surface Drainage.....	27
Chapter 2.5 : Evapotranspiration.....	30
Chapter 2.6 : Plant Growth.....	36
Chapter 2.7 : Geology.....	39
Chapter 2.8 : Soils.....	51
Chapter 2.9 : Surface Geophysical Investigations.....	57
Chapter 2.9.1 : Geophysical Survey of 1978.....	57
Chapter 2.9.2 : Geophysical Survey of 1982.....	59
Chapter 2.9.3 : Geophysical Survey of 2004.....	62
Chapter 2.9.4 : Geophysical Survey Discussion and Conclusions.....	69
Chapter 2.10 : Borehole Geophysical Investigations.....	79
Chapter 3 : Hydrogeology.....	82
Chapter 3.1 : General Hydrogeology.....	82
Chapter 3.2 : Groundwater Chemistry.....	89
Chapter 3.3 : Depth to Groundwater.....	92
Chapter 3.4 : Aquifer Transmissivity and Borehole Sustainable Yield Calculations....	98
Chapter 3.4.1 : Aquifer Transmissivity and Borehole Sustainable Yield Discussion.....	105
Chapter 3.5 : Recharge Estimations.....	108
Chapter 3.5.1 : Recharge Estimation Methodology.....	111
Chapter 3.5.2 : Recharge Estimation Methodology Application.....	119
Chapter 3.6 : Aquifer Storativity.....	127
Chapter 3.7 : Aquifer Sustainable Yield Calculations.....	128
Chapter 3.8 : Current Abstraction Volumes.....	132
Chapter 3.9 : Current and Future Sustainability Evaluation Calculations.....	135
Chapter 4 : Numerical Modelling.....	139
Chapter 4.1 : Background to Numerical Modelling.....	139

Chapter 4.2 : Construction and Calibration of the Model.....	154
Chapter 4.2.1 : Initial Calibration (No Abstraction).....	154
Chapter 4.2.2 : Calibration Taking Abstraction in Account.	156
Chapter 4.2.3 : Monitoring Data Calibrated Model - Grid.....	164
Chapter 4.2.4 : Monitoring Data Calibrated Model - Layers.....	164
Chapter 4.2.5 : Boundary Conditions.....	166
Chapter 4.2.6 : Monitoring Data Calibrated Model - Time Increments.....	166
Chapter 4.2.7 : Monitoring Data Calibrated Model - Observed Hydraulic Heads. .	166
Chapter 4.2.8 : Monitoring Data Calibrated Model - Transmissivity.....	167
Chapter 4.2.9 : Monitoring Data Calibrated Model - Storage Coefficient.....	167
Chapter 4.2.10 : Monitoring Data Calibrated Model - Recharge.....	168
Chapter 4.2.11 : Numerical Model Discussion.....	168
Chapter 4.3 : Model Applications.....	170
Chapter 5 : Conclusions and Recommendations.	174
Chapter 6 : References.....	195

LIST OF FIGURES

Figure 2.1.1: General Locality Map showing Zambia and the Mpongwe Study Area.	7
Figure 2.1.2: Locality Map - Mpongwe and Munkumpu Irrigational Areas.	8
Figure 2.1.3: Locality Map – Chambatata and Kabanga Farms.....	9
Figure 2.1.4: Locality Map – Kampemba and Ipumbu Farms.	10
Figure 2.2.1: Relatively Flat Topography of the Study Area.	13
Figure 2.2.2: Relatively Flat Topography of the Study Area (200ha Pivot Area).	14
Figure 2.2.3: Topography of the Study Area.	15
Figure 2.2.4: Three Dimensional Topography of the Study Area.....	16
Figure 2.3.1: Annual Rainfall – Mpongwe Mission April 1932 – March 1979.....	24
Figure 2.3.2: Annual Rainfall – Mpongwe Farm April 1979 – March 2003.....	25
Figure 2.3.3: Stationarity of the Mpongwe Mission and Mpongwe Farm Rainfall Records.	26
Figure 2.4.1: Kafue River.	29
Figure 2.5.1: Recorded Annual Evaporation Data.	34
Figure 2.5.2: Recorded Monthly Evaporation Data.....	35
Figure 2.6.1: Species <i>Brachystegia</i>	37
Figure 2.6.2: Natural Vegetation in the Study Area.....	38
Figure 2.7.1: General Geology of the Study Area.	40
Figure 2.7.2: North-South Cross Section through the Eastern Aquifer.	41
Figure 2.7.3: West-East Cross Section through the Eastern Aquifer.	42
Figure 2.7.4: Major Joint Set near Lake Nampamba.	45
Figure 2.7.5: Linear Outcropping of Dolomite near Lake Nampamba.....	46
Figure 2.7.6: Quartz Veining in the Dolomite.	47
Figure 2.7.7: Fractured White to Pink Limestone associated with High Yielding Areas..	48
Figure 2.7.8: Sandy Limestone.	49
Figure 2.7.9: Fractured and Weathered Limestone with Laterite.	50
Figure 2.8.1: Single Ring Infiltrometer Test.....	56
Figure 2.9.3.1: Geophysical Traverse Positions at Mpongwe (2004 Investigation).	68
Figure 2.9.4.1: Gravity Survey - Traverse 3.	75
Figure 2.9.4.2: Gravity vs. Electromagnetic Method.	76
Figure 2.9.4.3: Gravity vs. Magnetic Method.	77
Figure 2.9.4.4: Electromagnetic vs. Magnetic Method.	78

Figure 3.1.1: Chemical Weathering in Dolomite.....	83
Figure 3.1.2: Lake Nampamba.....	87
Figure 3.1.3: Lake Kashiba.	88
Figure 3.2.1: Piper Diagram indicating the Groundwater Character.	91
Figure 3.3.1: The Relationship between Water Level, Recharge and Abstraction Volumes for Lake Nampamba (Eastern Aquifer).	96
Figure 3.3.2: Groundwater Flow Contours in the Study Area.	97
Figure 3.4.1: Positions of the Boreholes Drilled during 1978, 1981 & 2004.....	99
Figure 3.5.1: Chloride Method – Calculation of Recharge Percentage.....	124
Figure 3.5.2: SVF Method – Calculation of Recharge Percentage.	125
Figure 3.5.3: CRD Method – Calculation of Recharge Percentage.	126
Figure 3.7.1: Estimated Annual Recharge to the Aquifers.	131
Figure 3.8.1: Dambo Areas along the Munkumpu Fault Zone Feeding Ipumbu Dam...	134
Figure 3.9.1: Sustainability Calculations: Current Abstraction Rates.....	137
Figure 3.9.2: Sustainability Calculations: Proposed Future Abstraction Rates.	138
Figure 4.1.1: Spatial Division of an Aquifer System used during Numerical Modelling.	144
Figure 4.1.2: Numerical Model Grid indicating the Block Centered Method.	145
Figure 4.1.3: Cell i,j,k and the Six Adjacent Cell Indices.....	148
Figure 4.1.4: Flow from Cell $i,j-1,k$ into Cell i,j,k	149
Figure 4.2.2.1: Correlation between Observed and Simulated Groundwater Levels. ...	159
Figure 4.2.3.1: Numerical Model Grid.	165
Figure 4.3.1: Predicted Groundwater Fluctuations based on Increased Abstraction Volumes.	173

LIST OF TABLES

Table 2.3.1: Rainfall Statistics.....	21
Table 2.3.2: Rainfall Intensity.....	21
Table 2.5.1: Evaporation Calculations.	32
Table 2.5.2: Comparative Evaporation Rates.	32
Table 2.9.1.1: Interpretation of the Geophysical Survey of 1978.....	58
Table 3.2.1: Chemical Analysis Results.....	89
Table 3.3.1: Hydrocensus Results	94
Table 3.3.1: Hydrocensus Results (Continued)	95
Table 3.4.1: Transmissivities and Specific Capacities as Calculated from Preliminary Aquifer Tests.....	100
Table 3.4.1: Transmissivities and Specific Capacities as Calculated from Preliminary Aquifer Tests (Continued).....	101
Table 3.4.2: Production Borehole Sustainable Yields.....	104
Table 3.5.1: Average Recharge Estimates in the Kabanga and Chambatata Areas. ...	108
Table 3.5.2: Landell Mills Associates Recharge Calculations (1979).	109
Table 3.5.2: Calculated Recharge Percentages – SVF and CRD Methods.....	123
Table 3.6.1: Aquifer Storativity.....	127
Table 3.7.1: Previous Estimated Sustainable Abstraction Rates.....	128
Table 3.7.2: Estimated Through Flow Through the Aquifer.	129
Table 3.7.3: Calculated Minimum and Maximum Annual Recharge Volumes.	130
Table 3.8.1: Current Abstraction Rates.....	133
Table 3.9.1: Proposed Future Abstraction Rates.....	135
Table 4.2.1.1: Initial Calibrated Model Parameters (No Abstraction).....	155
Table 4.2.2.1: Monitoring Data Used for Model Calibration.	160
Table 4.2.2.1: Monitoring Data Used for Model Calibration (Continued).	161
Table 4.2.2.2: Current Abstraction Rates.....	162
Table 4.2.2.3: Monitoring Data Calibrated Model Parameters.....	163
Table 4.3.1: Expected Future Abstraction Rates.	170
Table 4.3.2: Data Used in the Model Application.....	172

LIST OF APPENDICES

Appendix A: Geological Borehole Logs and Borehole Geophysical Data.

Appendix B: Surface Geophysical Investigation of 1982: VES Results.

Appendix C: Surface Geophysical Investigation of 2004: Gravity, EM and Magnetometer Results.

Appendix D: Aquifer Test Data and Borehole Sustainable Yield Calculations for 2004.

Chapter 1 : Background Information.

The aim of this study is to characterise the hydrogeological system surrounding the dolomitic aquifer situated in the Copperbelt Province, Northern Zambia. This includes determining the hydrogeological characteristics of the aquifer and identifying and expanding on the general surrounding conditions that influence the hydrogeological character of the aquifer. This study can also be used as a reference guide for any future hydrogeological studies in the study area or hydrogeological studies in other dolomitic regions.

The report is divided into three chapters. The first chapter (Chapter 2) centres on the general conditions surrounding the aquifer, which influence the hydrogeological system. These include general site conditions such as topography, plant growth, surface drainage features, soil characteristics, geology, rainfall occurrence, and evaporation.

Certain sections of Chapter 2 such as the soil investigations, plant growth and surface drainage either fall outside the author's area of expertise, or the original recorded data is not available for interpretation. However, it is the opinion of the author that these factors form an integral part of the determination of the sustainable yield of the aquifer and therefore need to be addressed and discussed. Reference has therefore been made to authors who have either had access to the original data, or who are specialists in the abovementioned fields and have previously addressed these issues in the study area (Landell Mills Associates (1978, 1979, 1980, and 1982); Macdonald and Partners Ltd. (1982); Rankin Engineering Consultants (1994, 1997); Scott Wilson Piésold (2003); and WLP U Consultants (1983)). Based on the available data and the author's knowledge of the subject matter, the author has evaluated the data compiled by previous specialists.

Technical aspects of the successful siting of production boreholes in the aquifer (refer to Chapter 2.9), and a characterisation of the aquifer based on borehole (down-the-hole) geophysical investigations (refer to Chapter 2.10), are also detailed in Chapter 2.

Chapter 3 focuses on the hydrogeological character of the dolomitic aquifer under investigation and incorporates the principles and conclusions discussed in Chapter 2. Topics contained in Chapter 3 include the general hydrogeological conditions, depth to

groundwater, aquifer transmissivity, recharge calculations, aquifer storativity and sustainable yields.

In Chapter 4 the construction and application of the numerical model is discussed.

In order to calculate the aquifer parameters, data from the Mpongwe Development Company (MDC) has been used. This data includes rainfall figures, abstraction volumes, water levels, geology, soils, evaporation, and plant growth information.

The MDC currently abstracts groundwater for irrigation purposes. The MDC land under irrigation spans two sub-catchment areas. These catchments are referred to as the eastern and western aquifers. Currently, approximately 12 300 000m³ and 13 000 000m³ of water is abstracted annually from the eastern and western aquifers respectively.

In the eastern aquifer, groundwater is currently abstracted directly from a sinkhole (Lake Nampamba) and eight production boreholes drilled into the dolomitic aquifer. In the western aquifer, water is released from the Ipumbu Dam. The dam is fed by surface runoff from rainfall and springs. Several dambo (wetland) areas occur on the Munkumpu fault zone that forms the contact between dolomite and quartzite, which underlies the Ipumbu dam.

The relative contribution of rainfall and spring flow to the Ipumbu Dam is not known. However, it is considered that spring flows supply the majority of the recharge to the dam. For modelling purposes the author has accepted the assumption that all the Ipumbu Dam water originates from springs that feed the dambo areas. It is believed that this approach will yield the most conservative estimations in terms of sustainable yield calculations.

Transmissivity values were obtained from two sources. The first source being aquifer tests that were previously performed in the study area, and the second source being aquifer tests performed during this hydrogeological study.

The aquifer tests conducted during this study were performed by conducting step drawdown tests followed by constant rate abstraction tests. During the step tests three

steps of one hour each were performed at increasing pumping rates. Following the three steps, the recovery of the water level was monitored for one hour.

The pumping rate used during the constant rate abstraction test was determined based on the results of the step tests. The transmissivities were calculated using the data obtained during the pumping (Theis and Cooper-Jacob methods) and recovery (Theis-Jacob method) phases of the constant rate aquifer tests.

The aquifer tests were carried out on ten boreholes. Five of these boreholes are existing boreholes that had been drilled during the 1979 and 1981-1982 investigations (Landell Mills Associates, 1978 and Macdonald and Partners Ltd., 1982). The remaining five boreholes were drilled during this hydrogeological investigation.

The aquifer tests and aquifer parameter calculations performed by Landell Mills Associates during the 1978 investigation took observation wells for boreholes IN3, F2000, F14500, and D7400 into account. During this study, no observation boreholes were monitored.

In order to be able to calculate the recharge to the study area, calculation methods developed by Bredenkamp *et al* (1995) were used. Specific methods that were applied include the Chloride, SVF, Equal Volume, and CRD methods.

The interconnectivity of the aquifers in the different sub-catchments was evaluated. Based on the recharge to the area and the interconnectivity of the aquifers a maximum sustainable yield was calculated (refer to Chapters 3.1 and 3.7).

No detailed water level monitoring data from the production boreholes is available. Definite differentiation between the water levels in closely spaced boreholes indicates the presence of small-scale compartmentalization in the dolomite. This is often a problem in dolomitic areas and limits the long-term sustainable abstraction from an aquifer. However, based on the high sustainable yields and long-term sustainability of the boreholes and Lake Nampamba, the author concludes that no small-scale compartmentalisation occurs in the area. This point is discussed in more detail in Chapter 3.1.

In order to substantiate all manual calculations a numerical groundwater model was constructed. The numerical model is based on the actual observed data and calculated aquifer parameters.

Due to the fact that the abstraction program as well as the natural factors such as rainfall, differ significantly between the dry season (April to October) and the wet season (November to March), the model was constructed in such a way as to be able to distinguish between and simulate the influence of the two seasons.

The model was first calibrated in the steady state using the trial and error method for the aquifer parameters without the external influence of the water abstraction. Calibration using the trial and error method entails changing the model parameters such as transmissivity, recharge, and storativity individually within realistic value ranges and running the model. The correlation between the actual observed values, such as water levels, can then be compared to those calculated by the numerical model. The calibration of the numerical model is achieved once observed and calculated values correlate.

Once the model was calibrated, the groundwater abstraction was incorporated into the numerical model. This was achieved by installing abstraction wells in positions where water is currently being abstracted from Lake Nampamba. Other data incorporated into the model includes actual recorded rainfall and water level fluctuations, calculated recharge percentages, transmissivities, and storage coefficients. The model is then run in transient state.

Further calibration or adjustments had to be made to the aquifer parameters in order to obtain the best correlation between the observed water level fluctuations and the values calculated by the numerical model. The level of confidence for the model was determined by comparing the observed and calculated water levels in Lake Nampamba.

The numerical model was applied by simulating the influence of the current and proposed future abstraction schedules on the groundwater levels and the sustainability of the abstraction programs.

Chapter 2 : General Site Conditions.

Chapter 2.1 : General Information.

The dolomitic aquifer of the Copperbelt Province occurs in the northern regions of Zambia (refer to Figure 2.1.1). The aquifer is of particular importance to the copper mines and farmers using irrigation, due to the large volumes of water contained within the aquifer. Mention of the aquifer is made in various hydrogeological studies of the copper mines situated within the region. However, specific hydrogeological information such as water levels and dewatering programs from the mines could not be obtained.

For the purpose of this study, data obtained from a large-scale irrigation farm was used. Four farms managed by the Mpongwe Development Company (MDC) abstract water from the aquifer for domestic and irrigation purposes. These farms are Kabanga, Chambatata, Kampemba, and Ipumbu.

The MDC farms part of the Commonwealth Development Company. As the name indicates, the farms are located near the village of Mpongwe in the Copperbelt Province of Zambia.

The general locality of Mpongwe is shown in Figure 2.1.1, and the locality of the four farms and the associated infrastructure are detailed in Figures 2.1.2, 2.1.3 and 2.1.4. Figure 2.1.2 indicates the relative positions of the Mpongwe and Munkumpu irrigation areas (eastern and western aquifers). Figure 2.1.3 specifies the Kabanga and Chambatata farms that together form the Mpongwe irrigation area and Figure 2.1.4 shows the Kampemba and Ipumbu farms that form the Munkumpu irrigation area.

In this paper mention is made of the eastern and western aquifers. The eastern aquifer refers to the aquifer contained within the sub-catchment in which Lake Nampamba is situated (refer to Figures 2.1.3 and 2.9.3.1). Using the WGS84 reference system Lake Nampamba is situated at approximately $X = 117\ 380$, $Y = -1\ 501\ 189$. The western aquifer underlies Ipumbu dam and the associated sub-catchment (refer to Figure 2.1.4).

As seen in Figure 2.1.2, the Kafue River forms a natural groundwater flow boundary to the West and to the North.

Currently groundwater is abstracted from a sinkhole (Lake Nampamba) in the dolomitic aquifer and the Ipumbu Dam. The Ipumbu Dam is fed by a combination of direct rainfall, run-off, and springs.

MDC irrigates a total of 4 150 hectares and abstracts approximately 12 300 000m³ of groundwater annually in the Mpongwe area. MDC releases approximately 13 000 000m³ of water from Ipumbu Dam annually for irrigation in the Munkumpu area.

MDC plans to expand the area of land under irrigation to a total of 6 500ha. Due to operational problems with the 200ha pivots, it is intended to limit the pivot size to either 100ha or 150ha. This means that another 16 to 25 pivots will need to be added to the existing infrastructure.

Detailed monitoring data is available from the MDC database. This monitoring data includes daily rainfall figures from 1931 to December 2003, abstraction volumes, daily groundwater levels at Lake Nampamba and the water level in the Ipumbu Dam for the time period 1979 to December 2003. This data was analysed and is discussed in Chapter 3.3.

Figure 2.1.1: General Locality Map showing Zambia and the Mpongwe Study Area.

General Locality Map showing Zambia and the Mpongwe Study Area

A general map indicating the position of the Mpongwe study area in Zambia. The area is relatively easily accessible through a 2.5hr flight from Johannesburg International Airport followed by a 1.5hr drive from Ndola to Mpongwe.



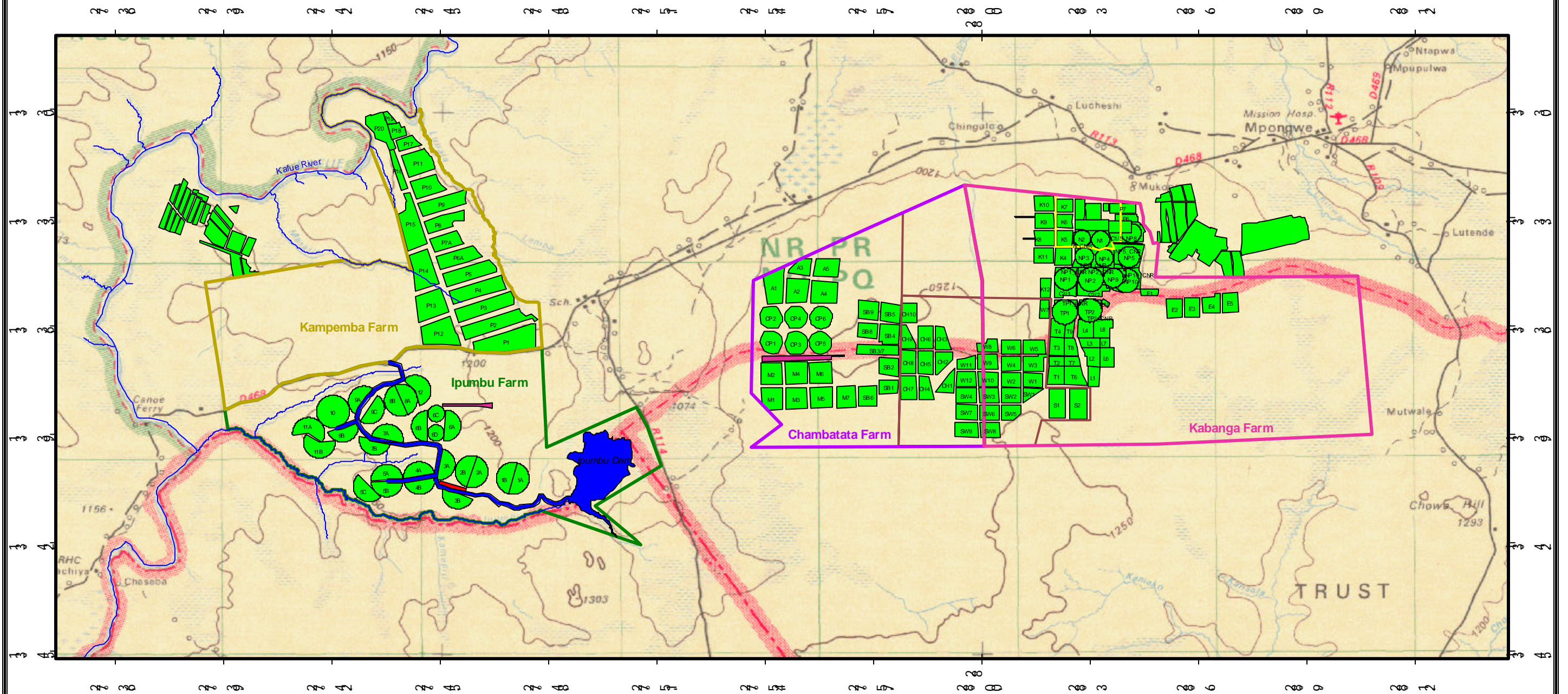
Figure No: 2.1.1

February 2005

Characterisation of the Dolomitic Aquifer in the Copperbelt Province, Northern Zambia.

Figure 2.1.2: Locality Map - Mpongwe and Munkumpu Irrigational Areas.

Locality Map - Mpongwe and Munkumpu Irrigational Areas



LEGEND:

	Canals		Buildings		Coffee area		Chambatata Farm
	Rivers		Dams		Other farm boundaries		Kampemba Farm
	Airstrips		Field boundaries		Ipumbu Farm		Kabanga Farm
							Luanshya_sd_35-7.tif

Figure No: 2.1.2

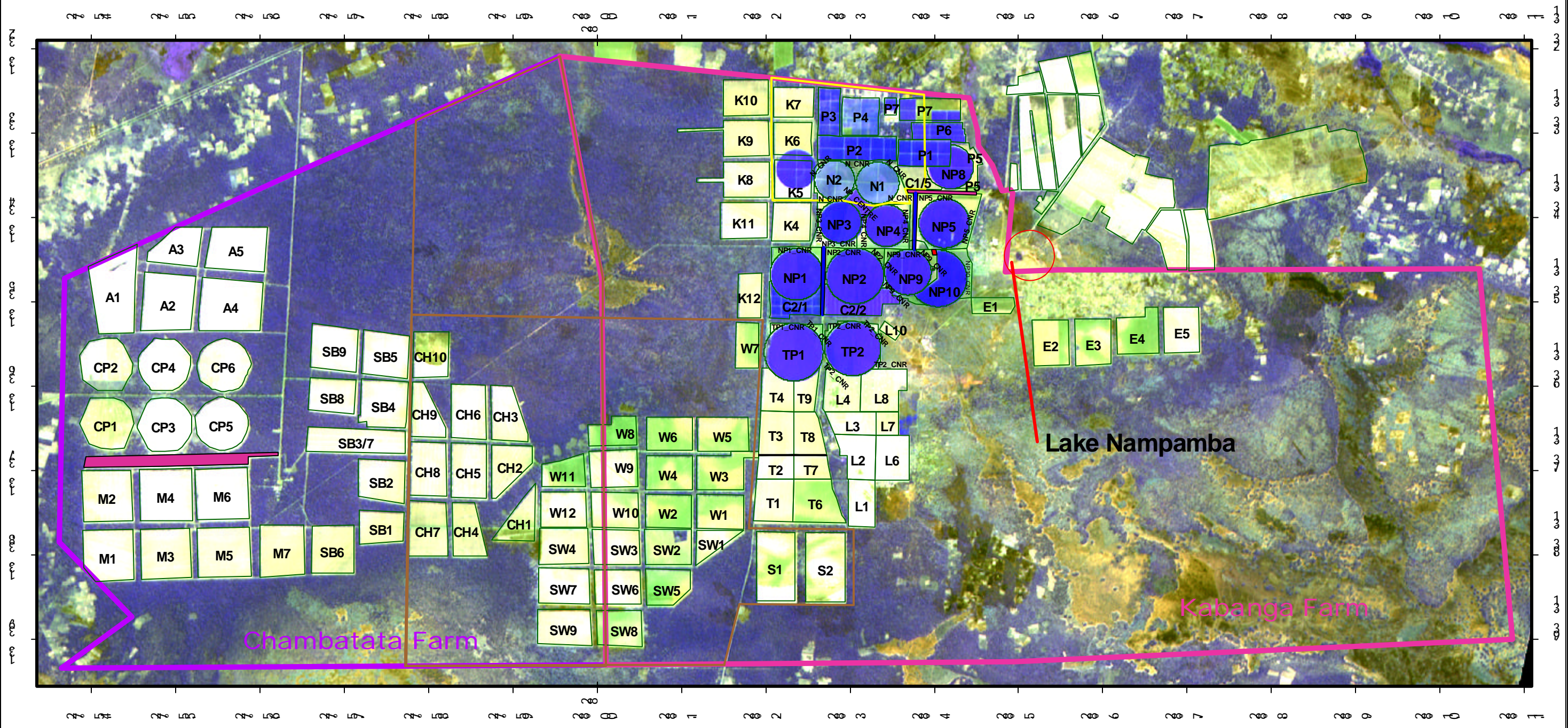
2 0 2 4 6 8 Kilometers



M.Sc Study - M. Prinsloo
Characterisation of the Dolomitic Aquifer
in the Copperbelt Province, Northern Zambia

Figure 2.1.3: Locality Map – Chambatata and Kabanga Farms.

Locality Map - Chambatata and Kabanga Farms



LEGEND:

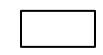


- | | | | | | | | |
|---|-----------|---|---------------------------|---|---------------------|-------|--|
|  | Canals |  | Coffee fields' boundaries |  | Farm_boundaries.shp | Image | R_10m_m_126-377_20020707_geo_wgs84_wgs84.tif => Spot4 of 7 July 2002 |
|  | Airstrips |  | Other field boundaries |  | Chambatata Farm | | |
|  | Buildings |  | Field boundaries | | Kabanga Farm | | |

Figure No: 2.1.3

Datum: WGS84
Spheroid: WGS84
Projection: Geographic

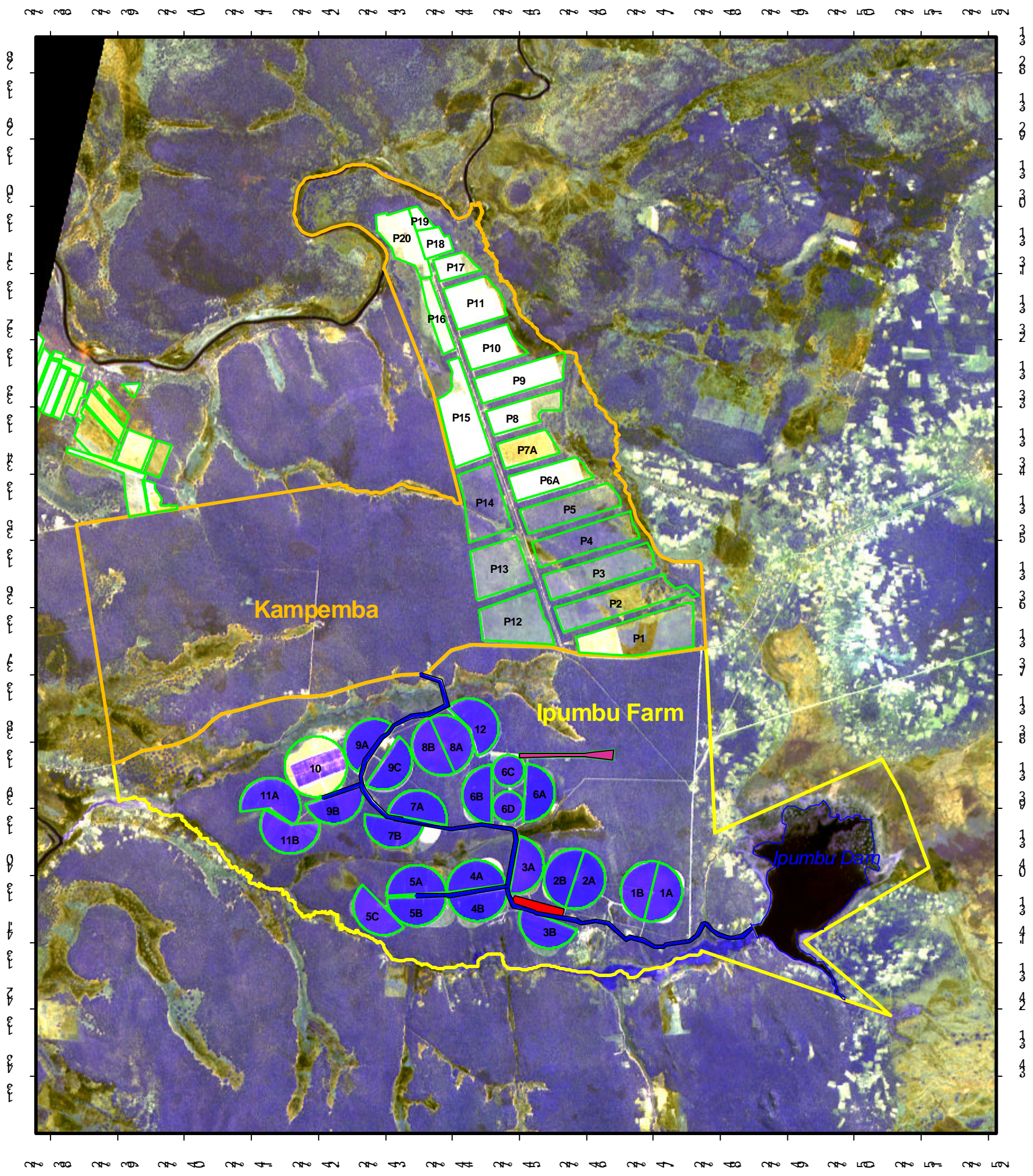
1 0 1 2 Kilometers



M.Sc Study - M. Prinsloo
Characterisation of the Dolomitic Aquifer
in the Copperbelt Province, Northern Zambia

Figure 2.1.4: Locality Map – Kampemba and Ipumbu Farms.

Locality Map - Kampemba and Ipumbu Farms



LEGEND:



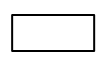

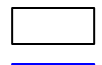
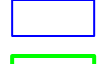
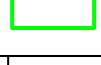
- | | | | |
|---|------------------|---|--|
|  | Canals |  | Kampemba Farm |
|  | Airstrips |  | Ipumbu Farm |
|  | Buildings | Image | R_10m_m_126-377_20020707_geo_wgs84_wgs84.tif => Spot4 of 7 July 2002 |
|  | Dam | | |
|  | Field boundaries | | |

Figure No: 2.1.4

Datum: WGS84
Spheroid: WGS84
Projection: Geographic



M.Sc Study - M. Prinsloo
Characterisation of the Dolomitic Aquifer
in the Copperbelt Province, Northern Zambia

Chapter 2.2 : Topography.

The topography within the study area is gently undulating. The topographic elevations are between 1 120 and 1 320 mamsl, and the topographical gradient ranges between 1:400 and 1:800. The topography slopes towards the northwest and the Kafue River. Figures 2.2.1 and 2.2.2 show photographs that indicate the relatively flat topography of the area and Figure 2.2.2 indicates the 200ha pivot area.

Figure 2.2.3 shows a two dimensional representation of the topography of the study area. The topography was obtained using six topographical maps of the area, which all form part of the Zambia topographical map series. The scale of the maps is 1:50 000.

The maps include:

- 1327B3
- 1327B4
- 1327D1
- 1327D2
- 1328A3
- 1328C1

Elevation on three of the maps (printed by the Director of Overseas Surveys, Tolworth, Surrey, England between 1965 and 1985) is shown in feet above mean sea level.

Due to the fact that the maps were only available in hard copy, the author has digitised the topographical contours, rivers and borders. Following the digitising, the elevations associated with each digitised point were then converted to metres above mean sea level (mamsl).

Digitising was performed using the computer software Surfer 8.00 – 11 February 2002 Surface Mapping Software developed by Golden Software, Inc. Conversion of the elevation from feet above mean sea level to metres above mean sea level was done using Windows Excel. The conversion factor between feet and metres was applied to each digitised point. The conversion factor from feet to metres is: 1ft = 0.3048m.

During digitising each digitised point is identified by X and Y coordinates. Elevations were attributed to the two-dimensional digitised contour points. The X, Y and Z data points were then used to construct a three-dimensional grid indicating the elevation at each digitised point. The areas between the digitised points were interpolated in Surfer using the Kriging method. The three dimensional topographical model of the study area is indicated in Figure 2.2.4.

Kriging is an estimation procedure applied in geostatistics using known values and a semi-variogram to determine unknown values (Dorsel and La Breche). Kriging was named after the South African, D. G. Krige. The procedures involved in Kriging incorporate measures of error and uncertainty when determining estimations. Based on the semi-variogram used, optimal weights are assigned to known values in order to calculate unknown values. Since the variogram changes with distance, the weights depend on the known sample distribution.

Punctual or Ordinary Kriging is the simplest form of Kriging (Dorsel and La Breche). It uses dimensionless points to estimate other dimensionless points, e.g. elevation contour plots. In punctual Kriging, the regionalised variable is assumed to be stationary i.e. no drift exists. This assumption allows for an estimate of an unknown value at point p, $Y_{E,P}$, to be calculated using a weighted average of the known values or control points:

$$Y_{E,P} = \sum W_i Y_i \quad (\text{Eq 2.2.1})$$

This estimated value will most likely differ from the actual value at point p, $Y_{A,P}$, and this difference is called the estimation error:

$$\varepsilon_P = (Y_{E,P} - Y_{A,P}) \quad (\text{Eq 2.2.2})$$

Figure 2.2.1: Relatively Flat Topography of the Study Area.

Relatively Flat Topography of the Study Area



The photograph show the flat topography of the study area.
The topographical gradient range between 1:400 and 1:800.

Figure 2.2.2: Relatively Flat Topography of the Study Area (200ha Pivot Area).

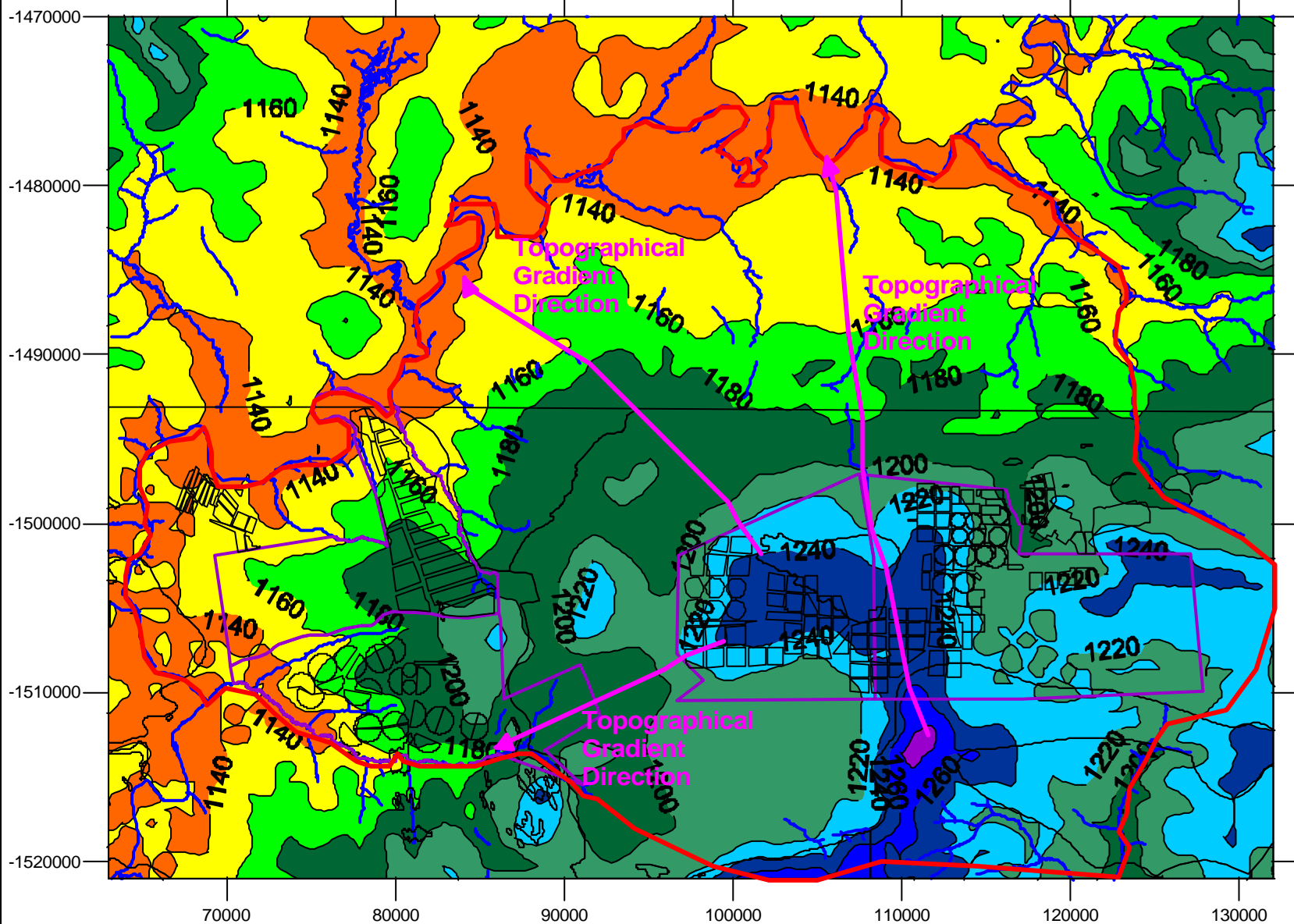
Relatively Flat Topography of the Study Area (200ha Pivot Area)

The photograph shows the relatively flat topography of the study area. Note the 200ha pivot area. This is one of several such pivots on the MDC farms. Note the dense natural plant growth in the undisturbed areas (Refer to Chapter 2.6 for more information on the plant growth).

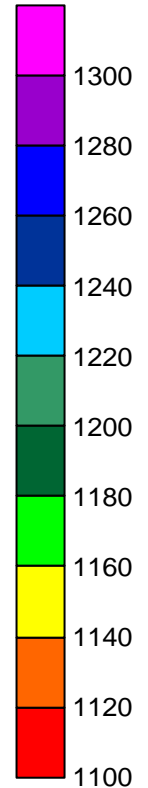
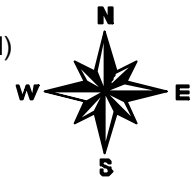


Figure 2.2.3: Topography of the Study Area.

Topography of the Study Area



Topography (mamsl)






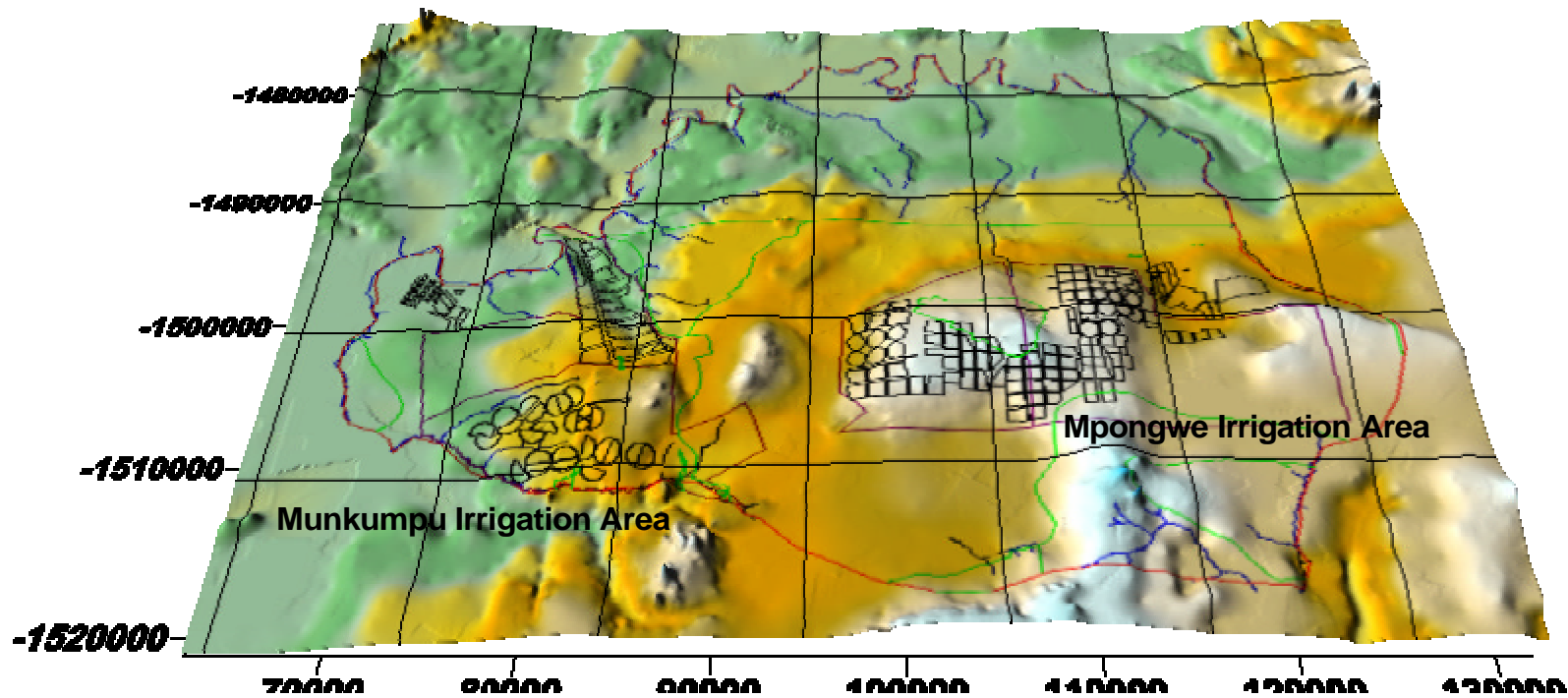
-  Catchment Area
-  Farm Boundaries and Fields
-  Perennial River

Figure No: 2.2.3

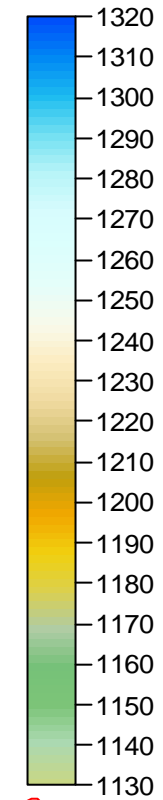
February 2005

Figure 2.2.4: Three Dimensional Topography of the Study Area.

Three Dimensional Topography of the Study Area



Topography (mamsl)






-  Catchment Area
-  Farm Boundaries and Fields
-  Perennial River

Figure No: 2.2.4

February 2005

If no drift exists and the sum of the weights used in the estimation is equal to one, then the estimated value is said to be unbiased. The scatter of the estimates about the true value is termed the error or estimation variance:

$$s_z^2 = \frac{\sum_{i=1}^n (Y_{E,P} - Y_{A,P})_i^2}{n} \quad (\text{Eq 2.2.3})$$

or as its square root, known as the standard error of the estimate:

$$s_z = \sqrt{s_z^2} \quad (\text{Eq 2.2.4})$$

The estimate and estimation error depend on the weights chosen. Ideally, Kriging tries to choose the optimal weights that produce the minimum estimation error. In order to derive the necessary equations for Kriging, extensive use of calculus is required - no detail of how the equations are formulated is discussed in this document. Optimal weights that produce unbiased estimates and have a minimum estimation variance are obtained by solving a set of simultaneous equations. For simplicity and to illustrate the methodology of Kriging, three unknown values, Y_1 , Y_2 , and Y_3 , will be used to estimate an unknown value at point p, $Y_{E,P}$. Three weights must be determined, W_1 , W_2 , and W_3 , to produce an estimate. The Kriging procedure begins with the following three simultaneous equations:

$$\begin{aligned} W_1\gamma(h_{11}) + W_2\gamma(h_{12}) + W_3\gamma(h_{13}) &= \gamma(h_{1p}) \\ W_1\gamma(h_{21}) + W_2\gamma(h_{22}) + W_3\gamma(h_{23}) &= \gamma(h_{2p}) \\ W_1\gamma(h_{31}) + W_2\gamma(h_{32}) + W_3\gamma(h_{33}) &= \gamma(h_{3p}) \end{aligned} \quad (\text{Eq 2.2.5})$$

where $\gamma(h_{ij})$ is the semi-variance between control points i and j corresponding to the distance between them, h. Since $h_{ij} = h_{ji}$, the left-hand matrix is symmetrical, with zeroes along the diagonal as the distance from a point to itself is zero. The values of the semi-variances are taken from the known or estimated semi-variogram.

To ensure that the solution is unbiased, a fourth equation is used:

$$W_1 + W_2 + W_3 = 1 \quad (\text{Eq 2.2.6})$$

A fourth variable is also introduced, called the Lagrange multiplier, λ , to ensure that the minimum possible estimation error is obtained. Therefore, the complete set of simultaneous equations is:

$$\begin{aligned} W_1\gamma(h_{11}) + W_2\gamma(h_{12}) + W_3\gamma(h_{13}) + \lambda &= \gamma(h_{1p}) \\ W_1\gamma(h_{21}) + W_2\gamma(h_{22}) + W_3\gamma(h_{23}) + \lambda &= \gamma(h_{2p}) \\ W_1\gamma(h_{31}) + W_2\gamma(h_{32}) + W_3\gamma(h_{33}) + \lambda &= \gamma(h_{3p}) \\ W_1 + W_2 + W_3 &= 1 \end{aligned} \quad (\text{Eq 2.2.7})$$

Separating these equations into matrix form yields:

$$\begin{bmatrix} \gamma(h_{11}) & \gamma(h_{12}) & \gamma(h_{13}) & 1 \\ \gamma(h_{21}) & \gamma(h_{22}) & \gamma(h_{23}) & 1 \\ \gamma(h_{31}) & \gamma(h_{32}) & \gamma(h_{33}) & 1 \\ 1 & 1 & 1 & 0 \end{bmatrix} \cdot \begin{bmatrix} W_1 \\ W_2 \\ W_3 \\ \lambda \end{bmatrix} = \begin{bmatrix} \gamma(h_{1p}) \\ \gamma(h_{2p}) \\ \gamma(h_{3p}) \\ 1 \end{bmatrix} \quad (\text{Eq 2.2.8})$$

This matrix equation is solved for the unknown coefficients [W]. The values in matrix A and matrix B are taken from the semi-variogram or the mathematical expression describing its form. Once the individual weights are known, an estimation can be made by:

$$Y_{E,p} = W_1Y_1 + W_2Y_2 + W_3Y_3 \quad (\text{Eq 2.2.9})$$

and an estimation variance can be calculated by:

$$s_z^2 = W_1\gamma(h_{1p}) + W_2\gamma(h_{2p}) + W_3\gamma(h_{3p}) + \lambda \quad (\text{Eq 2.2.10})$$

The methods used in Kriging have an advantage over other estimation procedures as the estimated values have a minimum error associated with them and this error is quantifiable.

It can be concluded that Kriging allowed for an accurate representation of the topography and the level of confidence of elevation data to be used during modelling is considered to be sufficient.

Chapter 2.3 : Rainfall.

The majority of the rainfall in the area occurs during the wet season (November to March). On average the rainy season spans 150 days. The dry season occurs from April to October and very little rain is experienced during this season.

Various sources of rainfall data have been identified by Landell Mills Associates (1979). These include:

- Mpongwe Mission (dating from 1931/32 to 1978/79)
- St. Anthony's Mission and Munkumpu School (dating from 1963/64 to 1978/79)
- Temporary rainfall stations set up by the Department of Water Affairs at Munkumpu Gauging Weir (dating from 1962/63 to 1969/70)
- Other stations at Mukubwe Agricultural Station, Mukubwe School, Kafue-Nduberi, and Mikata School (some dating back to 1955/56)

Since the Landell Mills Associates study, rainfall figures have been recorded by the Mpongwe Development Company (MDC) at Mpongwe farm from 1979 to December 2003. This data is shown in Figure 2.3.2.

The long-term record from Mpongwe Mission is complete and consistent and provides the most detailed information on long-term variations of rainfall over the study area. The annual rainfall observed at the Mpongwe Mission between 1931 and 1979 is shown in Figure 2.3.1. The Mission Farm, located just northwest of the MDC property, is now owned by Mr. Archibald. The farm is shown in Figure B1, which is listed in Appendix B.

It is estimated that these two observation points are less than 5km apart.

The longest continuous rainfall record was recorded at the Mpongwe Mission. The rainfall records indicate that the rainfall in the area is fairly consistent, with a slight seven to ten year cyclic pattern. The average annual rainfall, calculated from the data recorded at Mpongwe Mission farm, is 1 115mm. The annual rainfall displays a standard deviation of 207mm at Mpongwe Mission for the periods 1931 to 1979.

The 12-month period with the lowest recorded rainfall (635mm) occurred during April 1994 to March 1995. The most rainfall in a 12-month period (1722mm) was recorded during April 1977 to March 1978.

The rainfall data indicates that only once during the recorded history, did five consecutive years yield less than the average rainfall figures for the area. This occurred between April 1969 and March 1974. A 12-month period between 1 April and 31 March of the following year, with below average rainfall, is regarded as a “drought year”.

The rainfall occurrence statistics calculated by the author, based on the rainfall data recorded between 1931 and 2003 are summarised in Table 2.3.1.

Table 2.3.1: Rainfall Statistics.

Occurrence	Statistic
Maximum Rainfall over a 12 month period (1 April to 31 March)	1 722mm
Minimum Rainfall over a 12 month period (1 April to 31 March)	635mm
Average Rainfall over a 12 month period (1 April to 31 March)	1 115mm
Standard Deviation of Rainfall over a 12 month period (1 April to 31 March)	207mm
Recorded rainfall over a 12 month period with below average rainfall	54%
Recorded rainfall over a 12 month period that exceeds average rainfall	41%
Recorded rainfall over a 12 month period that achieves average rainfall	5%

The rainfall intensity was calculated by Landell Mills Associates (1979). Due to the fact that the rainfall time span has been lost over time, the rainfall intensities cannot currently be re-evaluated by the author and the values calculated by Landell Mills Associates (1979) for the Mpongwe Mission record (1931 – 1979) are therefore summarised in Table 2.3.2.

Table 2.3.2: Rainfall Intensity.

Occurrence	30 Minutes	1 Hour	2 Hours
Once yearly	28mm	38mm	46mm
Once in 5 years	41mm	53mm	63mm
Once in 50 years	56mm	74mm	89mm

In Chapters 3 and 4, calculations are performed based on both the Mpongwe Mission rainfall record (1931 to 1979) and the Mpongwe Farm rainfall record (1979 to 2003). The author has evaluated the accuracy of performing calculations based on both the data sets on the basis of stationarity.

Stationarity can be described as a condition of no systematical change in the mean and no systematical change in the variance. In hydrological terms stationarity means that except for cyclic or seasonal fluctuation, there is no permanent change in the record over time (Cornelius and du Plessis, 1997).

Stationarity can be tested either visually or numerically. Visual tests include:

- Cumulative mass plots: Cumulative data is plotted against time. In an ideal record the data points will display a straight-line correlation. Any tendencies in the rainfall records will be shown as deviations from the straight line.
- Double mass plots: A rainfall record is plotted against another closely located rainfall record. In this way periods of floods and droughts are likely to be neutralised and a straight line should be observed in the case of stationary records.
- Cusum plots: A series of cusum statistics (C_k) is calculated for a record and plotted against time. In effect, the cumulative deviations from the record mean are calculated and plotted. In the case of a stationary record the resulting plot should consist of a number of fluctuations around the zero line. Marked deviations from this ideal pattern will indicate a loss of stationarity.

Several numerical techniques are suitable for the analysis of change point data. Three of these are (Cornelius and du Plessis, 1997):

- Splines: This technique attempts to fit polynomial functions of different orders to different segments of a record.
- Segmented multiple linear regressions: This technique attempts to solve the change point problem by fitting different regressions to different segments of the rainfall record.

-
- Non-parametrical test for stationarity: This test is a non-parametrical version of a test that relies strongly on an analysis of the cusum graphs.

To prove the correlation and stationarity of the two rainfall records the cumulative mass plots method is employed. The cumulative rainfall of the two records over time is shown in Figure 2.3.3. The figure indicates that there is no discernable difference in slope or trend between the two rainfall records. This indicates stationarity between the two records and calculations can be based on a combination of the two rainfall records.

Fitting a linear trend line to the two consecutive data sets indicates a near 100% correlation.

Figure 2.3.1: Annual Rainfall – Mpongwe Mission April 1932 – March 1979.

Annual Rainfall - Mpongwe Mission April 1932 - March 1979

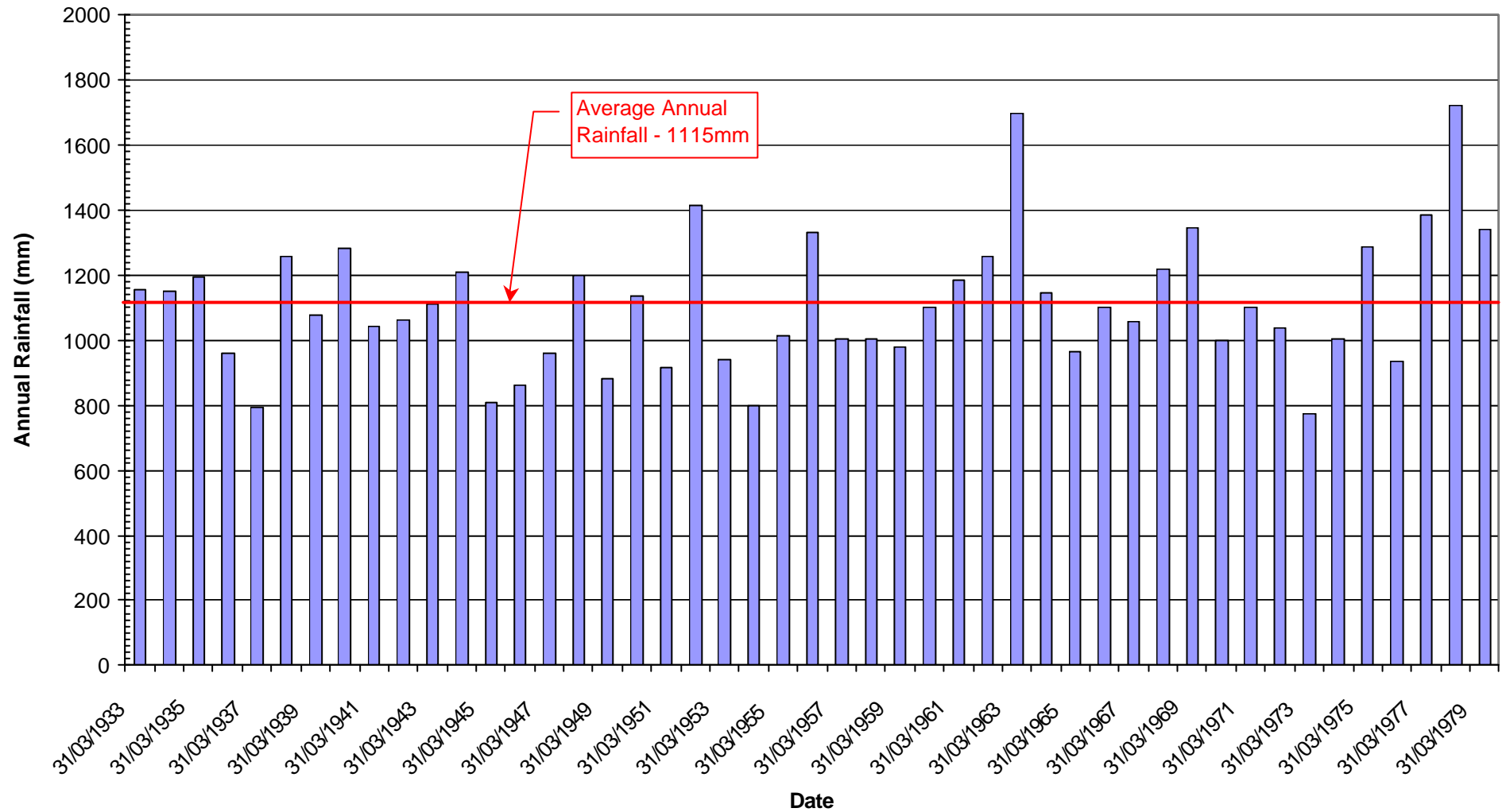


Figure No: 2.3.1

February 2005

Figure 2.3.2: Annual Rainfall – Mpongwe Farm April 1979 – March 2003.

Annual Rainfall - Mpongwe Farm April 1979 - March 2003

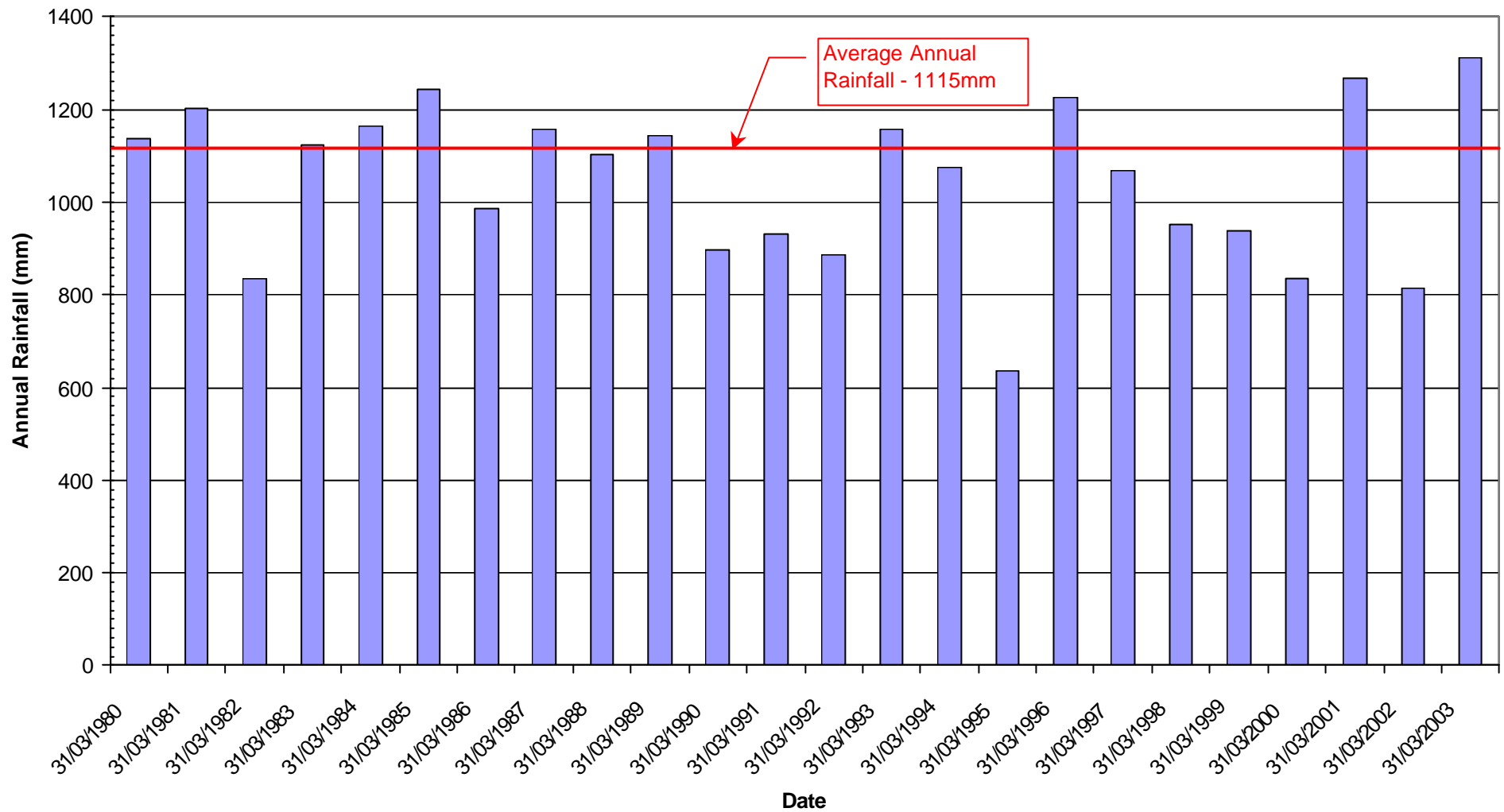
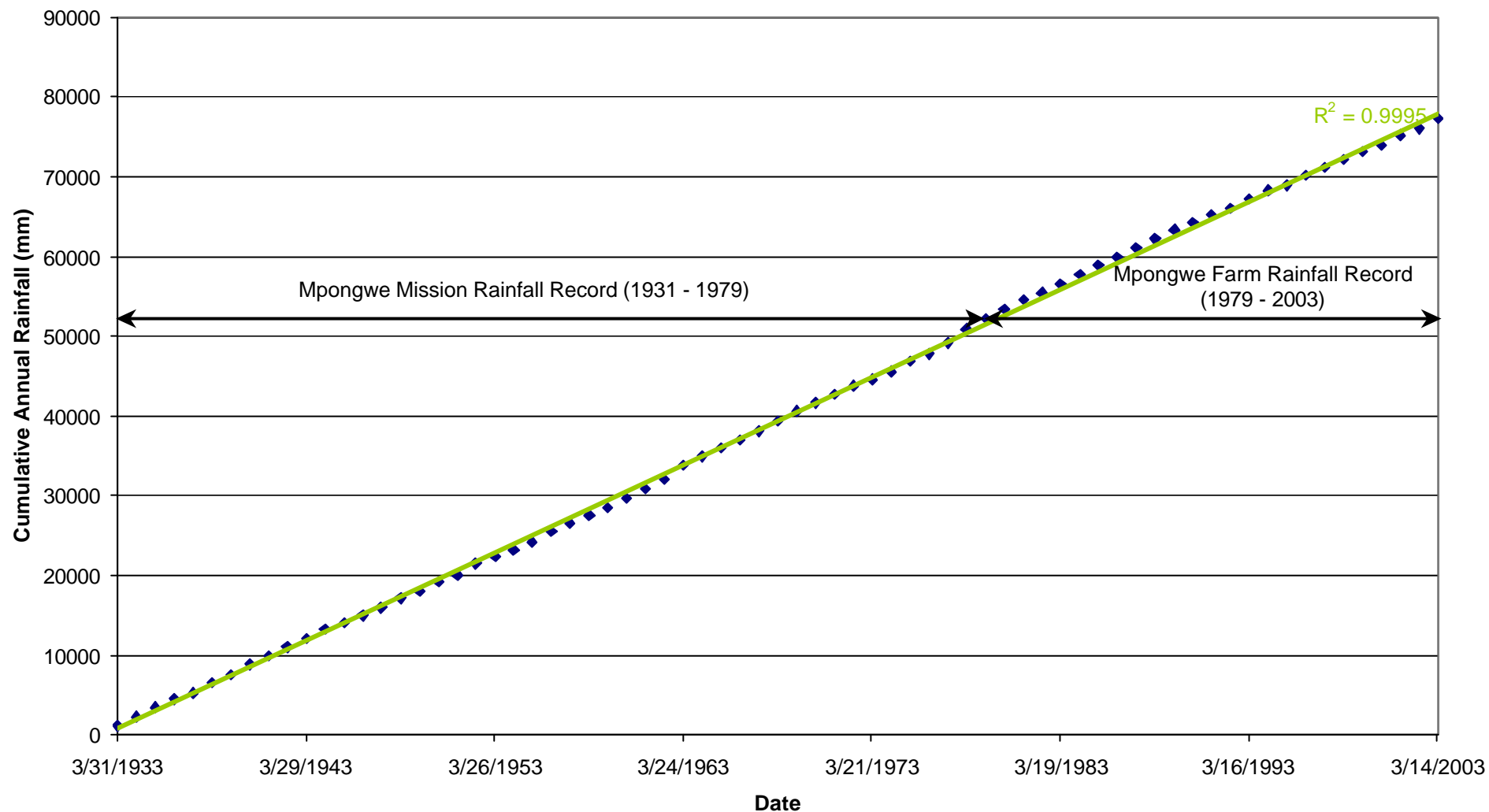


Figure No: 2.3.2

February 2005

Figure 2.3.3: Stationarity of the Mpongwe Mission and Mpongwe Farm Rainfall Records.

Stationarity of the Mpongwe Mission and Mpongwe Farm Rainfall Records



The Figure show the result of the stationarity analysis performed on the rainfall data from the two different rainfall stations. The cumulative annual rainfall data is plotted against time. The fact that the trends of the two stations are the same indicate a high stationarity. The similarity in trends is indicated by the 99.95% correlation of the trendline plotted through both sets of data. The high stationarity means that the two rainfall records can be used together in calculations without fear of anomalous results due to differences in rainfall character at the two stations.

Chapter 2.4 : Surface Drainage.

Despite the high rainfall volumes and high rainfall intensity, very few perennial surface run-off structures exist in the study area.

The main perennial surface run-off feature in the area is the Kafue River. This river is shown in Figures 2.1.2 and 2.4.1. The river is, on average, 10 to 20m wide and reportedly more than 3m deep. Flow in the river is relatively slow due to the low topographical gradients. No detailed flow records are available for the Kafue River in the study area.

It is considered that the dolomitic aquifer contributes a major portion of the base flow of the river. This presumption is based on the fact that very few tributaries to the Kafue River exist and also due to the fact that the soil infiltration rate is higher than the rainfall intensity. These factors, combined with the relatively flat topography (gradient ranging between 1:400 and 1:800) lead to the conclusion that base flow contributes a large portion of the river flow volume.

Scott Wilson Piésold (2003) suggests that base flow contributions to the Kafue River from the dolomitic aquifer dominate during periods of low flow volumes (dry season) based on observed increases and decreases in river flow volume in areas where it is expected that the dolomitic aquifer intersects the river (refer to Chapter 3.1).

Few non-perennial or rainfall related run-off channels exist in the study area. Only one rainfall related run-off feature exists in the area and feeds into the Ipumbu Dam. The feature is not indicated by the presence of an erosion channel or a “donga”, but rather represents a wide (50 to 100m) surface depression. The floor of the surface depression has a topographical height of approximately 3m below that of the regional topography.

Even though the rainfall intensity in the area is considered to be high (refer to Chapter 2.3) the rainfall does not exit the system directly in the form of surface run-off. This can be attributed to the generally low topographical gradients and the fact that the soil infiltration rates exceed the precipitation rates (Landell Mills Associates, 1979). The soil characteristics are discussed in detail in Chapter 2.8.

Wetland or vleis areas occur in the region. These areas are commonly referred to as “dambo” areas. The dambo areas occur where surface depressions intersect the groundwater table. In general, each dambo area is not very large in extent (less than 200m x 200m), however, in some areas the concentration of dambos is large and the total affected area is quite substantial.

The recharge percentage from rainfall to the aquifer in the dambo areas is uncertain. It is expected to be higher than the regional average due to the fact that the water is ponded and also due to the relatively high infiltration rate of the surrounding and underlying soils.

Evaporation occurs from the dambo areas. Evaporation data available from the MDC monitoring program at Mpongwe Farm for the time period April 1997 to April 2003 indicates that approximately 945mm of evaporation occurs annually. Evaporation is discussed in Chapter 2.5.

It is likely that the dambo areas remain wet well into the dry season, due largely to seepage along dambo edges. The seepage originates from slow sub-surface drainage from the higher lying areas between the dambos.

A relatively low percentage of the annual rainfall leaves the system through surface runoff and together with the high soil infiltration rate, the recharge percentage from rainfall in the region is elevated. The recharge to the groundwater system is discussed in detail in Chapter 3.5.

Figure 2.4.1: Kafue River.

Kafue River



The photograph show the Kafue River. The River is on average 10 to 20m wide and reportedly 3m deep. Flow in the river is relatively slow. The River is the only perennial surface runoff feature in the study area.

Figure No: 2.4.1

February 2005

Characterisation of the Dolomitic Aquifer in the Copperbelt Province, Northern Zambia.

Chapter 2.5 : Evapotranspiration.

Evaporation losses in the study area are mainly derived from water held on vegetation cover, from the phreatic zone and from the shallow ponding water in surface depressions such as the dambo areas. As evaporation from the soil dries the surface, water is abstracted through capillary action, allowing evaporation losses to continue until capillary water is no longer available.

Very little evaporation data is available for analysis by the author. The annual and monthly evaporation data as recorded by MDC is shown in Figures 2.5.1 and 2.5.2 respectively. It should be noted that this data reflects only positive net evaporation (total evaporation minus rainfall greater than zero). Due to the high rainfall, which exceeds the rate of evaporation during the rainy season, there is no positive net evaporation data for these periods on record. Therefore, even though evaporation does occur during the rainy season between rain showers, there is no data available on these evaporation rates.

The reason why only positive net evaporation is recorded is not known, but could possibly be due to problems associated with collecting the evaporation data during the rainy season.

The author has calculated the average annual net evaporation for the periods April 1997 to April 2003 to be 945mm.

Figure 2.5.1 shows that the annual evaporation data declines during the months of April to July. This is followed by a sharp increase in evaporation in August and particularly September. This decline and increase can be contributed to the influence of the temperature and number of daylight hours. During the months of April to July the average daily temperatures and number of daylight hours decrease until the winter solstice is reached on 21 June. During July, low temperatures and short days are experienced. In August, the seasons turn and daylight hours become slightly longer and temperatures rise markedly. During September, the daylight hours lengthen and temperatures increase to those that are expected during the rainy season (summer).

The potential evaporation from an open water surface, E_o , can also be estimated using various formulae (Penman, Turc and Blaney-Cridde equations) using meteorological data, or by using evaporation pans with the appropriate correction factor.

The difference between estimated and actual evaporation is variable. These variations are greatest during rainfall periods. This is possibly due to the difficulties encountered when measuring evaporation during rainfall. The degree of exposure, location and evaporation pan material can significantly affect the measured evaporation.

The available evaporation data as listed by Landell Mills Associates (1979) has been analysed by the author, and the potential evaporation has been calculated. The parameters used and results are shown in Table 2.5.1. The Penman equation was used during the analysis. The calculation was made using Microsoft Excel and follows the New Mexico Climate Center methodology (New Mexico Climate Center Website).

The calculated potential evaporation value of 1708mm/annum correlates well with the evaporation values calculated by Landell Mills Associates in 1979. The comparative values are summarised in Table 2.5.2.

In a simplified system the accuracy of the observed and calculated values can be evaluated with a basic calculation using the equation:

$$\begin{aligned} \text{Annual Rainfall} &= \text{Total evaporation} - \text{net evaporation} && \text{(Eq 2.5.1)} \\ &= 1\,700\text{mm/annum} - 945\text{mm/annum} \\ &= 755\text{mm/annum} \end{aligned}$$

However, in Chapter 2.3, it was shown that the average annual rainfall is approximately 1 115mm/annum, indicating a 365mm/annum discrepancy. This means that either the average annual rainfall is overestimated by 365mm or the average annual evaporation is underestimated by 365mm, or a combination of the two.

Table 2.5.1: Evaporation Calculations.

Parameter	Unit	Value
Maximum Temperature	°C	36.10
Minimum Temperature	°C	-2.20
Maximum Humidity	%	97.00
Minimum Humidity	%	28.00
Elevation	mamsl	1320.00
Wind Speed	Km/h	10.00
Barometric Pressure	mb	873.74
Average Temperature	°C	16.90
Minimum Saturated Vapour Pressure	mb	59.77
Minimum Air Vapour Pressure	mb	16.74
Maximum Saturated Vapour Pressure	mb	5.19
Maximum Air Vapour Pressure	mb	5.03
Actual Vapour Pressure at Mean Temperature	mb	10.88
Saturated Vapour Pressure at Mean Temperature	mb	32.48
Reflection Coefficient		0.21
Latent Heat of Vaporisation	cal/g	586.00
Net Radiation	cal/cm ² /day	317.25
Slope of Saturated Vapour Pressure Curve	mb/°C	1.22
Psychometric Constant	mb/°C	0.58
Penman Potential Evaporation	mm/day	4.68
Penman Potential Evaporation	mm/annum	1708.00

Table 2.5.2: Comparative Evaporation Rates.

Evaporation Calculation	Method	Evaporation (mm/annum)
M. Prinsloo (2004)	Penman	1 708
Landell Mills Associates (1979)	Penman	1 793
	Turc	1 488
	Blaney-Criddle	1 750

The author considers the rainfall data to be accurate. Based on this consideration, the uncertainties surrounding the methodology used during the recording of the evaporation data, and the non-recording of evaporation during the rainy season may be reasons for the 365mm discrepancy.

It is the opinion of the author that the shortcoming in the evaporation data and the subsequent 365mm discrepancy lies mostly with the non-recording of evaporation data during the rainy season. This opinion is discussed below.

Based on the recorded data the average net evaporation during the dry season is 945mm. Taking into consideration that very little to no rainfall occurs during the dry season, it can be assumed that the total evaporation during the dry season is equal to 945mm.

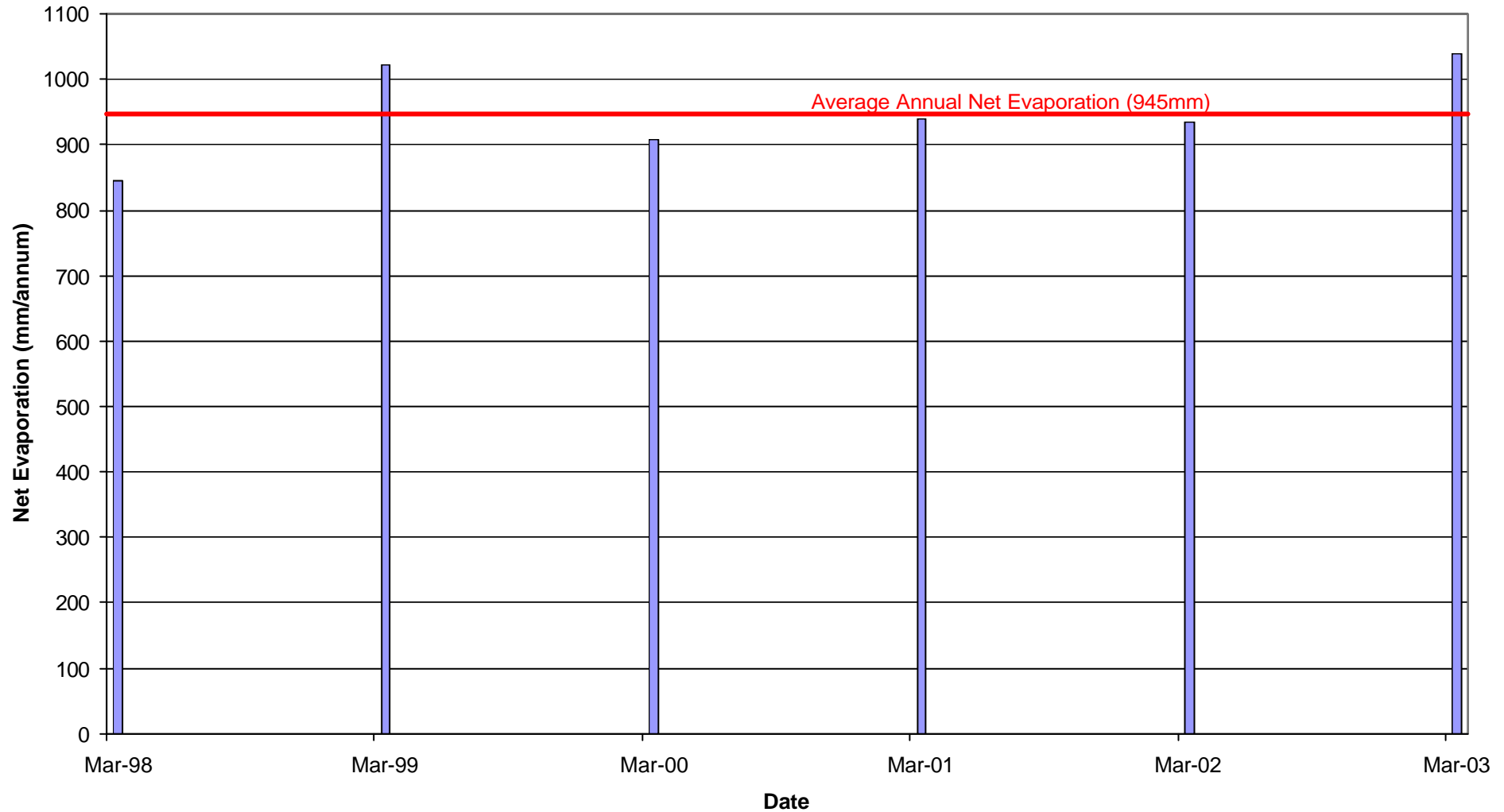
Based on an average dry season time span of 210 days, the evaporation rate equates to 4.5mm/day. The rainy season is on average 150 days. Using the dry season rate of evaporation, it can be calculated that 675mm of evaporation could theoretically occur during the wet season. The daily evaporation rate during the rainy season would, however, be influenced by the higher temperatures that would increase the evaporation on the one hand, whilst the increased humidity and rainfall would decrease the evaporation on the other hand.

There is, however, not enough meteorological and other data available to substantiate this opinion with scientific calculations.

Due to the uncertainties surrounding the evaporation data collection, and the non-collection of evaporation data during the rainy seasons, the author recommends that the evaporation data is not included in the water balance calculations, as this would negatively influence the confidence level of the calculation results.

Figure 2.5.1: Recorded Annual Evaporation Data.

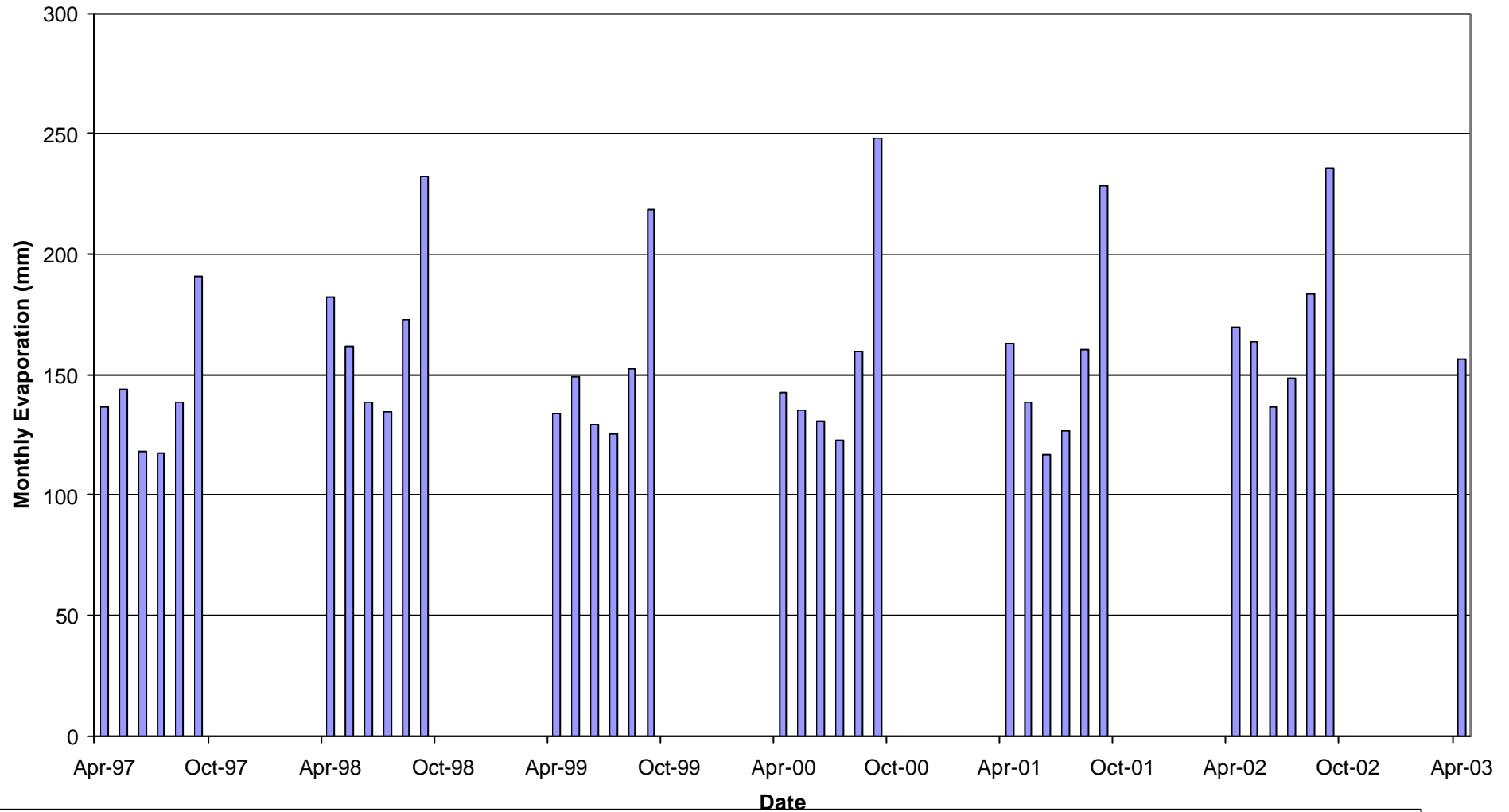
Recorded Annual Evaporation Data



The Figure indicate the recorded net annual evaporation. The average recorded net annual evaporation is calculated to be 945mm. Net evaporation is defined as the total evaporation minus the rainfall. MDC records only positive net evaporation. This occur only during the dry season (Refer Figure 2.5.2). Although evaporation occur during the rainy season, it is exceeded by rainfall, and is not recorded by MDC.

Figure 2.5.2: Recorded Monthly Evaporation Data.

Recorded Monthly Evaporation Data



The Figure indicate the recorded net monthly evaporation as measured at Mpongwe.
 The net evaporation is defined as the total evaporation minus the measured rainfall.
 During the dry season (April to October) a positive net evaporation exist due to the fact that very little to no rainfall occurs while evaporation continues.
 During the wet season (November to March) a negative net evaporation exist due to the high rainfall. MDC records no evaporation values for those months.

Chapter 2.6 : Plant Growth.

The area is in general covered by *Brachystegia – Tulbernardia* (Miombo) woodland (Landell Mills Associates, 1979). The dominant species is *Brachystegia*, with tree trunk diameters varying between 15 and 35cm (refer to Figures 2.6.1 and 2.6.2). The average tree density is approximately 500 trees per hectare. Grass cover found between the trees is widespread. In several areas, the tree cover is broken by the presence of dambos.

Miombo, or Miombo woodlands, are the largest continuous dry deciduous forests in the world (approximately 2 800 000km²). They extend across much of central, eastern and southern Africa, including Angola, DR Congo, Malawi, Mozambique, Tanzania, Zambia and Zimbabwe.

Authors such as Landell Mills Associates (1979) and The Community Based Natural Resource Management Network (ongoing study), which undertook a wide study of African water resources, concluded that the trees have had to adapt themselves to the amount of water available throughout the year, and have done so over a period of many years. They have developed root systems with long taproots that can easily draw water from a depth of up to 7m or more. Root depths of up to 40m have been reported.

The woodland is deciduous, losing most of its leaves and becoming semi-dormant during the dry season. The trees come into fresh leaf in September and October, often before any precipitation has occurred. The main growth period is confined from December to May.

The soil and climatic characteristics are such that agricultural plants such as mealies, wheat and coffee grow easily in the area. Yields from these crops are above average for African conditions and the MDC is one of the largest suppliers of agricultural crops in Zambia, as well as in Africa.

Figure 2.6.1: Species *Brachystegia*.

Species *Brachystegia*



The Figure indicate an example of Brachystegia.

Figure 2.6.2: Natural Vegetation in the Study Area.

Natural Vegetation in the Study Area



The photograph indicate the natural plant growth in the study area. Plant growth predominantly consist of Brachystegia woodland and grassland. On average there are 500trees/ha in undisturbed areas. The grass is thick and can be up to 2m tall.

Chapter 2.7 : Geology.

Anglo American Corporation performed a detailed geological investigation over the past three years. Application was made to Anglo American Corporation on behalf of MDC to obtain the data for the 2004 hydrogeological study. Anglo American Corporation approved the application and the data was made available. The geological maps resulting from the Anglo American Corporation investigation (1327D & 1328C) are shown in Figure 2.7.1.

The Mpongwe limestones and dolomites form part of the Upper Roan Group of the Katanga Supergroup. The surrounding formations are generally regarded as Lower Roan sandstones. However, schists have been encountered within the limestone and dolomite areas. An inlier of Lower Roan exists in the centre of the limestone and dolomite block at Mpongwe (refer to Figure 2.7.1).

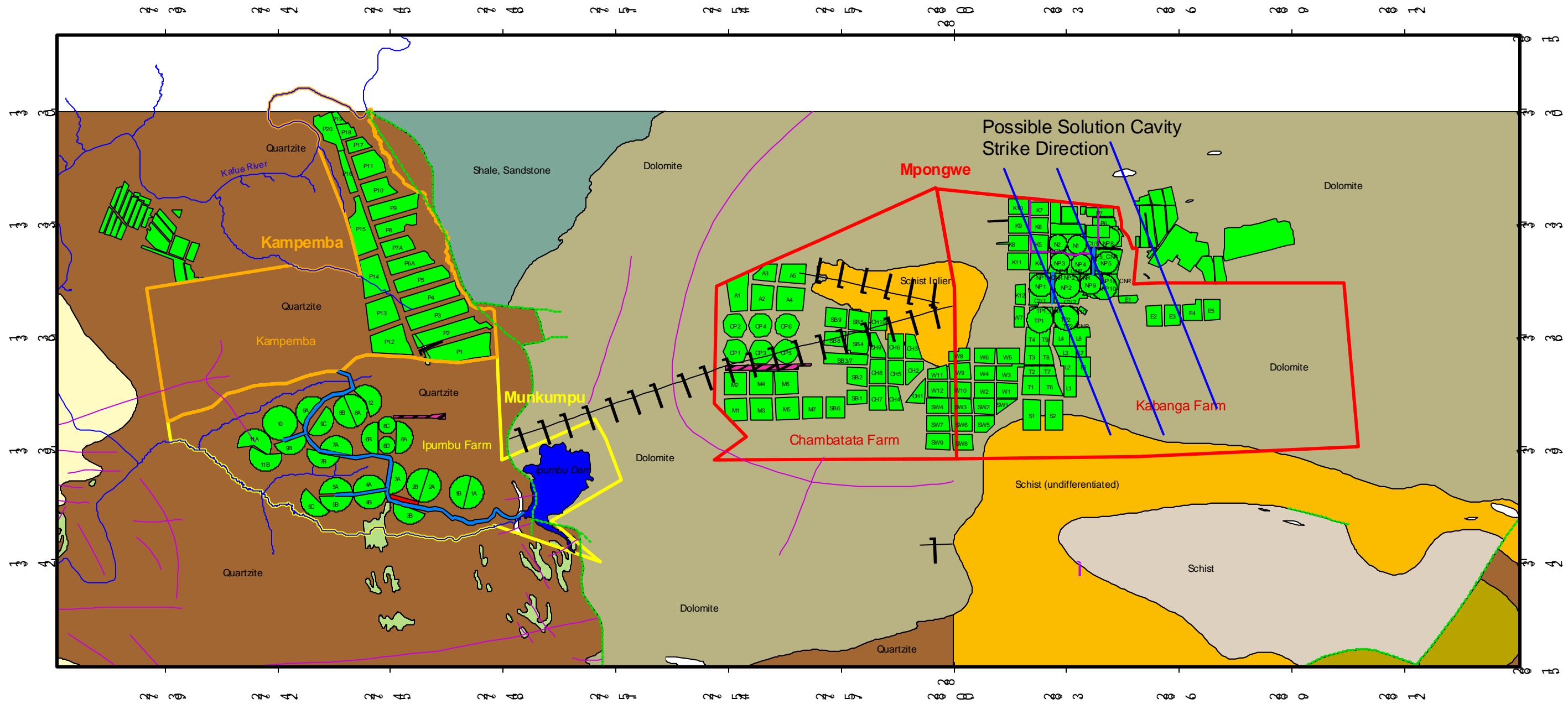
To the west, at Ipumbu Farm, the Munkumpu Fault zone forms a sharp contact between the limestone and dolomite to the east and meta-sedimentary siliclastic rocks or quartzite that underlies Ipumbu Farm.

North-south and east-west geological cross sections, constructed by the author, are shown in Figures 2.7.2 and 2.7.3 respectively. The cross sections are based on water borehole log data. Due to the fact that there is no data available for the Ipumbu Farm, the cross sections are limited to the Mpongwe area.

The limestone in the study area varies from pure white crystalline marble and dolomitic marble with saccharoidal texture to blue grey crystalline limestone to darker blue-grey argillaceous limestone often with a streaky texture and a variable degree of micaceous banding.

Figure 2.7.1: General Geology of the Study Area.

General Geology of the Study Area



LEGEND:

Canals	Structure.shp	Buildings	Coffee Boundary	Metasedimentary sandstone
Minerals.shp	fault: inferred undifferentiated	Airstrips	Field boundaries	Quartzite
copper	fold axis: undifferentiated	Farm_boundaries.shp	Geology.shp	Schist
iron	fold axis: vertical synform	Kampemba Arable Region	Banded limestone	Schist (undifferentiated)
pyrite	Rivers	Mpongwe Arable Region	Dolomite	Schist Inlier
	Dams	Munkumpu Arable Region	Metacglomerates	Shale, Sandstone

Figure No: 2.7.1



2 0 2 4 6 Kilometers

GEOLOGY DATA INFORMATION:

WESTERN PART:
Map Block: 1327D
Geological Map of the Mukutwe Area
Date: 1994
Capturing scale: 1:100 000

EASTERN PART:
Map Block: 1328C
Geological Map of the Mpongwe Mission-Lukanga River Area
Date: 2000
Capturing scale: 1:100 000

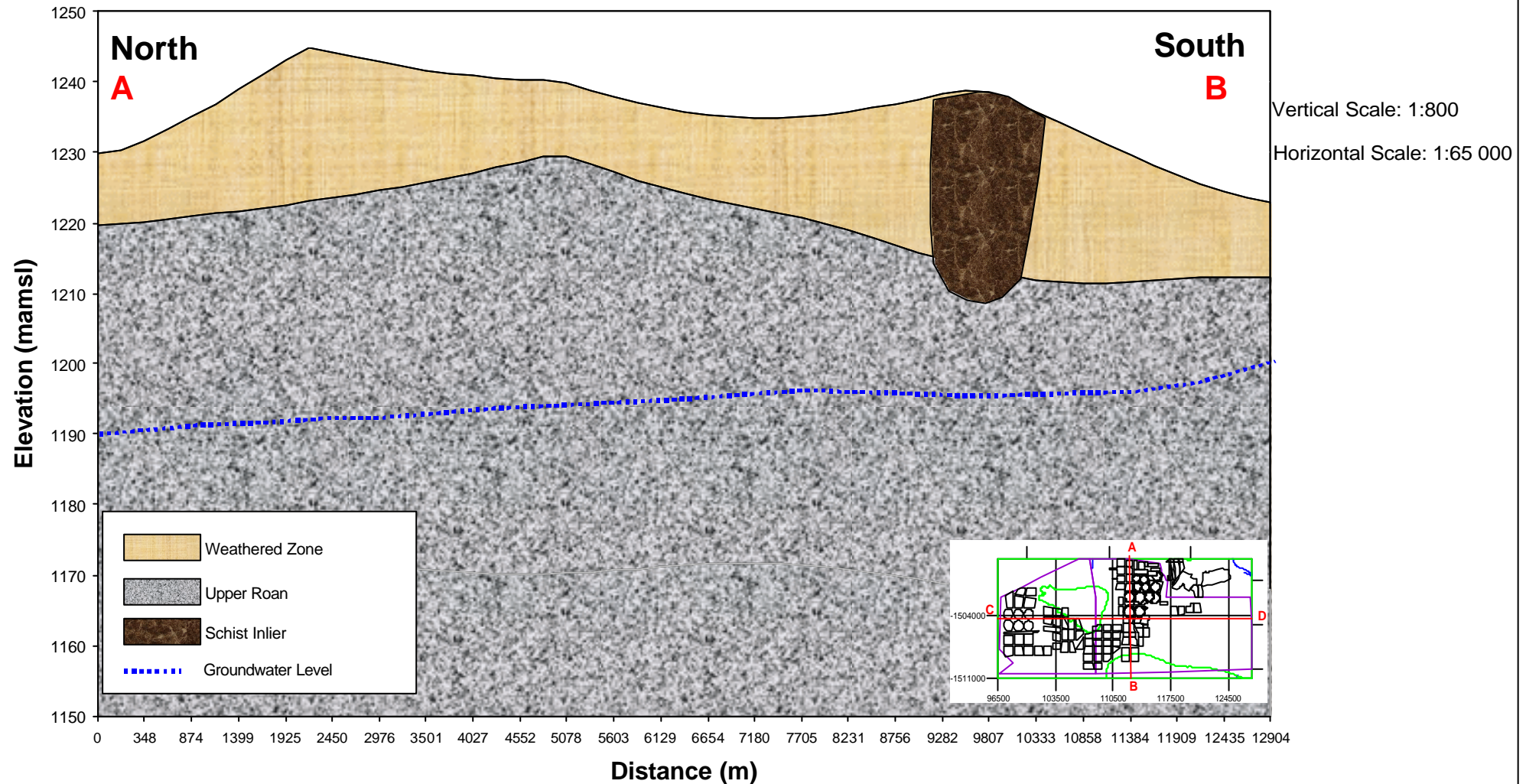
© Bought through GeorGIN from Anglo American (Nov 2003)

© Bought through GeorGIN from Anglo American (Nov 2003)

M.Sc Study - M. Prinsloo
Characterisation of the Dolomitic Aquifer
in the Copperbelt Province, Northern Zambia

Figure 2.7.2: North-South Cross Section through the Eastern Aquifer.

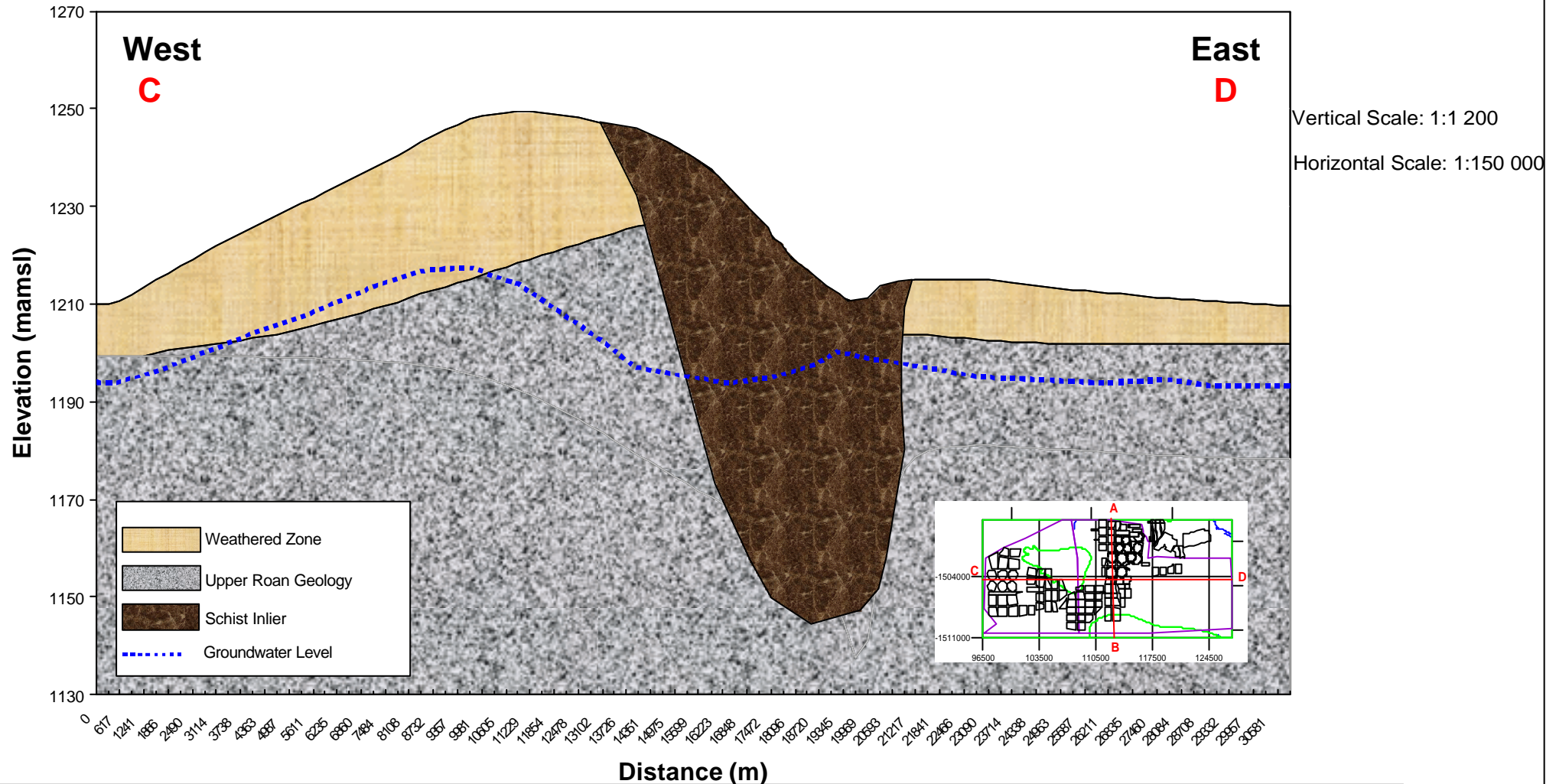
North-South Cross Section Through the Eastern Aquifer



The Figure indicate a north-south geological cross section through the Eastern Aquifer. The position of the cross section as well as the vertical and horizontal scales are indicated. The cross section is based on data obtained from the water borehole geological logs. Due to no data being available for the Munkumpu Irrigation Area, this is not included in the cross section. The exact shape of the schist inlier is not known and was interpreted as near as possible based on the water borehole geological data.

Figure 2.7.3: West-East Cross Section through the Eastern Aquifer.

West-East Cross Section Through the Eastern Aquifer



The Figure indicate a west-east geological cross section through the Eastern Aquifer. The position of the cross section as well as the vertical and horizontal scales are indicated. The cross section is based on data obtained from the water borehole geological logs. Due to no data being available for the Munkumpu Irrigation Area, this is not included in the cross section. The exact shape of the schist inlier is not known and was interpreted as near as possible based on the water borehole geological data.

Several types of schist can be recognised:

- Light blue grey calcareous schist
- Silvery brown highly micaceous schist
- Dark blue-grey schist, almost slate
- Green quartz-mica schist
- Grey-green schist
- Light greenish white schist with a soapy texture
- Black pyretic schist

The schistose rocks cannot be easily classified and stratigraphically related due to the lack of sufficient outcrop. However, hydrogeologically the schist behaves as a homogeneous unit and is interpreted as such.

Structural information can only be compiled from areas of natural outcrop. Outcrop areas are limited in the Mpongwe area and are largely confined to areas of limestone around the high lying plateau. Landell Mills Associates (1978) measured the orientation of the foliation in the schist in several borrow pits in the area. No other structural features were observed.

The outcropping limestone and dolomite foliation is usually visible. Extensive jointing occurs in the limestone and dolomite.

The limestone and dolomite beds display a generally shallow dip ranging between 5° and 20°, to the northwest or north-northwest. At Lake Kashiba the dip is as steep as 40° to 50°, but it still maintains the regional general strike direction.

Following Landell Mills Associates (1978), evidence of folding is very limited in the area and is only observed in two areas:

1. Lake Kashiba – very small-scale flow folds in more argillaceous and highly foliated bands of limestone.

-
2. The Chibili pavement displays small-scale drag folds and slightly larger folds with a wavelength of 2 to 3m. The axis of these folds trend at approximately 260°. The hinge line of the folds is near vertical.

Large scale folding of the area is uncertain. Major folding patterns would be more easily identifiable in the schist, however, limited outcrops in the area prevent any interpretation.

Jointing is common within the limestone and dolomite. Three major joint sets, all near vertical, are distinguished:

1. The dominant joint set with an orientation of 160°.
2. A secondary joint set with a 220° to 230° orientation.
3. A secondary joint set with a 270° orientation.

The principal joint set in the area is 160° and controls the orientation of Lake Nampamba (refer to Figures 2.7.4 and 3.1.2). Age relationships of the joint sets are not clear due to little offset between the different joint sets.

Evidence of extensive fracturing within the limestone and dolomite is found in the geological logs of the boreholes. The majority of the high yielding boreholes displayed significant fracturing of the limestone. Fracturing in the limestone is conducive for chemical weathering due to the fact that the fractures act as preferential pathways for groundwater flow. This will enhance the solution of the dolomitic geology in acidic water.

Outcrops at Lake Nampamba and Lake Kashiba display highly fractured and linear zones (refer to Figures 2.7.4 and 2.7.5). Calcite and quartz veining is common (refer to Figure 2.7.6).

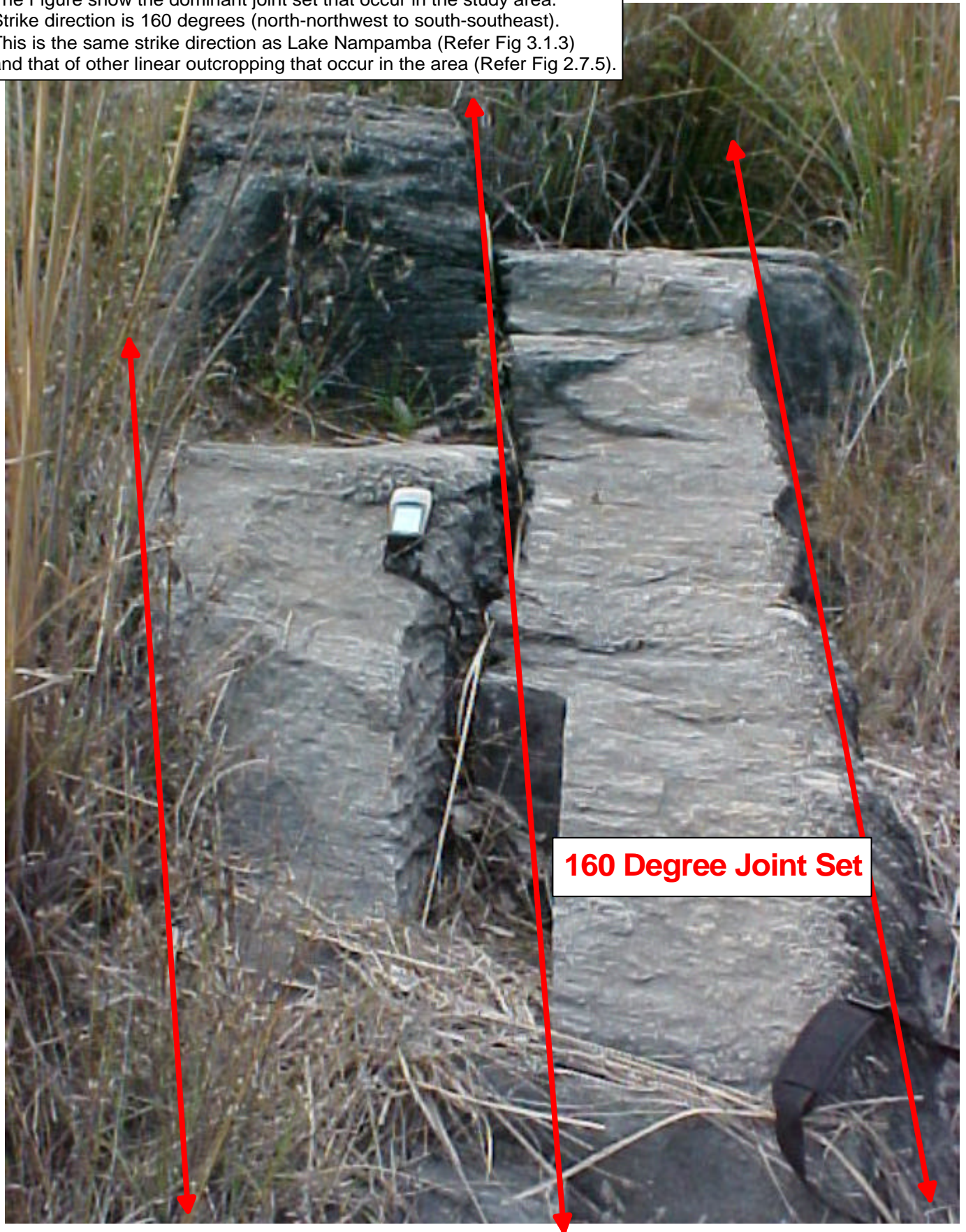
Due to the extensive soil cover the relationship and contact zones between the schist and the limestone are not clear.

Please refer to Figures 2.7.7 to 2.7.9 for photographs of some of the most prominent limestone and dolomitic lithologies in the study area.

Figure 2.7.4: Major Joint Set near Lake Nampamba.

Major Joint Set near Lake Nampamba

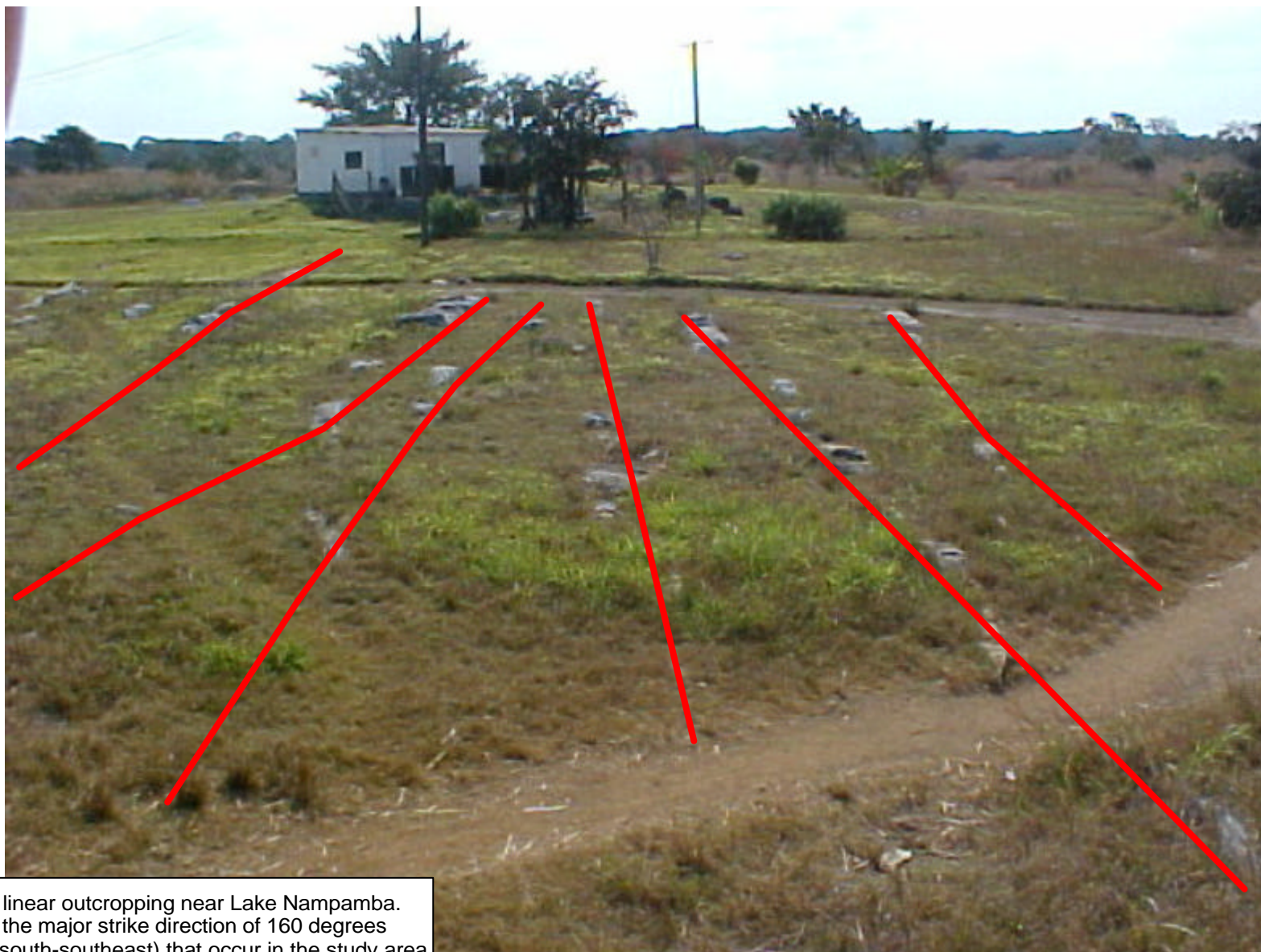
The Figure show the dominant joint set that occur in the study area. Strike direction is 160 degrees (north-northwest to south-southeast). This is the same strike direction as Lake Nampamba (Refer Fig 3.1.3) and that of other linear outcropping that occur in the area (Refer Fig 2.7.5).



160 Degree Joint Set

Figure 2.7.5: Linear Outcropping of Dolomite near Lake Nampamba.

Linear Outcropping of Dolomite near Lake Nampamba



The Figure indicate linear outcropping near Lake Nampamba. The lineation follow the major strike direction of 160 degrees (north-northwest to south-southeast) that occur in the study area.

Figure 2.7.6: Quartz Veining in the Dolomite.

Quartz Veining in the Dolomite

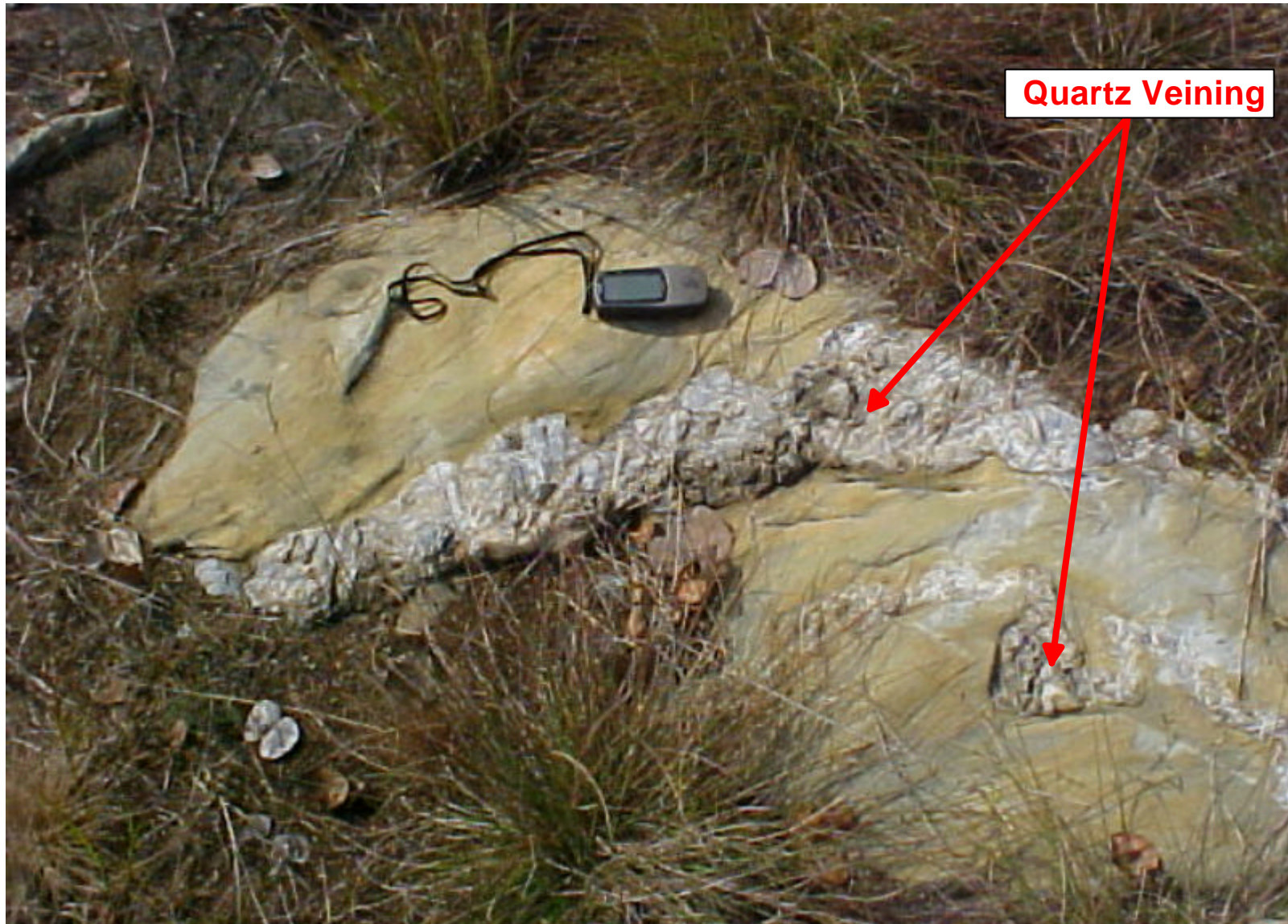


Figure No: 2.7.6

February 2005

Figure 2.7.7: Fractured White to Pink Limestone associated with High Yielding Areas.

Fractured White to Pink Limestone associated with High Yielding Areas



Example from Borehole MDP10A of the Fractured White to Pink Limestone Associated with high Yielding Areas. The larger drill chips average 3-5cm.

Figure 2.7.8: Sandy Limestone.

Sandy Limestone

Example of the Sandy Limestone from Borehole MDP10A. Note the sandy texture in comparison with Figure 2.7.7 that indicate the Fractured White to Pink Limestone.



Figure 2.7.9: Fractured and Weathered Limestone with Laterite.

Fractured and Weathered Limestone with Laterite



Example of the Fractured and Weathered Limestone. Example from Borehole MDP10A. Note the smaller chip size in relation to Figure 2.7.7. There is little to no sand present in the drill samples. The brown nodules is Laterite.

Chapter 2.8 : Soils.

An in-depth soil investigation has been carried out by Landell Mills Associates (1979). The soil cover overlying the limestone and schist areas is generally shallow, with an average depth of 8 to 12m. In some areas the soil depth reaches 35m (borehole E5000).

Rock outcrops can occur in the form of massive boulders of unweathered limestone or quartz, around which the soil can be several metres deep.

The soil characteristics influence the hydrological cycle as the characteristics influence water absorption, retention and infiltration. Considerable information is available on the soil types and soil characteristics to a depth of 2m.

The Zambian Department of Agriculture has performed extensive exploratory work in the study area. Landell Mills Associates (1979) refers to Tate And Lyle Technical Services Ltd. (1978) who also carried out a detailed soil investigation in the area.

Class 1 and Class 2 soils were identified and cover approximately 63% of the study area. These soils are suitable for agricultural purposes. The remaining 37% of the area is covered with marginal or unsuitable soil for agricultural purposes. The suitable soil types are described as follows:

- Class 1: Deep, well drained, dark reddish brown clay loam to clay over dark red clay.
- Class 2: Deep, well drained, dark reddish brown sandy clay loam and clay loam over yellowish red clay loam and clay. The soil possesses a high clay content (30-40%). This however, does not impair the drainage characteristics.

From slaking tests, the Class 1 and Class 2 soils are shown to be very stable. Slaking tests are performed by placing soil fragments or aggregates in water and estimating the degree of slaking (disintegration when combined chemically with water). The lighter, sandier soil on the central plateau area associated with the schist is markedly less stable than the Class 1 and 2 soils. A very stable soil will have a good resistance to impact from falling rain, and is less likely to break down into fines which then block the drainage

pores, creating an impervious surface skin and accentuating run-off during the latter part of rain storms.

The infiltration rate determines whether or not surface run-off will take place. Tate & Lyle Technical Services Ltd. performed ring infiltrometer tests in selected areas during 1978. Ring infiltrometer tests are performed in order to determine the rate of infiltration of fluid into soil. From this infiltration data the permeability of the unsaturated soil can be calculated.

Double or single ring infiltrometer tests can be performed (Brand, 2003). During double ring infiltrometer tests two open cylinders are driven into the ground, one inside the other, and partially filled with water. The volume of water added to the inner ring to maintain a constant water level is a measure of the volume of water that infiltrates the soil. The purpose of the outer ring is to promote one-dimensional vertical flow into the soil.

During single ring infiltrometer tests only a single ring is inserted into the ground (refer to Figure 2.8.1).

Infiltration rates are calculated using the following equations (Brand, 2003):

Downward flow rate:

$$i_w = i_n \pi r^2 / \pi (r+x)^2 \quad (\text{Eq 2.8.1})$$

Where:

- i_w = downward flow rate (L/t).
- i_n = last drop infiltration rate (L/t).
- r = radius of the infiltrometer ring (L).
- x = lateral extent of the wetting front (L).

The depth of the wetting front can be physically measured or calculated using the equation:

$$L = y_t \pi r^2 / n \pi (r+x)^2 \quad (\text{Eq 2.8.2})$$

Where:

- L = depth of wetting front (L).
- y_t = cumulative water level decline (L).
- r = radius of the infiltrometer ring (L).
- x = lateral extent of the wetting front (L).
- n = Porosity that can be filled (dimensionless).

Finally, the long-term infiltration rate is calculated using:

$$K_v = i_w L / z + L - h_{we} \quad (\text{Eq 2.8.3})$$

Where:

- K_v = long-term infiltration rate (L/t).
- i_w = downward flow rate (L/t).
- z = average depth to water in the infiltrometer ring during test (L).
- L = depth of wetting front (L).
- h_{we} = water entry value for soil.

The tests performed at Mpongwe in 1978 incorporated test areas in both undisturbed woodland soil and soil in the farming area. The results indicate that the infiltration rate is likely to exceed the rate of precipitation. This is subject to the condition that free drainage is not impaired, as the soil becomes water logged. Once free drainage is impaired, the infiltration rate will reduce.

The recorded depths of infiltration in Class 1 soils range between 260 and 460mm over a six-hour period. Infiltration rates average at 130mm for the first hour of the six-hour period. The rates decrease to approximately 40mm during the last three hours. The rates are higher for the Class 2 soils. Unfortunately, the specific data has been lost over time and is not available for evaluation by the author.

The field capacity of a soil is the volume of water retained after free drainage (seepage due to gravitational pull) has taken place. This moisture is retained in small pore spaces by capillary attraction, and as a film around individual soil particles. The field capacity of a soil is therefore to a large extent dependent on the porosity and the grading of the soil particle sizes.

Wilting point is the quantity of soil moisture at which the capillary and surface adhesion forces are greater than the soil suction forces exerted by plant roots. Wilting point is determined as the water remaining in the soil at a suction pressure of 15 atmospheres. In shallow soil layers water depletion will continue beyond the wilting point since evaporation is still active. Deep soil layers, however, are not affected by direct evaporation and will remain at the wilting point. The water potential of the soil reaches its minimum possible water content at the wilting point. The minimum wilting point depends on the physiological attributes of the plants that grow in the soil.

The soil characteristics at Mpongwe have been determined to be (Landell Mills Associates, 1979):

Field Capacity	= 290mm/m
Wilting Point	= 185mm/m

If it is assumed that the average water retaining properties of the soil apply throughout the depth of the entire study area, the volume of rainfall recharge held in the soil can be estimated.

It is considered unlikely that the soil moisture content will reduce to near wilting point capacity below 2m in depth during an average rainfall year.

The high density of woodland cover and the fact that growth does not appear to be limited indicates that *Brachystegia* species are capable of abstracting transpiration water from considerable depths.

Assuming an average depth of 2m, and a soil moisture content that has declined to wilting point capacity at the end of the dry season, the rainfall required to raise the soil

moisture content from wilting point to field capacity is approximately 105mm/m or 210mm (Landell Mills Associates, 1979). This, in addition to the evapotranspiration demand of the woodland, gives an indication of rainfall required before recharge to the underlying aquifer can occur.

Figure 2.8.1: Single Ring Infiltrometer Test.

Single Ring Infiltrometer Test

The volume of water added to the inner ring to maintain a constant water level is a measure of the volume of water that infiltrates into the soil.
The steel ring promote vertical flow into the soil.

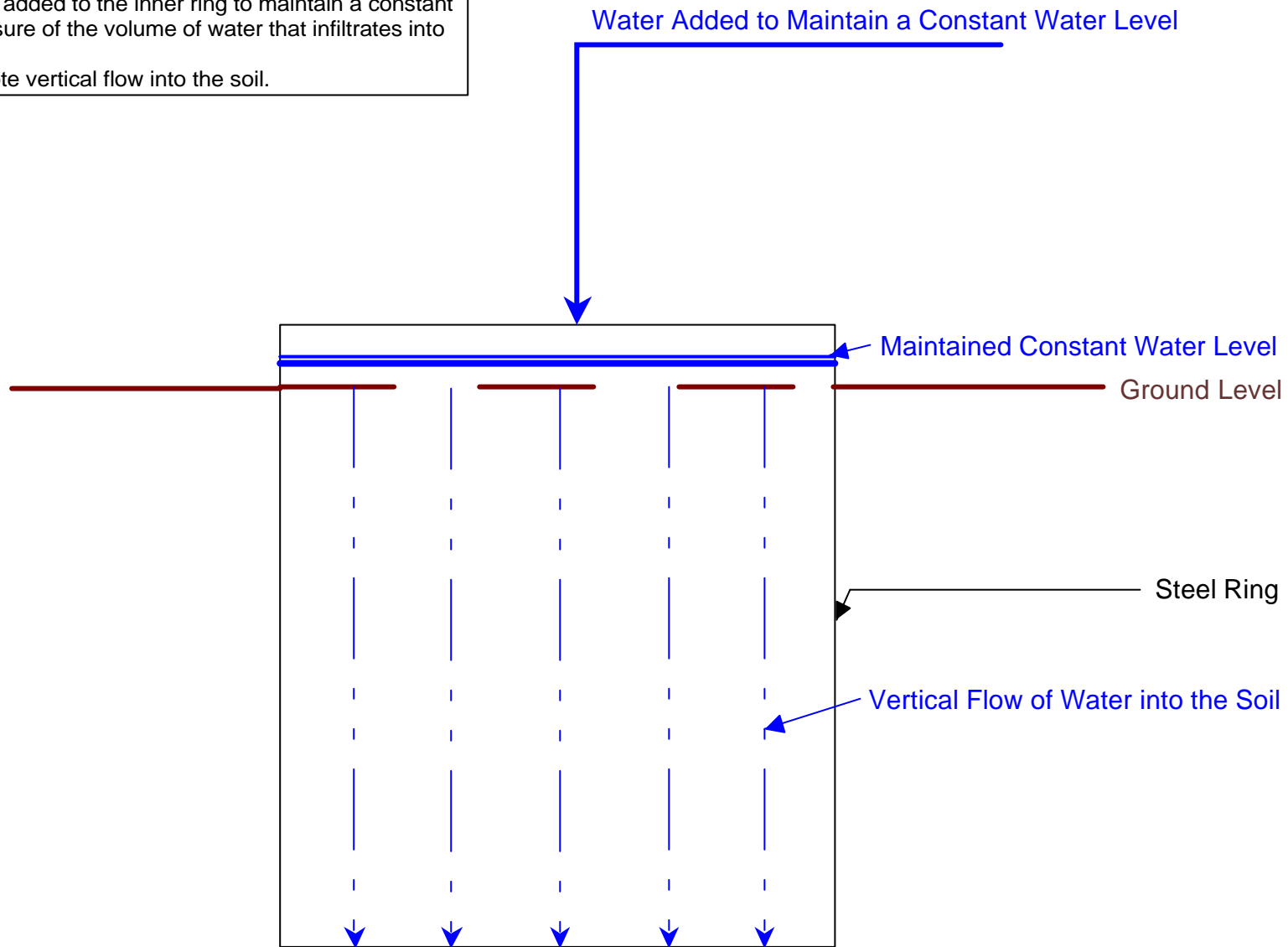


Figure No: 2.8.1

February 2005

Chapter 2.9 : Surface Geophysical Investigations.

Three documented geophysical surveys have been carried out in the Eastern Aquifer area. The first survey was held during 1978, the second during 1982, and the third during 2004. The aim of the investigations was to scientifically site boreholes for production purposes.

Chapter 2.9.1 : Geophysical Survey of 1978.

During 1978 Landell Mills Associates performed an extensive geophysical investigation. This included:

- 91.1km of electrical resistivity profiling
- 145.5km of magnetic profiling
- 145.5km of radiometric profiling
- 538 Vertical Electrical Soundings (VES)

The original data is not available and can therefore not be shown and independently evaluated by the author for this study. Landell Mills Associates (1978) compared the geophysical data to the results of the drilling program. The main conclusions reached by Landell Mills Associates are discussed below. The main findings and interpretations of the investigation are summarised in Table 2.9.1.1.

A large degree of electrical resistivity overlap occurs between water bearing limestone (30 to 300 Ω .m) and the weathered and unweathered schists (50 to 400 Ω .m).

One is unable to distinguish between the schists and the water bearing limestone, using only the VES method.

Due to the electrical overlap, the resistivity traversing performed was unable to discriminate between the water bearing limestone and schists.

A study of the magnetic and radiometric profiles indicated that these methods are also unable to distinguish between the two main rock types.

Table 2.9.1.1: Interpretation of the Geophysical Survey of 1978.

Simplified Geological Succession	Simplified Geo-electrical Succession
Soil and superficial deposits.	Red soil sometimes with quartz pebbles. This also includes ferricrete, laterite and the transition zone between soil and the underlying rock. Resistivity range from 1 000 – 6 000Ω.m. Infrequently exceeds 6 000Ω.m. In a few places the range is less than 200Ω.m.
Schist.	Marginal aquifer / aquiclude. Resistivity range between 50 - 400Ω.m - usually between 100-200Ω.m.
Mineralised schist.	Acts as a conductor. Resistivity less than 10Ω.m
Partly weathered limestone.	Marginal aquifer. Resistivity range from 300 to 1 400Ω.m, usually in excess of 1 000Ω.m.
Crystalline limestone with development of fractures and karst features.	Aquifer. Variable thickness - in places in excess of 60m. Resistivity range between 100-300Ω.m
Weathered argillaceous limestone.	Aquifer. Variable thickness - in places in excess of 50-60m. Resistivity range from 30-110Ω.m

It was noted that once the geological boundary between the schist and the limestone was identified, the VES method was capable of delineating the water bearing structures within the limestone.

It was concluded that lateral changes in resistivity typical of a karst environment could be clearly identified from field data.

From the calibration soundings performed by Landell Mills Associates (1978) it was concluded that the optimum resistivity range for water bearing karstic limestone ranges between 100 and 300Ω metres. The resistivity of the water bearing argillaceous limestone ranges between 30 and 110Ω metres.

It was concluded that the identification of the schist – limestone boundary is of utmost importance. Once the boundary has been identified the use of the VES method will allow the selection of borehole sites to be made with confidence.

Chapter 2.9.2 : Geophysical Survey of 1982.

During the 1982 investigation (Macdonald and Partners Ltd.) it was decided to perform additional VES soundings in the Eastern Aquifer area. In addition, a limited amount of resistivity profiling was planned even though this profiling was not recommended in the 1978 study results. The investigation covered the southern borehole field where the MDP boreholes occur and extended to include a small sinkhole approximately 4km east of Kabanga Farm.

The results of the VES investigation are summarised in Appendix B. The survey positions are indicated in Figure B1. Note that the coordinates indicated on the figure do not reflect the WGS84 system that has been used for all the other coordinates in this report. The coordinate system used by Macdonald and Partners Ltd. (1982) cannot be identified with certainty. Therefore, the positions of the survey points could not be accurately transferred to a more recent map produced by the author and the figure was thus copied from the original Macdonald and Partners Ltd. report.

During the electrical resistivity investigation the Wenner array was used. For a Wenner array survey, two current electrodes and two potential electrodes are placed in line with each other, equidistant from one another, and centered on an arbitrary selected location.

The apparent resistivity computed from the measurements of voltage, ΔV , and current, i , is given by the relatively simple equation (Colorado School of Mines, course notes, 2004):

$$\rho_a = 2\pi a \frac{\Delta V}{i} \quad (\text{Eq 2.9.2.1})$$

By plotting the apparent resistivity versus the electrode spacing, the resistivity variation with depth can be interpreted.

The Wenner array is relatively sensitive to vertical changes in sub-surface resistivity below the centre of the array. However, it is less sensitive to horizontal changes in sub-surface resistivity.

Compared to other arrays, the Wenner array has a moderate depth of investigation (Loke, 2000). The median depth of investigation is approximately 0.5 times the “a” spacing used. Electrode spacing for the 1982 investigation ranged from 5 to 200m. It is calculated that the theoretical depth of investigation ranges between 2.5 and 100mbgl.

An electrode spacing of 100m was used during the 1982 profiling survey, resulting in a theoretical depth of investigation of 50mbgl.

The results of the investigation (MacDonald and Partners Ltd., 1982) are summarised as follows:

Accurate values of bedrock resistivity were obtained from the results of the investigation. However, it was much more difficult to define the depth of the bedrock. When plotted, results should lie on or close to sections of smooth line in order to be able to match the data. In many result sets the curve sections were too short and any matching that was done was highly subjective. In other cases the curve gradients were too steep to be matched against the existing standard curves.

The problems with interpreting resistivity data may be attributed to two sources:

1. Near surface layers are heterogeneous. For successful interpretation of VES data, the contacts between layers of contrasting resistivity must be almost horizontal over at least the section extending between the outer electrodes. Anomalies in results will occur if this is not the case. Furthermore, the nearer to the surface the irregular formation contacts occur, the greater the anomalies will be.

Drilling results indicate that the laterite overburden has a considerable variation in thickness over short distances.

-
2. Lateral variations in bedrock electrical resistivity will contribute to anomalies occurring. The results from the drilling program indicate that frequent lateral variations in rock type occur over short distances within the study area.

Macdonald and Partners Ltd. compared the findings of the geophysical investigation with the results of the 1982 drilling program.

It can be concluded that formations with typical, relatively high resistivity values (2 000 to 10 000 Ω .m) consist of the less argillaceous crystalline limestone, commonly white or grey marbles and weathered calcareous sandstone.

Formations with lower resistivity values consist typically of more argillaceous thin-bedded limestone with sandstone, shale and schists. The geology often displays a very high degree of weathering. These formations display resistivity values of less than 200 Ω .m.

By comparing the sustainable yields of the boreholes tested during the 1982 investigation with the obtained VES measurements at the point nearest to the boreholes, Macdonald and Partners Ltd. attempted to correlate the VES and the sustainable yield of specific areas. However, it was concluded that no significant correlation exists.

A point of interest highlighted by Macdonald and Partners Ltd. was that while the 1978 report of Landell Mills Associates lists the resistivity of karstic limestone range between 100 and 300 Ω .m (refer to Table 2.9.1.1), the results of the VES survey performed adjacent to Lake Nampamba, station V44, indicate a resistivity of 5 000 Ω .m. It would therefore seem that the general resistivity range for the karstic limestone cannot be applied to what is considered to be the most extensively fissured limestone area in the Eastern aquifer.

As stated in the 1978 Landell Mills Associates report, and verified by Macdonald and Partners Ltd. in 1982, if karstic limestone exists as an extensive aquifer within the catchment, it can not be distinguished from the other rock types by resistivity.

Chapter 2.9.3 : Geophysical Survey of 2004.

During 2004 the author was involved in a brief geophysical investigation conducted at Mpongwe. Three different geophysical methods were used:

- Gravimetric
- Electromagnetic
- Magnetic

The positions of the 2004 geophysical traverses are shown in Figure 2.9.3.1

A geophysical contracting company performed the gravity survey, while the author performed the electromagnetic and magnetic surveys.

Gravity is widely acknowledged as the most effective method for use in dolomitic areas or areas of karstification and dissolution.

The earth's gravitational attraction at a particular site is a function of the density of the surface sediments and the underlying rock units. Gravity meters can measure extremely small differences in the Earth's gravitational field caused by sub-surface density variations.

The theory, on which gravity geophysics is based, is a direct deduction from Newton's Law of Gravity. According to this law two masses m_1 and m_2 a distance r apart will attract each other with a force:

$$F = \frac{GM_1M_2}{r^2} \quad (\text{Eq 2.9.3.1})$$

where G is a gravity constant ($6.67 \times 10^{-11} \text{Nm}^2/\text{kg}^2$)

The acceleration **a** of a mass m_2 due to the gravitational pull of mass m_1 can be calculated using:

$$a = \frac{Gm_1}{m_2} \quad (\text{Eq 2.9.3.2})$$

To be able to apply the gravity method the equation can be changed to:

$$g = \frac{GM}{R^2} \quad (\text{Eq 2.9.3.3})$$

where:

- g = the force per unit mass at the earth's surface (gal or cm/sec)
- G = gravity constant ($6.67 \times 10^{-11} \text{Nm}^2/\text{kg}^2$)
- M = mass of the earth in grams
- R = diameter of the earth in cm

The value of **g** is the average calculated value for the force of gravity at the earth's surface. The variance in **g** is usually so small that it is measured in milligal.

The calculated gravity data can then be contoured using a software package such as Surfer. From the contoured data, areas of low density associated with karstic features can be identified.

Using the electromagnetic equipment, a time varying magnetic field can be induced. Should any conductive material be present in the artificially induced magnetic field, an electric potential will be induced in the conducting material, which can lead to electrical stream flow within the conducting material. This electrical flow within the conductor will be the source of a secondary magnetic field. At any given point in the original magnetic field, the total magnetic field will be equal to the sum of the primary and secondary magnetic fields.

When using the electromagnetic method, the sub-surface conducting material will be the source of the secondary magnetic field. The amplitude of the magnetic field as well as

the phase difference between the primary and secondary magnetic fields is used to identify the position of the conducting material.

The magnetic method relies on the assumption that there is a measurable difference in the permanent magnetism of the host geology and water bearing features, such as a fracture and fault zones, or in the case of dolomite the host geology and the solution cavity.

The interaction between the earth's magnetic field and the lithologies situated in the earth's crust cause a distortion or an anomaly of the earth's magnetic field.

Initially, it was planned that only the gravimetric method would be employed during the 2004 geophysical investigation. The gravity survey consisted of four survey traverses. The reduced gravity data is summarised in Appendix C. The accompanying graphs for the four traverses are shown in Figures C1, C2, C3 and C4 respectively.

Due to the fact that existing borehole logs from the 1978 and 1981 investigations indicated that the main water bearing cavities and fracture zones are situated between 30 and 50mbgl, it was decided that the gravity station interval would be 30m. A *Sodin* gravimeter was used and the relative station elevations were determined using a dumpy level (Engineering & Exploration Geophysical Services cc Report, 2004). The relative station elevations are used during the gravity calculations where corrections have to be made for elevation changes.

Data reduction followed procedures typical of dolomite investigations. The field data was reduced to relative Bouguer values using an elevation correction and a theoretical gravity gradient of 0,21 and 0,00037 mGals per metre respectively. The Bouguer values of both data sets were adjusted by the removal of regional trends that were determined by fitting planes to the data. The values were further adjusted by constants so that the maximum gravity values were less than zero, generating 'residual' data sets.

The data indicated broad changes in gravity. This can be seen in Traverse 3 (refer to Figure C3). These broad changes have a wavelength of more than a kilometre and are probably caused by deep structures of no interest to the present study.

Following Engineering & Exploration Geophysical Services cc (2004), depressions one to several hundred metres in width that were superimposed on the broader changes may be of importance. Examples of these shorter-wavelength anomalies are:

- Traverse 1 from station 100 to 110 (only partly defined, but of high amplitude).
- Traverse 1 from stations 140 to the end of the traverse (several depressions superimposed on a broader depression).
- Traverse 3 from the start of the traverse to station 330 (possibly two separate anomalies, depending on the definition of the broader background change).

Gravity lows are usually associated with preferential weathering of potential water-bearing fracture zones, but relatively high yielding boreholes such as MDP1/19Ab, E3700 and MPD1/11 (refer to Figure C1) are located on relative gravity highs, whilst dry borehole E3000 which is located just to the east of Traverse 1 is probably situated in a gravity low.

Two possible explanations for this apparent anomalous result are (Engineering & Exploration Geophysical Services cc, 2004):

- Some gravity lows may be associated with schist, a poor aquifer; for example the low at the western end of traverse 1 where E3000 encountered only schist before the hole was stopped at 32½ metres.
- Gravity lows may be caused by thick soil, such as found at borehole E5000(1) where the overburden is 30m thick (compared to ten to fifteen metres elsewhere).

It is believed that the cavities which form the main water bearing feature in several boreholes, are too small to be detected using a thirty-metre station separation, and are unlikely to be mapped by even the closest practical gravity grid.

Two boreholes (GCS1 and GCS2) were drilled based on the gravity data. Neither of these boreholes yielded more than 0.5l/s. It was decided to employ the electromagnetic and magnetic methods to correlate the gravimetric data. The author performed these investigations.

The Electromagnetic (EM) Survey was performed using Geonics EM34-3 equipment. A 40m coil separation was used in order to obtain the deepest penetration.

The electromagnetic and magnetic methods were used on a section of the gravity Traverse 3. The EM and magnetometer investigation included the area from gravity station 385 to station 419. As stated above, the gravity survey was performed at a 30m station interval. The EM survey was performed at a 20m interval and the Magnetometer survey was performed using a 5m interval.

Additional electromagnetic and magnetometer survey traverses were performed, which did not correspond with the positions of the gravity traverses. The data is included in Appendix C in Figures C5 and C6 respectively.

The data from traverse “Turnbull” (Figure C5) indicates definite anomalies between stations 120 and 260 in the EM34 data. This anomaly is not as clear in the corresponding magnetometer data. Another anomaly on this traverse exists between stations 580 and 710 on both the EM34 and magnetometer data.

Traverse “Turnbull Cross” (Figure C6) indicates anomalies in the electromagnetic data between stations 240 and 420 and again between stations 620 and 820. The magnetometer data does not indicate an anomaly between stations 240 and 420. However, it does confirm the anomaly between stations 620 and 820.

The magnetic method was employed performing four traverses (Archibald 1-4) in the vicinity of known high yielding boreholes (Arch1 and Arch3). The graphs indicating the magnetic data are shown in Figures C7 to C10.

The magnetic data for traverse Archibald 1 indicates an anomaly from station 35 onwards. This is attributed to the high yielding fracture zone or dissolution cavity into which the high yielding borehole Arch3 is drilled.

The magnetic data for traverse Archibald 2 does not indicate any distinctive anomaly even though the traverse crossed the suspected strike direction of the fracture zone at

borehole Arch3. It is believed that this is due to the artificial influence from the pipeline and power cable for borehole Arch3.

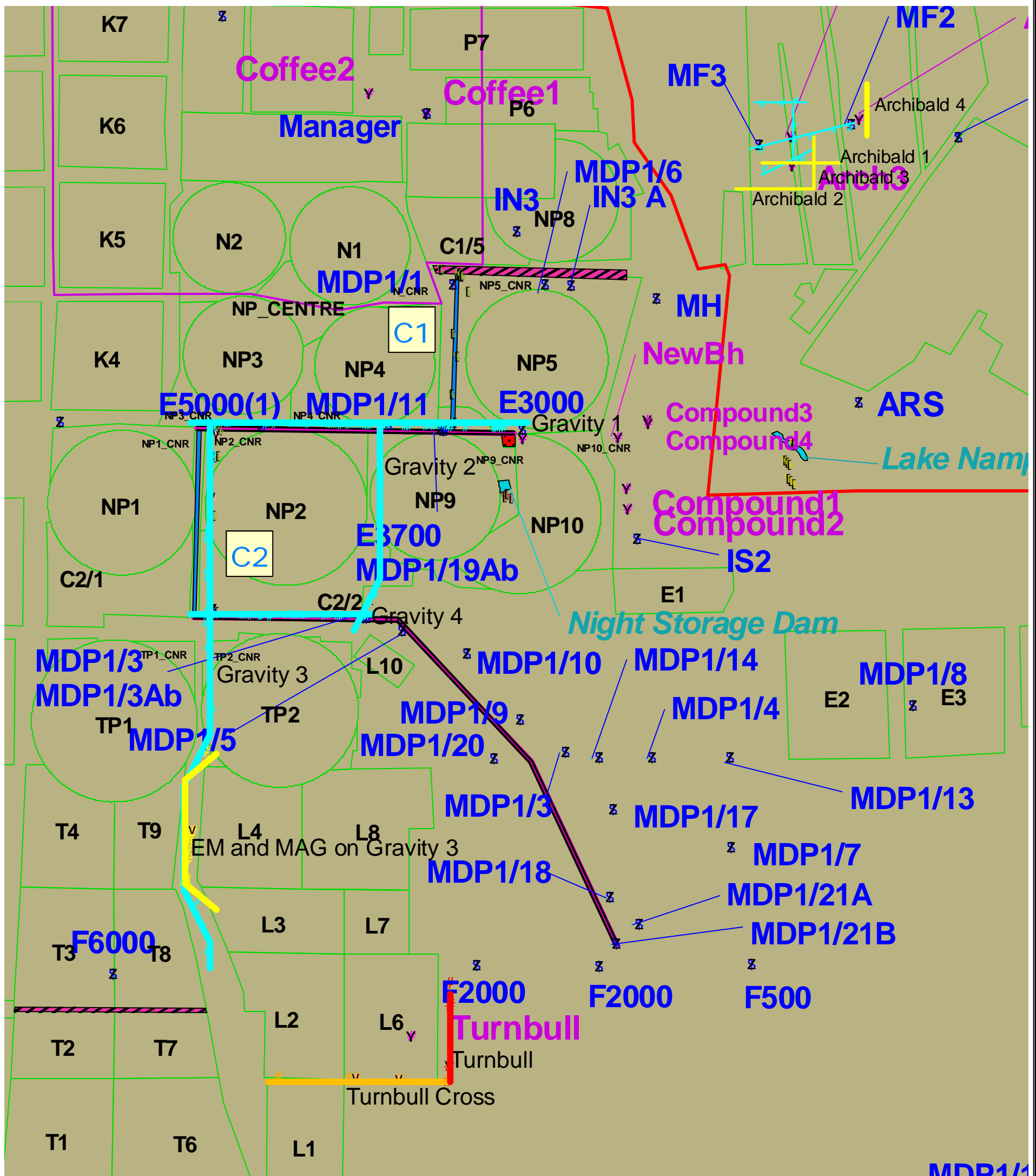
The magnetic data for traverse Archibald 1 indicates an anomaly between stations 5 and 45. This is attributed to the high yielding fracture zone or solution cavity into which the high yielding borehole Arch3 is drilled.

The magnetic data for traverse Archibald 4 indicates an anomaly between stations 20 and 50. The anomaly is attributed to the fracture zone or solution cavity into which borehole Arch1 is drilled.

The anomalies in Traverses Archibald 1, Archibald 3, and Archibald 4 together with boreholes Arch1 and Arch3 form a lineation. It is assumed that the two boreholes are situated on the same fracture zone or solution cavity.

Figure 2.9.3.1: Geophysical Traverse Positions at Mpongwe (2004 Investigation).

Geophysical Traverse Positions at Mpongwe (2004 Investigation)



LEGEND:

v	Boreholes drilled 2004	z	Gravity Stations	⊞	Pumps in Night Storage Dam	Farm_boundaries.shp	○	Field boundaries	⊞	Schist (undifferentiated)	
Traverses_geophysics.dbf		z	Boreholes 1982 & 1994 reports	~	Pipes (hand drawn)	○	Mpongwe Arable Region	Geology.shp	⊞	Schist Inlier	
#	Traverse1	Y	Boreholes not in reports - GPS by GCS Nov2003	~	Existing Canals	▨	Airstrips	○	Dolomite	○	Shale, Sandstone
+	Traverse2	⊞	Pumps in C1 & C2 Canals	⊞	Dams	⊞	Buildings	○	Quartzite		
+	Traverse3	⊞	Pumps at Nampamba Lake			○	Coffee Boundary	○	Schist		

Figure No: 2.9.3.1



M.Sc Study - M. Prinsloo
Characterisation of the Dolomitic Aquifer
in the Copperbelt Province, Northern Zambia

Chapter 2.9.4 : Geophysical Survey Discussion and Conclusions.

During the 2004 geophysical investigation the gravity, electromagnetic and magnetic methods were used. The effectiveness and applicability of these methods are evaluated from the data collected during the surveys.

As stated above, the gravity survey was conducted first. A total of four traverses were performed at a 30m station spacing. Due to the first two boreholes being drilled on targets identified by the gravity method, it was decided to perform an electromagnetic and magnetic survey in an attempt to confirm the drilling targets indicated by the gravity survey.

Traditionally, the gravity method is considered to be the most effective way of identifying possible borehole positions in dolomitic terrain because it is capable of detecting the small changes in the earth's gravitational field due to the presence of sub-surface solution cavities that cause sub-surface density variations. These variations can be identified at depths of 100m or more. The solution cavities are usually indicated by areas of relatively low gravity values due to the reduced underlying rock mass.

However, it is the opinion of the author that the gravity method proved to be ineffective as a singular means of identifying high yielding zones within the geology in the study area. This conclusion is based on the evidence that the schist that occurs in the area appears to possess an almost equal gravitational force to the karstic (solution cavity) dolomitic geology. This equal gravitational force is shown on gravity Traverse 3 (refer to Figure 2.9.4.1).

The figure indicates two areas of gravity low, with approximately equal values. These are:

- Between 0 and 1 000m
- Between 3 150 and 4 170m.

A zone of relative gravity high separates the two areas of gravity low. Prior to the drilling of boreholes GCS1 and GCS2, it was argued that both areas of gravity low indicated high yielding karstic dolomitic aquifers.

However, when drilling began, it soon became apparent that the gravity low between 0 and 1 000m represents the contact zone between schist and the dolomite. The borehole log for borehole GCS1 (drilled at station 90) indicates a schist lens between 61 and 64m in depth within the dolomite, and metamorphosed schist from 72m downwards. Borehole GCS2 (drilled at station 780) indicates extensive weathering, with some limestone between 40 and 55m depth, as well as clay. Please refer to the borehole logs of boreholes GCS1 and GCS2 in Appendix A for a graphic display of the boreholes. It is believed that the schist dips sharply from GCS1 towards GCS2, and therefore this borehole is too shallow (only 60m) to have intersected any schist if it is present in this area.

The weathering profile in these boreholes also extends deeper than the average of 10 to 20m in other areas. This is possibly due to the contact between the dolomite and schist, facilitating weathering by acting as a preferential pathway for groundwater movement.

The gravity low between 3 150 and 4 170m is caused by karstification. Boreholes GCS7 and GCS8 have been drilled at stations 3 180 and 4 080 respectively. Unfortunately, no detail logs are available for these boreholes. These boreholes reportedly intersected extensive fracturing during drilling and subsequent aquifer tests performed on the boreholes revealed extremely high transmissivities and sustainable yields. This point is discussed in more detail in Chapter 3.4.

No boreholes have been drilled into the area of gravity high between stations 1 110 and 2 490. It is however believed that the dolomite becomes more competent and less weathered in this area. It is expected that boreholes drilled within this area will be relatively low yielding due to less fractures and less solution of the dolomite than in the area between stations 3 150 and 4 170.

The gravity data indicates areas where smaller fracture zones and/or lesser weathering occur. Examples of these on Traverse 3 are:

- Between stations 1 350 and 1 500
- Between stations 1 560 and 1 710
- Between stations 2 250 and 2 490

It is believed that boreholes drilled into these areas would be relatively low yielding due to the lesser development of fractures and/or weathering zones.

This example highlights the importance of detailed knowledge of the geology of the study area. The extent of the dolomitic aquifer and the locality of schist inliers must be known when scientifically siting boreholes. Once the dolomitic aquifer has been delineated, the gravity method is capable of distinguishing between potentially low and high yielding zones within the dolomite.

In order to validate the gravity survey, the electromagnetic and magnetic surveys were first performed along a section of gravity Traverse 3. The correlation between the different methods are shown in the Figures below:

- Gravity vs. electromagnetic method (Figure 2.9.4.2)
- Gravity vs. magnetic method (Figure 2.9.4.3)
- Electromagnetic vs. magnetic method (Figure 2.9.4.4)

The figures indicate a marked correlation between the point of gravity low at Station 3 180 and anomalies in the EM34-3 and magnetometer data in this area.

As discussed above, the gravity data indicated a gravity low in this area, and borehole GCS7 has been drilled at station 3 180.

The electromagnetic data indicates a sharp anomaly between stations 3 050 and 3 250 in the vertical dipole mode, and also in the available data for the horizontal dipole mode.

The horizontal dipole measurements could not be recorded accurately at all the stations due to erratic fluctuation in the measurements. It is the opinion of the author that these fluctuations can be attributed to three factors:

- The shallow sub-surface ferricreaceous material that occurs in the area. The ferricreaceous material is high in iron content. This influences the electric current and artificial magnetic field induced by the electromagnetic method. Due to the highly conductive nature of this material, the electric current and induced magnetic field mainly travels along this layer.

The 40m coil separation was used in an effort to obtain the deepest possible penetration. Using the 40m coil separation yields a maximum theoretical penetration depth of 20m in the horizontal dipole configuration and 60m in the vertical dipole configuration.

This is the maximum spacing that can be used with the EM34-3 data. The longer the station spacing, the higher the interference by external factors, especially on the horizontal dipole measurements. If a shorter coil separation, for example 20m, was used the interference and fluctuations would probably have been less, however, depth of penetration would have been halved to 10m in the horizontal dipole configuration and 30m in the vertical dipole configuration. As stated earlier, the main water bearing features are situated between 30 and 50m, and they would therefore not have been recorded using a 20m-coil separation.

- The change in lithology over short distances, as observed by Macdonald and Partners Ltd. in 1982 (refer to Chapter 2.9.2). Macdonald and Partners Ltd. experienced difficulties fitting the obtained resistivity to the calibration curves to obtain depth to bedrock. They were of the opinion that a possible reason for this could be the changes in lithology over short distances, as was evident from the borehole logs drilled during the 1981 investigation.

These changes in lithology would definitely have an effect on the obtained measurements. It is also the opinion of the author that such changes would in addition influence the vertical dipole configuration.

It is the opinion of the author that the fluctuations in the horizontal dipole configuration are best explained by the ferricreaceous nature of the shallow sub-surface soil. The ferricrete can be observed on the surface and also from the drilling logs.

The magnetic method indicates a large anomaly between stations 3 045 and 3 200. This is accompanied by what appears to be possibly two sympathetic anomalies between stations 3 200 and 3 385.

The magnetic method presents some relatively erratic data, with fluctuations in the order of 20 to 50nT being common. This could also be attributed to the ferricreaceous nature of the shallow sub-surface soil.

The electromagnetic and magnetic methods have also been used in other areas where the gravity method was not used (refer to Traverses “Turnbull” and “Turnbull Cross” in Chapter 2.9.3). Boreholes drilled on sites identified using the two methods have been relatively successful with three out of five holes drilled yielding large volumes of water (50 to 100l/s). The sustainable yields for these boreholes are discussed in Chapter 3.4.

Borehole GCS6 was drilled at station 380 on Traverse “Turnbull Cross”. From aquifer test data, the transmissivity of this borehole was calculated to be 6 900m²/day. This is the highest transmissivity of all the boreholes drilled in the study area since 1978. Using the FC method, the sustainable yield of this borehole is estimated to be approximately 100l/s.

The conclusion for this particular study area, where the main water bearing features are located between 30 and 50mbgl, is that the electromagnetic and magnetic methods can be employed with a relatively high success rate.

The electromagnetic and magnetic methods have not been tested against distinguishing between the schist and dolomite and, therefore, no conclusion on this aspect can be reached.

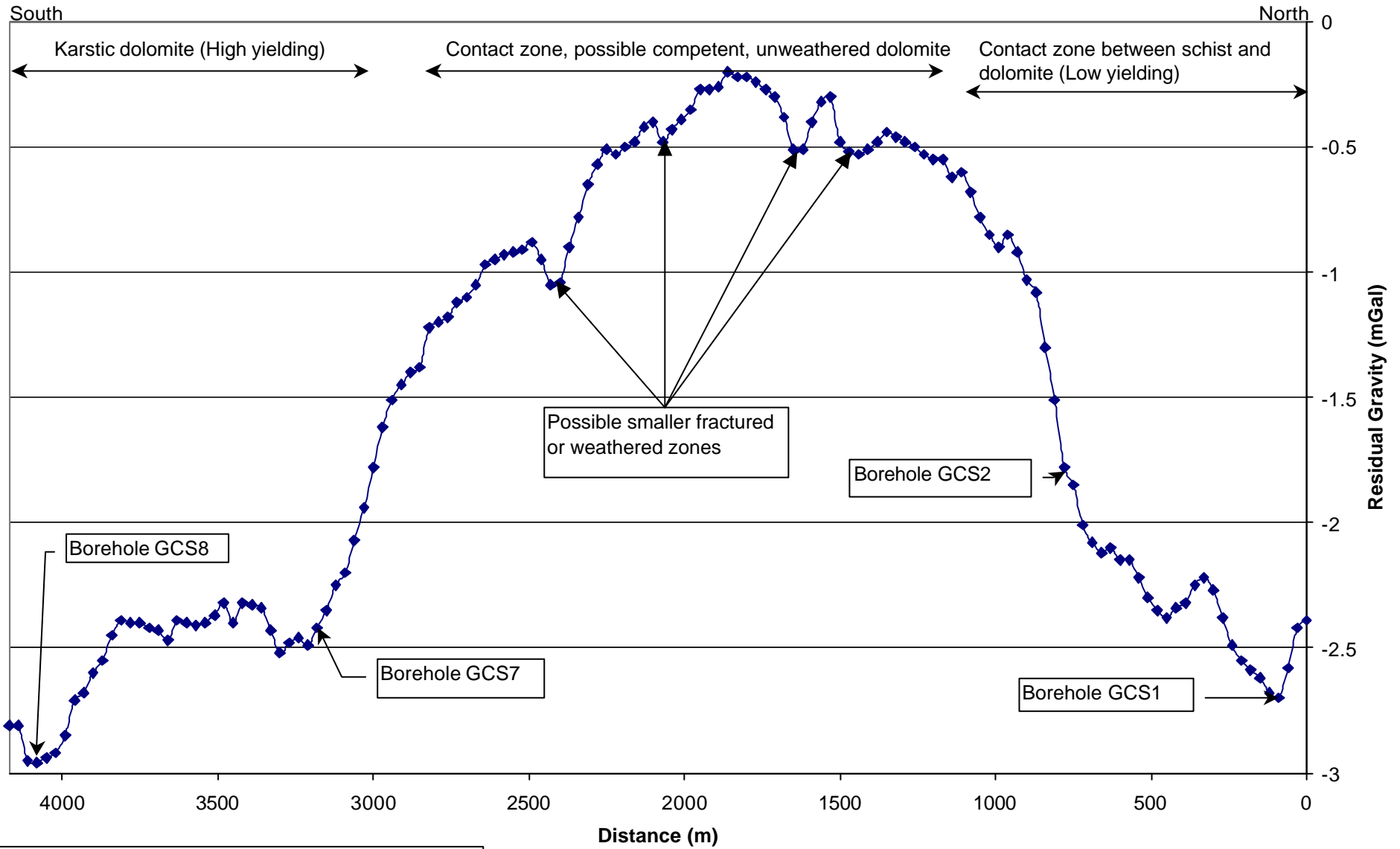
The 1979 and 1982 geophysical investigations conclude that the resistivity methods suffer from the same limitations as the gravity survey of 2004 revealed, namely, that the

investigations are not able to distinguish between the water bearing dolomitic areas and the surrounding lower yielding lithologies.

It is concluded that the geophysical methods are unable to distinguish between high yielding and lower yielding lithologies. However, once high yielding lithologies have been identified, any of the geophysical methods are able to determine the positions of fracture zones and solution cavities associated with high yielding boreholes.

Figure 2.9.4.1: Gravity Survey - Traverse 3.

Gravity Survey - Traverse 3



The graph indicate the gravity values recorded along Traverse 3

Figure 2.9.4.2: Gravity vs. Electromagnetic Method.

Gravity vs. Electromagnetic Method

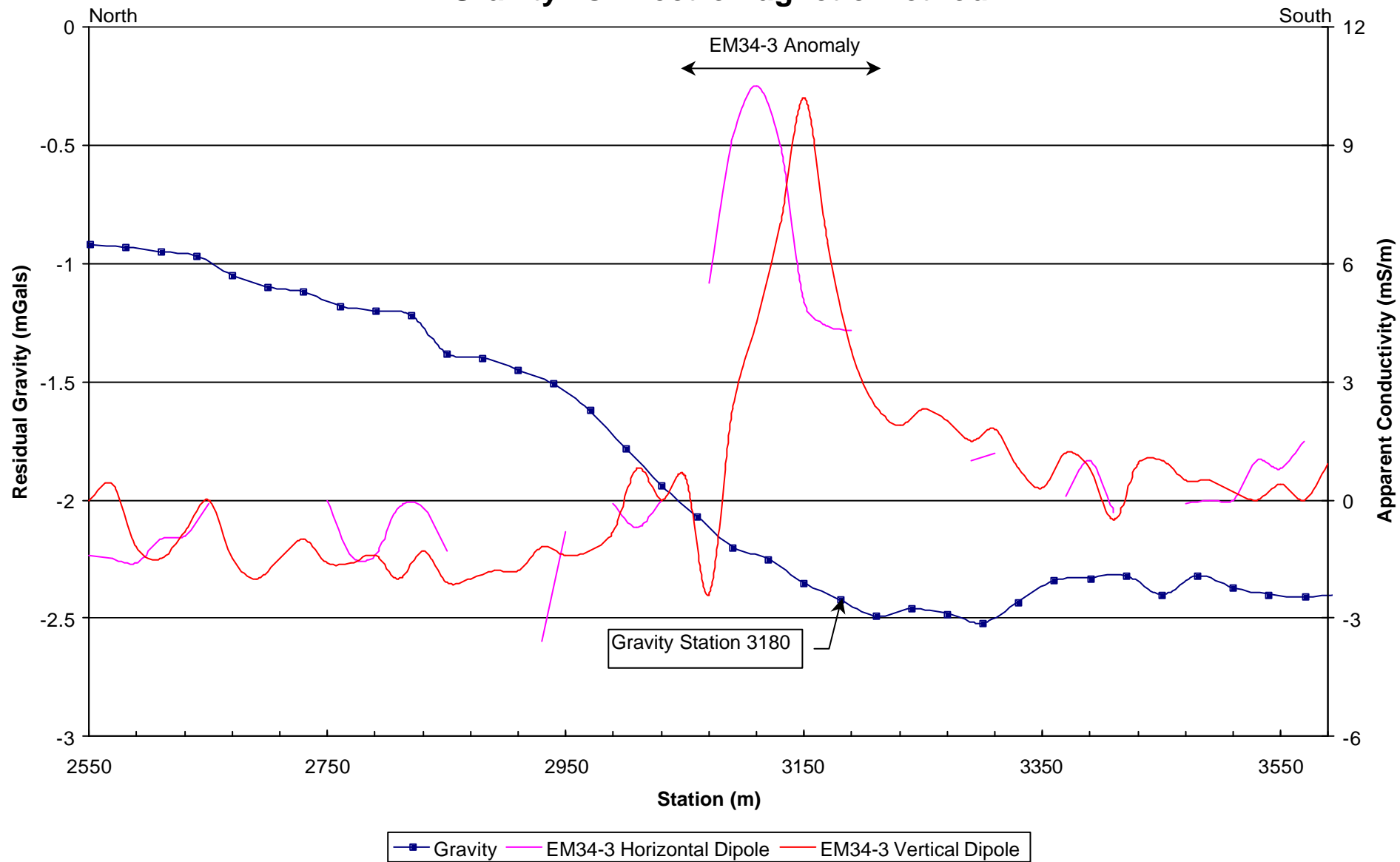


Figure 2.9.4.3: Gravity vs. Magnetic Method.

Gravity vs. Magnetic Method

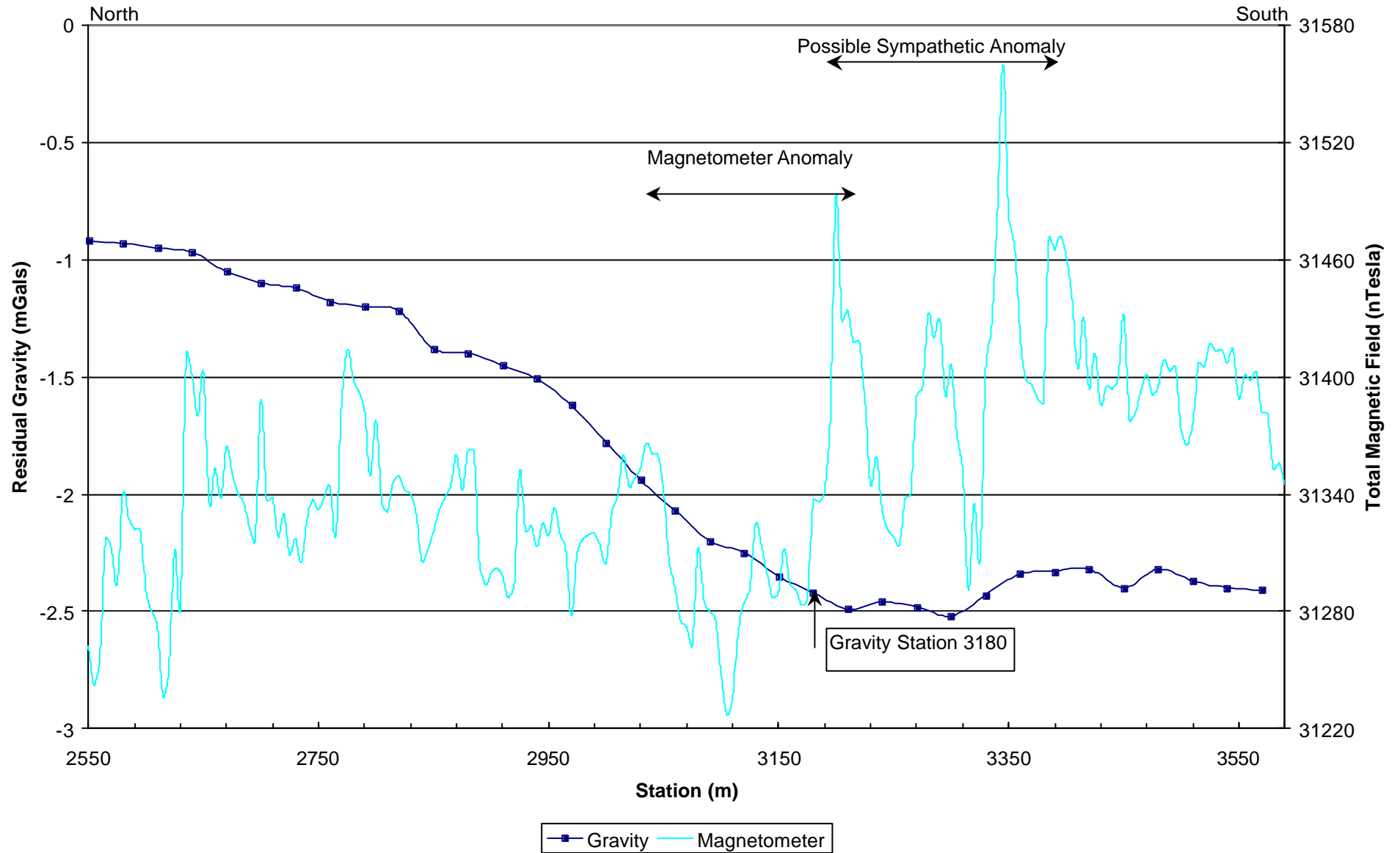
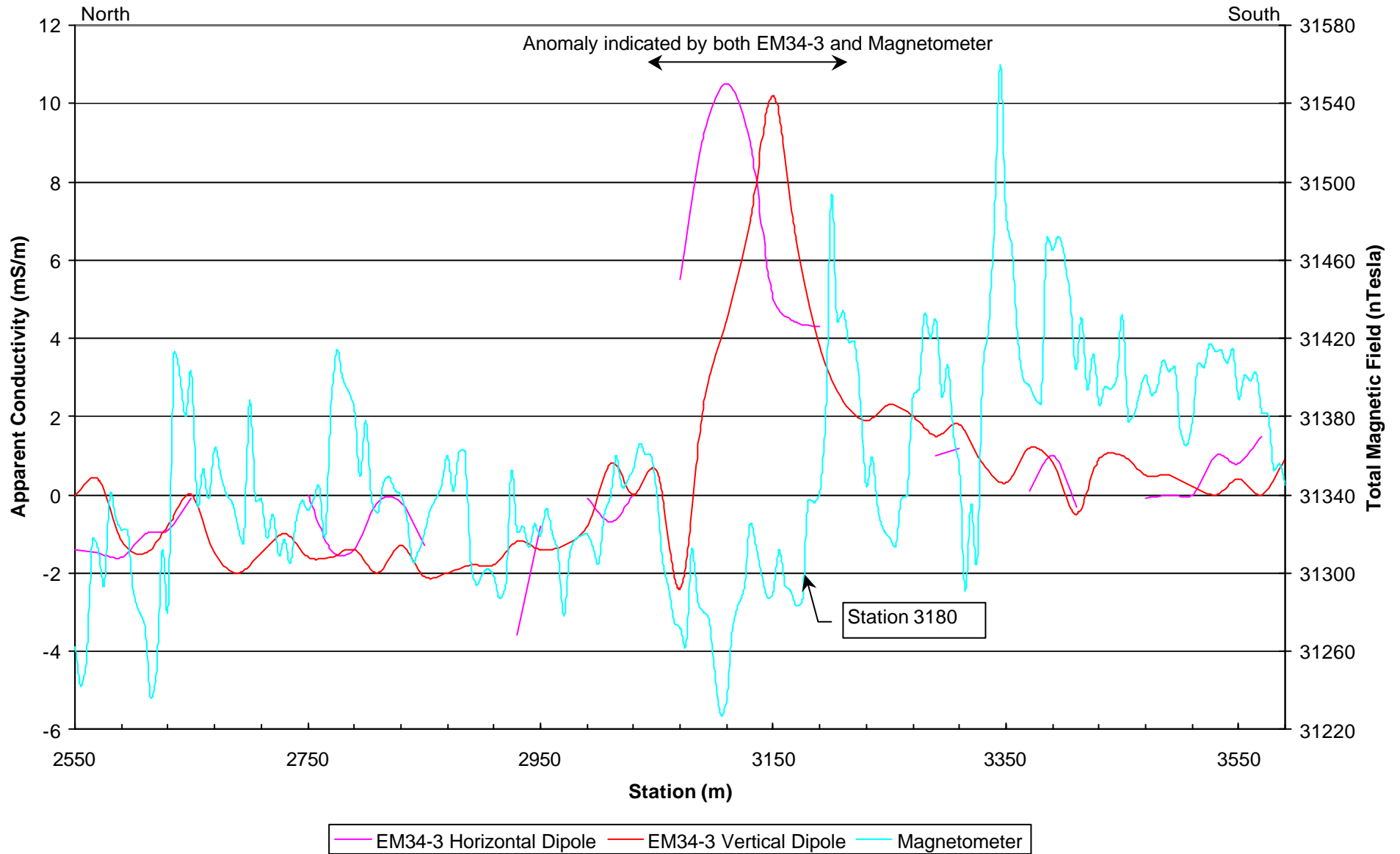


Figure 2.9.4.4: Electromagnetic vs. Magnetic Method.

Electromagnetic vs. Magnetic Method



Chapter 2.10 : Borehole Geophysical Investigations.

Geophysical logging of boreholes MDP1 to MDP21A as well as E3700 and IN3A was performed in 1982 (Macdonald and Partners Ltd.). The acquired logs are included as Appendix A. The purpose of this investigation was to supplement borehole information recorded during the drilling of these boreholes. From this information, a better understanding of the rock types and depth of fissure zones could be obtained.

A Mount Sopris model 1 000C battery powered logger was used (Macdonald and Partners Ltd., 1982). Three different logs were obtained:

- 1 Natural Gamma: This measures the concentration of radioactive potassium in the geology. As potassium is present in clays and their metamorphosed derivatives, the log distinguishes crystalline limestone and dolomite from mudstone, shale, schist and more argillaceous carbonaceous rocks.
- 2 Single Point Resistance: This measures electrical resistivity between an electrode in the borehole and the surface. In general, resistance increases with grain size and decreases with borehole diameter, density of water bearing fractures, and increasing dissolved solids concentration of borehole fluid. As with resistivity measurements, rock types can be disguised using this log and large water bearing fracture zones identified.
- 3 Spontaneous Potential: This is generally used where drilling mud has been introduced into the borehole. It measures the difference in natural voltage between the probe and a surface grounded electrode. This method is sensitive to pore water chemistry, which is greatly influenced by the lithology of the sub-surface. Generally, coarser grained sandy units induce a positive voltage difference while fine-grained clay units induce a negative potential. It can be used to indicate the positions of bedrock boundaries.

Single point resistance and spontaneous potential data collection is limited to fluid filled open boreholes.

Gamma logs for boreholes penetrating pure crystalline limestone and calcareous sandstone show a lack of gamma activity. The overburden-bedrock contact can be easily identified from the large change in natural gamma.

Spontaneous potential and single point resistance both indicate a high degree of fluctuation. This is possibly due to the variation in geology at many of the boreholes. The high resistance encountered in several of the boreholes prevented continuous logging of the point resistance log.

However, it can be stated that single point resistance logs do correspond well with the fracture zones and solution cavities indicated by the drilling logs.

In several of the boreholes the spontaneous potential (SP) and single point resistance (SPR) could not be recorded continuously due to the parameters being too high for the logger to record. This explains the discontinuous data in boreholes such as MDP5 (SPR), MDP7 (SPR), MDP8 (SPR), MDP10 (SPR) etc.

Other techniques that might be considered in the down-the-hole logging of boreholes include the use of calliper, fluid resistivity, fluid temperature and water flow logs. These methods are effective in characterising the aquifer and determining water strike depths and the direction and rate of groundwater movement. Each of these methods is discussed briefly below. Mention is made of the principle on which each method is based and the recorded parameters used.

Calliper logs provide a continuous record of average borehole diameter, which is related to fractures, dissolution zones or cavities, lithology and drilling technique. Calliper logs can be used to identify fractures and water bearing openings such as solution cavities in the dolomite. Correlation of calliper logs with fluid resistivity and fluid temperature logs are used to identify water producing and water receiving fractures or zones.

Fluid temperature logs provide a continuous record of the temperature of the fluid in the borehole. Fluid temperature logs can be used to identify the water producing cavities and fracture zones. They can also be used to determine intervals of vertical borehole flow. Solution cavities and fracture zones will be identified by intervals of sharp changes

in temperature. A small or no temperature gradient identifies areas of vertical borehole flow.

Fluid resistivity logs measure the electrical resistance of fluid in a borehole. Resistance is the reciprocal of fluid conductivity, and fluid resistivity logs reflect the changes in the dissolved solids concentration of the borehole fluid.

The direction and rate of water movement within a borehole can be measured using a high-resolution heat pulse flow meter. The heat pulse flow meter operates by diverting nearly all the flow to the centre of the tool where a heating grid slightly heats a thin zone of water. If vertical borehole flow occurs, the water moves up or down the borehole to one of two sensitive thermistors (heat sensors). When a peak temperature is recorded by one of the thermistors, a measurement of direction and rate is calculated.

By determining the flow rate and direction of flow of the water in the borehole, fracture zones and solution cavities can be identified.

Chapter 3 : Hydrogeology.

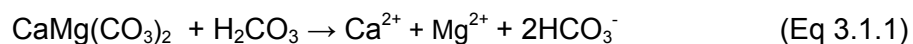
Chapter 3.1 : General Hydrogeology.

Several previous studies have described the hydrogeology of the area. These studies include those performed by Landell Mills Associates (1978, 1979, 1980, 1982), Macdonald and Partners Ltd. (1982), Rankin Engineering Consultants (1994, 1997), Scott Wilson Piésold (2003), and WLP U Consultants (1983). The information collected during these studies has been incorporated into the conclusions reached during the 2004 investigation.

Two hydrogeological cross sections with groundwater levels are shown in Figures 2.7.2 and 2.7.3. A north-south cross section (Figure 2.7.2) was drawn between boreholes A3000 and MDP16. The groundwater level and gradient is influenced by the presence of the schist inlier.

The dolomitic lithology is susceptible to chemical weathering and subsequent karstification or formation of solution cavities. The solution cavities have exceptionally high transmissivities and large volumes of water can be stored in the cavities when they are developed below the regional groundwater level.

The chemical weathering of the dolomitic geology develops according to the following reactions:



A simplified representation of the chemical weathering processes involved in dolomite is shown in Figure 3.1.1.

It is unclear to what extent the solution cavities are interconnected. However, based on the high sustainable yields of the boreholes, it is the opinion of the author that an extensive and well connected network of solution cavities exists in the area. This presumption is supported by the relatively shallow drawdown compared to the high abstraction rate for Lake Nampamba.

Figure 3.1.1: Chemical Weathering in Dolomite.

Chemical Weathering in Dolomite

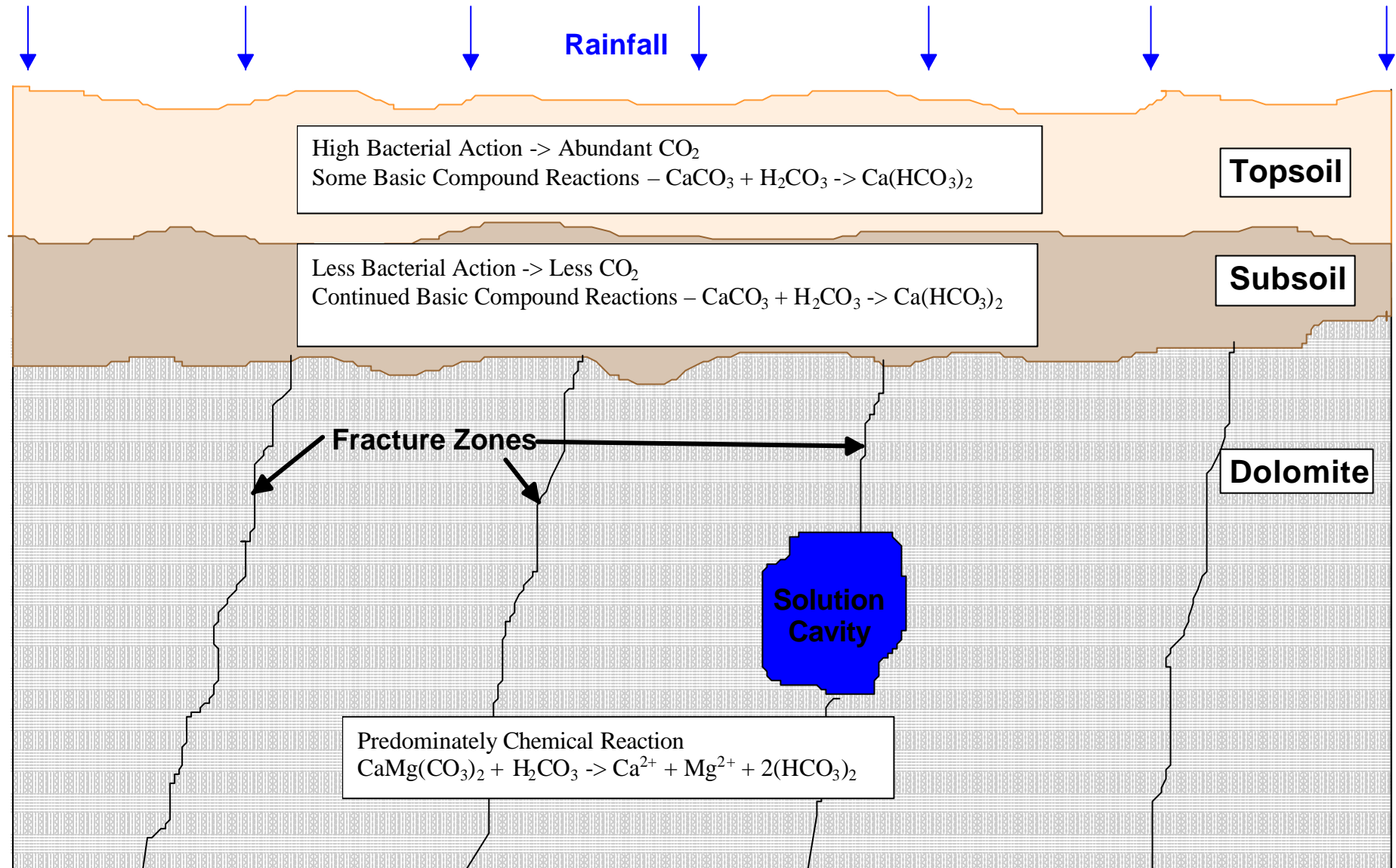


Figure No: 3.1.1

February 2005

It is considered that the solution cavities generally strike in a south-southeast to north-northwest direction, as indicated in Figure 2.7.1. This strike direction corresponds to that of the major joint set (refer to Chapter 2.7). This considered strike direction is supported by the detail resistivity investigations conducted during 1979 and 1982, the short gravity, electromagnetic and magnetic surveys conducted during 2004 (refer to Chapter 2.9 for the discussion on the surface geophysical investigation), the major strike direction of joint patterns in the dolomite, the strike and shape of Lake Nampamba and the observed surface fracturing and solution features close to Lake Nampamba (refer to Chapter 2.7 for the discussion on the geology) as well as the suggestion which has been made by several authors that Lake Nampamba is hydraulically connected to the Kafue River to the north.

No detailed water level monitoring data from the production boreholes is available. Definite differentiation between the water levels in closely spaced boreholes indicates the presence of small-scale compartmentalization in the dolomite. This is often a problem in dolomitic areas and limits the long-term sustainable abstraction from an aquifer. However, based on the high sustainable yields and long-term sustainability of the boreholes and Lake Nampamba, it is concluded that no small-scale compartmentalisation occurs in the area. This conclusion is further supported by the fact that both the geological data obtained from the latest mapping and the borehole logs show no indication of intrusive material.

The influence of compartmentalisation by dolerite intrusions in South African dolomitic aquifers has been extensively investigated by the South African Department of Water Affairs and Forestry (van Dyk, (1993 & 1997), Janse v Rensburg *et al.* (1987) and Lynch and Hodgson (1987)).

Three prominent karstic features occur in the study area. These are Lake Nampamba, Lake Kashiba and the “Chibili pavement”. Lake Nampamba and Lake Kashiba are well known features in the area and are considered to be collapse structures in the dolomite. The depth of both the lakes is unknown, but reportedly, both lakes are deeper than 100m. These lakes represent “windows” into the aquifer where direct abstraction of groundwater can be undertaken.

The position of Lake Nampamba is indicated in Figure 3.4.1. Lake Kashiba is situated approximately 20km northwest of Lake Nampamba, and due to the distance, the locality is not shown on any of the maps. Reportedly, the “Chibili pavement” is located directly south of Chambatata Farm. However, the author never visited this feature and the exact location is uncertain. Figures 3.1.2 and 3.1.3 show photographs of Lake Nampamba and Lake Kashiba respectively.

The boreholes drilled at Mpongwe are less than 100m deep. As far as could be established the deepest production borehole is MDP4. This borehole was drilled to a completed depth of 93.3m. This raises the question whether an even larger water source exists at depth, which has not been intersected or exploited by the boreholes.

The deepest recorded borehole is A12500 at 100m. Unfortunately, this borehole is located in unweathered schist and therefore gives no indication of dolomitic conditions at this depth.

The “Chibili pavement” was not visited during the 2003 site visit. However, it reportedly has several shallow passages and rectangular joints open to the surface. Sub-surface water movement can be heard (Scott Wilson Piésold, 2003).

It has been suggested by various authors that the Mpongwe karstic features (Lake Nampamba), Lake Kashiba at St. Anthony’s Mission, the “Chibili pavement” and the Kafue River are all interconnected. Quoted evidence for this assumption includes:

- The groundwater flow gradient is approximately 1:400. Extrapolating this to the Kafue River, the groundwater level coincides with the level of the Kafue River (Scott Wilson Piésold, 2003).
- Low flow volumes in the Kafue River when groundwater base flow contributions dominate suggests that there is an apparent gain of upstream flow at Ndubeni and a corresponding loss downstream. This suggests that the Kafue River may be fed by the Mpongwe groundwater system above Ndubeni. The river recharges the groundwater system below Ndubeni. This stretch of the river coincides with the area of connection and possibly karstic connection north of Lake Kashiba between the Mpongwe limestone and Lake Kashiba (Scott Wilson Piésold, 2003).

-
- Rankin Engineering Consultants (1997) states that it is clear that the Northern Zone of Ipumbu Farm is connected to the St. Anthony Aquifer. The Central Zone may be connected to the Ipumbu Aquifer. The possibility that the Ipumbu and St. Anthony's aquifers are connected cannot be ruled out. The evidence on which these conclusions are based is not shown and therefore the author cannot comment on it.

Recharge calculations performed by the author during the 2004 study are discussed in Chapter 3.5. The recharge calculations indicate a definite connection between the eastern aquifer that underlies the Mpongwe irrigation area and western aquifer that underlies the Munkumpu irrigation area. This connection is confirmed by the influence of abstraction volumes from the Munkumpu area on the correlation between observed and calculated water levels in Lake Nampamba that is situated in the Mpongwe Area. This subject matter is discussed in more detail in Chapter 3.5.

Interconnectivity of the aquifers indicates that the solution cavities span several sub-catchment areas and are thus not bound by normal hydrogeological boundaries such as catchment water divides and rivers.

Figure 3.1.2: Lake Nampamba.

Lake Nampamba

The photograph shows Lake Nampamba. The lake is a 150m x 30m sinkhole and reportedly more than 100m deep. Lake Nampamba is considered to be a direct reflection of the water level in the Eastern Aquifer. The lake strike north-northwest to south-southeast, following the major joint set striking 160 degrees that occur in the area. Jointing can be clearly seen in the sidewalls of Lake Nampamba. MDC currently have a license to abstract 1000l/s from the lake.



Figure No: 3.1.2

February 2005

Figure 3.1.3: Lake Kashiba.

Lake Kashiba



The Figure show a photograph of Lake Kashiba. The lake is a large square (100m x 100m) sinkhole, and reportedly more than 100m deep. During the rainy season the water level rise and decanting occurs.

Chapter 3.2 : Groundwater Chemistry.

MDC supplied the author with three water samples taken from unidentified boreholes. The water samples were submitted to a SANAS accredited laboratory for chemical analysis. The results of the analysis are summarised below in Table 3.2.1.

The results are compared to the South African Water Quality Guidelines (SAWQG) for Domestic Use. Both the SAWQ target and critical values are listed. Constituents that exceed the guideline values are highlighted.

Table 3.2.1: Chemical Analysis Results.

Constituent	Units	SAWQG – Target Values	SAWQG – Critical Values	Sample H	Sample U	Sample W
pH		6-9	<4 and >11	6.6	6.6	6.4
Conductivity	mS/m	0-70	0-300	71.7	58.9	59.2
Calcium	mg/l	0-32	0-80	86	72	102
Magnesium	mg/l	0-30	0-100	50	40	18.2
Sodium	mg/l	0-100	0-400	0.2	1.2	1.8
Potassium	mg/l	0-50	0-100	<0.1	<0.1	<0.1
Total Alkalinity	mg/l	NG	NG	400	308	312
Bicarbonate	mg/l	NG	NG	488	375	380
Chloride	mg/l	0-100	0-1200	1.0	3.2	2.1
Sulphate	mg/l	0-200	0-400	0.7	1.3	1.7
Nitrate	mg/l	0-6	0-20	3.9	4.6	1.5
Fluoride	mg/l	0-1	0-100	0.2	0.2	0.1
Iron	mg/l	0-0.1	0-10	<0.01	<0.01	<0.01

NG = No Guideline

mS/m = milliSiemens/metre

Exceeds SAWQ Target Guidelines

Exceeds SAWQ Critical Guidelines

Constituents that exceed the SAWQ target guidelines in all three samples are calcium and magnesium. The samples also display elevated bicarbonate concentrations. This is attributed to the dolomitic environment in which the aquifer is situated.

The chemical character of the groundwater is shown in Figure 3.2.1 on a Piper diagram. The figure indicates that the groundwater is relatively recently recharged. This corresponds with the high recharge percentage calculated for the study area (refer to Chapter 3.5). The groundwater displays a calcium-magnesium and bicarbonate-carbonate dominant character. This is expected in dolomitic formations as discussed above.

The pH of the water is lower than would generally be expected for dolomitic terrains. However, it is considered that although the groundwater displays a recently recharged character, ion exchange has occurred in order to enrich the groundwater in calcium and magnesium. Acid rain of relatively low pH that enters the groundwater system will be attenuated by the acid neutralising capacity of the dolomitic geology. During the neutralising process the karstic nature of the dolomite will be enhanced by dissolution of the rock material into the acidic water. Calcium and magnesium will go into solution resulting in elevated concentrations of the constituents. The relatively low pH of the acidic water will be neutralised during this process.

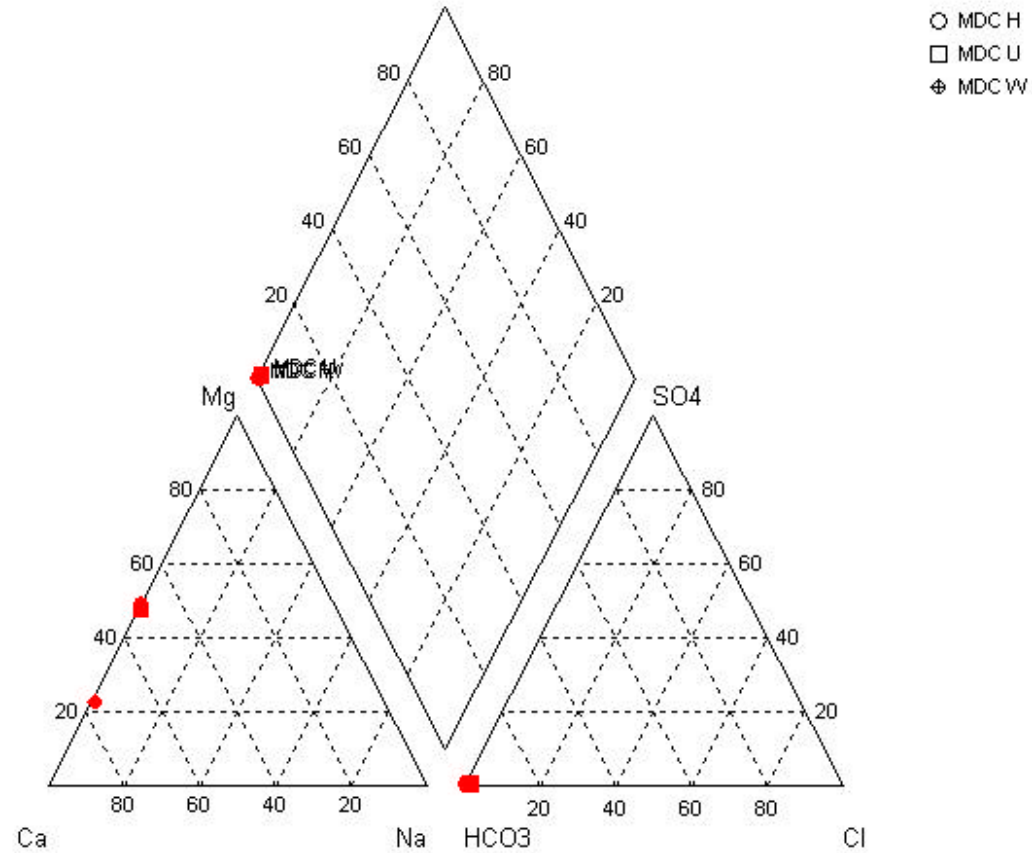
Even though the calcium and magnesium concentrations exceed the target values, it is considered that, from an inorganic perspective, the groundwater is suitable for human consumption. The calcium and magnesium critical values as specified by the SAWQ guidelines are 80mg/l and 100mg/l respectively.

However, at a concentration of 80mg/l calcium has no adverse effect on human health - it only influences the scaling effect in kettles and impairs the lathering of soap.

At a concentration of 100mg/l the taste of the water becomes aesthetically unacceptable. Diarrhoea will occur in most new users of the water.

Figure 3.2.1: Piper Diagram indicating the Groundwater Character.

Piper Diagram Indicating the Groundwater Character



The Figure indicate the piper diagram for the groundwater chemistry. Note that all three samples plot in the extreme left hand corner of the diamond. This indicates that the water was relatively recently recharged.

Chapter 3.3 : Depth to Groundwater.

The depth to groundwater is listed in several of the previous studies. These studies include Landell Mills Associates (1978, 1979, 1980, 1982), Macdonald and Partners Ltd. (1982), Rankin Engineering Consultants (1994, 1997), Scott Wilson Piésold (2003), and WLPU Consultants (1983). The author measured the depth to groundwater during a site visit conducted in November 2003. The results of the 2003 hydrocensus are summarised in Table 3.3.1. Please note that the coordinate system used refers to the WGS84 datum point.

The geometric mean depth to groundwater as determined from the data collected by the author in November 2003 is calculated to be 17.68m.

Lake Nampamba is a sinkhole that reflects the groundwater level in the area. From the Lake Nampamba monitoring data it is evident that the groundwater level in the area declines during the dry season and rebounds during the wet season. Groundwater abstraction volumes for irrigation purposes are six times greater during the dry season than during the wet season. Figure 3.3.1 indicates the relationship between the water level in Lake Nampamba, the calculated recharge from the rainfall and the volume of water abstracted from the eastern dolomitic aquifer for the time period April 1991 to March 2003, as calculated by the author. The recharge calculations are discussed in Chapter 3.5. The abstraction volumes are discussed in detail in Chapters 3.8 and 3.9.

Figure 3.3.1 indicates that while the water level starts recovering immediately after the first rainfall, there exists a one to two month delay between maximum monthly rainfall and maximum groundwater level. This can clearly be seen for each rainy season where maximum monthly rainfall occurs mostly between December and February while the maximum water level is recorded only in March or April.

Following the theory of a large interconnected network of solution cavities, it can be argued that this delay in maximum groundwater level can be attributed to the water having to migrate from an up-gradient recharge point. The water migrates down-gradient as a pulse through the aquifer, causing a seasonally fluctuating water level.

Figure 3.3.1 also indicates that during years of low rainfall, the water level in Lake Nampamba does not rise as high as during years with higher rainfall. An example of this is the rainy seasons of 1993-1994 and 1994-1995. The rainy season of 1993-1994 yielded relatively high rainfall figures and subsequent recharge to the aquifer. This caused the water level to rise to the highest recorded level of approximately 1195mamsl. The rainy season of 1994-1995 produced relatively low rainfall figures and recharge to the aquifer was low. The maximum water level recorded was approximately 1189mamsl. This equates to a difference of 6m in maximum water level.

It is believed that the groundwater fluctuations are a combined result of the natural seasonal fluctuations (the change in recharge from rainfall) and abstraction for irrigation purposes. Additional possible discharges from groundwater to the Kafue River that have an effect on the groundwater level are discussed in Chapter 3.1.

Figure 3.3.2 indicates the typical groundwater contours in the area. Groundwater flow is in a north-north westerly direction. The groundwater flow gradient is in the order of 1:400.

Table 3.3.1: Hydrocensus Results

Borehole No.	X-Coord	Y-Coord	Elevation (mamsl)	Pump	Pump Depth (mbgl)	Static Water Level (mbgl)	Static Water Level (mamsl)	Comment
ARS	118123	-1501135	1207.00	Hand pump	ND	ND	ND	No access.
B6500	112025	-1501261	1241.00	None	N/A	Dry	Dry	Dry borehole, never equipped.
CHAMBATATA1	97324	-1505791	1214.00	None	N/A	Collapsed	Collapsed	The only high yielding borehole in the area. Water level was measured in March 2003 at approximately 17m. Collapsed
CHAMBATATA2	97362	-1505709	1216.00	None	N/A	26.3	1189.7	Earth has collapsed in a 1m radius around borehole.
CHAMBATATA3	96789	-1505623	1222.00	None	N/A	20.2	1201.8	Never equipped.
CHAMBATATA4	96638	-1505290	1222.00	None	N/A	Dry	Dry	Set of 3 boreholes 10m apart.
CHAMBATATA5	96857	-1502382	1204.00	None	N/A	Collapsed	Collapsed	Borehole damaged. Will have to be rehabilitated.
CHAMBATATA6	96878	-1501896	1214.00	None	N/A	Sealed	Sealed	No access.
CHAMBATATA7	102316	-1507477	1225.00	Submersible	ND	Sealed	Sealed	Used for domestic purposes – Chambatata compound.
COFFEE1	114842	-1498863	1216.00	Submersible	ND	Sealed	Sealed	Domestic water for the general manager. 20 000l reservoir, 4 or 5-inch pipe.
COFFEE2	114398	-1498704	1213.00	Submersible	ND	Sealed	Sealed	4-inch distribution pipe. Domestic use.
COFFEE3	114565	-1497995	1216.00	None	N/A	19.6	1196.4	No pump, new borehole, never used.
COFFEE4	116292	-1501394	1201.00	None	N/A	15.15	1185.85	Never equipped.
COMPOUND1	116354	-1501797	1210.00	None	N/A	16.19	1193.81	Low yielding borehole. Dry in winter, water level in winter reportedly lower than 30mbgl.
COMPOUND2	116358	-1501958	1218.00	None	N/A	16.97	1201.03	Pump removed to pump test Coffee 4, but was broken in process. Head of borehole is situated in a cement pit sunk 1mbgl. Dry in winter.
COMPOUND3	116515	-1501265	1207.00	None	N/A	13.07	1193.93	Was used for compound, pump removed 3 years ago. Cement pit sunk 1mbgl.
COMPOUND4	116519	-1501288	1200.00	Submersible	ND	Sealed	Sealed	4-inch distribution pipes, no electricity, no flow meter.

mamsl = metres above mean sea level

mbgl = metres below ground level

ND = No Data

N/A = Not Applicable

All coordinates shown are in WGS84 format.

Table 3.3.1: Hydrocensus Results (Continued)

Borehole	X-Coord	Y-Coord	Elevation (mamsl)	Pump	Pump Depth (mbgl)	Static Water Level (mbgl)	Static Water Level (mamsl)	Comment
E3000	115557	-1501336	1220.00	None	N/A	Dry	Dry	Dry borehole. Never equipped.
E3700	114951	-1501344	1217.00	None	N/A	20.49	1196.51	Borehole collapsed. Equipment removed.
E5000	113559	-1501299	1222.00	None	N/A	Collapsed	Collapsed	Never equipped.
IN3A	115521	-1499788	1210.00	Submersible	29m	Pumping	Pumping	Pump from MDP21.
MDP2	115931	-1503802	1206.60	Submersible	39m	17.22	1189.38	Production borehole.
MDP3	114330	-1502801	1212.70	Submersible	32.5m	ND	ND	Production borehole.
MDP10	115031	-1503101	1206.58	None	N/A	ND	ND	Never equipped. Reportedly high yielding borehole.
MDP12	113130	-1502701	1227.60	None	N/A	Collapsed	Collapsed	Never equipped.
MDP18	116331	-1504902	1210.09	None	Was 24m	11.49	1198.6	Pump removed in September 2003 for repairs.
MDP21	116431	-1505202	1210.10	None	Was 29m	13.94	1196.16	Pump removed to IN3A, 8 November 2003.
MDP1900	114931	-1501321	1214.25	None	N/A	20.49	1193.76	Borehole collapsed, pump removed.
MF1 (Arch6)	118897	-1499065	1208	None	N/A	Sealed	Sealed	Never equipped.
MF2 (Arch5)	118074	-1498961	1216	Submersible	ND	Sealed	Sealed	Used to be a windpump. Currently pumps at 7l/s.
MF3 (Arch2)	117376	-1499120	1207	Submersible	42m	Pumping	Pumping	Pumped at 11l/s. Earth collapsing around the borehole.
Arch1	117622	-1499053	1208	Submersible	39m	Pumping	Pumping	Pumped at 10l/s
Arch3	117633	-1499284	1208	Submersible	30m	Pumping	Pumping	Pumped at 45l/s. Cavity 49-52.5m depth.
Arch4	118147	-1498919	1200	None	N/A	23.55	1176.45	Never equipped.
MH	116588	-1500319	1211	None	N/A	Collapsed	Collapsed	Never equipped.
OFFICE BH	115559	-1501407	1213	None	N/A	Collapsed	Collapsed	Collapsed at 7m.
TURNBULL	114695	-1506064	1220	Submersible	34m	Sealed	Sealed	Provided domestic water.

mamsl = metres above mean sea level

mbgl = metres below ground level

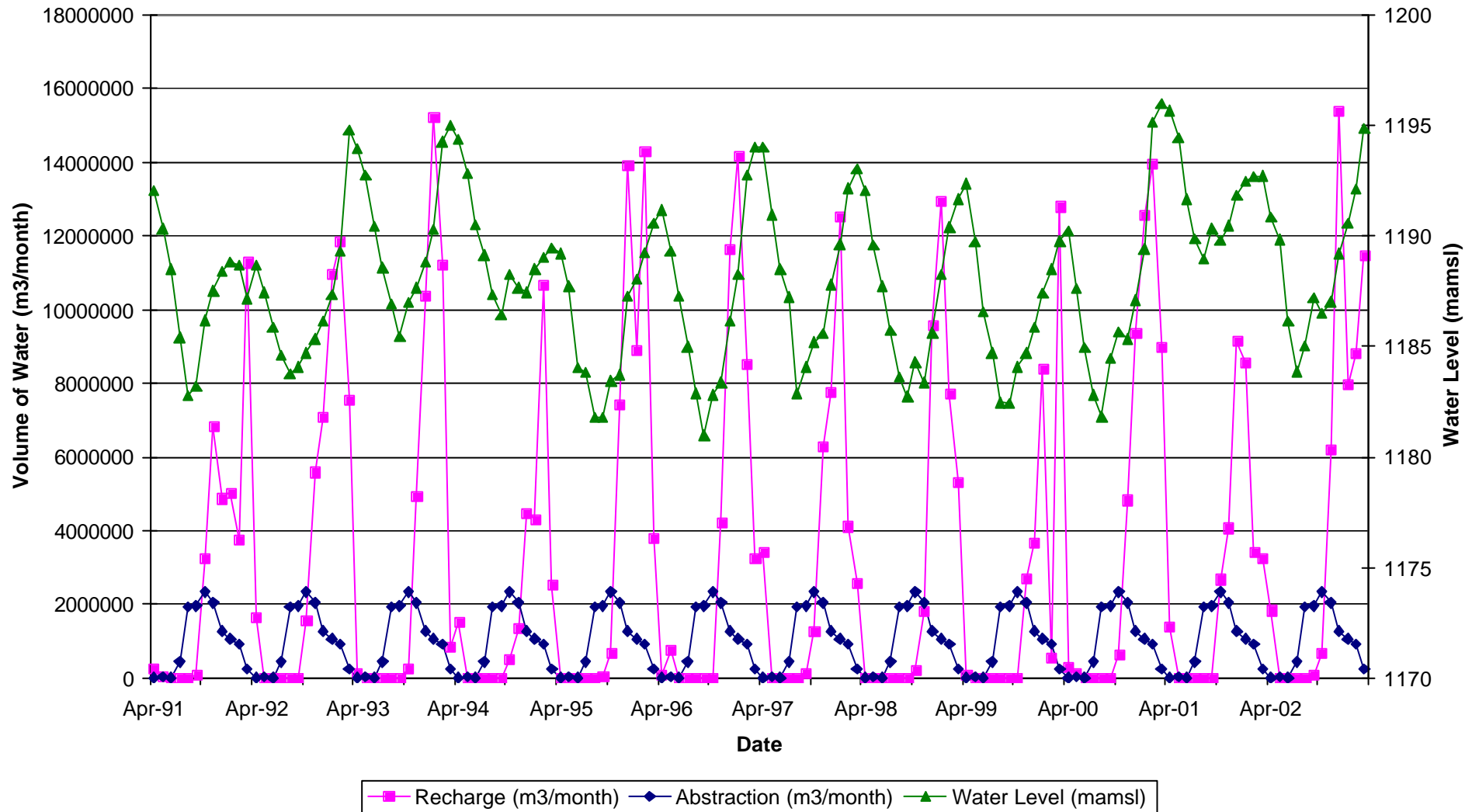
ND = No Data

N/A – Not Applicable

All coordinates shown are in WGS84 format.

Figure 3.3.1: The Relationship between Water Level, Recharge and Abstraction Volumes for Lake Nampamba (Eastern Aquifer).

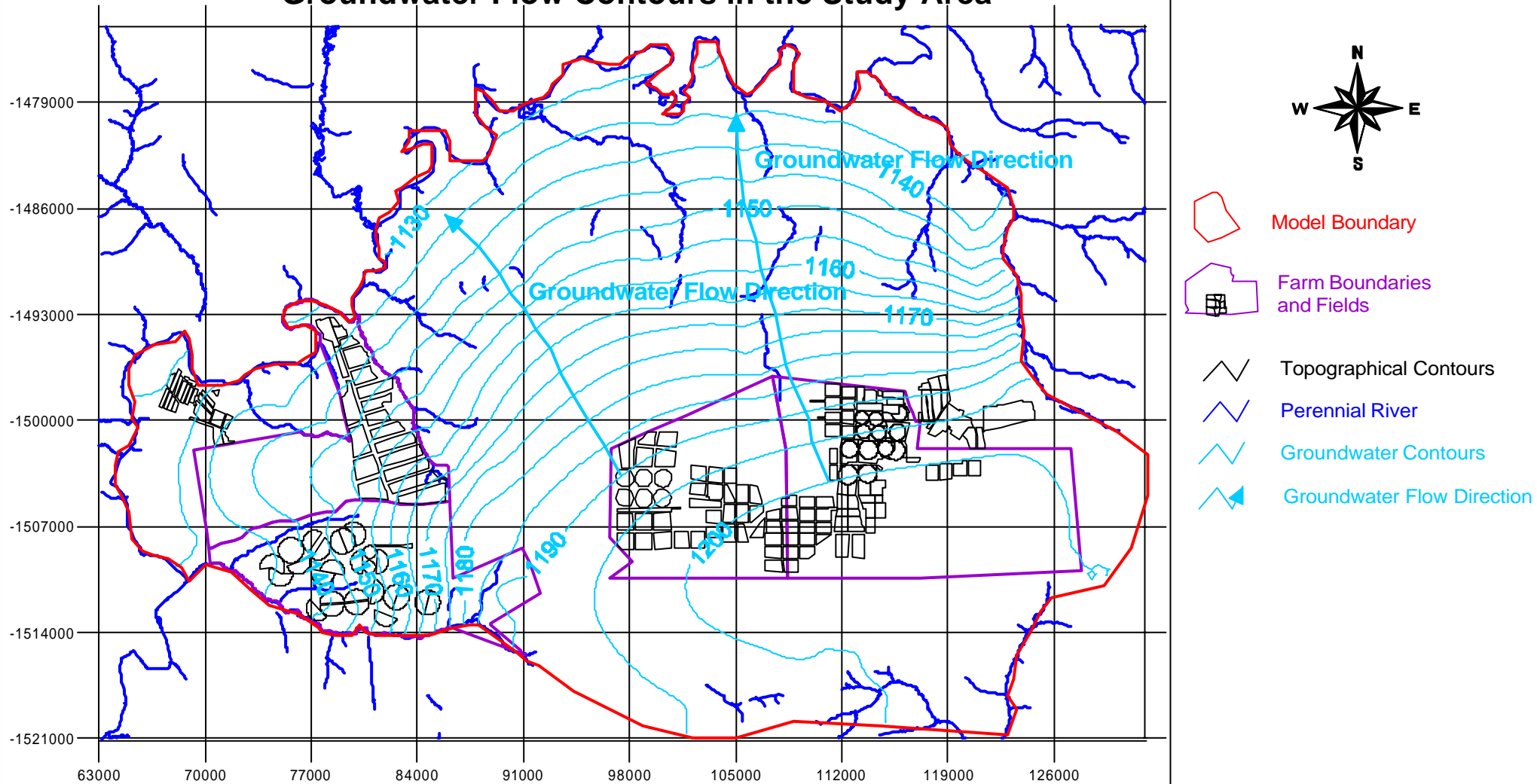
The Relationship between Water Level, Recharge and Abstraction Volumes for Lake Nampamba (Eastern Aquifer)



The Figure indicate the relationship between Recharge to the Eastern Aquifer, Water Level in Lake Nampamba and the Abstraction Rate from the Eastern Aquifer. The Figure indicate a decrease in water level during the dry season when there is no recharge from rainfall and a high abstraction rate. During the rainy season the water level recover. The water level start to recover almost immediately after the start of the rainy season. Peak water levels occur approximately 2 months after the peak rainfall.

Figure 3.3.2: Groundwater Flow Contours in the Study Area.

Groundwater Flow Contours in the Study Area



The figure indicates the groundwater flow contours as derived from the groundwater level data. Due to the clustering of the boreholes it is practically impossible to indicate the positions of the boreholes on this figure. For borehole positions please refer to Figure 3.4.1.

Figure No: 3.3.2

February 2005

Chapter 3.4 : Aquifer Transmissivity and Borehole Sustainable Yield Calculations.

The Mpongwe Development Company (MDC) has drilled a total of 65 boreholes on Kabanga farm in the Mpongwe irrigation area. The positions of the boreholes are shown in Figure 3.4.1. Of these 65 boreholes, 33 were drilled during 1978, a total of 22 during 1982 and 10 in 2004. The geological logs of the boreholes are shown in Appendix A.

During the three mentioned hydrogeological investigations, aquifer tests were performed on a total of 34 of the 65 drilled boreholes to determine the aquifer transmissivity and the borehole sustainable yields.

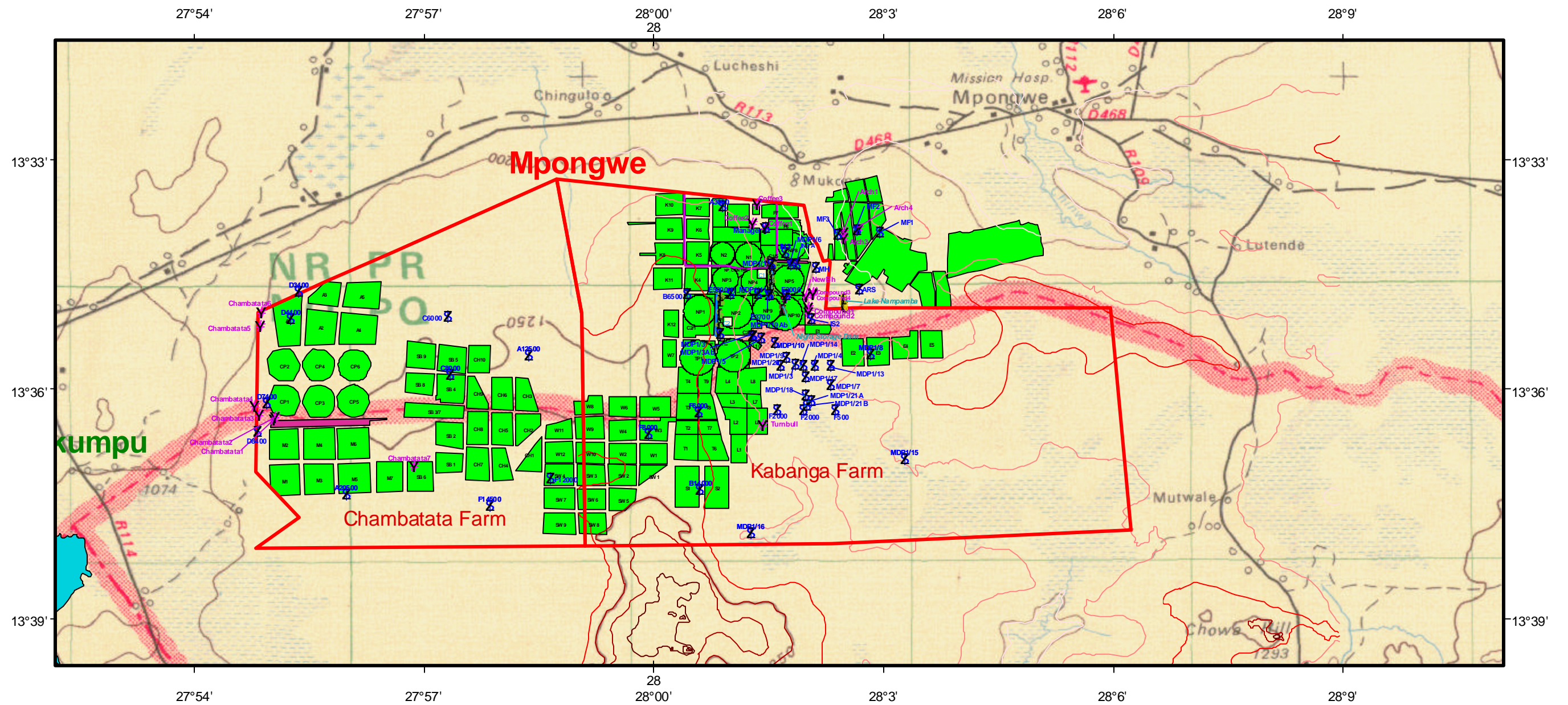
The transmissivity and specific capacity of 8 boreholes was determined in 1978 by Landell Mills Associates. The transmissivity calculations performed during the 1978 investigation were done by applying the Cooper-Jacob equation to constant rate aquifer test data. The boreholes for which the calculations were performed are:

- ARS (Agricultural Research Station)
- D4400
- D7400
- F500
- F2000
- F3000
- F14500
- IN3A

Preliminary aquifer tests were performed on 25 of the boreholes in 1982 (Macdonald and Partners Ltd.). The aquifer test data was used to calculate the transmissivity of the aquifer. Following the 1978 methodology of Landell Mills Associates, the Cooper-Jacob method was applied during the transmissivity calculations.

Figure 3.4.1: Positions of the Boreholes Drilled during 1978, 1981 & 2004.

Positions of Boreholes Drilled During 1978, 1981 and 2004



LEGEND:

	Boreholes 1982 & 1994 reports		Pumps in Night Storage Dam		Existing Canals		Contours_1328c1.shp		1250 - 1260		Coffee Boundary
	Boreholes not in reports - GPS by GCS Nov2003		Farm_boundaries.shp		Rivers		1180 - 1200		1280 - 1320		Field boundaries
	Pumps in C1 & C2 Canals		Mpongwe Arable Region		Dams		1220		Airstrips		Luanshya_sd_35-7.tif
	Pumps at Nampamba Lake		Dams		Buildings		1240		Buildings		

Figure No: 3.4.1

1 0 1 2 3 4 Kilometers



Datum: WGS84
Spheroid: WGS84
Projection: Geographic

Characterisation of the Dolomitic Aquifer in the Copperbelt Province, Northern Zambia

Table 3.4.1: Transmissivities and Specific Capacities as Calculated from Preliminary Aquifer Tests.

Borehole	Date Drilled	Date Tested	Transmissivity (m ² /day)	Specific Capacity (l/s/m)	Test Yield (l/s)
ARS	N/A	09/11/1978	845	21.5	17
D4400	04/11/1978	18/11/1978	230	1	6
D7400	20/10/1978	07/12/1978	4 400	16.5	27
E3700	20/03/1979	15/06/1981	917	15.8	29
E3700	20/03/1979	03/05/2004	992	11.1	25.1
F500	23/10/1978	31/10/1978	400	6.9	17
F2000	10/10/1978	22/11/1978	500	2.2	35
F3000	18/10/1978	13/11/1978	960	12	16.25
F14500	31/10/1978	30/11/1978	235	1	18
GCS6	April 2004	06/06/2004	6 900	83	25
GCS7	April 2004	11/06/2004	3 139	34	25
GCS8	April 2004	01/06/2004	803	34	25
IN3A	12/09/1978	03/11/1981	1 050	9.1	18
MDP1	24/04/1981	25/04/1981	<1	<0.1	1
MDP2	29/04/1981	09/05/1981	224	5.5	29
MDP3	20/08/1981	02/10/1981	206	5.7	31
MDP3Ab	09/05/1981	02/10/1981	N/A	3.8	28
MDP4	01/09/1981	09/09/1981	65	0.7	20
MDP5	20/05/1981	Not tested – low yielding borehole			
MDP6	22/05/1981	10/06/1981	422	8.11	28
MDP7	05/06/1981	19/06/1981	242	5.7	28
MDP8	18/06/1981	29/06/1981	N/A (Fluctuating Water level)		30
MDP9	06/10/1981	23/10/1981	59	N/A	21

Table 3.4.1: Transmissivities and Specific Capacities as Calculated from Preliminary Aquifer Tests (Continued).

Borehole	Date Drilled	Date Tested	Transmissivity (m²/day)	Specific Capacity (l/s/m)	Test Yield (l/s)
MDP10	25/06/1981	10/07/1981	49	1.7	14
MDP10A	April 2004	29/05/2004	67	0.63	10.5
MDP11	01/07/1981	06/07/1981	195	1	6.9
MDP12	05/07/1981	16/07/1981	41	1.2	10
MDP13	20/07/1981	30/07/1981	221	4.8	14
MDP14	17/07/1981	23/07/1981	N/A	1.6	9.5
MDP15	19/07/1981	Not tested – low yielding borehole			
MDP15	19/07/1981	24/04/2004	177	2.7	11.2
MDP16	22/07/1981	04/08/1981	14	0.4	6.4
MDP17	05/08/1981	Not tested – low yielding borehole			
MDP18	09/09/1981(82.3m)	23/09/1981	158	9.3	27
MDP18	09/09/1981(82.3m)	01/05/2004	547	11.4	25
MDP19	07/09/1981	18/09/1981	733	14.5	21.8
MDP19	07/09/1981	05/05/2004	970	1.7	14.2
MDP19Ab	19/08/1981	Not tested – borehole collapsed on 19/08/1981			
MDP20	20/08/1981 (60m)	25/08/1981	271	1.3	24
MDP20A	April 2004	09/06/2004	235	0.86	13
MDP21A	24/09/1981	01/10/1981	1 066	21.8	31
MDP21B	28/10/1981	01/11/1981	852	N/A	29
MDP21B	28/10/1981	27/04/2004	1 555	31	25.6

Boreholes on which preliminary aquifer tests were performed in 1981 and 1982 are:

- MDP1 to MDP21B (except MDP5, MDP8, MDP15 and MDP17 which were low yielding boreholes, and MDP19Ab which had collapsed). Boreholes MDP10A and MDP20A were only drilled in 2004.
- E3700
- IN3A

From the results of these preliminary aquifer tests, eight boreholes were identified to serve as production boreholes to supplement the abstraction of water from Lake Nampamba. The eight boreholes are:

- E3700.
- IN3A.
- MDP2, MDP3, MDP18, MDP19, MDP21A, MDP21B.

The eight boreholes were reamed to a larger diameter and boreholes MDP2, MDP9, MDP18 and MDP20 were drilled deeper in an effort to increase the sustainable yields that could be obtained from the boreholes.

Following the reaming and drilling, final aquifer tests were conducted on the eight boreholes and the transmissivity along with the sustainable yield and specific capacity was determined based on the aquifer test data. Both the pumping and recovery data were considered during the transmissivity calculations. The transmissivities and sustainable yields calculated for the eight boreholes are included in Table 3.4.2.

The sustainable yields of these boreholes as calculated in 1982 by Macdonald and Partners Ltd. range between 20 and 60l/s (630 000 to 1 890 000m³/annum). The total combined sustainable yield from the eight production boreholes is estimated at 264l/s (8 325 500m³/annum).

A total of ten boreholes were drilled during the 2004 drilling program. Five of these boreholes were sufficiently high yielding for aquifer tests to be performed. These boreholes are:

- GCS6, GCS7, GCS8 (newly drilled based on the 2004 geophysical investigation – refer to Chapter 2.9).
- MDP10A, MDP20A (newly drilled to replace the collapsed existing boreholes drilled during 1982).

Aquifer tests were also performed on existing boreholes:

- E3700.
- MDP 15, MDP18, MDP19, MDP21B.

The **AquiferTest for Windows** software (Version 2.01) developed by Waterloo Hydrologic Inc. was used by the author to calculate the transmissivity of the aquifer. Calculations were based on both the pumping and recovery data.

The sustainable yields listed in Table 3.4.2 are based on a combination of sustainable yields calculated by the Flow Characteristics (FC) method and those calculated based on the specific capacity and a maximum drawdown of 5m. The aquifer test data and sustainable yield calculations are shown in Appendix D.

The FC-method was developed by the Institute for Groundwater Studies at the University of the Free State, South Africa. Sustainable yields calculated using the FC-method are based on a recharge percentage of between 5 and 10%. In Chapter 3.5, it is shown that the regional recharge is estimated at 25% and therefore 5 to 10% is considered to be conservative.

The aquifer transmissivities calculated using AquiferTest and the sustainable yields calculated using the FC-method are summarised in Table 3.4.2.

Table 3.4.2: Production Borehole Sustainable Yields.

Borehole	Date Tested	Depth (mbgl)	Transmissivity (m ² /day)	Sustainable Yield (l/s)	Sustainable Yield (m ³ /annum)
E3700	23/09/1981	68.3	917	25	788 400
E3700	03/05/2004	68.3	992	60	1 892 200
GCS6	06/06/2004	65.0	6 900	100	3 153 600
GCS7	11/06/2004	79.0	3 139	50	1 576 800
GCS8	01/06/2004	42.0	803	80	2 522 900
IN3A	02/12/1981	54.0	1 050	60	1 892 200
MDP2	09/05/1981	62.5	224	32	1 009 000
MDP3	02/10/1981	73.2	202	35	1 104 000
MDP10A	29/05/2004	59.0	67	8.5	270 000
MDP15	24/04/2004	55.8	177	15	473 000
MDP18	23/09/1981	82.3	158	27	851 500
MDP18	01/05/2004	82.3	547	55	1 734 500
MDP19	18/09/1981	68.3	733	20	630 700
MDP19	05/05/2004	68.3	970	10	315 400
MDP20A	09/06/2004	72.0	271	5	157 700
MDP21A	01/10/1981	60.0	1 066	30	946 000
MDP21B	01/11/1981	40.0	852	35	1 104 000
MDP21B	27/04/2004	40.0	1 555	80	2 522 900

mbgl = metres below ground level

During the 2004 investigation the specific capacity of the boreholes, as calculated from the aquifer test data, was taken into account during the estimation of sustainable yields of boreholes due to the high transmissivities.

The specific capacity of an aquifer is calculated using the equation:

$$\text{Specific Capacity} = \text{Aquifer Test Yield} / \text{Maximum Drawdown} \quad (\text{Eq 3.4.1})$$

The specific capacity is expressed as l/s/m and simply put determines the volume of water that can be abstracted from the aquifer for every metre of drawdown in the borehole.

For the purpose of this study, it was assumed that the specific capacity follows a linear trend. Sustainable yields calculated based on the specific capacity depends on a maximum drawdown of five (5) metres. This yield is obtained by multiplying the specific capacity obtained using Equation 3.4.1 by five.

A maximum drawdown of 5m is used as it is considered to be conservative. The maximum drawdown will occur during the dry season when abstraction increases and no recharge from rainfall occurs. The normal seasonal groundwater fluctuations can be up to 15m. Compared to this figure, a drawdown of 5m during the dry season due to increased abstraction is deemed to be acceptable. It is assumed that during the rainy season, the aquifer will be fully recharged. Please refer to Chapters 3.5, 3.8 and 3.9 for detailed recharge and aquifer sustainability discussions.

Chapter 3.4.1 : Aquifer Transmissivity and Borehole Sustainable Yield Discussion.

Transmissivities calculated from the aquifer test data range between 1 and 6 900m²/day (refer to Table 3.4.1). This is typical of karstic areas with the relatively low transmissivities being associated with areas where no or very little karstic development occurred, and the high transmissivities occurring in areas where karstic development is pronounced.

Table 3.4.1 indicates that boreholes MDP1, MDP5, MDP15 and MDP17 are low yielding boreholes. Blow yields of these boreholes yielded less than 1l/s. In dolomitic lithologies, blow out yield is not always indicative of the potential yield of a borehole. This is due to the fact that when solution cavities are intersected, the compressed air used during normal percussion drilling is absorbed by the cavity space, and little to no drill chip or water return occurs.

However, on closer inspection of the lithological logs of the abovementioned boreholes, it is clear that these boreholes are indeed low yielding boreholes.

Borehole MDP1 is drilled partially into the schist, which is a low yielding lithology. No fracture zones or solution cavities are recorded in the limestone that was intersected between 30 and 48mbgl.

Borehole MDP5 was drilled into the limestone. The limestone to the completed depth is generally unweathered.

Boreholes MDP15 and MDP17 are drilled into the schist. This lithology is low yielding.

The total sustainable yield from the fourteen boreholes as listed in Table 3.4.2 is estimated at 620.5l/s (19 570 000m³/annum). This figure is calculated based on the latest results i.e. if a borehole was tested in both 1981 and 2004, the 2004 sustainable yield as calculated by the author was used. Sustainable yields calculated for the individual boreholes range between 5 to 100l/s (157 700 to 3 153 600m³/annum).

The sustainable yield of borehole GCS7 is indicated as 50l/s. The regional average depth to water level is calculated to be 13.68m (refer to Chapter 3.3). Borehole GCS7 indicates an anomalous water level for the area (34.29mbgl). This water level is possibly due to construction problems encountered during the installation of the steel casing.

Due to the possibility of the borehole collapsing, it is the author's opinion that the pump can only be inserted to 39m in depth, leaving an available drawdown of 5m. Owing to this fact, a conservative sustainable yield calculated from the specific capacity is based on a maximum drawdown of 2m, in contrast to the 5m used for the other boreholes. The main water strike occurred in a solution cavity 40 to 42mbgl. If this borehole was drilled deeper, the recommended sustainable yield could increase substantially.

Boreholes drilled into the solution cavities, or cavity associated fracture zones, are generally high yielding as can be seen from boreholes GCS6, GCS7, GCS8, MDP19, MDP21A, MDP21B, IN3A and E3700.

The fine crystalline unweathered or slightly fractured rock displays a lower transmissivity and storativity than the solution cavities. These areas will usually yield less water. Relative to the karstic aquifer, the yield from the fractured rock aquifer is negligible.

During the 1981 - 1982 investigation (Macdonald and Partners Ltd.), MDP11 was classified as a low yielding borehole. However, during 2004 closer investigation of the borehole geological log by the author indicated extensive fissuring below the regional groundwater level. This corresponds to similar fissuring reported in high yielding boreholes such as MDP21A and MDP21B. The fissuring is further highlighted by the single point resistance being completely off-scale (refer to Chapter 2.9 and Appendix A). The aquifer test data from 1982 indicates that the borehole was tested at a rate of 6.9l/s.

Drawdown of the water level in the borehole stabilised after 18 minutes at approximately 7m drawdown where it oscillated at approximately 28 to 29mbgl until the test was stopped after an hour. The oscillation level corresponds well to the fissure zone indicated in the drill log between 27 and 47m in depth.

Due to the oscillation of the water level during the last 40 minutes (two thirds of the testing time), Macdonald and Partners Ltd. only fitted a trend line to the early time data (first 20 minutes). This yielded the stated transmissivity of $195\text{m}^2/\text{day}$ (refer to Table 3.4.1).

The oscillation occurs due to the fact that the aquifer test was performed at too low a rate. Once the hydrogeological system is in motion the influx of water into the borehole is higher than what the pump can extract and a surging motion develops.

It is the opinion of the author that should this borehole be tested at a higher rate of 25 or 30l/s the oscillation effect can be avoided and a better estimation of the transmissivity can be obtained. It is the belief of the author that this borehole also has the potential to be high yielding. Unfortunately, it was not possible to prove this theory during the 2004 investigation.

Chapter 3.5 : Recharge Estimations.

Previous studies in the Mpongwe area have estimated groundwater recharge as a percentage of the annual rainfall. The estimated recharge from these studies is shown in Table 3.5.1.

Table 3.5.1: Average Recharge Estimates in the Kabanga and Chambatata Areas.

Reference	Recharge
Landell Mills Associates (1979)	10% (110 – 120mm/annum)
Macdonald and Partners Ltd. (1982)	6 – 22% (70 – 250mm/annum) – natural state 67% (750mm/annum) – cultivated land
Wimpey (1983)	45% (500mm/annum) -thin soil cover 28% (300mm/annum) - average soil cover

The recharge estimation by Landell Mills Associates (1979) is based on a conceptual model and calculates the recharge in the sub-catchment area. Lake Nampamba is situated within the sub-catchment area. Rainfall and water level data is available for the sub-catchment area and was used to determine the recharge percentage.

Due to little data being available at the time, Landell Mills Associates developed what was termed a preliminary conceptual model. The model made several assumptions. These assumptions include:

- The schist inlier is impervious, and underlies most of the potential farm area.
- The dolomitic aquifer surrounds the schist inlier.
- The high and moderately yielding dolomitic areas are both uniform and isotropic.
- The soil is on average free draining over the whole area to its full depth, and vertical drainage is complete in less than one month after the end of the rainy season.
- Evapotranspiration losses are confined to the removal of water from the soil and do not draw significantly from groundwater in the aquifer.

Based on subsequent studies, it is now known that the first assumption is not true. Geological evidence from subsequent drilling programs and geological studies indicate that the schist inlier is localised (refer to Chapter 2.7).

Landell Mills Associates (1979) used the change in storage (saturated thickness) reflected by Lake Nampamba water level records to calculate the recharge percentage. This requires knowledge of the regional storage coefficient S in association with Lake Nampamba and regional water levels.

Landell Mills Associates (1979) used the aquifer tests performed in 1978 to calculate the storage coefficient. Based on data from boreholes IN3A and F2000 and Lake Nampamba, an average storage coefficient of 0.002 (or 0.2%) was calculated. This was considered to be conservative.

The findings of the Landell Mills Associates (1979) calculations are summarised in Table 3.5.2. Following Landell Mills Associates' (1979) calculations, this indicates an effective recharge of 110 to 120mm. The Total Recharge Volume (Mm^3) is calculated based on the area under the recession graph and using a storage coefficient of 0.002.

Table 3.5.2: Landell Mills Associates Recharge Calculations (1979).

Year	Rainfall (mm)	Total Recharge Volume (Mm^3)	Equivalent Rainfall Recharge (mm)	Percentage of Annual Rainfall
1973 to 1974	1 105	10.0	65	5.9%
1974 to 1975	1 196	15.4	100	8.4%
1975 to 1976	1 075	18.8	122	11.3%
1976 to 1977	1 295	17.4	112	8.6%

Recharge estimations performed by the author in 2004 indicate a storage coefficient of 0.02 (or 2%). These calculations are discussed in Chapter 3.6. This is an order of magnitude larger than that used by Landell Mills Associates in 1979. The above calculations incorporating the storage coefficient would therefore change. Unfortunately, the original recession curves are not available, and thus the author could not interrogate the calculations.

Macdonald and Partners Ltd. (1982) calculated the recharge as part of a detailed water balance. Following Macdonald and Partners Ltd., the water balance was calculated based on the equation:

$$\text{Precipitation} = \text{Run-off} + \text{Actual Evapotranspiration} + \text{Recharge}$$

Macdonald and Partners Ltd. used the rainfall record from the Mpongwe Mission farm for the precipitation figure.

The evapotranspiration was poorly defined and Macdonald and Partners Ltd. calculated the evapotranspiration based on:

- Rainfall
- Interception storage
- Potential evaporation
- Coefficients for the woodland equivalent to crop coefficients (k_c)
- Effective rooting depths of the woodland
- Factors taking into account the decrease in transpiration of the woodland when soil moisture levels decrease below freely available water, and
- The antecedent moisture content.

The equations used in these calculations are not listed or explained by Macdonald and Partners Ltd., and the author is therefore not able to comment on these calculations.

Having calculated the evapotranspiration, Macdonald and Partners Ltd. (1982) calculated the monthly soil moisture content. If the soil moisture is greater than the field capacity, the excess water is assumed to recharge the underlying aquifer.

Based on the calculated and assumed values, a recharge range of 70 to 250mm/annum was calculated by Macdonald and Partners Ltd. for natural areas.

Changing the parameters for cropping coefficients and rooting depths, Macdonald and Partners Ltd. calculated a recharge in cultivated areas of 750mm/annum.

This increase in recharge from natural to cultivated state is mainly due to the decrease in initial rainfall required to make up the smaller soil moisture deficit existing over the greatly reduced rooting depth at the beginning of the wet season (Macdonald and Partners Ltd, 1982). A rainy season yielding average rainfall will see recharge to the underlying aquifer in cultivated areas as early as November, compared to January for natural woodland areas.

The Wimpey report could not be located and the values as stated in Rankin Engineering Consultants (1994) were used.

Chapter 3.5.1 : Recharge Estimation Methodology.

A considerable amount of research has been undertaken on the recharge of dolomitic aquifers in South Africa (Bredenkamp *et al.*, 1995). Several methods have been successfully developed to estimate the recharge to the groundwater in dolomitic aquifers from rainfall. Methods that are applicable to this study are:

- Chloride Method
- SVF Method
- CRD Method

The chloride method can be considered to be one way of determining the mass balance of the unsaturated zone. The chloride, which is a conservative tracer element, enters the soil as part of the infiltrating rainwater and is subsequently concentrated by transpiration from plants, and by direct evaporation from the soil.

The method allows recharge to be calculated, and in its simplest form the relationship can be represented as:

$$RE = \frac{Cl_{input}}{Cl_{gw}} \cdot Rf \quad (\text{Eq 3.5.1.1})$$

where

RE = Recharge

Cl_{input} = chloride from the rainfall as well as from dry depositioning

Cl_{gw} = chloride in the groundwater

Rf = Rainfall

The essential requirement for the application of the method is that the chloride concentration of the rainfall must be known.

Generally, the recharge percentages estimated using the chloride method correspond well with those obtained using other, more detailed and accurate methods, such as the SVF and CRD methods. The simplicity of the chloride method and the relative ease of sampling mean that this method can be useful in obtaining a provisional recharge percentage for an area.

The Saturated Volume Fluctuation (SVF) method incorporates a lumped parameter approach whereby the status of the aquifer, based on the water level fluctuations of the monitoring boreholes, is integrated and its variation with time analysed.

By means of a network of finite elements the piezometric levels from the observations points are integrated to yield the saturated volume status for the entire aquifer. The network of elements is constructed using the water level monitoring points or points of abstraction as nodal points for the grid network.

An arbitrary value for the base thickness is assigned, usually in such a way that the saturated volumes are always positive values. In this study, the base thickness is selected as 100m, the maximum depth of the boreholes in the area.

The boundaries of the system are the contact with the surrounding geology, specifically the quartzite to the west. The Kafue River to the north is also taken into consideration.

Mathematically the method is based on the saturated flow equation:

$$I - O + RE - Q = S \times (\Delta V / \Delta t) \quad (\text{Eq 3.5.1.2})$$

Where:

- I = $(I_1 + I_2) / 2$ that is, the mean lateral inflow during the time increment Δt
- O = $(O_1 + O_2) / 2$ that is, the average lateral outflow from the system
- RE = groundwater recharge to the system, which is the unknown parameter to be estimated
- Q = net discharge or abstraction from the groundwater system
- S = the aquifer storativity
- ΔV = change in saturated volume of the aquifer
- Δt = $t_2 - t_1$ that is, the time increment over which the water balance is executed

The aquifer storativity (S) is an essential element in the water balance. However, it is difficult to determine the storativity due to the interdependence of the water level response on both recharge and storativity. Generally, in the estimation of the aquifer storativity from water balances or by means of aquifer tests, it is assumed that the inferred storativity is uniform over the full thickness of the aquifer.

According to Bredenkamp *et al*, it was shown by Enslin and Kriel (1967), by means of an analysis of the core recoveries of diamond drill holes that the porosity of a dolomitic aquifer in the West Rand (South Africa) decreases with depth. This may not hold true for the dolomitic aquifer in northern Zambia. This assumption is based on the possibility that both Lake Nampamba and Lake Kashiba are fed from a groundwater source that is higher yielding than those intersected by the production boreholes. This source would be deeper than 100m below surface, as this is the maximum depth of the boreholes. Divers have established that both the lakes (sinkholes) are deeper than 100m.

Another example where major water bearing features such as solution cavities exist in the dolomite at great depths is in the Petit region, South Africa, where major water

strikes associated with the dolomitic aquifer reportedly occur between 100 and 120m, with an average depth of approximately 112m.

However, it is agreed that secondary water yielding features such as fractures will decrease in frequency, transmissivity and associated yield with depth.

An additional method to the SVF method is the “Equal volume” method. This method corresponds more closely to average rainfall situations in as much as the equal volume includes spells of both above average and below average rainfall.

When the change in groundwater storage over a selected period of time is zero (thus $\Delta V = 0$), the storativity of the aquifer is eliminated from the equation. When the inflow and outflow terms are assumed to cancel each other out, the recharge from rainfall would be equal to the abstraction Q , which is the volume of water being abstracted from the dolomitic aquifer.

Following these assumptions the SVF equation can be reduced to:

$$RE = (A_2 \times T_0) - (A_1 \times T_1) + Q \quad (\text{Eq 3.5.1.3})$$

Or $RE = Q$ if inflow = outflow (Eq 3.5.1.4)

The successful application of the SVF method, or any water balance method, requires that the abstraction (Q) must be known. When natural losses such as evapotranspiration are not incorporated as part of the abstraction, the inferred recharge only represents the effective or exploitable recharge of the aquifer, which is obviously smaller than the total recharge.

The Cumulative Rainfall Departure (CRD) method follows the concept that equilibrium conditions develop in an aquifer over time until the average rate of losses equals the average rate of recharge to the system. The CRD method was first used as early as 1936 (Wenzel). In South Africa, Temperley (1980) applied this method extensively.

In using the moving average rainfall the weight assigned to early rainfall records is progressively reduced, and at the same time, the effect caused by future rainfall events eliminated.

The CRD method is applicable to both natural and exploited aquifer conditions. The CRD method is based on the argument that an equilibrium exists between average annual rainfall and the hydrological response in terms of run-off, recharge, evaporation, plant growth etc. This equilibrium can be expressed as (Bredenkamp *et al*, 1995):

$$Rf_{av} = RO_{av} + RE_{av} + EVT_{av} \quad (\text{Eq 3.5.1.5})$$

Where:

Rf_{av} = Average rainfall

RO_{av} = Average run-off

RE_{av} = Average recharge

EVT_{av} = Average evapotranspiration

The CRD method assumes that the bulk of the precipitation is returned to the atmosphere by evaporation and evapotranspiration. These evaporative losses are caused by the biological pumps, which are controlled by the type of vegetation that has established itself over many years in accordance with the available soil moisture and its temporal distribution. For this reason the natural vegetation in humid areas is much more dense and lush, creating high evapotranspiration losses.

The relationship between the CRD method and the groundwater level response can be derived from first principles.

The recession part of the groundwater hydrograph follows an exponential decline if the recharge is zero (Ernst, 1962; Gieske, 1992) i.e.:

$$h_t = h_0 e^{-yt} \quad (\text{Eq 3.5.1.6})$$

Where:

- h_t = the piezometric level above the aquifer base.
- h_0 = the initial level.
- y = the decline factor.

According to the simplified approach of Ernst (1962) the exponential decline of the water level (Equation 3.5.1.6) can be approximated by:

$$h = h_0(1-yt) \quad (\text{Eq 3.5.1.7})$$

$$= h_0 \times c \quad (\text{Eq 3.5.1.8})$$

Where:

- c = (1-yt)
- t = the time interval.

The response of the piezometric level is controlled by recharge and recession in the following way, assuming that the recharge is added at the end of the chosen time interval:

$$h_i = h_{i-1}c + \frac{RE_i}{S} \quad (\text{Eq 3.5.1.9})$$

where the recharge is usually represented by a simple equation:

$$RE_i = a(Rf_i - b) \quad (\text{Eq 3.5.1.10})$$

Where:

- b = a constant.
- a = the fraction of rainfall that constitutes recharge.
- Rf_i = rainfall for period i .

The change in water level over the selected time interval dt is:

$$\Delta h_i = h_i - h_{i-1} \quad (\text{Eq 3.5.1.11})$$

Therefore:

$$\Delta h_i = h_{i-1}(c-1) + \frac{a}{S}(Rf_i - b) \quad (\text{Eq 3.5.1.12})$$

where S is the storativity of the aquifer, and over the long-term, integrating from j = i backwards over a period for which equilibrium conditions have been established:

$$\sum_{j=1}^{j=i} \Delta h_j = \sum_{j=1}^{j=i} h_{j-1}(c-1) + \frac{a}{S} \sum_{j=1}^{j=i} (Rf_j - b) \quad (\text{Eq 3.5.1.13})$$

Where j represents the present status in relation to the antecedent period of i increments;

As $\sum \Delta h_i \cong 0$ over a period long enough for equilibrium conditions to apply, Equation 3.5.1.13 reduces to:

$$\sum_{j=1}^{j=i} h_{j-1}(c-1) = \frac{-a}{S} i(Rf_{av} - b) \quad (\text{Eq 3.5.1.14})$$

having incorporated i time increments. Therefore, for the previous increment, assuming that equilibrium has set in:

$$h_{i-1}(c-1) = \frac{-a}{S}(Rf_{av} - b)$$

Thus Equation 3.5.1.12 becomes:

$$\begin{aligned}\Delta h_i &= \frac{a}{S}(Rf_i - b) - \frac{a}{S}(Rf_{av} - b) \\ &= \frac{a}{S}(Rf_i - Rf_{av})\end{aligned}\quad (\text{Eq 3.5.1.15})$$

which can be written as:

$$\frac{a}{S}(Rf_i - k.Rf_{av}) \quad (\text{Eq 3.5.1.16})$$

where $k = 1$ indicates that natural conditions apply.

The above Equation 3.5.1.16 indicates that the change in water level will respond according to the cumulative rainfall departure from the mean, with a proportionality coefficient (a/S). This is in agreement with the concept illustrated by Gieske (1992) that the water level builds up over several years to reach an equilibrium condition representing the average status, which is balanced by the average outflow from the aquifer.

It is evident that the final equilibrium water level of an aquifer will be the result of the incremental water level changes over the long term.

The trend of the natural fluctuations of the groundwater levels is maintained even when substantial pumping occurs, provided that the pumping remains reasonably constant. Therefore the pumping could be set to equal an effective constant loss factor, which can be incorporated as:

$$k + \Delta k$$

Where:

$$\Delta k = \frac{Q_p}{Rf_{av} \cdot Area}$$

Where:

Area = the area of the aquifer.

This allows the relationship:

$$RE = a(Rf - k.Rf_{av}) \quad (\text{Eq 3.5.1.17})$$

to be used to determine the effective recharge according to the natural water balance applied to a selected time interval where:

$k = 1$ represent the natural situation.

$k > 1$ indicates the system is being exploited.

The Equation 3.5.1.17 indicates that:

- Positive recharge occurs when the rainfall is more than the average for the selected time interval.
- Negative recharge occurs when the rainfall is less than the average for the selected time interval.
- The effect of pumping (Δk) is incorporated inside the brackets i.e. its influence is reduced depending on the value of a , which is normally less than 1.

Chapter 3.5.2 : Recharge Estimation Methodology Application.

The available data was interpreted using the **Recharge** software. This is an Excel based spreadsheet program developed by G. van Tonder and Y. Xu of the Institute for Groundwater Studies (University of the Free State, South Africa). The software was developed with the aim of estimating groundwater recharge and the associated groundwater reserve for catchment areas.

Several recharge estimation methods are contained in the software such as the SVF method, CRD method, chloride method, isotope analysis and the qualified guess method.

The qualified guess method is only applicable to South Africa and could therefore not be used for this study. No isotope analyses have been performed.

Following the chloride method the percentage recharge from rainfall is estimated based on the annual rainfall, chloride concentration in the rainfall, the dry deposition chloride and the chloride concentration in the groundwater.

No rainfall could be collected during the time of the site visit as the visit fell outside of the rainy season. Therefore the chloride concentration in the rainwater had to be estimated. The chemical analysis of three groundwater samples indicates that the chloride concentration ranges between 1 and 3.2mg/l. Unfortunately, the boreholes were not identified (refer to Chapter 3.2).

The chloride concentration in the water will increase from the time that recharge from rainfall into the soil occurs until the water is abstracted from the aquifer. This is based on the assumption that the chloride concentration will increase due to transpiration from plants and by direct evaporation from the soil (Bredenkamp *et al*, 1995).

Accepting this reasoning, it follows that the chloride concentration in the rainwater cannot be higher than that recorded in the groundwater. Therefore, the chloride concentration in rainfall will be equal to or less than 1mg/l.

The average annual rainfall for the study area is 1 115mm. Following the reasoning above, the chloride concentration in the rainfall should be equal to or less than 1mg/l. It was decided to calculate the recharge percentage based on values ranging between 0.1 and 1 mg/l.

Using the **Recharge** software, it is recommended that the dry deposition chloride concentration should be calculated as 0.1 times the rainfall chloride concentration in inland areas where no forests occur. The dry chloride concentration should be calculated as 2.5 times the rainfall chloride concentration in areas where forests occur. As shown in Chapter 2.6, the natural plant growth occurring in the area is *Brachystegia* woodland with a density of 500 trees per hectare. Figures 2.2.2 and 2.6.2 show the natural plant growth and how the natural woodland was cleared for agricultural purposes.

Therefore, based on the facts that the study area is situated far inland, with cleared areas for agricultural purposes and the presence of natural forest over large areas, the author concludes that the actual dry chloride deposition versus the rainfall chloride concentration ratio will fall between 0.1 and 2.5. Taking all the plant growth and geographical conditions into consideration, it is the opinion of the author that the ratio is closer to 0.1 than 2.5.

The harmonic mean groundwater chloride concentration calculated from the available data is 1.667mg/l.

Due to the fact that both the rainfall chloride concentration and the rainfall chloride concentration versus the dry chloride deposition ratio are uncertain, the recharge percentage is calculated as a range based on the discussed ranges of these two parameters. The expected range of recharge percentage is shown in Figure 3.5.1.

Figure 3.5.1 shows that for a rainfall chloride concentration versus a dry chloride deposition ratio of 0.1, the recharge percentage ranges between 7 and 65%, depending on the rainfall chloride concentration. For a rainfall chloride concentration versus a dry chloride deposition ratio of 2.5, the recharge percentage ranges between 21 and 208%.

A recharge percentage higher than 100% would mean that there is more water recharge than total rainfall volume. This can only occur if water is artificially recharged to the aquifer from an external source, which does not happen in the study area. In reality recharge percentages higher than 50% are rarely achieved under natural conditions, depending on site-specific conditions such as recharge pathways, soil cover, topography and slope, infiltration rates, fracturing and outcropping of the competent rock and rainfall intensity.

It is generally considered that a chloride concentration of 0.1mg/l in rainwater is too low, and should be nearer to between 0.8 and 1mg/l. However, Figure 3.5.1 indicates that even at a rainfall chloride concentration versus a dry chloride deposition ratio of 0.1, a chloride concentration of 1mg/l indicates a 65% recharge percentage, which is considered to be high for this hydrogeological system.

At 0.8mg/l chloride concentration in rainfall, and a ratio of 0.1, recharge is calculated to be approximately 50%. This is also considered to be too high for this system.

It is concluded that the chloride method cannot be applied with confidence to this particular area. This is possibly due to the large distance from the coast (approximately 1 400km), or the relatively high rainfall figures. Investigation of the **Recharge** software indicates that most inland locations for which recharge has been benchmarked have a rainfall figure of less than 600mm/annum, which is half of the figure that is recorded at Mpongwe. Distance from the coast for the points benchmarked in the software is also generally less than 800km.

The SVF and CRD methods were used to calculate the recharge to the Mpongwe aquifer for a higher degree of accuracy. Due to most of the data being available for the eastern aquifer (Mpongwe area), analysis focussed on this area. The calculated recharge values could then be extrapolated to the western aquifer (Munkumpu Area). Data analysed includes:

- Monthly rainfall data – January 1991 to December 2003.
- Average monthly water level in Lake Nampamba – January 1991 to December 2003.
- Abstraction volumes from Lake Nampamba – Actual volumes for 2000 and 2002, average volumes for 1991 to 1999, 2001 and 2003.
- Sub-catchment area of 160km² as specified by Macdonald and Partners Ltd. (1982) for the eastern aquifer.
- Sub-catchment area of 328km² as calculated by Rankin Engineering Consultants for the western aquifer.

Using the **Recharge** software the recharge percentage was calculated by correlating the actual observed water levels in Lake Nampamba to calculated water levels. The calculated water levels are based on the actual observed rainfall and abstraction data. In addition to this, the correlation between the observed and calculated water levels is influenced by the storativity.

The results of the recharge calculations are shown in Table 3.5.2. The graphs indicating correlation between the observed and the estimated volumes are shown in Figures 3.5.2 and 3.5.3 for the SVF and the CRD methods respectively.

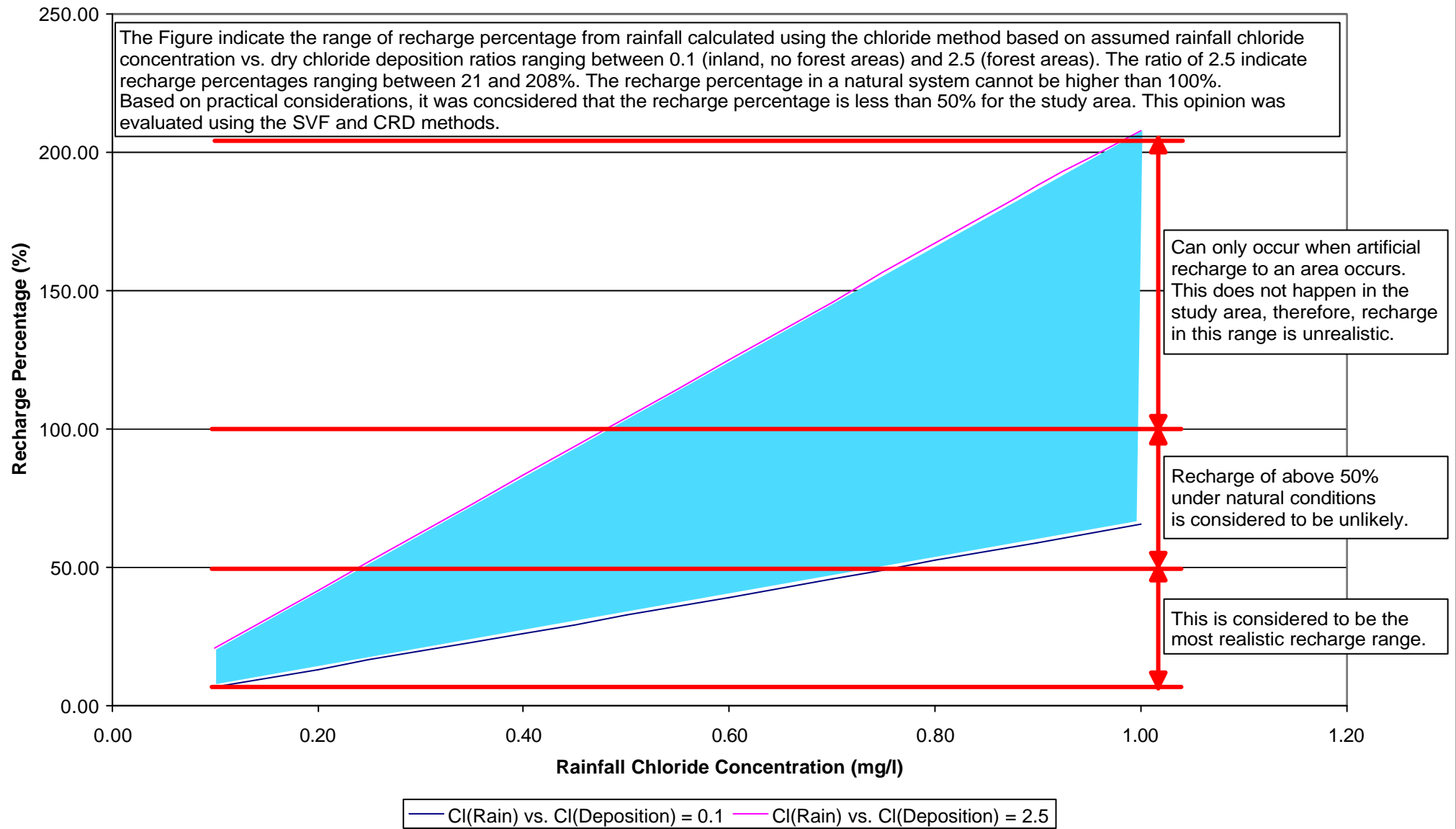
Table 3.5.2: Calculated Recharge Percentages – SVF and CRD Methods.

Method	Recharge
Chloride	7 to 208% (80 to 2 320mm/annum)
SVF	25% (280mm/annum)
SVF – Equal Volume	24.97% (280mm/annum)
CRD	25% (280mm/annum)

It should be noted that the recharge percentage is dependent on the storativity (S). The storativity value obtained by the author during the investigation is discussed in Chapter 3.6.

Figure 3.5.1: Chloride Method – Calculation of Recharge Percentage.

Chloride Method - Calculation of Recharge Percentage

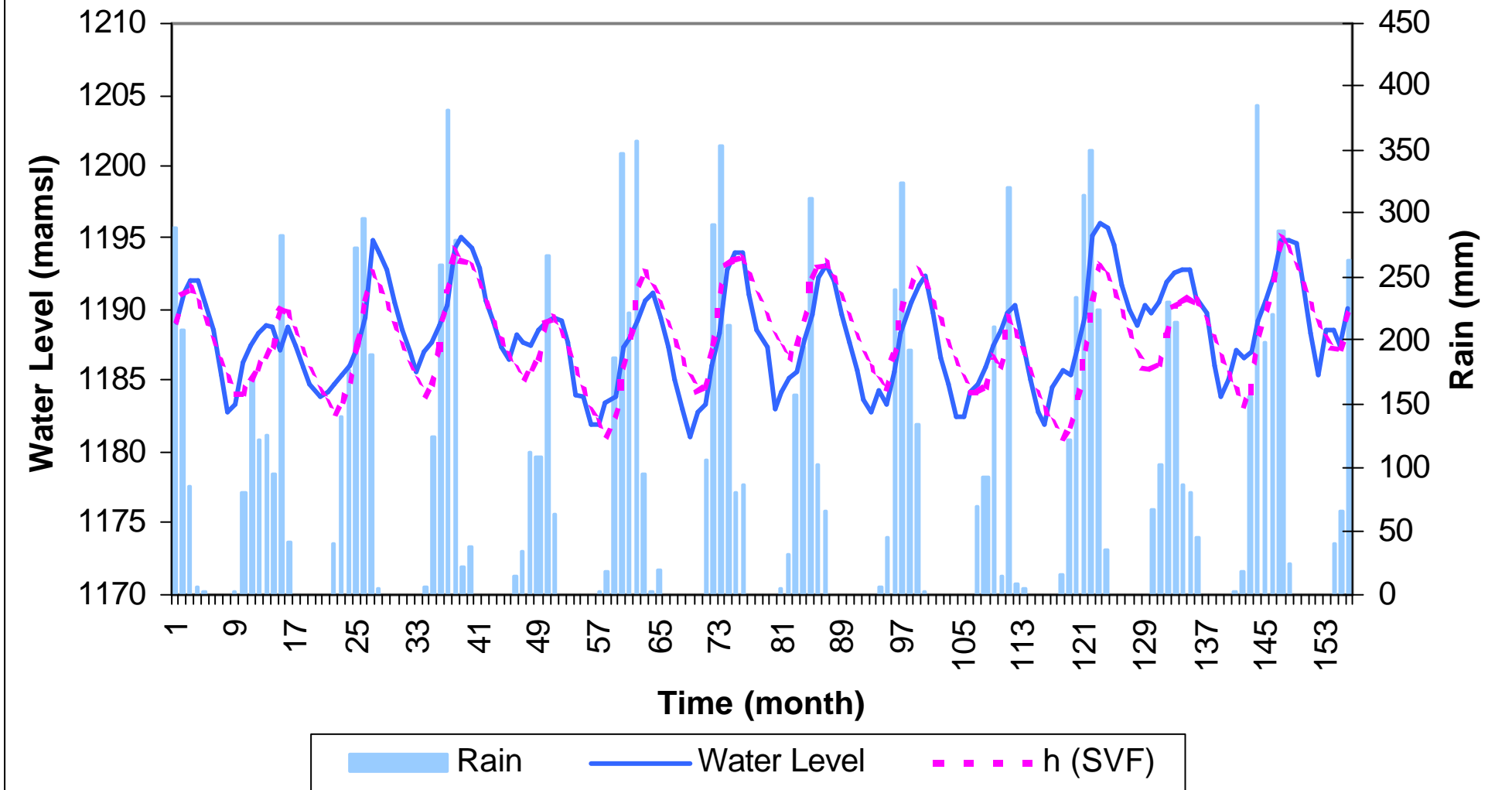


The Figure indicate the range of recharge percentage from rainfall calculated using the chloride method based on assumed rainfall chloride concentration vs. dry chloride deposition ratios ranging between 0.1 (inland, no forest areas) and 2.5 (forest areas). The ratio of 2.5 indicate recharge percentages ranging between 21 and 208%. The recharge percentage in a natural system cannot be higher than 100%. Based on practical considerations, it was considered that the recharge percentage is less than 50% for the study area. This opinion was evaluated using the SVF and CRD methods.

Figure 3.5.2: SVF Method – Calculation of Recharge Percentage.

SVF Method - Calculation of Recharge Percentage

SVF: Rech% = 25, S = 0.02; Month 1 = January 1991, Month 155 = December 2003

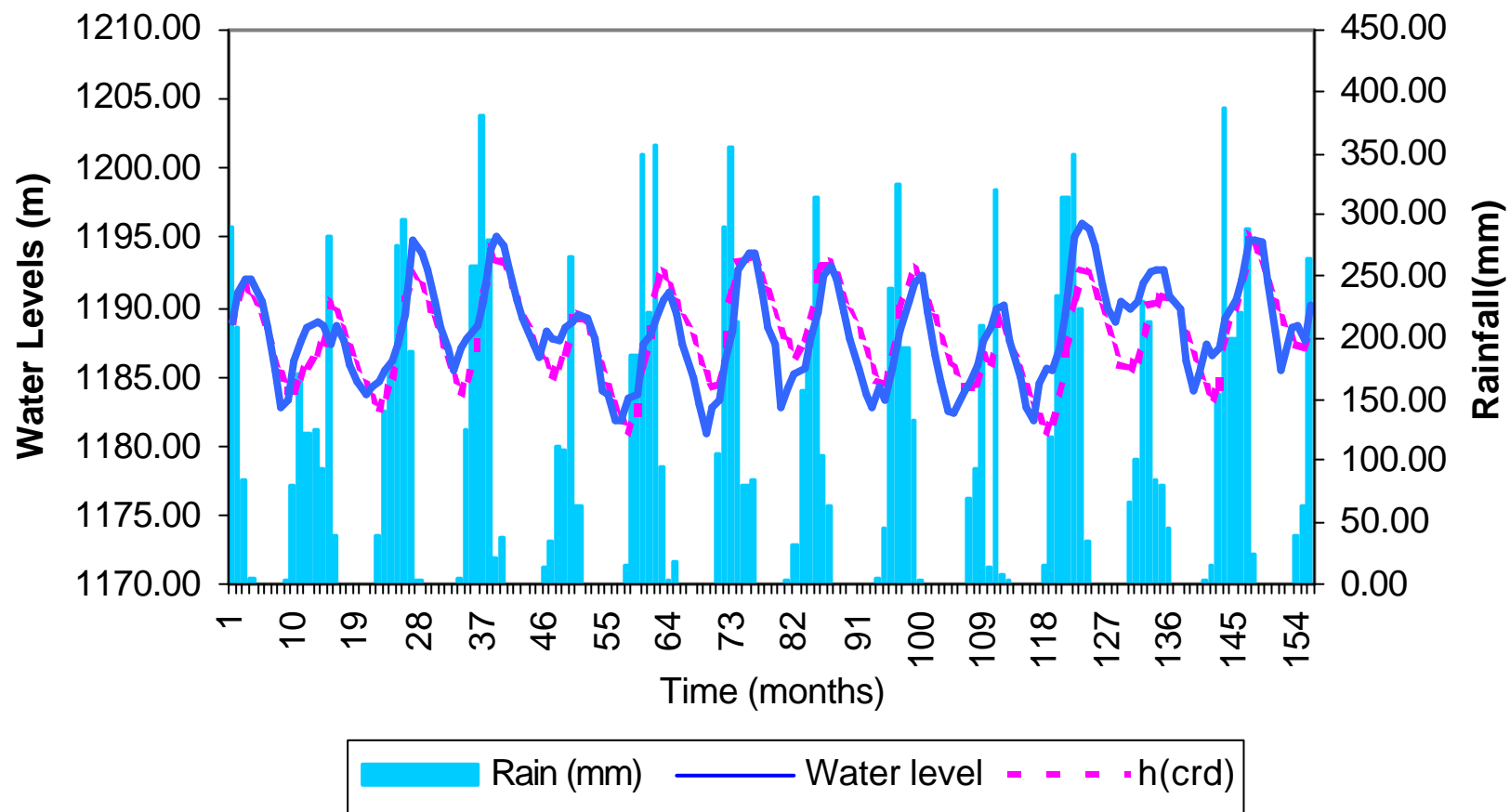


The Figure indicate the observed water levels in Lake Nampamba (Blue Line) and the water levels calculated using the SVF method (pink dotted line). The observed rainfall is indicated by the light blue bars. The recharge percentage and storativity parameters used during the calculations are indicated.

Figure 3.5.3: CRD Method – Calculation of Recharge Percentage.

CRD Method - Calculation of Recharge Percentage

CRD: Rech% = 25; S = 0.02; Month 1 = January 1991; Month 155 = December 2003



The Figure indicate the observed water levels in Lake Nampamba (Blue Line) and the water levels calculated using the CRD method (pink dotted line).
 The observed rainfall is indicated by the light blue bars.
 The recharge percentage and storativity parameters used during the calculations are indicated.

Chapter 3.6 : Aquifer Storativity.

The storativity of a saturated confined aquifer of thickness D is defined as the volume of water released from storage per unit surface area of the aquifer per unit decline in the component of hydraulic head normal to that surface. In a vertical column of unit area extending through the confined aquifer, the storativity “ S ” equals the volume of water released through the aquifer when the piezometric surface drops over a unit distance (Kruseman & de Ridder, 2000).

As storativity involves a volume of water per volume of aquifer, it is a dimensionless quantity.

As stated in Chapter 3.5, the storativity of the aquifer is an important parameter. Using the SVF and CRD methods of the **Recharge** software, the storativity has to be calibrated in order to adjust and obtain the best fit between the observed and calculated water levels.

The storativities as obtained from the data analysis are listed in Table 3.6.1. The calculated storativities calculated using the **Recharge** software are also indicated in Figures 3.5.2 and 3.5.3.

Table 3.6.1: Aquifer Storativity.

Method	Storativity
SVF	0.02
CRD	0.02
Recession analysis	0.0182

These storativity values of between 0.0182 and 0.02 correspond well with the values obtained for other dolomitic aquifers by other authors. In 1987 Lynch and Hodgson obtained a storativity value of 0.01 for the Sishen dolomitic aquifer in South Africa. Janse van Rensburg *et al* (1987) calculated a storativity of 0.028 for the Grootfontein Compartment in South Africa.

Chapter 3.7 : Aquifer Sustainable Yield Calculations.

The maximum sustainable yield of an aquifer can be defined as the maximum volume of water that can be abstracted annually without negatively impacting on the volume of water in storage in the aquifer. A negative impact on the volume of water stored within the aquifer will manifest itself through a year on year regional declining trend in the groundwater level. The declining trend will continue as long as the excessive abstraction continues, or until inflows into the system increase sufficiently to sustain the outflows from the system.

The decline in groundwater level is the result of more water being abstracted annually than what is recharged to the area. This shortfall of water has to be supplemented from the water in storage, thus resulting in a year on year decline in groundwater level.

The sustainable yield of the dolomitic aquifer has been previously estimated based on the size of the sub-catchment area and recharge percentage. These sustainable yields are summarised in Table 3.7.1.

Table 3.7.1: Previous Estimated Sustainable Abstraction Rates.

Reference	Sub-Catchment (km ²)	Sustainable Yield (Mm ³ /annum)	Sustainable Yield (m ³ /day)
Macdonald and Partners Ltd. (1982)	160km ² (Eastern Aquifer only)	19.55Mm ³ /annum	53 400m ³ /day
Rankin Engineering Consultants (1994)	328km ² (Western Aquifer only)	72.5Mm ³ /annum	200 000m ³ /day

Scott Wilson Piésold (2003) calculated the sustainable yield from the aquifer based on the through flow. The estimation follows the equation:

$$Q = k \times i \times A \quad (\text{Eq 3.7.1})$$

Where:

Q = Flow through aquifer.

k = hydraulic conductivity.

i = groundwater flow gradient (0.0025).

A = Cross sectional area (20 000m).

The hydraulic conductivity can be calculated using the equation:

$$k = T / D$$

Where:

T = Transmissivity (range 250 to 2 000m²/day).

D = Saturated thickness of the aquifer.

The estimated through flow is summarised in Table 3.7.2.

Table 3.7.2: Estimated Through Flow Through the Aquifer.

Transmissivity (m²/day)	Sustainable Yield (Mm³/annum)	Sustainable Yield (m³/day)
250	4.6Mm ³ /annum	12 500m ³ /day
1 000	18.25Mm ³ /annum	50 000m ³ /day
2 000	36.5Mm ³ /annum	100 000m ³ /day

The volume of 18.25Mm³/annum based on a transmissivity of 1 000m²/day corresponds to the volume of 19.55Mm³/annum calculated by Macdonald and Partners Ltd. (1982). The transmissivity of 1 000m²/day corresponds with the transmissivity at which the numerical model reached calibration for solution cavities for the current study (refer to Chapter 4.1).

For the current study the recharge volume was calculated for the eastern aquifer, the western aquifer, the combined eastern and western aquifers, and the whole of the known dolomitic area.

Analysis of the data during the CRD, SVF and equal volume method calculations indicated that the eastern and western aquifers are definitely connected. This conclusion is discussed in detail in Chapters 3.1 and 3.5. It is believed that the eastern and western aquifers should be evaluated as one entity. Based on this assumption, the combined yield of the eastern and western aquifers was calculated.

Recharge to the whole of the dolomitic area was calculated as discussed above.

The area covered by each aquifer is:

- Eastern Aquifer: 160km² (Macdonald and Partners Ltd., 1982)
- Western Aquifer: 328km² (Rankin Engineering Consultants, 1994)
- Eastern and Western Aquifers: Combined area of 488km²
- Dolomitic Aquifer: At least 1190km² (Based on 1: 100 000 geological map)

The annual estimated recharge to the area is shown in Figure 3.7.1. The figure indicates that the calculated recharge intensity to the area is relatively constant with little variance. The rainy seasons of 1994 / 1995, 1999 / 2000 and 2001 / 2002 indicate a noticeably lower than average recharge. The rainy seasons of 1995 / 1996, 2000 / 2001 and 2002 / 2003 indicate a noticeably higher than average recharge.

Maximum and minimum annual recharge volumes are summarised in Table 3.7.3. For maximum recharge calculations the data for April 2002 to March 2003 was used and for the minimum recharge calculations the data from April 1994 to March 1995.

As stated above, it is considered that the eastern and western aquifers are interconnected. However, it is uncertain whether the solution cavities and fracture zones of the eastern and western aquifers are interconnected with features further away such as Lake Kashiba and the Kafue River.

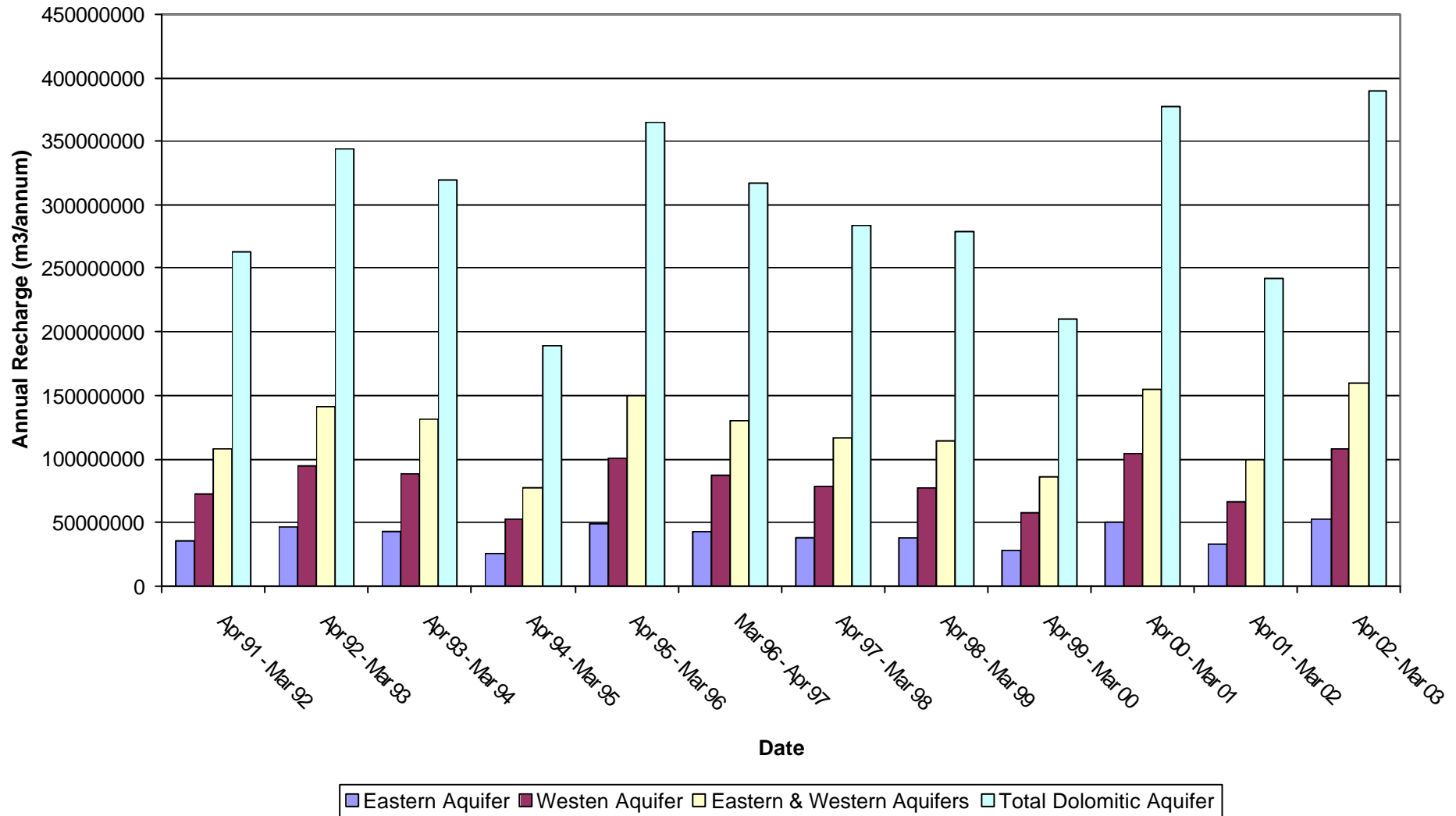
Table 3.7.3: Calculated Minimum and Maximum Annual Recharge Volumes.

Aquifer	Minimum Recharge (m³)	Maximum Recharge (m³)
Eastern	25 400 000	44 600 000
Western	52 070 000	91 430 000
Eastern & Western	77 470 000	136 030 000
Total Dolomitic	188 912 500	331 712 500

Based on a combined area of 488km² and a recharge percentage of 25% of the lowest recorded annual rainfall (635mm, during the time period April 1994 to March 1995), it is calculated that the total volume of water that can safely be abstracted from the combined eastern and western aquifers is 77 470 000m³/annum. Based on the 50 year average rainfall of 1 115mm, a maximum total volume of 136 030 000m³ can be abstracted per annum from the combined eastern and western aquifers.

Figure 3.7.1: Estimated Annual Recharge to the Aquifers.

Estimated Annual Recharge to the Aquifers



The Figure indicate the calculated annual recharge to the various aquifers. The recharge is calculated based on the actual observed rainfall. Recharge is calculated as 25% of the annual rainfall.

Figure No: 3.7.1

February 2005

Chapter 3.8 : Current Abstraction Volumes.

Very little abstraction data is available. Abstraction rates were inferred from recorded pumping hours and pump capacities.

From data supplied by MDC for the years 2000 and 2002, it is calculated that the current MDC abstraction is approximately 12 300 000m³/annum from the dolomitic aquifer at Kabanga Farm. A total volume of approximately 13 000 000m³/annum is released annually from Ipumbu dam for irrigation purposes.

Infrastructure and abstraction licenses at Lake Nampamba (Kabanga Farm) allows for the abstraction of 1 000l/s (86 400m³/day or 31 540 000m³/annum). The production boreholes as listed in Table 3.4.2 contribute to abstraction from the eastern aquifer in the Mpongwe Irrigation area.

Approximately 11 000 000m³ is abstracted from Lake Nampamba during the dry season. Based on a time period of seven months (210 days), an average of 52 380m³ is abstracted daily.

At Ipumbu farm, which forms part of the Munkumpu Irrigation area, water is released from the Ipumbu Dam for irrigation purposes. The water is routed to the centre pivots through a lined canal system. Approximately 13 000 000m³ of water is released from Ipumbu Dam annually for irrigation purposes. Approximately 1 300 000m³ and 11 700 000m³ of water is released during the wet and dry seasons respectively.

The dam is recharged through a combination of surface water run-off from rainfall and springs. The landscape within the dam is dotted with several dambo areas in the vicinity of the Munkumpu fault zone that forms the contact between the dolomitic aquifer and the neighbouring quartzite (refer to Figure 3.8.1).

Recharge from rainfall or surface run-off water is considered to be minimal due to the fact that there is only one non-perennial surface run-off feature that feeds into the dam. Therefore, the majority of the non-groundwater related water that recharges the dam would be from direct rainfall.

It is therefore considered that the majority of the water in the Ipumbu Dam originates from the dambo areas, and thus from the groundwater.

Therefore, for the purpose of calculations in this paper, the volume of water released from Ipumbu dam is considered to be the volume of water abstracted from the aquifer.

The calculated current abstraction volumes for the wet and dry seasons are shown in Table 3.8.1.

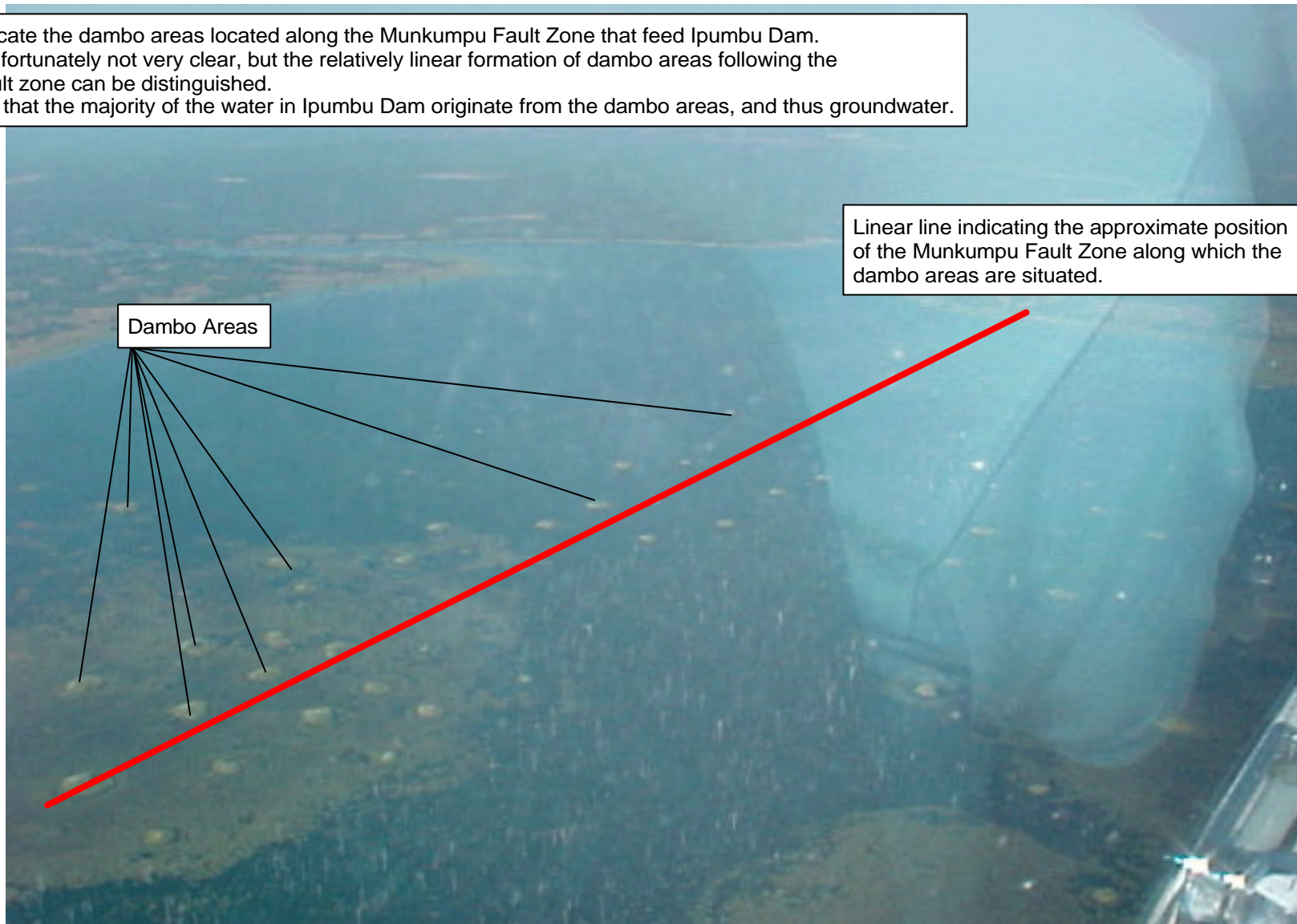
Table 3.8.1: Current Abstraction Rates.

Abstraction Point	Wet Season	Dry Season
Lake Nampamba	8 700m ³ /day	52 380m ³ /day
Ipumbu Dam	8 700m ³ /day	55 700m ³ /day

Figure 3.8.1: Dambo Areas along the Munkumpu Fault Zone Feeding Ipumbu Dam.

Dambo Areas along the Munkumpu Fault Zone Feeding Ipumbu Dam

The Figure indicate the dambo areas located along the Munkumpu Fault Zone that feed Ipumbu Dam. The photo is unfortunately not very clear, but the relatively linear formation of dambo areas following the Munkumpu Fault zone can be distinguished. It is considered that the majority of the water in Ipumbu Dam originate from the dambo areas, and thus groundwater.



Chapter 3.9 : Current and Future Sustainability Evaluation Calculations.

MDC plans to expand the irrigable land from 4 150ha to 6 500ha. Due to operational problems with the 200ha pivots, it is intended to limit the pivot size to 100ha or 150ha. Another 16 to 25 pivots will therefore need to be installed.

Based on the proposed expansion, the volume of water required to meet the annual irrigation demands can be calculated as follows:

Table 3.9.1: Proposed Future Abstraction Rates.

Abstraction Point	Wet Season	Dry Season
Lake Nampamba	13 700m ³ /day	82 800m ³ /day
Ipumbu Dam	16 700m ³ /day	107 000m ³ /day

Incorporating the above data in the calculations, it is possible to evaluate the sustainability of the current and the future abstraction rates from the aquifer. In a simplified system, this can be done by comparing the recharge to the system from rainfall to the abstraction rate through the equation:

$$\text{Net Groundwater Volume} = \text{Recharge} - \text{Abstraction} \quad (\text{Eq 3.9.1})$$

A negative net groundwater volume indicates that dewatering of the system occurs.

In order to illustrate the sustainability of the abstraction program from the combined eastern and western aquifers, recharge calculated from actual observed rainfall data for the time period January 1991 to December 2003 is plotted against the calculated average abstraction rates in Figure 3.9.1.

Figure 3.9.1 indicates that the net volume of water in the combined eastern and western aquifers varies with time according to the annual recharge volume. However, the net volume of water is positive at all times, indicating that the annual recharge exceeds the annual abstraction.

In order for the groundwater system to stay in equilibrium the excess (positive net volume) water leaves the system at another unknown point, possibly the Kafue River as suggested by Scott Wilson Piésold (2003).

Baseline calculations indicate that under natural conditions as much as 44 000 000m³ can flow annually into the Kafue River as base flow contribution.

Figure 3.9.2 indicates the influence of the proposed future abstraction regime on the net groundwater volume in storage in the aquifer. This figure indicates that the aquifer can sustain the proposed abstraction volumes.

Figure 3.9.1: Sustainability Calculations: Current Abstraction Rates.

Sustainability Calculations: Current Abstraction Rates

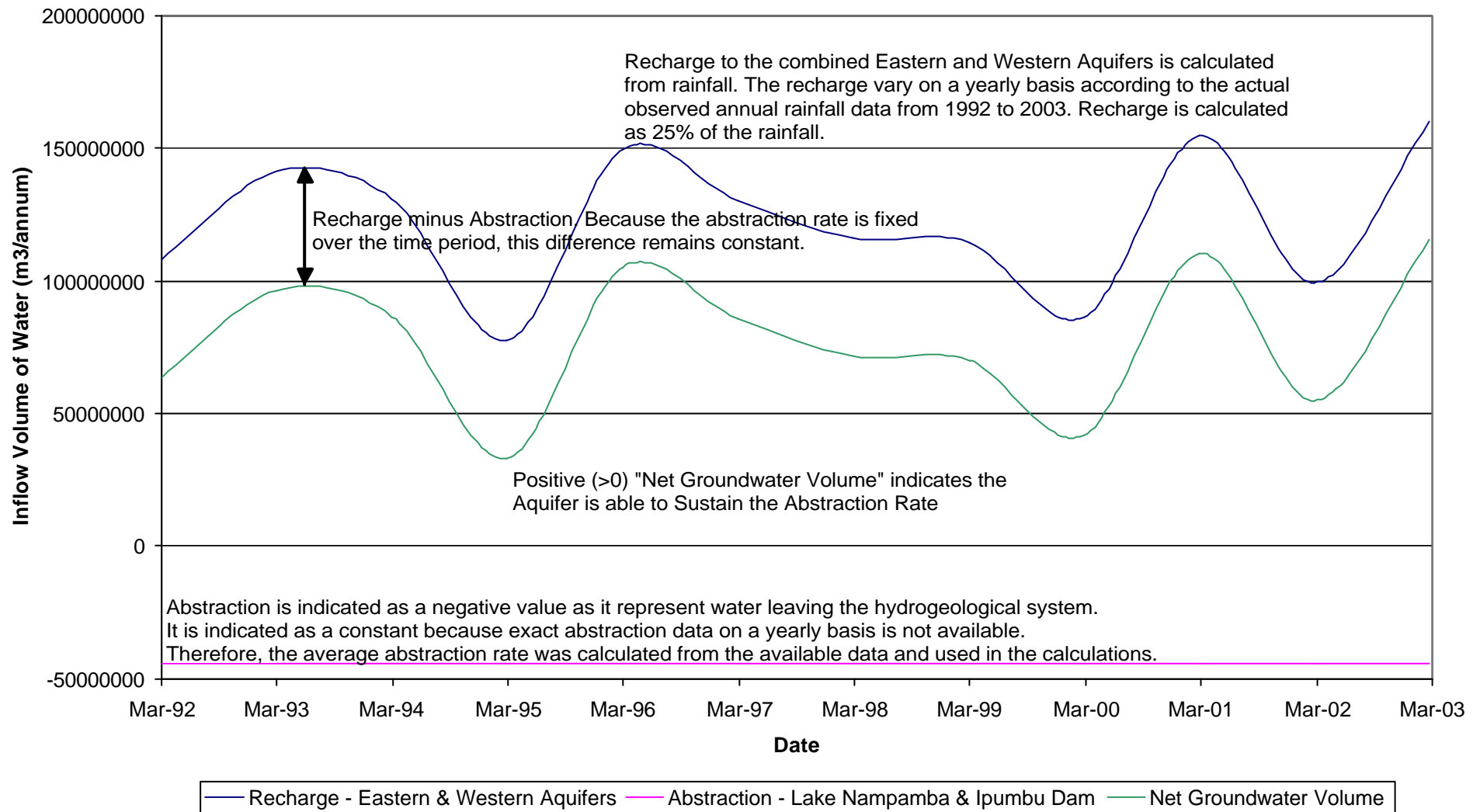


Figure No: 3.9.1

February 2005

Figure 3.9.2: Sustainability Calculations: Proposed Future Abstraction Rates.

Sustainability Calculations: Proposed Future Abstraction Rates

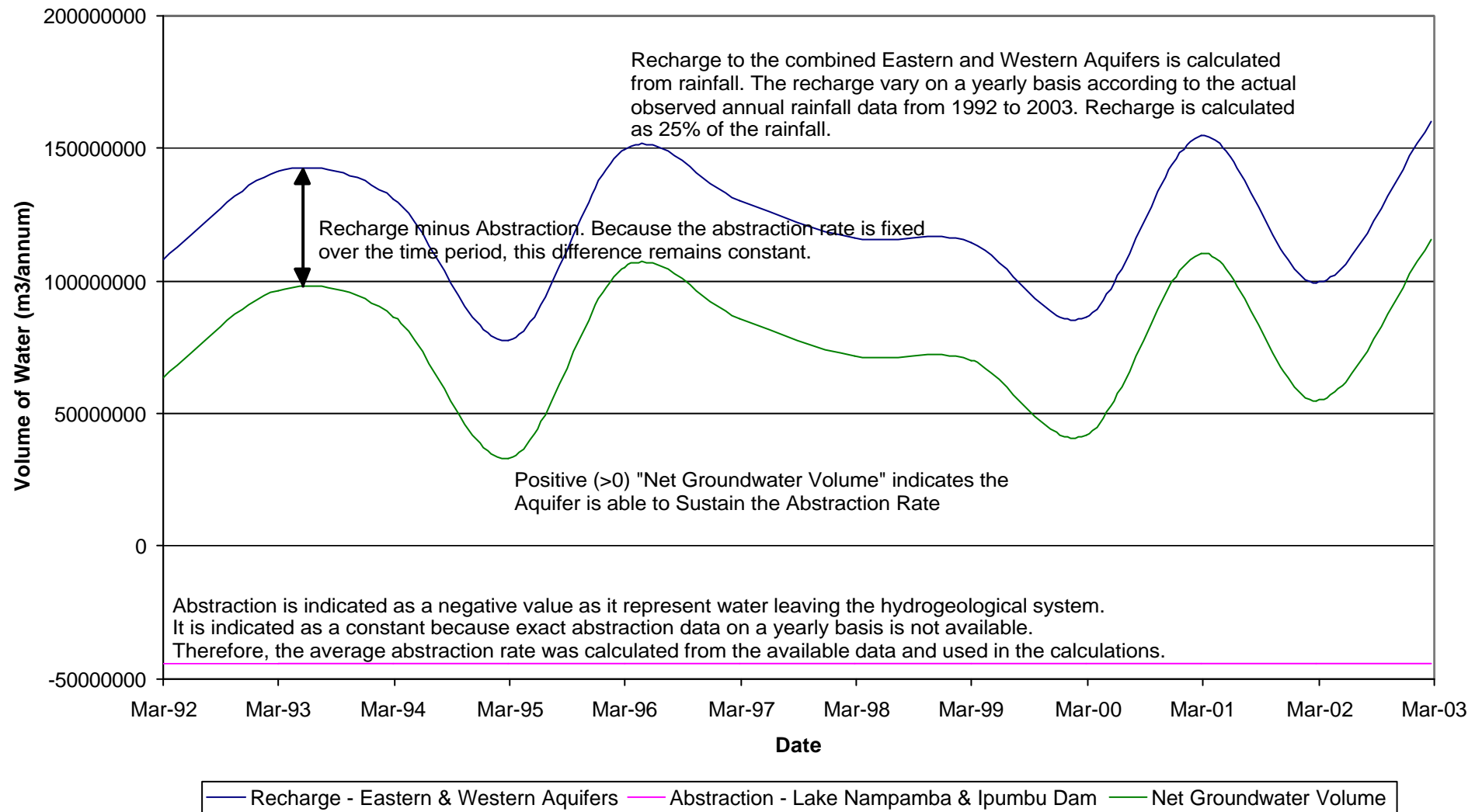


Figure No: 3.9.2

February 2005

Chapter 4 : Numerical Modelling.

Chapter 4.1 : Background to Numerical Modelling.

Numerical modelling was performed in order to substantiate the calculations and assumptions discussed in Chapters 2 and 3. The numerical model is based on mathematical equations representing the groundwater flow in the area. The calculated aquifer parameters were used and adjusted during the construction and calibration of the model.

Following the calibration of the numerical model the current and proposed groundwater abstraction scenarios were modelled in order to confirm and illustrate whether the aquifer is capable of sustaining the abstraction regimes.

The model was constructed using the Processing Modflow (version 5.1.7) software. The software was developed under copyright (1991 to 1997) of W.-H Chiang and W. Kinzelbach.

Because they provide the most versatile approach to groundwater problems, numerical models have outclassed all other types of groundwater models. The well-earned popularity of numerical models, however, may lead to overestimation of their potential. Groundwater systems are complicated and are often beyond our capability of evaluating them in too fine a detail.

In order to understand the groundwater problem under investigation, assumptions and simplifications are required. In most groundwater investigations it is not practical to monitor all aspects of the groundwater flow and solute distribution. Information between and beyond monitoring points and in the future is needed to understand the site and make more informed decisions.

No matter how sophisticated a numerical model is, it will never be able to describe the groundwater system under investigation without deviation of model simulations from the actual physical processes. As a consequence, in applying a numerical model to a field

investigation, the model user should always understand the implications of simplifying assumptions. Every reliable model is based and calibrated on accurate field data.

In designing a groundwater model, the model user combines various modelling components. These components are (Spits and Moreno, 1996):

- Natural system for which the model is designed.
- Conceptual model as an idealised representation of the natural system.
- Mathematical model representing controlling mechanisms in mathematical terms.
- Solution of the mathematical model.
- Calibration of the solution by adjusting simulated to actual observed responses of the natural system.
- Validation of the accuracy of the model predictions.
- Simulations based on the calibrated solution of the conceptual model.

Numerical modelling is a tool used to solve problems, but in itself, is not a solution to the problems. Numerical models do not give accurate answers to insufficiently defined problems. Neither do the models magically release the model users from their responsibility to carefully study the groundwater system. Numerical modelling is not a question of understanding the numerical techniques, but of understanding the model application and limitations.

Numerical models follow two approaches. These are:

- Finite difference calculations.
- Finite element calculations.

Both of these approaches have advantages and disadvantages. Processing Modflow is based on the finite difference approach.

The fundamentals of the mathematical equations and calculation methodology used during numerical modelling are described below. The explanation is based on the explanatory notes provided by the United States Geological Survey (USGS) in 1988.

The three dimensional movement of groundwater of constant density through porous material may be described by the partial-differential equation.

The partial-differential equation is shown below:

$$\frac{\partial}{\partial x} \left(K_{xx} \frac{\partial h}{\partial x} \right) + \frac{\partial}{\partial y} \left(K_{yy} \frac{\partial h}{\partial y} \right) + \frac{\partial}{\partial z} \left(K_{zz} \frac{\partial h}{\partial z} \right) - W = S_s \frac{\partial h}{\partial t} \quad (\text{Eq 4.1.1})$$

where:

K_{xx} , K_{yy} and K_{zz} are values of hydraulic conductivity along the x, y and z coordinate axes, which are assumed to be parallel to the major axes of hydraulic conductivity (Lt^{-1}).

h is the potentiometric head (L)

W is a volumetric flux per unit volume and represents sources and/or sinks of water (t^{-1})

S_s is the specific storage of the porous material (L^{-1}), and

t is time (t)

In general, S_s , K_{xx} , K_{yy} and K_{zz} may be functions of space ($S_s = S_s(x,y,z)$, etc). W may be a function of space and time ($W = W(x,y,z,t)$). Equation 4.1.1 describes the groundwater flow under non-equilibrium conditions in a heterogeneous and anisotropic medium, provided the principal axes of hydraulic conductivity are aligned with the coordinate directions.

Equation 4.1.1, together with specification of flow and/or head conditions at the boundaries of an aquifer system and specification of initial head conditions, constitutes a mathematical representation of a groundwater flow system.

A solution of Equation 4.1.1, in an analytical sense, is an algebraic expression giving $h(x,y,z,t)$ such that when the derivative of h with respect to space and time are substituted into Equation 4.1.1, the equation and its initial and boundary conditions are satisfied.

A time varying head distribution of this nature characterizes the flow system, in that it measures both the energy of flow and the volume of water in storage, and can be used to calculate directions and rates of movement.

Except for very simple systems, analytical solutions of Equation 4.1.1 are rarely possible. Due to this, various numerical methods must be employed to obtain approximate solutions.

One approach is the finite difference method. The finite difference method replaces the continuous system described by Equation 4.1.1 with a finite set of discrete points in space and time. The partial derivatives are replaced by terms calculated from the differences in head values at these points.

The process leads to systems of simultaneous linear algebraic difference equations. Solutions of these equations yields the head (water level) values at specific points and times. These water level values constitute an approximation to the time varying head distribution that would be given by an analytical solution of the partial differential flow equation.

The finite difference approach is best described in Figure 4.1.1. The figure indicates the spatial division of an aquifer system through the use of a three dimensional sketch. The blocks are called cells. The location of each cell is described in terms of rows, columns and layers. General practice follows an i,j,k indexing system.

For a system consisting of “ n ” rows, “ n ” columns, and “ n ” layers, i is the row index, j is the column index and k is the layer index. As an example, Figure 4.1.1 indicates a system with $nrow = 4$, $ncol = 7$ and $nlay = 4$.

The model is usually constructed in such a way that the layers correspond to horizontal hydrogeological units or intervals.

Thus, in Cartesian coordinates, the k index denotes the changes along the vertical direction (z). General practice has it that the layers are numbered from the top down, thus an increase in the k index indicates a decrease in elevation.

Similarly, the rows are considered to be parallel to the x-axis so that increments in the row index (*i*) would correspond to decreases in the y-direction. Columns are considered to be parallel to the y-axis. Increments in the column index, *j*, would correspond to increases in the x-direction.

Following the conventions used in Figure 4.1.1, the width of the cells in the row (*j*) direction is expressed as Δr_j , the width of the cells in the column direction at a given row, *i*, is designated Δc_i and the thickness of the cells in a given layer, *k*, is designated Δv_k . Thus the cell with coordinates $(i,j,k) = (3,5,3)$ has a volume of $\Delta r_3 \times \Delta c_5 \times \Delta v_3$.

The centre of each cell is called the node at which the water level (head) is calculated. Two methods of defining the cell configuration in relation to the location of the node exist. The first is the block centred approach and the second is the point centred approach. Discussion in this document will be limited to the block centred approach as this is the methodology used in the construction of the numerical model.

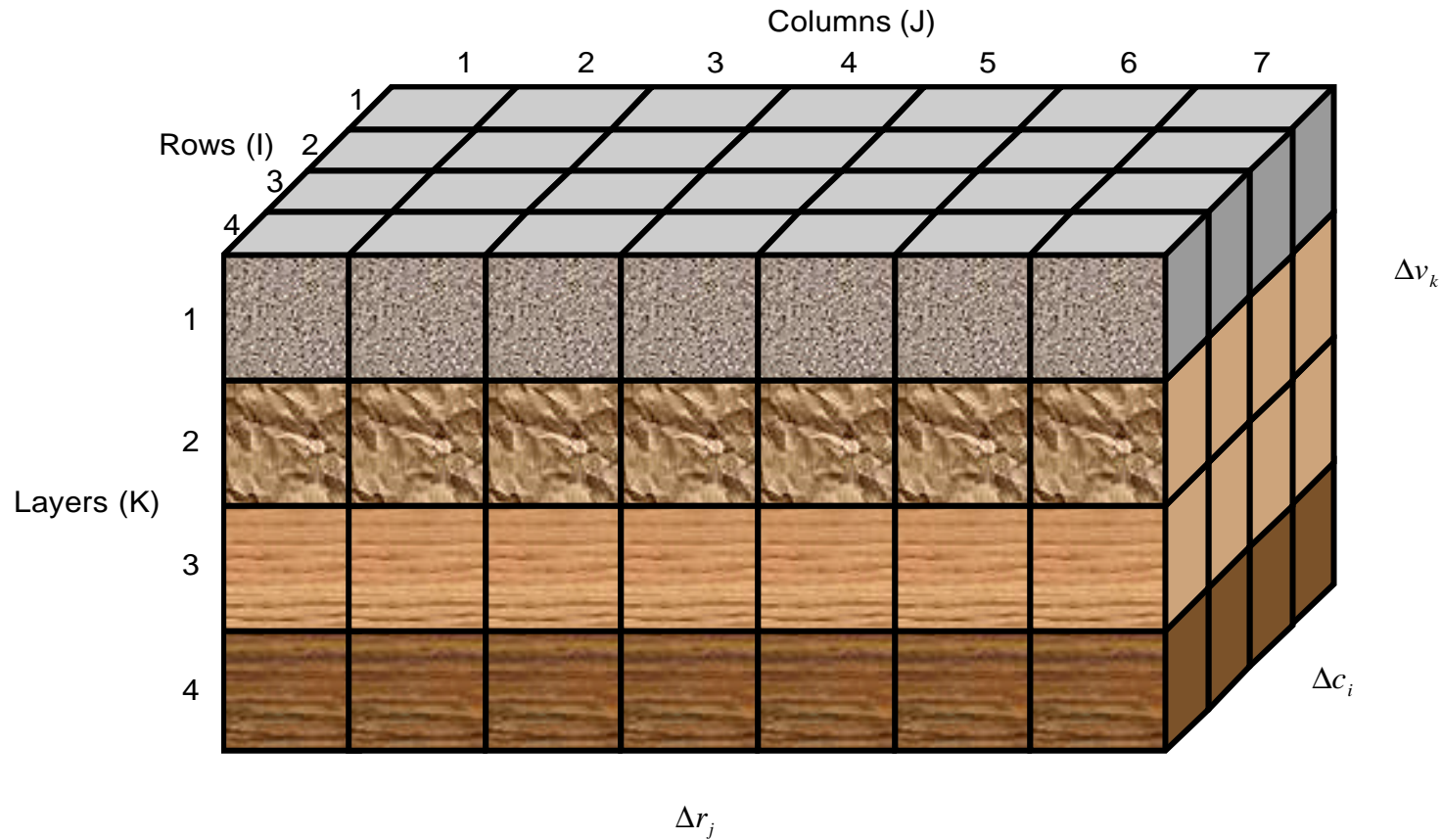
Figure 4.1.2 illustrates, in two dimensions, the block centred convention. The blocks formed by the parallel lines are the cells, with the nodes located at the centre of the blocks.

Spacing of the nodes should be such that the hydraulic properties of the system are generally uniform over the extent of the cell.

The finite difference flow equation is deduced from the application of the continuity equation. This equation states that the sum of all flows into and out of a cell must be equal to the rate of change in storage within that cell.

Figure 4.1.1: Spatial Division of an Aquifer System used during Numerical Modelling.

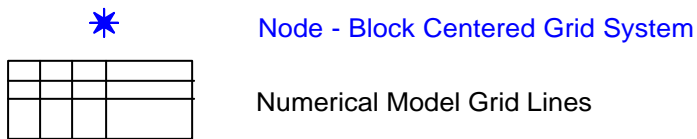
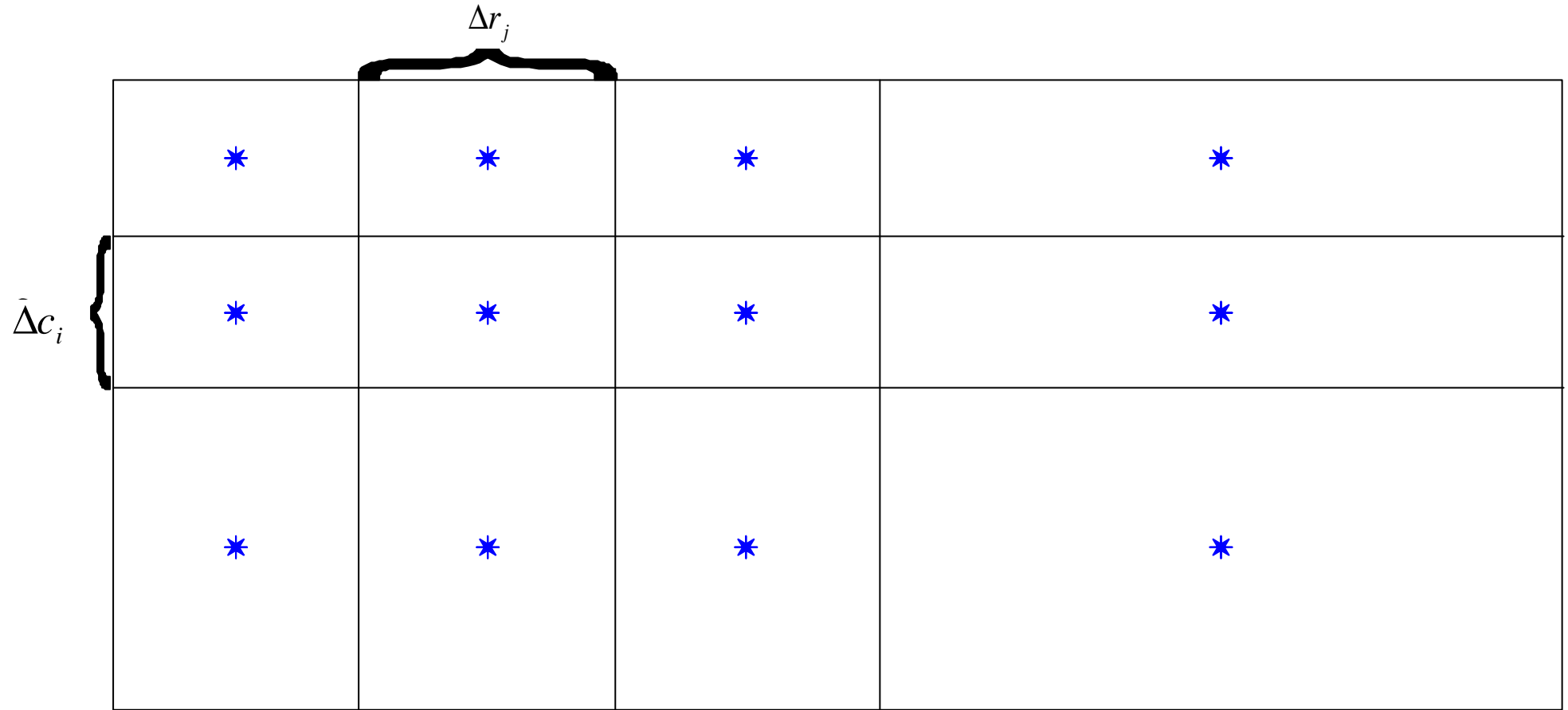
Spatial Division of an Aquifer System used during Numerical Modelling



- Δr_j = Dimension of cell along the row direction. Subscript (J) indicates the number of the column
- Δc_i = Dimension of cell along the column direction. Subscript (I) indicates the number of the row
- Δv_k = Dimension of cell along the vertical direction. Subscript (K) indicates the number of the layer

Figure 4.1.2: Numerical Model Grid indicating the Block Centered Method.

Numerical Model Grid indicating the Block Centered Method



The Figure show a plan view of a theoretical model with 4 columns and 3 rows. The blue star indicate the centre of each cell. Following the Block Centered Method calculations are performed at the centre of each cell.

Assuming that the density of groundwater is constant, the continuity equation for expressing the balance of flow in a cell is expressed as (USGS, 1988):

$$\sum Q_i = S_s \frac{\Delta h}{\Delta t} \Delta V \quad (\text{Eq 4.1.2})$$

where:

- Q_i = the flow rate into the cell (L^3t^{-1}).
- S_s = the specific storage in the finite difference equation (L^{-1}).
- ΔV = the volume of the cell (L^3).
- Δh = the change in head over a time interval of length Δt .

The right hand side term can be described as the volume of water taken into storage over a time interval Δt given a change in head of Δh .

Equation 4.1.2 is stated in terms of inflow and storage gain. Outflow and loss are represented by defining outflow as negative inflow and loss as negative gain.

Figure 4.1.3 shows a cell i,j,k and six adjacent aquifer cells. These cells are:

- $i-1,j,k$
- $i+1,j,k$
- $i,j-1,k$
- $i,j+1,k$
- $i,j,k-1$
- $i,j,k+1$

In order to simplify the explanation, flows are considered to be positive when it enters cell i,j,k and the negative sign usually incorporated into Darcy's law has been omitted from all terms.

Following these conventions, flow into cell i,j,k in the row direction from cell $i,j-1,k$ (refer to Figure 4.1.4) is given by Darcy's law as:

$$q_{i,j-\frac{1}{2},k} = KR_{i,j-\frac{1}{2},k} \Delta c_i \Delta v_k \frac{(h_{i,j-1,k} - h_{i,j,k})}{\Delta r_{j-\frac{1}{2}}} \quad (\text{Eq 4.1.3})$$

where:

- $h_{i,j,k}$ = the head at node i,j,k
- $h_{i,j-1,k}$ = the head at node $i,j-1,k$
- $q_{i,j-\frac{1}{2},k}$ = the volumetric fluid discharge through the face between cells i,j,k and $i,j-1,k$ (L^3t^{-1})
- $KR_{i,j-\frac{1}{2},k}$ = the hydraulic conductivity along the row between nodes i,j,k and $i,j-1,k$ (Lt^{-1})
- $\Delta c_i \Delta v_k$ = the area of the cell faces normal to the row direction (L^2).
- $\Delta r_{j-\frac{1}{2}}$ = the distance between the nodes i,j,k and $i,j-1,k$ (L).

The term $KR_{i,j-\frac{1}{2},k}$ refers to the entire region between the nodes and is normally calculated as a harmonic mean. Following this, Equation 4.1.3 gives the exact flow, for a one dimensional steady state case, through a block of aquifer extending from node $i,j-1,k$ to node i,j,k and having a cross sectional area $\Delta c_i \Delta v_k$.

Similar expressions can be written approximating the flow into the cell through the remaining five faces (refer to Figure 4.1.3), i.e., for flow in the row direction through the faces i,j,k and $i,j+1,k$:

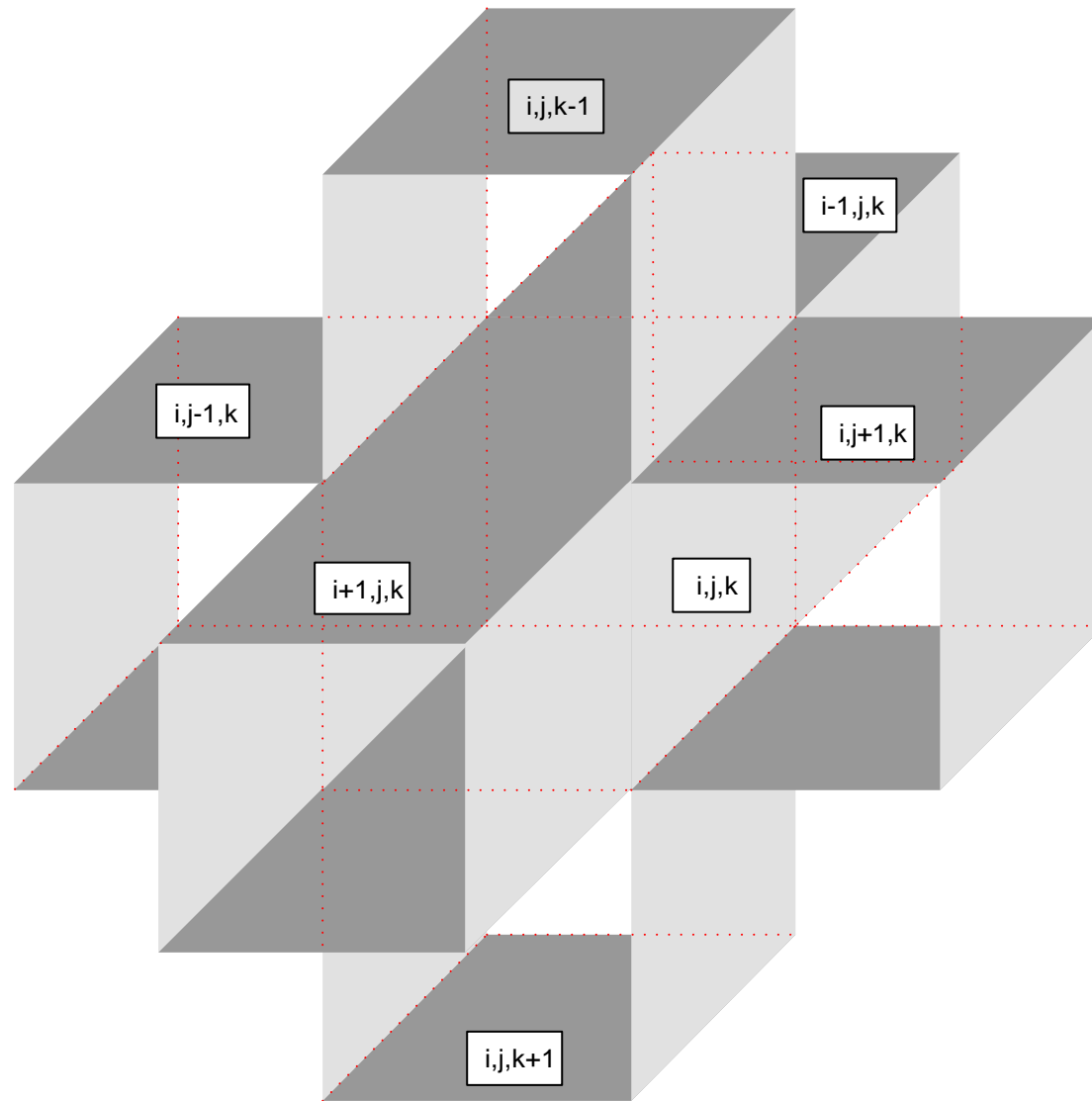
$$q_{i,j+\frac{1}{2},k} = KR_{i,j+\frac{1}{2},k} \Delta c_i \Delta v_k \frac{(h_{i,j+1,k} - h_{i,j,k})}{\Delta r_{j+\frac{1}{2}}} \quad (\text{Eq 4.1.4})$$

while for the column direction, flow into the block through the forward face is:

$$q_{i+\frac{1}{2},j,k} = KC_{i+\frac{1}{2},j,k} \Delta r_j \Delta v_k \frac{(h_{i+1,j,k} - h_{i,j,k})}{\Delta c_{i+\frac{1}{2}}} \quad (\text{Eq 4.1.5})$$

Figure 4.1.3: Cell i,j,k and the Six Adjacent Cell Indices.

Cell i,j,k and the Six Adjacent Cell Indices



The Figure indicates cell i,j,k , which is located in the middle, and the six adjacent cells. Each of the six adjacent cells is located on a different face of cell i,j,k . The indices for each cell is indicated.



Numerical Model Cell



Hidden Line

Figure 4.1.4: Flow from Cell $i,j-1,k$ into Cell i,j,k .

Flow from Cell $i,j-1,k$ into Cell i,j,k

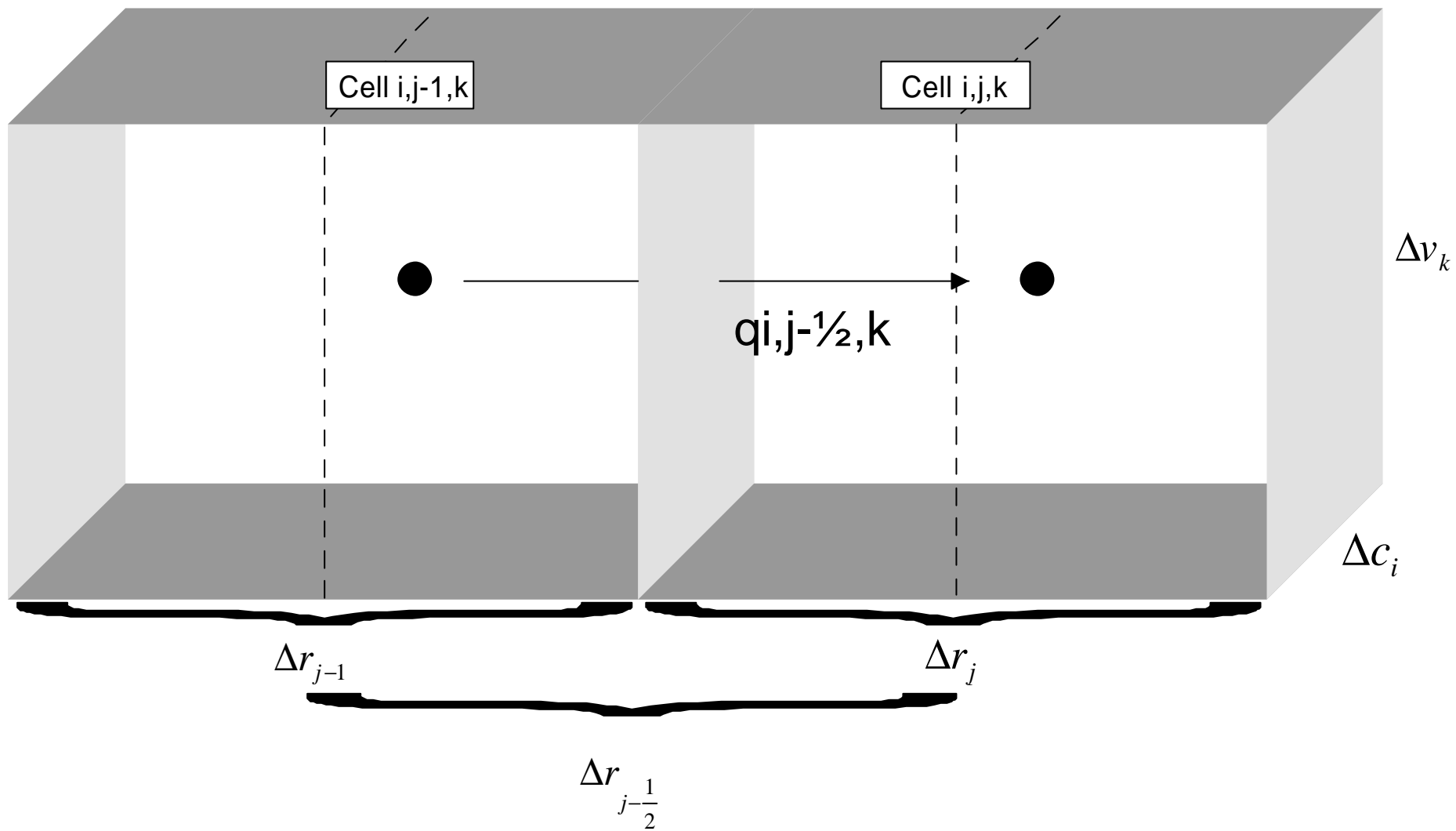


Figure No: 4.1.4

February 2005

and flow into the block through the rear face is:

$$q_{i,-\frac{1}{2},j,k} = KC_{i-\frac{1}{2},j,k} \Delta r_j \Delta v_k \frac{(h_{i-1,j,k} - h_{i,j,k})}{\Delta c_{i-\frac{1}{2}}} \quad (\text{Eq 4.1.6})$$

For the vertical direction, inflow through the bottom face is:

$$q_{i,j,k+\frac{1}{2}} = KV_{i,j,k+\frac{1}{2}} \Delta r_j \Delta c_i \frac{(h_{i,j,j+1} - h_{i,j,k})}{\Delta v_{k+\frac{1}{2}}} \quad (\text{Eq 4.1.7})$$

while inflow through the upper face is represented by:

$$q_{i,j,k-\frac{1}{2}} = KV_{i,j,k-\frac{1}{2}} \Delta r_j \Delta c_i \frac{(h_{i,j,j-1} - h_{i,j,k})}{\Delta v_{k-\frac{1}{2}}} \quad (\text{Eq 4.1.8})$$

Each of the Equations 4.1.3 to 4.1.8 express inflow through a face of cell i,j,k in terms of heads, grid dimensions and hydraulic conductivity. The notation can be simplified by combining the grid dimensions and hydraulic conductivity into a single constant, the hydraulic conductance, e.g.:

$$CR_{i,j-\frac{1}{2},k} = KR_{i,j-\frac{1}{2},k} \frac{\Delta c_i \Delta v_k}{\Delta r_{j-\frac{1}{2}}} \quad (\text{Eq 4.1.9})$$

where:

$$CR_{i,j-\frac{1}{2},k} = \text{the conductance in row } i \text{ and layer } k \text{ between nodes } i,j-1,k \text{ and } i,j,k \text{ (L}^2\text{t}^{-1}\text{)}.$$

Conductance is thus the product of hydraulic conductivity and cross sectional area of flow divided by the length of the flow path (distance between the nodes).

Substituting conductance from Equation 4.1.9 into Equation 4.1.3 yields:

$$q_{i,j-\frac{1}{2},k} = CR_{i,j-\frac{1}{2},k} (h_{i,j-1,k} - h_{i,j,k}) \quad (\text{Eq 4.1.10})$$

Similarly, Equations 4.1.4 to 4.1.8 can be re-written to yield:

$$q_{i,j+\frac{1}{2},k} = CR_{i,j+\frac{1}{2},k} (h_{i,j+1,k} - h_{i,j,k}) \quad (\text{Eq 4.1.11})$$

$$q_{i-\frac{1}{2},j,k} = CC_{i-\frac{1}{2},j,k} (h_{i-1,j,k} - h_{i,j,k}) \quad (\text{Eq 4.1.12})$$

$$q_{i+\frac{1}{2},j,k} = CC_{i+\frac{1}{2},j,k} (h_{i+1,j,k} - h_{i,j,k}) \quad (\text{Eq 4.1.13})$$

$$q_{i,j,k-\frac{1}{2}} = CV_{i,j,k-\frac{1}{2}} (h_{i,j,k-1} - h_{i,j,k}) \quad (\text{Eq 4.1.14})$$

$$q_{i,j,k+\frac{1}{2}} = CV_{i,j,k+\frac{1}{2}} (h_{i,j,k+1} - h_{i,j,k}) \quad (\text{Eq 4.1.15})$$

where the conductances are defined analogously to $CR_{i,j-\frac{1}{2},k}$ in Equation 4.1.9.

Equations 4.1.10 to 4.1.15 account for the flow into cell i,j,k from the six adjacent cells. To account for flows into the cell from external features or processes such as rivers, recharge or drains, additional terms are necessary. Flow from outside the aquifer is represented by:

$$a_{i,j,k,n} = p_{i,j,k,n} h_{i,j,k} + q_{i,j,k,n} \quad (\text{Eq 4.1.16})$$

where:

$a_{i,j,k,n}$ = flow from the n^{th} external source into cell i,j,k (L^3t^{-1}) and
 $p_{i,j,k,n}$ and $q_{i,j,k,n}$ are constants ((L^2t^{-1}) and (L^3t^{-1}) respectively).

In general, if there are N external sources or stresses affecting a single cell, the combined flow is expressed as:

$$QS_{i,j,k} = \sum_{n=1}^N a_{i,j,k,n} = \sum_{n=1}^N p_{i,j,k,n} h_{i,j,k} + \sum_{n=1}^N q_{i,j,k,n} \quad (\text{Eq 4.1.17})$$

Defining $P_{i,j,k}$ and $Q_{i,j,k}$ by the expressions:

$$P_{i,j,k} = \sum_{n=1}^N p_{i,j,k,n} \quad (\text{Eq 4.1.18})$$

$$Q_{i,j,k} = \sum_{n=1}^N q_{i,j,k,n} \quad (\text{Eq 4.1.19})$$

The general external flow term for cell i,j,k is:

$$QS_{i,j,k} = P_{i,j,k} h_{i,j,k} + Q_{i,j,k} \quad (\text{Eq 4.1.20})$$

Applying the continuity Equation 4.1.2 and taking into account the flows from the six adjacent cells, as well as the external flow rate, QS , yields:

$$q_{i,j-\frac{1}{2},k} + q_{i,j+\frac{1}{2},k} + q_{i-\frac{1}{2},j,k} + q_{i+\frac{1}{2},j,k} + q_{i,j,k-\frac{1}{2}} + q_{i,j,k+\frac{1}{2}} + QS_{i,j,k} = SS_{i,j,k} \frac{\Delta h_{i,j,k}}{\Delta t} \Delta r_j \Delta c_i \Delta v_k \quad (\text{Eq 4.1.21})$$

where:

$$\frac{\Delta h_{i,j,k}}{\Delta t} = \text{a finite difference approximation for the derivative of head with respect to time (Lt}^{-1}\text{).}$$

$$SS_{i,j,k} = \text{the specific storage of cell } i,j,k \text{ (L}^{-1}\text{)}$$

$$\Delta r_j \Delta c_i \Delta v_k = \text{the volume of the cell } i,j,k \text{ (L}^3\text{).}$$

Equations 4.1.10 to 4.1.15 and 4.1.20 can be substituted into Equation 4.1.21 to yield the finite difference approximation for the cell i,j,k .

$$\begin{aligned} & CR_{i,j-\frac{1}{2},k} (h_{i,j-1,k} - h_{i,j,k}) + CR_{i,j+\frac{1}{2},k} (h_{i,j+1,k} - h_{i,j,k}) \\ & + CC_{i-\frac{1}{2},j,k} (h_{i-1,j,k} - h_{i,j,k}) + CC_{i+\frac{1}{2},j,k} (h_{i+1,j,k} - h_{i,j,k}) \\ & + CV_{i,j,k-\frac{1}{2}} (h_{i,j,k-1} - h_{i,j,k}) + CV_{i,j,k+\frac{1}{2}} (h_{i,j,k+1} - h_{i,j,k}) \\ & P_{i,j,k} h_{i,j,k} + Q_{i,j,k} = SS_{i,j,k} \frac{\Delta h_{i,j,k}}{\Delta t} (\Delta r_j \Delta c_i \Delta v_k) \end{aligned}$$

(Eq 4.1.22)

The numerical model utilises iterative methods in order to obtain the solution to the system of finite difference equations for each time step. The ideal would be to stop the iteration process when the calculated heads are suitably close to the exact position. However, because the exact solution is unknown, an indirect method of specifying when to stop iterating is employed.

The most commonly used method is to specify the required difference in subsequent iterations. Once the change in head is less than the specified value, the iteration process for the time step is completed. This value is usually in the order of 0.01 to 0.001m (1cm to 1mm).

Chapter 4.2 : Construction and Calibration of the Model.

During the construction of the numerical model the aquifer parameters, as estimated during this study by the author and by previous consultants, were analysed and incorporated into the model. Due to the fact that the pumping regime and the natural factors such as rainfall differ significantly between the dry season (April to October) and the wet season (November to March), the model was constructed in such a way as to be able to distinguish between the two seasons.

Due to the fact that the hydrogeological conditions in the eastern and western aquifers, such as lithology, flow gradients, and nature of the aquifer, are the same and the two aquifers are considered to be interconnected (refer to Chapter 3) the numerical model does not distinguish between the two aquifers by way of different transmissivities, storativities or a flow barrier between the two aquifer.

Chapter 4.2.1 : Initial Calibration (No Abstraction)

The numerical model was first constructed and calibrated in the steady state. During this phase the aquifer parameters such as transmissivity, recharge and storage coefficient were varied within acceptable ranges to obtain a modelled transient state water level that corresponds with that observed by the author during the 2003 hydrocensus.

Once the model was calibrated in the steady state environment, running the model in the transient state and noting whether the water levels increased or decreased with time further tested the accuracy of the calibration. The time parameter was set at one stress period of 500 years, divided into 50 equal time steps of 10 years each. This time period is considered to be of sufficient length so that any variations in the simulated transient state water level will be shown.

The model parameters at which an acceptable level of calibration was reached are summarised briefly in Table 4.2.1.1.

The Table indicates that the transmissivity of the aquifers falls within the expected range. Transmissivity of the known solution cavity areas (Lake Nampamba) was calibrated at

5 000m²/day, while the general transmissivity of the limestone and dolomitic aquifer is 1 000m²/day. These values correspond well with transmissivities shown in Chapter 3.4.

Table 4.2.1.1: Initial Calibrated Model Parameters (No Abstraction).

Parameter	Unit	Calibrated Value
Time	Days	182 500
Transmissivity (Areas of known solution cavities such as Lake Nampamba)	m ² /day	5 000
Transmissivity (Areas of strongly suspected cavities from geological and geophysical data)	m ² /day	2 000
Transmissivity (Rest of study area where solution cavities might occur)	m ² /day	1 000
Transmissivity (Schist)	m ² /day	3.5
Storage Coefficient (Area of known solution cavities - Lake Nampamba)		1
Storage Coefficient (Rest of study area)		0.02
Recharge (Limestone / Dolomitic Area)	% of average annual rainfall)	8
Recharge (Schist)	% of average annual rainfall)	3
Recharge (Ipumbu Dam)	% of average annual rainfall)	35
Solver used		pcg2
Preconditioning method		Modified Incomplete Cholesky
Outer Iteration (MXITER)		30
Inner Iteration (ITER1)		200
Convergence Criteria (Head Change)	m	0.01
Convergence Criteria (Residual)	m	0.01
Modflow Version		PMWIN 4.X

The storage coefficient was calibrated at 0.02 (2%). This corresponds exactly with the aquifer storativity calculated in Chapter 3.6.

Recharge percentages in the limestone and schist areas were much lower than expected based on the calculations shown in Chapter 3.5. Manual recharge calculations

shown in Chapter 3.5 indicated a range of approximately 25% of annual rainfall. However, the manual calculations took the current abstraction volumes into account, whereas this initial calibration of the model did not. Incorporating abstraction while maintaining the observed groundwater level would necessitate higher recharge percentages. Therefore, it is to be expected that a model that does not take the abstraction into account would underestimate the recharge.

Recharge at Ipumbu Dam is calibrated at 35% of mean annual rainfall. This is considered to be higher than the actual value. However, due to the inherent difficulties in simulating the water level in a surface water body using a groundwater model, and the absence of groundwater level data in the vicinity of the dam due to the fact that no boreholes are located in its vicinity, it was not possible to obtain a better estimation, or to determine the flow gradient between the dam and the groundwater.

Based on the above, the author decided to focus more on the transmissivity and storativity of the aquifer, calibrating it to within realistic values indicated by the calculations shown in Chapter 3. Values for transmissivity and storativity were fixed as listed in Table 4.2.1.1.

Chapter 4.2.2 : Calibration Taking Abstraction in Account.

Once the model was calibrated as stated above, the ability of the numerical model to accurately predict the groundwater level fluctuations due to seasonal changes in rainfall and abstraction volumes was tested by incorporating the actual observed water levels and rainfall for the time period April 1997 (beginning of a dry season) to October 2002 (end of a wet season) into the model.

Some parameter adjustments had to be made in order to obtain the best correlation between the observed water level fluctuations and the values calculated by the numerical model.

Calibration of the model was performed by comparing the actual water levels in Lake Nampamba to those calculated using the numerical model. Points taken into consideration when comparing the observed and simulated groundwater levels include:

-
- General decreasing or increasing trend with time
 - Amplitude of water level variations
 - Vertical displacement between observed and simulated water levels in metres above mean sea level
 - Do the simulated water levels fluctuate correctly (decreasing during dry seasons and increasing during wet seasons)?
 - Does the simulated data appear realistic and natural?

It was attempted to simulate the change in water level in Ipumbu Dam because it is believed that water level fluctuations in the dam can at least partially be attributed to seasonal changes in yield from the dambo areas located within the dam area (refer to Figure 3.8.1). However, the water level in the surface water body could not be simulated accurately due to the inherent nature of the groundwater modelling package. The package is unable to directly simulate water levels in surface water bodies such as dams.

The best dam water level estimations can be made by assuming that the water level in the dam will reflect the immediately surrounding groundwater level. As a matter of interest, this water level is shown along with the simulated water level in Lake Nampamba in Figure 4.2.2.1.

Incorporating the actual observed rainfall and Lake Nampamba water level data with time into the numerical model meant that the model could be calibrated much more accurately than would be the case when the model is calibrated based on water levels observed at one point in time only. The data used during the calibration is summarised in Table 4.2.2.1. Note that pumps 4, 5 and 6 listed in the Table abstract water from Lake Nampamba. No detail abstraction data from Ipumbu Dam is available.

The average water levels in Lake Nampamba have been calculated based on the daily water level as measured at 12h00 (midday).

Rainfall data incorporated into the model was obtained from the Mpongwe Farm records supplied by MDC. The rainfall data was grouped into seasonal volumes. Based on this

actual rainfall data and the recharge percentage, a unique daily recharge flux was calculated for each season.

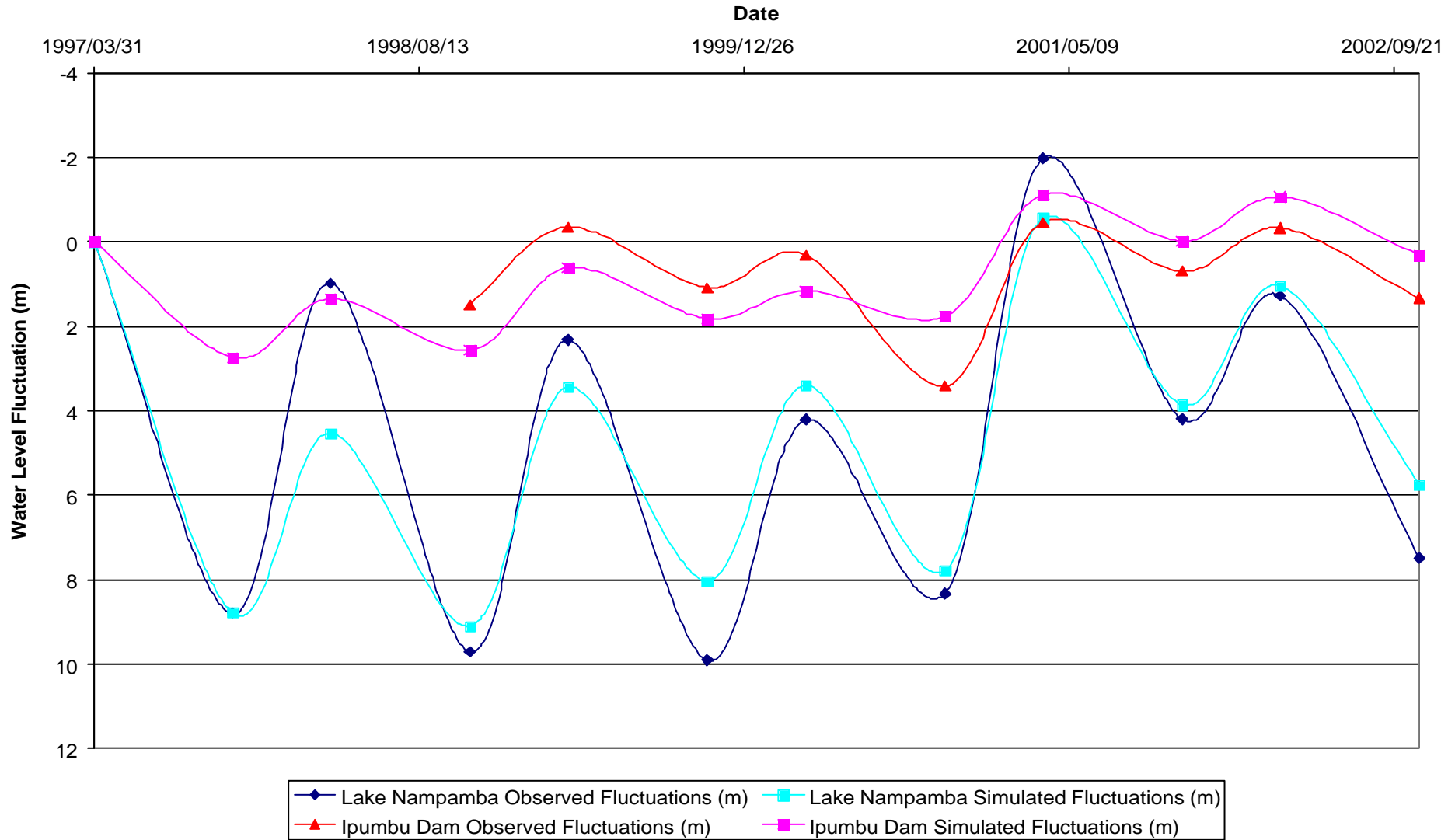
Very little abstraction data is available. Abstraction volumes were inferred from recorded pumping hours and the pump capacities. From data supplied by MDC for the years 2000 and 2002 it was calculated that approximately 12 300 000m³/annum is abstracted from the dolomitic aquifer at Kabanga Farm. A total volume of approximately 13 000 000m³ of water is released annually from Ipumbu dam for irrigation purposes.

Approximately 11 000 000m³ of water is abstracted from Lake Nampamba during the dry season. Based on a time period of seven months (210 days), an average of 52 380m³ of water is abstracted daily.

Reportedly approximately 13 000 000m³ of water is released from Ipumbu Dam annually for irrigation purposes. Approximately 1 300 000m³ and 11 700 000m³ of water is released during the wet and dry seasons respectively. As the relative contribution of rainfall run-off and spring flows to the dam is unknown, it is assumed that all the water in the dam is derived from the aquifer. This is considered to be a conservative approach in calculating the sustainable abstraction potential of the aquifer.

Figure 4.2.2.1: Correlation between Observed and Simulated Groundwater Levels.

Correlation between Observed and Simulated Groundwater Levels.



The Figure indicate the observed water level fluctuations vs. the water level fluctuations simulated using the numerical model. The fluctuations simulated using the numerical model takes into account 20% recharge from the seasonally variable rainfall and average abstraction from the aquifer. Storage coefficient was set at 0.02 and transmissivity ranged between 1000 and 5000m²/day.

Table 4.2.2.1: Monitoring Data Used for Model Calibration.

Date	Average Lake Nampamba Water Level (mamsl)	Rainfall (mm/month)	Average Ipumbu Dam Water Level (mamsl)	Pump 4		Pump 5		Pump 6	
				Pumping hours per month	Pumped volumes (m ³ /month)	Pumping hours per month	Pumped volumes (m ³ /month)	Pumping hours per month	Pumped volumes (m ³ /month)
Apr-97	1193.99	86	ND	ND	ND	ND	ND	ND	ND
May-97	1190.98	0	ND	ND	ND	ND	ND	ND	ND
Jun-97	1188.5	0	ND	ND	ND	ND	ND	ND	ND
Jul-97	1187.23	0	ND	ND	ND	ND	ND	ND	ND
Aug-97	1182.87	0	ND	ND	ND	ND	ND	ND	ND
Sep-97	1184.09	3	ND	ND	ND	ND	ND	ND	ND
Oct-97	1185.19	32	ND	ND	ND	ND	ND	ND	ND
Nov-97	1185.6	157	ND	ND	ND	ND	ND	ND	ND
Dec-97	1187.79	194	ND	ND	ND	ND	ND	ND	ND
Jan-98	1189.62	313	ND	ND	ND	ND	ND	ND	ND
Feb-98	1192.14	103	1191.25	ND	ND	ND	ND	ND	ND
Mar-98	1193.02	64	1192.44	ND	ND	ND	ND	ND	ND
Apr-98	1192.03	0	1192.5	ND	ND	ND	ND	ND	ND
May-98	1189.58	0	1192.3	ND	ND	ND	ND	ND	ND
Jun-98	1187.72	0	1192.11	ND	ND	ND	ND	ND	ND
Jul-98	1185.72	0	1191.87	ND	ND	ND	ND	ND	ND
Aug-98	1183.61	0	1191.5	ND	ND	ND	ND	ND	ND
Sep-98	1182.74	0	1191.3	ND	ND	ND	ND	ND	ND
Oct-98	1184.28	5	1190.95	ND	ND	ND	ND	ND	ND
Nov-98	1183.36	45	1190.68	ND	ND	ND	ND	ND	ND
Dec-98	1185.62	239	1190.97	ND	ND	ND	ND	ND	ND
Jan-99	1188.27	324	1191.53	ND	ND	ND	ND	ND	ND
Feb-99	1190.4	193	1191.09	ND	ND	ND	ND	ND	ND
Mar-99	1191.67	133	1192.79	ND	ND	ND	ND	ND	ND
Apr-99	1192.35	2	1192.71	ND	ND	ND	ND	ND	ND
May-99	1189.72	0	1192.6	ND	ND	ND	ND	ND	ND
Jun-99	1186.56	0	1192.39	ND	ND	ND	ND	ND	ND
Jul-99	1184.72	0	1192.1	ND	ND	ND	ND	ND	ND
Aug-99	1182.47	0	1191.78	ND	ND	ND	ND	ND	ND
Sep-99	1182.42	0	1191.6	ND	ND	ND	ND	ND	ND
Oct-99	1184.08	0	1191.36	ND	ND	ND	ND	ND	ND
Nov-99	1184.7	68	1191.13	ND	ND	ND	ND	ND	ND
Dec-99	1185.85	92	1191.2	ND	ND	ND	ND	ND	ND

ND = No Data

mamsl = metres above mean sea level

Table 4.2.2.1: Monitoring Data Used for Model Calibration (Continued).

Date	Average Lake Nampamba Water Level (mamsl)	Rainfall (mm/month)	Average Ipumbu Dam Water Level (mamsl)	Pump 4		Pump 5		Pump 6	
				Pumping hours per month	Pumped volumes (m ³ /month)	Pumping hours per month	Pumped volumes (m ³ /month)	Pumping hours per month	Pumped volumes (m ³ /month)
Jan-00	1187.41	210	1191.48	5	7200	0	0	12	17280
Feb-00	1188.48	144	1191.7	5	7200	0	0	10	14400
Mar-00	1189.78	320	1192.13	8	11520	0	0	0	0
Apr-00	1190.22	7	1192.15	200	288000	33	47520	69	99360
May-00	1187.61	3	1191.8	561	807840	433	623520	432	622080
Jun-00	1184.95	0	1191.37	655	943200	614	884160	439	632160
Jul-00	1182.81	0	1190.83	620	892800	538	774720	486	699840
Aug-00	1181.83	0	1190.26	686	987840	629	905760	235	338400
Sep-00	1184.45	0	1190.12	291	419040	245	352800	130	187200
Oct-00	1185.66	16	1189.02	266	383040	231	332640	85	122400
Nov-00	1185.35	121	1189.55	249	358560	191	275040	69	99360
Dec-00	1187.09	234	1189.61	57	82080	15	21600	16	23040
Jan-01	1189.41	314	1191.5	ND	ND	ND	ND	ND	ND
Feb-01	1195.14	349	1192.1	ND	ND	ND	ND	ND	ND
Mar-01	1195.97	224	1192.9	ND	ND	ND	ND	ND	ND
Apr-01	1195.66	35	1192.78	ND	ND	ND	ND	ND	ND
May-01	1194.44	0	1192.6	ND	ND	ND	ND	ND	ND
Jun-01	1191.65	0	1192.46	ND	ND	ND	ND	ND	ND
Jul-01	1189.89	0	1192.18	ND	ND	ND	ND	ND	ND
Aug-01	1188.93	0	1191.19	ND	ND	ND	ND	ND	ND
Sep-01	1190.32	0	1191.87	ND	ND	ND	ND	ND	ND
Oct-01	1189.79	67	1191.75	ND	ND	ND	ND	ND	ND
Nov-01	1190.45	102	1191.9	ND	ND	ND	ND	ND	ND
Dec-01	1191.82	229	1192.1	ND	ND	ND	ND	ND	ND
Jan-02	1192.49	214	1192.56	0	0	2	2880	9	12960
Feb-02	1192.66	86	1192.85	0	0	6	8640	8	11520
Mar-02	1192.72	81	1192.77	0	0	5	7200	7	10080
Apr-02	1190.86	46	1192.71	0	0	130	187200	187	269280
May-02	1189.81	0	1192.6	126	181440	524	754560	595	856800
Jun-02	1186.14	0	1192.15	392	564480	299	430560	333	479520
Jul-02	1183.85	0	1191.73	556	800640	594	855360	468	673920
Aug-02	1185.03	0	1191.48	526	757440	411	591840	354	509760
Sep-02	1187.19	2	1191.5	799	150560	562	809280	445	640800
Oct-02	1186.51	17	1191.11	313	450720	299	430560	298	429120

ND = No Data

mamsl = metres above mean sea level

The calculated current abstraction volumes for the wet and dry seasons are shown in Table 4.2.2.2.

Table 4.2.2.2: Current Abstraction Rates.

Abstraction Point	Wet Season	Dry Season
Lake Nampamba	8 700m ³ /day	52 380m ³ /day
Ipumbu Dam	8 700m ³ /day	55 700m ³ /day

Initially it was attempted to vary the simulated abstraction rate from the aquifer on a seasonal basis. However, this led to exaggerated calculated groundwater fluctuations at Lake Nampamba. These fluctuations could not be moderated without using unrealistic values for the storage coefficient “S”. Using a varying abstraction rate, an acceptable fit to the actual observed water levels could only be obtained by applying a storage coefficient of 15 for the Lake Nampamba area. However, the principles of hydrogeology dictate that this value cannot be larger than one (1), without implying the presence of constant head conditions in the numerical model. This would yield erroneous simulation results. Therefore, these scenarios using a storage coefficient of 15 have to be rejected.

Eventually, it was decided to apply a constant abstraction rate. Logic dictates that the combined wet and dry seasonal abstraction be combined and then divided into 365 days to obtain an average daily abstraction rate. However, when applying this, the simulated groundwater level in Lake Nampamba indicates an increasing trend (rising water level) with time. This increasing trend is present, even at low recharge rates, irrespective of changes in transmissivity and storage coefficient.

Applying the trial and error method by varying the model parameters within realistic ranges showed that the increasing trend could only be controlled by increasing the daily abstraction rate to that used during the dry season. This allowed for a recharge rate of 20% in the limestone area, which is close to the 25% calculated in Chapter 3.

The comparison between actual observed and calculated water levels is shown in Figure 4.2.2.1.

The model parameters at which an acceptable level of calibration was reached are summarised briefly in Table 4.2.2.3, and discussed in more detail below.

The preconditioning method had to be changed to the Neumann Series Polynomial due to the fact that the Modified Incomplete Cholesky method experienced oscillation and the iteration process could not reach the convergence criteria.

Table 4.2.2.3: Monitoring Data Calibrated Model Parameters.

Parameter	Unit	Calibrated Value
Mesh Size	m	50 x 50 up to 200 x 200
Layer Type		Confined (Type 0)
Time	Days	2 010
Stress Periods	Each	11 (6 x dry seasons & 5 x wet seasons)
Time Steps	Each	60 (7 for each dry season & 5 for each wet season)
Transmissivity (Areas of known solution cavities such as Lake Nampamba)	m ² /day	5 000
Transmissivity (Areas of strongly suspected cavities from geological and geophysical data)	m ² /day	2 000
Transmissivity (Rest of study area where solution cavities might occur)	m ² /day	1 000
Transmissivity (Schist)	m ² /day	3.5
Storage Coefficient (Area of known solution cavities - Lake Nampamba)		1
Storage Coefficient (Ipumbu Dam area)		0.1
Storage Coefficient (Rest of study area)		0.02
Recharge (Limestone / Dolomitic Area)	% of average annual rainfall)	20
Recharge (Schist)	% of average annual rainfall)	3
Recharge (Ipumbu Dam)	% of average annual rainfall)	20
Solver used		pcg2
Preconditioning method		Neumann Series Polynomial
Outer Iteration (MXITER)		500
Inner Iteration (ITER1)		200
Convergence Criteria (Head Change)	m	0.01
Convergence Criteria (Residual)	m	0.01
Modflow Version		PMWIN 4.X

Chapter 4.2.3 : Monitoring Data Calibrated Model - Grid.

The numerical model grid was constructed in such a way that the grid directions were compatible with the general aquifer characteristics such as groundwater flow direction and transmissivity.

The grid was constructed with a minimum cell size of 50 x 50m and a maximum cell size of 200 x 200m (refer to Figure 4.2.3.1). The smaller cells are located in the area where, based on current abstraction patterns, most groundwater flow and groundwater level fluctuations are expected.

Chapter 4.2.4 : Monitoring Data Calibrated Model - Layers.

Due to the fact that only the dolomitic aquifer is under investigation, it was decided that the numerical model would comprise of only one layer. There is little regional data available on the upper contact of the dolomitic layer. The only available data is from the borehole logs. Most of the boreholes are situated in a tight cluster in the eastern section of the Mpongwe irrigation area, with only a few boreholes present in the western section of the Mpongwe irrigation area. No boreholes exist in the Munkumpu irrigation area (refer to Figure 3.4.1). Due to the clustering of the boreholes, there is insufficient spatially representative data available to interpolate the top of the dolomitic aquifer throughout the whole of the study area.

As stated in Chapter 2.2 the topographical maps were digitised, and thus a large amount of topographical data of the study area is available. Assuming that the top of the competent dolomitic rock to a large extent mimics topography, it was decided to interpolate the top of the dolomitic aquifer based on the available topographical data.

The bottom of the layer was specified at 100m below the top. This is based on the fact that no data more than 100m below surface is available and therefore any values below 100m will be based on speculation.

Figure 4.2.3.1: Numerical Model Grid.

Numerical Model Grid

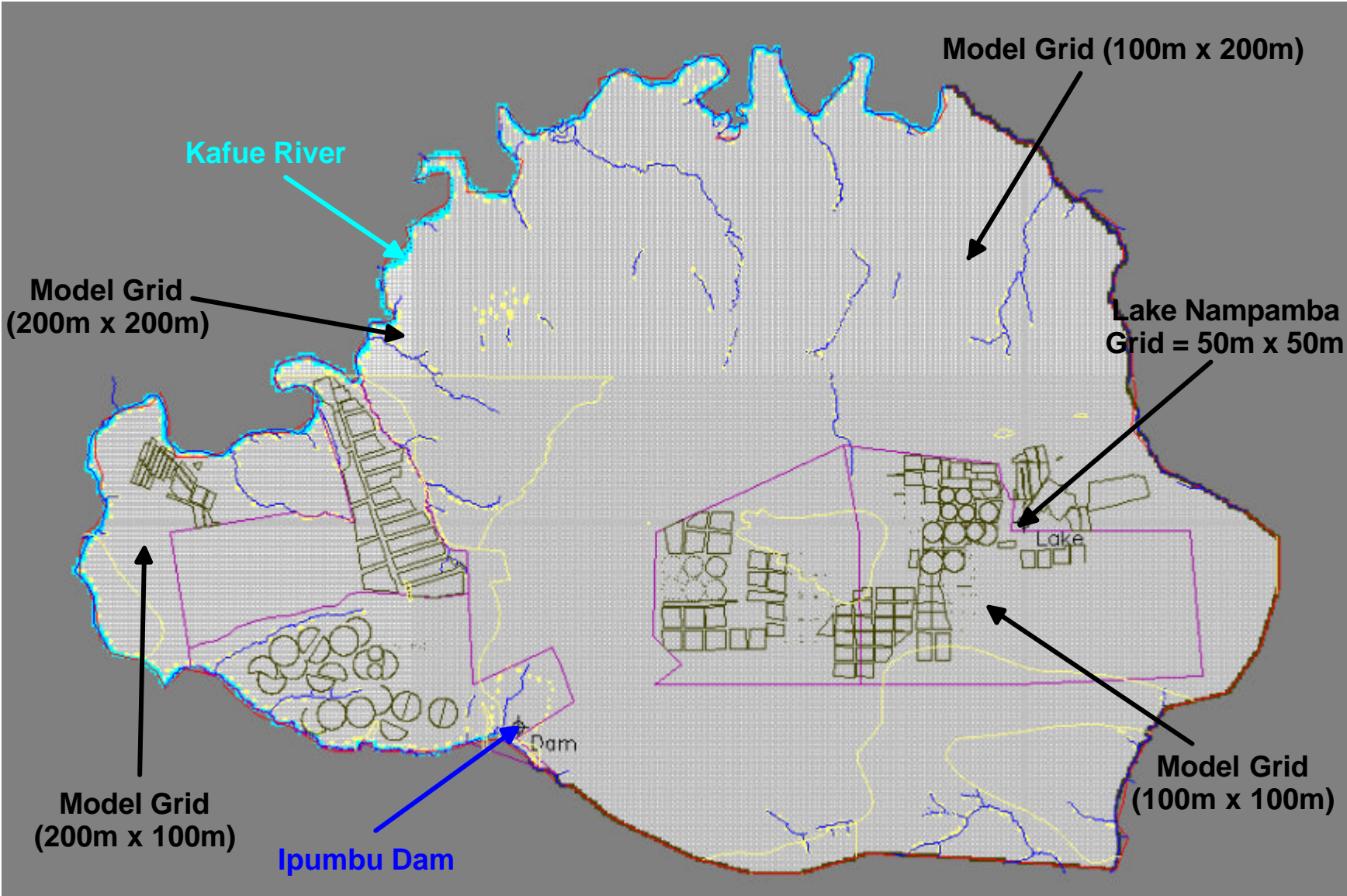


Figure No: 4.2.3.1

The layer type was specified as being confined (Type 0), therefore, parameters such as horizontal hydraulic conductivity, vertical hydraulic conductivity and specific yield are not applicable and do not have to be specified.

Chapter 4.2.5 : Boundary Conditions.

Where possible, natural groundwater flow boundaries were used as model boundaries. In the southwest, west and north, the Kafue River and its perennial tributaries were used as boundaries. In the south and east the boundary follows what is considered to be flow divides (refer to Figure 2.2.3). However, the topography is gently sloping and as discussed previously in this report, it is considered that sub-catchments are connected through the solution cavity network.

The Kafue River and tributaries are simulated using river cells. Inactive cells represent the no flow boundaries. General head boundaries were used in places. No constant head boundaries were employed in the construction of the numerical model.

Chapter 4.2.6 : Monitoring Data Calibrated Model - Time Increments.

The time parameter reflects the seasonal time increments. To be able to incorporate the time period April 1997 to October 2002, the time parameter was divided into eleven (11) stress periods. Each of the stress periods reflects either a dry or a wet season.

Each dry season was sub-divided into seven (7) time steps (months) and the wet seasons into five (5) time steps (months).

The model was set to simulate a transient flow type.

Chapter 4.2.7 : Monitoring Data Calibrated Model - Observed Hydraulic Heads.

The average monthly water levels as observed in Lake Nampamba and Ipumbu Dam for the time period were incorporated into the model. These average water levels were calculated based on the daily water level measurements recorded by MDC.

During the calibration process the observed water levels with time were compared to the simulated water levels. Due to the fact that the model did not simulate each month separately, it was not possible to assess the capability of the numerical model to simulate the two-month delay between maximum rainfall and peak groundwater level. However, due to the fact that the maximum groundwater level coincides with the end of the rainy season, it is considered that the model is capable of simulating the maximum groundwater level accurately.

Chapter 4.2.8 : Monitoring Data Calibrated Model - Transmissivity.

The transmissivity of the area as calculated from the aquifer tests ranges between 1 and 6 900m²/day. Values used in the calibration of the numerical model are:

- Transmissivity of known solution cavity areas: 6 900m²/day.
- Transmissivity of areas where it is considered that solution cavities might occur from geological and geophysical data: 2 000m²/day.
- Transmissivity of the rest of the limestone / dolomitic aquifer: 1 000m²/day.
- Transmissivity of the schist: 3.5m²/day.

It is considered that the calibrated transmissivities fall within an acceptable and realistic range.

Chapter 4.2.9 : Monitoring Data Calibrated Model - Storage Coefficient.

The storage coefficients used in the calibration of the numerical model are:

- Storage coefficient of known solution cavity areas: 1.
- Storage coefficient for the rest of the limestone / dolomitic aquifer: 0.02.

A storage coefficient of 1 was used in the vicinity of the Lake Nampamba sinkhole because there is little rock material in the solution cavities that will reduce the storage coefficient. In nature Lake Nampamba measures approximately 150m x 30m (4 500m²). In the numerical model, Lake Nampamba is represented by 4 cells, which measure 50m x 50m, thus spanning an area of 2 500m².

The storage coefficient for the rest of the limestone / dolomitic aquifer was calibrated at 0.02. This corresponds to the storage coefficient calculated by the author in Chapter 3.

Chapter 4.2.10 : Monitoring Data Calibrated Model - Recharge.

Recharge to the study area was calculated using the SVF, Equal Volume and CRD methods:

- Recharge to the limestone / dolomite aquifer in the study area as a percentage of the annual rainfall: 25% initially. However, the model calibrated at 20% recharge.
- Recharge to the schist: 3%.

Chapter 4.2.11 : Numerical Model Discussion.

The numerical model was calculated using the trial and error method. Initial parameter values were based on values calculated from the data. Through adjustment of these values within realistic ranges the model was calibrated. The final values are listed above.

The parameters used fall within the expected range. Recharge to the area calibrated at 20% corresponds well to the calculated figure of 25%, as determined in Chapter 3 using the SVF, Equal Volume and CRD methods. This figure is slightly higher than the 10% of Landell Mills Associates (1978) and falls within the upper segment of the 6 to 22% calculated by Macdonald and Partners Ltd. (1982). However, taking into consideration the dambo areas, relatively flat topography, absence of major surface water drainage canals, high rainfall, the fact that soil infiltration rates exceed precipitation rates (Landell Mills Associates, 1979) and elevated recharge in irrigated areas due to return flow, this figure is considered to be conservative.

Sensitivity analyses indicate that the numerical model is relatively insensitive to changes in the parameters. The model is influenced by storativity, transmissivity, and recharge. The model is most sensitive for changes in transmissivity and recharge.

Figure 4.2.2.1 shows the correlation between actual observed water levels in Lake Nampamba and Ipumbu Dam and the water levels simulated using the numerical model.

The figure indicates a high correlation between the observed and calculated values at Lake Nampamba.

As mentioned previously, the water levels in the surface water body of Ipumbu Dam could not be simulated accurately. However, the figure indicates that there does exist a correlation between observed and calculated water levels in the dam.

The correlation is considered to be sufficient so that the numerical model can be applied to simulate various theoretical scenarios and obtain reasonably acceptable results.

The Kafue River and some of the perennial tributaries were incorporated into the model as flow boundaries in the southwest, west and north. Due to the fact that no flow data is available for the Kafue River, it is not possible to evaluate the accuracy of the numerical model in predicting the interaction between the aquifer and the river.

Chapter 4.3 : Model Applications.

The calibrated numerical model can be applied to evaluate different hydrogeological scenarios and perform various predictions. For the purposes of the current study, the numerical model was applied by evaluating expected future abstraction rates from the dolomitic aquifer in the study area. By using the numerical model the sustainability of the proposed abstraction program may be evaluated.

The rainfall data as observed during the time period April 1991 to October 2003 was incorporated into the numerical model. The numerical model evaluation thus spanned a 25 cycle (12.5-year) time period.

Recharge to the aquifer was calculated based on the actual observed rainfall data for the time period and the calibrated 20% recharge. The rainfall and recharge data used is summarised in Table 4.3.2.

Aquifer parameters such as transmissivity and storage coefficient were not changed from those used in the model in Chapter 4.2 to evaluate the current abstraction program. These values are summarised in Table 4.2.2.3.

The proposed future abstraction program was discussed in Chapter 3.9. The expected future abstraction volumes are summarised in Table 4.3.1, with separate figures for the expected different seasonal abstraction programs.

Table 4.3.1: Expected Future Abstraction Rates.

Abstraction Point	Wet Season	Dry Season
Lake Nampamba	13 700m ³ /day	82 800m ³ /day
Ipumbu Dam	16 700m ³ /day	107 000m ³ /day

However, based on the results of the water level fluctuations modelled in Chapter 4.2, it was decided not to vary the abstraction rate per season, as this would lead to anomalously high fluctuations in water level. Following the methodology of Chapter 4.2, the dry season abstraction rate for Lake Nampamba was used.

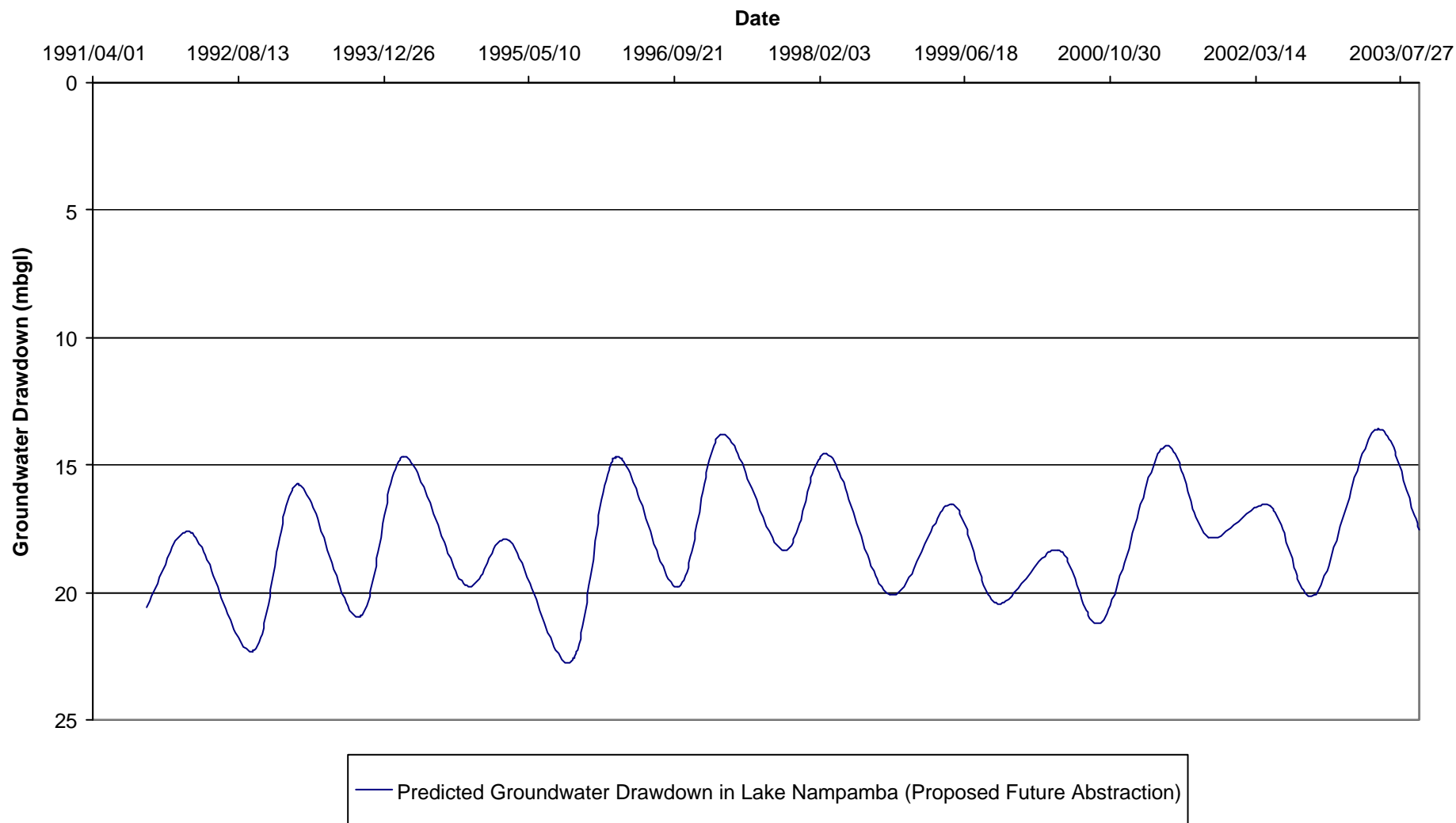
The predicted water level fluctuations over the 25 seasons are shown in Figure 4.3.1. The groundwater level declines during the dry season due to the effect of little recharge from rainfall. The groundwater level rebound occurs during the rainy season. There is no long-term declining trend in groundwater level that would indicate dewatering of the aquifer. A declining groundwater trend indicates that more water is being removed from storage than is recharged and the aquifer is thus being dewatered. Based on the absence of such a declining trend, it is concluded that the dolomitic aquifer can sustain the proposed future abstraction rates.

Table 4.3.2: Data Used in the Model Application.

Date	Season	Rainfall (mm/season)	Calculated Recharge (m/day)
April 1991 – October 1991	Dry	90	8.571×10^{-5}
November 1991 – March 1992	Wet	795	1.060×10^{-3}
April 1992 – October 1992	Dry	80	7.619×10^{-5}
November 1992 – March 1993	Wet	1076	1.435×10^{-3}
April 1993 – October 1993	Dry	9	8.571×10^{-6}
November 1993 – March 1994	Wet	1065	1.420×10^{-3}
April 1994 – October 1994	Dry	51	4.857×10^{-5}
November 1994 – March 1995	Wet	584	7.787×10^{-4}
April 1995 – October 1995	Dry	18	1.714×10^{-5}
November 1995 – March 1996	Wet	1208	1.611×10^{-3}
April 1996 – October 1996	Dry	21	2.000×10^{-5}
November 1996 – March 1997	Wet	1045	1.393×10^{-3}
April 1997 – October 1997	Dry	121	1.152×10^{-4}
November 1997 – March 1998	Wet	831	1.108×10^{-3}
April 1998 – October 1998	Dry	5	4.762×10^{-6}
November 1998 – March 1999	Wet	934	1.245×10^{-3}
April 1999 – October 1999	Dry	2	1.905×10^{-6}
November 1999 – March 2000	Wet	704	1.112×10^{-3}
April 2000 – October 2000	Dry	26	2.476×10^{-5}
November 2000 – March 2001	Wet	1242	1.656×10^{-3}
April 2001 – October 2001	Dry	102	9.714×10^{-5}
November 2001 – March 2002	Wet	712	9.493×10^{-4}
April 2002 – October 2002	Dry	65	6.190×10^{-5}
November 2002 – March 2003	Wet	1246	1.661×10^{-3}
April 2003 – October 2003	Dry	64	6.095×10^{-5}

Figure 4.3.1: Predicted Groundwater Fluctuations based on Increased Abstraction Volumes.

Predicted Groundwater Fluctuations based on Increased Abstraction Volumes.



The Figure indicate the predicted water level fluctuations simulated using the numerical model. The proposed future abstraction rates was used in conjunction with observed rainfall data from April 1991 to October 2003. It is reasoned that should the proposed abstraction rate be sustainable based on recorded past data, it will most likely also be sustainable in future. No general downward trend in water level occurs with time, indicating that the aquifer can sustain the proposed future abstraction program.

Chapter 5 : Conclusions and Recommendations.

Based on the considerations, simplifications and calculations described in the previous chapters, several conclusions can be reached.

The topography is relatively flat, ranging between 1:400 and 1:800. This, combined with the fact that the soil infiltration potential is higher than the rainfall intensity, contributes to recharge to the underlying aquifer as the low topographical gradient does not induce surface run-off, but rather retards it.

The average annual rainfall in the study area is calculated as 1 115mm. Daily rainfall data from 1931 to 2003 indicates a seven to ten year cyclic pattern. The average annual rainfall displays a standard deviation of 207mm. The lowest recorded annual rainfall was 635mm, while the highest annual rainfall figure was 1 722mm.

There exists a high seasonal variability in rainfall with high rainfall volumes and rainfall intensities during the rainy season (November to March), and very little to no rainfall during the dry season (April to October). The seasonal change in groundwater level in the dolomitic aquifer is partly attributed to this seasonal variation in rainfall.

The rainfall intensity in the area is relatively high (28mm/30minutes once yearly) and as such it would be expected that a large percentage of the annual rainfall would exit the hydrological system in the form of surface run-off. However, due to the high infiltration rate of the soil, a large proportion of the rainfall enters the hydrogeological system and replenishes the underlying aquifers. Obvious evidence of this is the fact that very few surface run-off features exist in the study area - only one perennial surface run-off structure exists in the study area.

The Kafue River is on average 10 to 20m wide and 3m deep. It is considered that the base flow contribution from the dolomitic aquifer constitutes a large portion of the flow volume of the river. This is partially based on the fact that there are very few tributaries to the Kafue River. Another contributing factor, as Scott Wilson Piésold noted in 2003, is that the river flow volumes increase and decrease in areas where the dolomitic aquifer

intersects the river. These increases and decreases indicate that the dolomitic aquifer is in hydraulic contact with the river.

This indicates that at the river the groundwater level is at or slightly above the riverbed (3m below surface). In Chapter 3.3 it was stated that the average depth to groundwater level in the boreholes visited during the 2003 hydrocensus was calculated at 17.68m. However, it should be borne in mind that the boreholes are situated far away from the Kafue River, and on topographically relatively higher lying areas. As with most natural instances the groundwater level will be deeper in the higher lying areas, than in the lower lying areas.

Only one rainfall related surface run-off structure exists in the study area. This feature feeds into Ipumbu Dam.

Wetland or vlei areas occur in the study area. These areas are commonly referred to as “dambo” areas and occur where surface depressions intersect the groundwater table. Generally, the dambo areas are not very large in extent, less than 200m x 200m. However, in some areas the concentration of dambos is large and the total affected area can be quite extensive.

Evaporation losses from the study area will derive mainly from water held on vegetative cover, from the phreatic zone and from the shallow ponding water in surface depressions such as the dambo areas.

Very little evaporation data is available for analysis. MDC records only positive net evaporation (total evaporation minus rainfall greater than zero), thus, evaporation data is only available for the dry season. From the available data, it is calculated that the net annual evaporation is 945mm. The available data indicates a decrease in evaporation during April to July. This is followed by a sharp increase during August and particularly September. This trend is attributed to the influence of temperature and the number of daylight hours. During April to July the average daily temperatures and number of daylight hours decrease until the winter solstice is reached on 21 June. During July, low temperatures and short days are experienced. In August, the seasons change with daylight hours becoming slightly longer and temperatures rising markedly. During

September, the daylight hours lengthen and the temperatures increase to those that are expected during the rainy season.

The Penman equation was used to calculate the potential evaporation in the study area. The potential evaporation was calculated to be 1 708mm/annum. However, after comparing the theoretical annual rainfall based on this value and the actual observed rainfall, this value is believed to be erroneous.

It is believed that the rainfall data is more accurate than the evaporation data due to uncertainties surrounding the methodology used during recording of the evaporation data and the non-recording of evaporation during the rainy season.

Due to the fact that the evaporation data is believed to be erroneous, it is recommended that the evaporation data is not included in the water balance calculations.

Plant growth in the area is lush with *Brachystegia – Tulbernardia* (Miombo) woodland being the dominant species. The average plant density is in the order of 500 trees per hectare, with tree diameters varying between 15 and 35cm. Grass cover that is found between the trees is widespread. The grass can be very thick in undisturbed places and can reach heights of more than 2m. In some areas the grassland and tree cover is broken by the presence of dambos.

The Mpongwe limestones and dolomites form part of the Upper Roan Group of the Katanga Supergroup. The surrounding formations are generally regarded as Lower Roan sandstones. However, schists have been encountered within the limestone and dolomite area. An inlier of Lower Roan exists in the centre of the limestone block at Mpongwe.

The limestone in the study area varies between pure white crystalline marble and dolomitic marble to dark blue grey crystalline limestone.

Several types of schist occur. The schistose rocks cannot be easily classified and stratigraphically related due to the lack of sufficient outcrop. However, hydrogeologically the schist behaves as a homogenous unit, and is interpreted as such.

The limestone beds generally display a shallow dip ranging between 5° and 20°, to the northwest and north-northwest.

Extensive jointing occurs in the limestone and dolomite. Three major joint sets, all near vertical can be distinguished. The first is the dominant joint set with an orientation of 160°. Two secondary joint sets occur, the one shows an orientation of 220° to 230°, and the other an orientation of 270°.

The principal joint set in the area (160°) controls the orientation of Lake Nampamba, and the other sub-surface solution cavities.

Age relationships between the joint sets are not clear due to little offset between the different joint sets.

Evidence of extensive fracturing within the limestone and dolomite is found in the geological logs of the drilled boreholes. The majority of high yielding boreholes display significant fracturing of the geology. Fracturing in the dolomite and limestone will be conducive for chemical weathering due to the fact that the fractures will act as preferential pathways for groundwater flow. This will enhance solution of the lithology in acidic water.

To the west, at Ipumbu Farm, the Munkumpu Fault zone forms a sharp contact between the limestones to the east and meta-sedimentary siliclastic rocks or quartzite that underlies Ipumbu Farm.

This contact is outlined on the surface by several dambo areas. These dambo areas contribute to the Ipumbu dam in conjunction with surface run-off from rainfall. It is considered that seepage from the dambo areas contributes the majority of the water to the Ipumbu dam.

Two classes of soil have been identified in the study area (Landell Mills Associates, 1979). The first is classified as Class 1, a deep, well-drained, dark reddish brown clay loam to clay over dark red clay.

The second is Class 2, a deep, well-drained, dark reddish brown sandy clay loam and clay loam over yellowish red clay loam and clay. The soil possesses a high clay content (30-40%). This however, does not impair the drainage characteristics.

From slaking tests, the Class 1 and Class 2 soils are shown to be very stable. The lighter, sandier soil on the central plateau area is however noticeably less stable. The stable soil has a high resistance to impact from falling rain, being less likely to break down into fines which then block the drainage pores, creating an impervious surface skin and accentuating run-off during the latter part of rain storms. It can thus be concluded that the soils in the study area indicate characteristics conducive to high infiltration rates.

The infiltration rate determines whether or not surface run-off will take place. Infiltrometer tests performed in the study area (Landell Mills Associates, 1979) indicate that the infiltration rate is likely to exceed the rate of precipitation. This is subject to the condition that free drainage is not impaired, as the soil becomes water logged.

The depths of infiltration in Class 1 soils range between 260 and 460mm over a six-hour period.

The field capacity and wilting point of the soil have been determined as 290mm/m and 185mm/m respectively. Assuming an average depth of 2m, and that the soil moisture content has declined to wilting point capacity at the end of the dry season, the rainfall required to raise the soil from wilting point to field capacity is approximately 105mm/m or 210mm. This, in addition to the evapotranspiration demand of the woodland, gives an indication of rainfall required before recharge to the underlying aquifer can occur.

It is unclear to what extent the solution cavities are interconnected. No detailed water level monitoring data from the production boreholes is available. Definite differentiation between the water levels in closely spaced boreholes indicate the presence of small-scale compartmentalization in the dolomite. This is often a problem in dolomitic areas and limits the long-term sustainable abstraction from an aquifer.

It can be argued that the high sustainable yields can be attributed to the high transmissivity (up to 6 900m²/day). However, in the event that compartmentalisation

does occur in the study area, the borehole would only be able to yield high volumes of water until a flow boundary (edge of the compartment) was reached. On reaching such a flow boundary, the yield of the borehole would substantially decrease or even stop. However, in none of the aquifer tests performed, is there evidence of such an occurrence.

Based on the high sustainable yields and long term sustainability of the boreholes and Lake Nampamba, it can be concluded that no small-scale compartmentalisation occurs in the area. This is further supported by the fact that both the geological data obtained from the latest mapping and the borehole logs show no indication of intrusive material.

It is considered that the solution cavities generally strike in a south – southeast to north-northeast direction, as is indicated on Figure 2.7.1. This strike direction corresponds to that of the major joint set. This considered strike direction is supported by the detail resistivity investigations conducted during 1979 and 1982, the short gravity, electromagnetic and magnetic surveys conducted during 2004 of the area (refer to Chapter 2.9 for the discussion on the surface geophysical investigation), the major strike direction of joint patterns in the dolomite, the strike and shape of Lake Nampamba and the observed surface fracturing and solution features close to Lake Nampamba (refer to Chapter 2.7 for the discussion on the geology) as well as the suggestion made by several authors that Lake Nampamba is hydraulically connected to the Kafue River to the north.

Three prominent karstic features occur in the study area. These are Lake Nampamba, Lake Kashiba and the “Chibili pavement”. Lake Nampamba and Lake Kashiba are well known features in the area and are considered to be collapsed structures in the dolomite. The depth of both the lakes is unknown. However, both lakes are reportedly deeper than 100m. These lakes represent “windows” into the aquifer where direct abstraction of groundwater can be undertaken.

The “Chibili pavement” was not visited during the site visits. However, it reportedly has several shallow passages and rectangular joints open to the surface. Sub-surface water movement can be heard (Scott Wilson Piésold 2003).

It has been suggested by various authors that the Mpongwe karstic features, Lake Kashiba at St. Anthony's Mission, the "Chibili pavement" and the Kafue River are all interconnected. Evidence quoted for this assumption includes:

The groundwater flow gradient is approximately 1:400. Extrapolating this to the Kafue River, the groundwater level coincides with the level of the Kafue River (Scott Wilson Piésold 2003).

Low flow volumes in the Kafue River when groundwater baseflow contributions dominate suggests that there is an apparent gain of upstream flow at Ndubeni and a corresponding loss downstream. This suggests that the Kafue River may be effluent from the Mpongwe groundwater system above Ndubeni and influent to the groundwater system below. This stretch of the river coincides with the area of connection and possibly karstic connection north of Lake Kashiba between the Mpongwe limestone and Lake Kashiba (Scott Wilson Piésold 2003).

Rankin Engineering Consultants (1997) states that it is clear that the Northern Zone of Ipumbu Farm is connected to the St. Anthony Aquifer. The Central Zone may be connected to the Ipumbu Aquifer. The possibility that the Ipumbu and St. Anthony's aquifers are connected cannot be ruled out.

Interconnectivity of the aquifers indicates that the solution cavities span several sub-catchment areas and are thus not bound by normal hydrogeological boundaries such as water divides and rivers.

The chemical character of the groundwater is shown in Figure 3.2.1 on a Piper diagram. The figure indicates that the groundwater has been somewhat recently recharged. This fact corresponds with the high recharge percentage calculated for the study area. The groundwater displays a calcium-magnesium and bicarbonate-carbonate dominant character. This is expected in dolomitic formations.

The pH of the water is lower than would generally be expected for dolomitic terrains. However, although the groundwater displays a recently recharged character, ion exchange has occurred in order to enrich the groundwater in calcium and magnesium.

Acid rain of relatively low pH that enters the groundwater system will be attenuated by the acid neutralising capacity of the dolomitic geology. During the neutralising process the karstic nature of the dolomite will be enhanced by dissolution of the rock material into the acidic water. Calcium and magnesium will go into solution resulting in elevated concentrations of the constituents. The relatively low pH of the acidic water will be neutralised during this process.

Even though the calcium and magnesium concentrations exceed the target values, it is deemed, from an inorganic perspective, that the groundwater is suitable for human consumption. The calcium and magnesium critical values as specified by the SAWQ guidelines are 80mg/l and 100mg/l respectively.

The geometric mean depth to groundwater as determined in November 2003 is calculated to be 17.68m.

Lake Nampamba is a sinkhole that reflects the groundwater level in the area. From the Lake Nampamba monitoring data it is evident that the groundwater level in the area declines during the dry season and rebounds during the wet season. Groundwater abstraction volumes for irrigation purposes are six times greater during the dry season than during the wet season.

The water level starts recovering immediately after the first rainfall, however, there exists a one to two month delay between maximum monthly rainfall and maximum groundwater level. Rainfall and water level data indicate that maximum monthly rainfall mostly occurs between December and February while the maximum water level is recorded only in March or April.

Following the theory of a large interconnected network of solution cavities, it can be argued that this delay in maximum groundwater level can be attributed to the water having to migrate from an up-gradient recharge point. The water migrates down gradient as a pulse through the aquifer, causing a seasonally fluctuating water level.

During years of low rainfall, the water level in Lake Nampamba does not rise as high as during years of high rainfall. An example of this is the rainy seasons of 1993-1994 and

1994-1995. The rainy season of 1993-1994 yielded relatively high rainfall and subsequent recharge to the aquifer. This caused the water level to rise to the highest recorded level of approximately 1 195mamsl. The rainy season of 1994-1995 yielded relatively low rainfall and recharge to the aquifer. The maximum water level recorded was only approximately 1 189mamsl. This gives rise to a difference of 6m in the maximum water level.

It is considered that the groundwater fluctuations are a combined result of the natural seasonal fluctuations (the change in recharge from rainfall) and abstraction for irrigation purposes. Additional possible discharges from groundwater to the Kafue River that have an effect on the groundwater level are discussed in Chapter 3.1.

Groundwater flow is in a north-north westerly direction. The groundwater flow gradient is in the order of 1:400.

Transmissivities calculated from the aquifer test data ranges between 1 and 6 900m²/day (refer to Table 3.4.1). This is typical of karstic areas with relatively low transmissivities being associated with areas where very little or no karstic development occurred, and the high transmissivities occurring in areas where karstic development is pronounced.

Boreholes MDP1, MDP5, MDP15 and MDP17 are low yielding boreholes. Blow yields of these boreholes yielded less than 1l/s. In dolomitic lithologies, blow out yield is not always indicative of the potential yield of a borehole. This is due to the fact that when solution cavities are intersected the compressed air used during normal percussion drilling is absorbed by the cavity space and little to no drill chip or water return occurs.

However, on closer inspection of the lithological logs of the abovementioned boreholes, it is clear that these boreholes are indeed low yielding.

Borehole MDP1 is drilled partially into the schist, which is a low yielding lithology. No fracture zones or solution cavities are recorded in the limestone that was intersected between 30 and 48mbgl.

Borehole MDP5 was drilled into the limestone. The limestone to the completed depth is generally unweathered.

Boreholes MDP15 and MDP17 are drilled into the schist. This lithology is low yielding.

The total sustainable yield from the 14 high yielding boreholes identified in the area is estimated at 620.5l/s (19 570 000m³/annum). Sustainable yields calculated for the individual boreholes range between 5 and 100l/s (157 700 to 3 153 600m³/annum).

The sustainable yield of borehole GCS7 is indicated as 50l/s. The regional average depth to water level is calculated to be 17.68m. Borehole GCS7 indicates an anomalous water level for the area (34.29mbgl). This water level is possibly due to construction problems encountered during the installation of the steel casing.

Due to the possibility of the borehole collapsing, it is the author's opinion that the pump can only be inserted to 39m depth, leaving an available drawdown of 5m. The main water strike occurred in a solution cavity 40 to 42mbgl. If this borehole was drilled deeper, the recommended sustainable yield could substantially increase.

Boreholes drilled into the solution cavities, or cavity associated fracture zones, are generally high yielding as can be seen from boreholes GCS6, GCS7, GCS8, MDP19, MDP21A, MDP21B, IN3A and E3700.

The fine crystalline unweathered or slightly fractured rock displays a lower transmissivity and storativity than the solution cavities. These areas will usually yield less water. Relative to the karstic aquifer, the yield from the fractured rock aquifer is negligible.

During the 1981 – 1982 investigation MDP11 was classified as a low yielding borehole. However, during 2004 closer investigation of the borehole geological log by the author indicated extensive fissuring below the regional groundwater level. This corresponds to similar fissuring reported in high yielding boreholes such as MDP21A and MDP21B. The fissuring is further highlighted by the single point resistance being completely off-scale. The aquifer test data from 1982 indicates that the borehole was tested at a rate of 6.9l/s.

Drawdown of the water level in the borehole stabilised after 18 minutes at approximately 7m drawdown where it oscillated at approximately 28 to 29m depths until the test was stopped after an hour. The oscillation level corresponds well with the fissure zone indicated in the drill log between 27 and 47m depth.

Due to the oscillation of the water level during the last 40 minutes (two thirds of the testing time), Macdonald and Partners Ltd. (1982) only fitted a trend line to the early time data (first 20 minutes). This yielded the stated transmissivity of 195m²/day (refer to Table 3.4.1).

The oscillation occurs due to the fact that the aquifer test was performed at too low a rate. Once the hydrogeological system is in motion the influx of water into the borehole is higher than what the pump can extract and a surging motion develops.

It is the opinion of the author that should this borehole be tested at a higher rate of 25 or 30l/s the oscillation effect can be avoided and a better estimation of the transmissivity can be obtained. It is the opinion of the author that this borehole also has the potential to be high yielding. Unfortunately, it was not possible to prove this theory during the 2004 investigation.

Previous studies in the Mpongwe area have estimated groundwater recharge as a percentage of the annual rainfall. The estimated recharge from these studies ranged between 6 and 45% in uncultivated areas. During the 2004 investigation, the author made use of the Chloride, SVF, Equal Volume and CRD methods.

The chemical analysis of three groundwater samples indicates that the chloride concentration ranges between 1 and 3.2mg/l. The chloride concentration in the water will increase from the time that recharge from rainfall into the soil occurs until the water is abstracted from the aquifer. This is based on the assumption that the chloride concentration will increase due to transpiration from plants and by direct evaporation from the soil (Bredenkamp *et al*, 1995).

Following this reasoning, it is accepted that the chloride concentration in the rainwater cannot be higher than that recorded in the groundwater. Therefore, the chloride concentration in rainfall will be less than 1mg/l.

The average annual rainfall for the study area is 1 115mm. Following the reasoning above, the chloride concentration in the rainfall should be less than 1mg/l. It was decided to calculate the recharge percentage based on values ranging between 0.1 and 1 mg/l.

Based on the facts that the study area is situated far inland, with cleared areas for agricultural purposes and the presence of natural forest over large areas, the author concludes that the actual dry chloride deposition versus the rainfall chloride concentration ratio will fall between 0.1 and 2.5. Taking all the plant growth and geographical conditions into consideration, it is the opinion of the author that the ratio will be closer to 0.1 than 2.5.

The harmonic mean groundwater chloride concentration calculated from the available data is 1.667mg/l.

Due to the fact that both the rainfall chloride concentration and the rainfall chloride concentration versus the dry chloride deposition ratio are uncertain, the recharge percentage is calculated as a range based on the discussed ranges of these two parameters.

For a rainfall chloride concentration versus a dry chloride deposition ratio of 0.1, the recharge percentage ranges between 7 and 65%, depending on the rainfall chloride concentration. For a rainfall chloride concentration versus a dry chloride deposition ratio of 2.5, the recharge percentage ranges between 21 and 208%.

A recharge percentage higher than 100% would mean that there is more water recharge than total rainfall volume. This can only occur if water is artificially recharged to the aquifer from an external source, and this does not happen in the study area. In reality recharge percentages higher than 50% are rarely achieved under natural conditions, depending on site specific conditions such as recharge pathways, soil cover, topography

and slope, infiltration rates, fracturing and outcropping of the competent rock and rainfall intensity.

It is generally considered that a chloride concentration of 0.1mg/l in rainwater is too low, and should be nearer to between 0.8 and 1mg/l. However, Figure 3.5.1 indicates that even at a rainfall chloride concentration versus a dry chloride deposition ratio of 0.1, a chloride concentration of 1mg/l indicates a 65% recharge percentage that is considered to be high for this hydrogeological system.

At 0.8mg/l chloride concentration in rainfall, and a ratio of 0.1, recharge is calculated to be approximately 50%. This is also believed to be too high.

It is concluded that the chloride method cannot be applied with confidence to this particular area. This is possibly due to the large distance from the coast, or the relatively high rainfall figures. Investigation of the **Recharge** software indicates that most inland locations for which recharge has been benchmarked have a rainfall figure of less than 600mm/annum, half of the figure recorded at Mpongwe, and is located less than 800km from the coast. Mpongwe is located approximately 1 400km from the coast.

The SVF and CRD methods were used to calculate the recharge to the Mpongwe aquifer to a higher degree of accuracy. Due to most of the data being available for the eastern aquifer (Mpongwe area), analysis focussed on this area. The calculated recharge values could then be extrapolated to the western aquifer (Munkumpu Area).

Based on the CRD, SVF and Equal Volume methods, it is calculated that approximately 25% of the annual rainfall recharges the aquifer. The calculated recharge percentage correlates well with recharge percentages obtained for other dolomitic areas (van Dyk (1993 & 1997); Bredenkamp *et al* (1995), Janse van Rensburg *et al* (1987)).

The aquifer storativity (S) is an essential element in the water balance. However, it is difficult to determine the storativity due to the interdependence of the water level response on both recharge and storativity. Generally, in the estimation of the aquifer storativity from water balances or by means of aquifer tests, it is assumed that the inferred storativity is uniform over the full thickness of the aquifer.

Based on the recorded rainfall and water level data the aquifer storativity is calculated as approximately 2%. This correlates with storage coefficients calculated for other dolomitic aquifers.

Analysis of the data during the CRD, SVF and Equal Volume method calculations indicated that the eastern and western aquifers are definitely connected. This is based on the influence of abstraction from the western aquifer on recharge calculations. Incorporating abstraction from the western aquifer yields more realistic recharge and storativity values, than without incorporating abstraction. Based on this, the combined sustainable yield of the eastern and western aquifers was calculated.

Based on a combined area of 488km² and a recharge percentage of 25% of the lowest recorded annual rainfall (635mm, during the time period April 1994 to March 1995), it is calculated that the total volume of water that can safely be abstracted from the combined eastern and western aquifer is 77 470 000m³/annum. Based on the 50-year average rainfall of 1 115mm, a maximum total volume of 136 030 000m³ can be abstracted per annum from the combined eastern and western aquifers.

MDC plans to expand the irrigable land from 4 150ha to 6 500ha. Due to operational problems with the 200ha pivots, the pivot size will be limited to either 100 or 150ha. Another 16 to 25 pivots will therefore need to be installed.

Based on the proposed expansion, it is expected that a combined total of 30 400m³/day will be abstracted from Lake Nampamba and Ipumbu Dam during the wet season and 189 800m³/day during the dry season.

Using the above data, it is possible to evaluate the sustainability of the current and the future abstraction rates from the aquifer. In a simplified system, this can be done by comparing the recharge to the system from rainfall to the abstraction rate through the equation:

$$\text{Net Groundwater Volume} = \text{Recharge} - \text{Abstraction}$$

It can generally be stated that a negative net groundwater volume calculated by the above equation indicates that dewatering of the groundwater system occurs.

The net volume of water in the combined eastern and western aquifers varies with time according to the annual recharge volume. However, the net volume of water for current and future abstraction rates is positive, indicating that the annual recharge exceeds the annual abstraction.

In order for the groundwater system to stay in equilibrium the excess (positive “net volume”) water leaves the system at another unknown point, possibly the Kafue River, as suggested by Scott Wilson Piésold (2003).

Baseline calculations indicate that under natural conditions as much as 44 000 000m³ of water flows annually into the Kafue River as base flow contribution.

The numerical model was used to correlate and substantiate the water balance calculations. A numerical model was constructed to evaluate the assumptions put forward, and confirmed the calculated values of the manual calculations. The model was calibrated using the trial and error method.

The aquifer parameters fall within the expected range. Recharge to the area calibrated at 20%, which corresponds well to the calculated figure of 25% using the SVF, Equal Volume and CRD methods. This is slightly higher than the figure of 10% by Landell Mills Associates (1978) and falls within the upper segment of the 6 to 22% calculated by Macdonald and Partners (1982). However, taking into consideration the dambo areas, relatively flat topography, absence of major surface water drainage canals, high rainfall, the fact that soil infiltration rates exceed precipitation rates (Landell Mills Associates, 1979) and elevated recharge in irrigated areas due to return flow, this figure is believed to be conservative.

Sensitivity analyses indicate that the numerical model is relatively insensitive to changes in the parameters. The model is influenced by storativity, transmissivity, and recharge.

The numerical model confirms that the combined eastern and western aquifers are capable of sustaining the current and future abstraction programs.

Traditionally, the gravity method is considered to be the most effective way of identifying possible borehole positions in dolomitic terrain as it is capable of detecting the small changes in the earth's gravitational field due to the presence of sub-surface solution cavities which cause sub-surface density variations. These variations can be identified at depths of 100m and more. The solution cavities are usually indicated by areas of relatively low gravity values due to the reduced underlying rock mass.

However, it is the opinion of the author that the gravity method proved to be ineffective as a singular means of identifying high yielding zones within the geology in the study area. This conclusion is based on the evidence that the schist, which occurs in the area, appears to possess an almost equal gravitational force to the karstic (solution cavity) dolomitic geology. This equal gravitational force is shown on gravity Traverse 3 (Figure 2.9.4.1).

The figure indicates two areas of gravity low, with approximately equal values. These two areas are located between 0 and 1 000m, and between 3 150 and 4 170m. A zone of relative gravity high separates the two areas of gravity low.

When drilling, it became apparent that the gravity low between 0 and 1 000m represents the contact zone between schist and the dolomite. The borehole log for borehole GCS1 (drilled at station 90) indicates a schist lens between 61 and 64m depth within the dolomite, and metamorphosed schist from 72m downwards. Borehole GCS2 (drilled at station 780) indicates extensive weathering, and some limestone between 40 and 55m depth, as well as clay. It is considered that the schist dips sharply from GCS1 towards GCS2, and therefore this borehole is too shallow (only 60m) to have intersected any schist which may be present in this area.

The weathering profile in these boreholes also extends deeper than the average of 10 to 20m, which occurs in other areas. This is possibly due to the contact between the dolomite and schist facilitating weathering by acting as a preferential pathway for groundwater movement.

The boreholes yielded very little (seepage) to no water.

The gravity low between 3 150 and 4 170m is caused by karstification. Boreholes GCS7 and GCS8 have been drilled at stations 3 180 and 4 080 respectively. Reportedly, these boreholes intersected extensive fracturing during drilling and subsequent aquifer tests performed on the boreholes revealed relatively high transmissivities (3 139m²/day and 803m²/day respectively) and sustainable yields (25l/s for both).

No boreholes have been drilled in the area of gravity high between stations 1 110 and 2 490, however, it is believed that the dolomite becomes more competent and less weathered in this area. It is expected that boreholes drilled in this area will be relatively low yielding due to less fractures and less solution of the dolomite than in the area between stations 3 150 and 4 170.

The gravity data indicates areas where smaller fracture zones and/or lesser weathering occur. It is considered that boreholes drilled in these areas would be relatively low yielding due to the lesser development of fractures and/or weathering zones.

This example highlights the importance of detailed knowledge of the geology of the study area. The extent of the dolomitic aquifer and the locality of schist inliers must be known when scientifically siting boreholes. Once the dolomitic aquifer has been delineated, the gravity method is capable of distinguishing between potentially low and high yielding zones within the dolomite.

In order to validate the gravity survey, the electromagnetic and magnetic surveys were performed along a section of gravity Traverse 3. The data indicates a marked correlation between the point of gravity low at Station 3 180 and anomalies in the EM34-3 and magnetometer data in this area.

As discussed above, the gravity data indicated a gravity low in this area, and borehole GCS7 has been drilled at station 3 180.

The electromagnetic data indicates a sharp anomaly between stations 3 050 and 3 250 in the vertical dipole mode, as well as in the available data for the horizontal dipole mode.

The horizontal dipole measurements could not be recorded accurately at all the stations due to erratic fluctuation in the measurements. It is the opinion of the author that these fluctuations are attributed to two factors.

The first factor is the shallow sub-surface ferricreaceous material that occurs in the area. The ferricreaceous material is high in iron content. This influences the electric current and artificial magnetic field induced by the electromagnetic method. Due to the highly conductive nature of this material, the electric current and induced magnetic field mostly travels along this layer.

The 40-metre coil separation was used in an effort to obtain the deepest possible penetration. Using the 40-metre coil separation yields a maximum theoretical penetration depth of 20m in the horizontal dipole configuration and 60m in the vertical dipole configuration.

This is the maximum spacing that can be used with the EM34-3. The longer the station spacing, the higher the interference by external factors, especially on the horizontal dipole measurements. If a shorter coil separation, for example 20m, was used, the interference and fluctuations would probably have been less; however, the depth of penetration would have been halved to 10m in the horizontal dipole configuration and 30m in the vertical dipole configuration. As stated earlier, the main water bearing features are situated between 30 and 50m, and they would therefore not have been recorded using a 20-metre coil separation.

The second factor is the change in lithology over short distances, as commented on by Macdonald and Partners in 1982 (refer to Chapter 2.9.2). Macdonald and Partners Ltd. experienced difficulties fitting the obtained resistivity to the calibration curves to obtain depth to bedrock. Macdonald and Partners Ltd. was of the opinion that a possible reason for this could be the changes in lithology over short distances, as was evident from the borehole logs drilled during the 1981 investigation.

These changes in lithology would definitely have an effect on the obtained measurements. However, it is the opinion of the author that such changes would also influence the vertical dipole configuration.

It is the opinion of the author that the fluctuations in the horizontal dipole configuration are best explained by the ferricreaceous nature of the shallow sub-surface soil. The ferricrete can be observed on the surface and also from the drilling logs.

The magnetic method indicates a large anomaly between stations 3 045 and 3 200. This is accompanied by what appears to be possibly two sympathetic anomalies between stations 3 200 and 3 385.

The magnetic method displays some relatively erratic data, with fluctuations in the order of 20 to 50nT being fairly common. This could also be attributed to the ferricreaceous nature of the shallow sub-surface soil.

It is concluded that for this particular study area, where the main water bearing features are located between 30 and 50mbgl, the electromagnetic and magnetic methods can be employed with a relatively high success rate. The electromagnetic and magnetic methods have not been tested against distinguishing between the schist and dolomite, and therefore no conclusion on this aspect can be reached.

The 1979 and 1982 geophysical investigations conclude that the resistivity methods suffer from the same limitations as the gravity survey of 2004 revealed, namely that it is not able to distinguish between the water bearing dolomitic areas and the surrounding lower yielding lithologies.

Generally, it is concluded that the geophysical methods are unable to distinguish between high yielding and lower yielding lithologies. However, once high yielding lithologies have been identified, any of the geophysical methods are able to determine the positions of fracture zones and solution cavities associated with high yielding boreholes.

Based on the conclusions of this study several recommendations can be made.

The daily rainfall data and Lake Nampamba water level data collection should be continued. It is important to keep this data collection up-to-date should any additional future studies have to be performed.

In addition to the existing data collection the water levels in the production boreholes should be monitored at least on a weekly basis. This will provide more data for model calibration, monitor levels to see whether a dewatering trend develops, and identify any compartmentalisation.

It is recommended that a deep exploration borehole be drilled close to Lake Nampamba in order to determine the source of water for Lake Nampamba. As discussed, none of the boreholes were drilled deeper than 100m, while both Lake Nampamba and Lake Kashiba are deeper than 100m. It is possible that a deeper, even higher yielding source of water exists, than what is currently accessed by the boreholes. Fracture or solution cavity zones should be recorded. If possible, the borehole should be pump tested on reaching 100m in depth, and again should further water strikes be reached deeper than 100m. This way the sustainable yield and relative contribution of the deeper fracture zones can be determined. It should be noted that this borehole should be drilled at a diameter of at least 254mm (10”), in order to be able to install a sufficiently large pump to be able to perform meaningful aquifer tests.

Additional aquifer tests should be performed on boreholes with an observation borehole close by. By recording the groundwater level fluctuation in the observation borehole, additional storativity calculations can be performed.

As discussed, borehole MDP11 appears to be high yielding, even though not identified as such by Landell Mills Associates. It is proposed that an aquifer test be performed on this borehole to determine the true transmissivity of the aquifer in that area.

It is recommended that an isotope study of the groundwater quality be undertaken. Using deuterium or Oxygen¹⁸, additional recharge percentage estimations that are more accurate than the chloride method, and possibly also the SVF and CRD methods, can be performed.

Evaporation data should be recorded properly and on a daily basis in order for the data to be able to be incorporated into the water balance calculations.

Flow data from the Kafue River should be obtained. From this data the base flow contribution from the dolomitic aquifer in different areas can be assessed.

It is recommended that additional soil infiltration tests be performed in order to correlate the Landell Mills Associates (1979) data. The soil infiltration tests should be performed in undisturbed and agricultural areas in order to determine the influence of the mining activities on the soil.

It is recommended that a detailed geological investigation be performed in the area. This should include surface mapping, data analysis from the existing borehole logs and a detailed three-dimensional geological model. The three-dimensional model will help immensely with the conceptualisation of the aquifer interactions and processes. From the geological model, potentially high yielding dolomitic areas can be identified. These identified areas can then be the aim of future geophysical investigations.

Chapter 6 : References.

Brand, CC (June 2003). Paper presented at the 11th Biennial Symposium on Groundwater Recharge, Phoenix, AZ. *Groundwater Recharge Potential in the Upper Black Squirrel Creek Basin, Colorado.*

Bredenkamp, DB; Botha, LJ; van Tonder, GJ and van Rensburg, HJ (June 1995). Water Research Commission Report TT73/95. *Manual on the Quantitative Estimation of Groundwater Recharge and Aquifer Storativity.*

Colorado School of Mines, Course notes, 2004. *Resistivity Soundings.* Website: http://www.mines.edu/fs_home/tboyd/GP311/MODULES/RES/NOTES/sounding.html

Community-Based Natural Resource Management Network, The. Ongoing study. Website: <http://www.cbnrm.net/resources/topics/biomes/miombo.html>

Cornelius, FP and du Plessis, JA (April 1997). *Short Course on Hydrological Modelling. Vol 1: Text.*

Department of Water Affairs and Forestry (1996). *South African Water Quality Guidelines (Vol 1, 2nd Edition): Domestic Use.*

Dorsel, D and La Breche, T. *Environmental Sampling & Monitoring Primer: Kriging.* Website: http://www.ce.vt.edu/program_areas/environmental/teach/smprimer/kriging/kriging.html

Engineering & Exploration Geophysical Services cc Report, 30 March 2004. *Gravimetric Survey in Mpongwe District, Zambia.*

Janse van Rensburg, H; van Tonder, GJ; Botha, JF and Bredenkamp, DB (March 1987). Water Research Commission Report No. 171/1/87. *'n Ondersoek na die Benutting van Grondwater in die Grootfonteinkompartement.*

Kruseman, G.P & de Ridder, N.A. (2000). ILRI Publication 47: *Analysis and Evaluation of Pumping Test Data*. 2nd Edition (Completely Revised). ISBN 90 70754 207.

Landell Mills Associates (December 1978). Report to the Ministry of Lands and Agriculture, Republic of Zambia. Commission of the European Communities European Development Fund. Account No. 4100.033.56.14. Financing Agreement No 2188/ZAM. *Mpongwe Pilot Project. Interim Report on the Assessment of Groundwater Resources*.

Landell Mills Associates (March 1979). Report to the Ministry of Agriculture and Water Development, Republic of Zambia. Commission of the European Communities European Development Fund. *Mpongwe Pilot Project. Preliminary Report on Water Resources*.

Landell Mills Associates (March 1980). *Mpongwe Pilot Project. Final Report on 1979 Hydrological Monitoring Programme*.

Landell Mills Associates (March 1982). *Mpongwe Development Project. Final Report on 1981 Hydrological Monitoring Programme*.

Loke, MH Dr (2000). *Electrical imaging surveys for environmental and engineering studies. A practical guide to 2-D and 3-D surveys*.

Lynch, SD and Hodgson, FDI (November 1987). Water Research Commission Report No. 113/2/87. *Parameter Identifikasie en Modelling van die Sishen Akwifereer*.

Macdonald, M. and Partners Ltd. (February 1982). Report to the Ministry of Agriculture and Water Development, Government of the Republic of Zambia. European Development Fund Project Account Nr. 4100.033.56.44. Financing agreement Nr. 2505/ZAM. *Mpongwe Development Company – Phase 1. Groundwater Report*.

New Mexico Climate Center Website. <http://www.nmsu.edu/math/penmans.html>.

Rankin Engineering Consultants (November 1994). Mpongwe Development Company Limited. Review of Literature and Data Related to Western Aquifers.

Rankin Engineering Consultants (July 1997). Mpongwe Development Corporation. Western Aquifer Drilling Report.

Scott Wilson Piésold (August 2003). Report to the Ministry of Energy and Water Development OPPPI/ZESCO Limited. Integrated Kafue River Basin Environmental Impact Assessment Study. Strategic Environmental Impact Assessment Report. Copy of Appendix B: Groundwater at Mpongwe.

Spits, K and Moreno, J (1996). A practical guide to groundwater and solute transport modeling.

Topographical Map 1327b3, 2nd Edition (1965). Scale 1:50 000. Published by the Director of Overseas Surveys, Tolworth, Surrey, England (4110/8/65/2087/0S). Grid: UTM Zone35. Projection: Transverse Mercator. Spheroid: Clarke 1880 (Modified). Meridian of Origin: 27°00' East of Greenwich. Latitude of Origin: Equator. Datum: New (1950) Arc.

Topographical Map 1327b4, 2nd Edition (1965). Scale 1:50 000. Published by the Director of Overseas Surveys, Tolworth, Surrey, England (4100/9/65/1178/SPC). Grid: UTM Zone35. Projection: Transverse Mercator. Spheroid: Clarke 1880 (Modified). Meridian of Origin: 27°00' East of Greenwich. Latitude of Origin: Equator. Datum: New (1950) Arc.

Topographical Map 1327d1, Series 51, 1ZS 1985 Edition (1985). Scale 1:50 000. Published by the Surveyor General, Lusaka (11/85/851423M). Grid: UTM Zone35. Projection: Transverse Mercator. Spheroid: Clarke 1880 (Modified). Meridian of Origin: 27°00' East of Greenwich. Latitude of Origin: Equator. Datum: New (1950) Arc.

Topographical Map 1327d2, 2nd Edition (1965). Scale 1:50 000. Published by the Director of Overseas Surveys, Tolworth, Surrey, England (4110/9/65/2112/0S). Grid:

UTM Zone35. Projection: Transverse Mercator. Spheroid: Clarke 1880 (Modified). Meridian of Origin: 27°00' East of Greenwich. Latitude of Origin: Equator. Datum: New (1950) Arc.

Topographical Map 1328a3, Series 51, 1ZS 1984 Edition (1984). Scale 1:50 000. Published by the Surveyor General, Lusaka. Grid: UTM Zone35. Projection: Transverse Mercator. Spheroid: Clarke 1880 (Modified). Meridian of Origin: 27°00' East of Greenwich. Latitude of Origin: Equator. Datum: New (1950) Arc.

Topographical Map 1328c1, Series ZS51, 1-ZS 1985 Edition (1985). Scale 1:50 000. Published by the Surveyor General, Lusaka (2/86/851654M). Grid: UTM Zone35. Projection: Transverse Mercator. Spheroid: Clarke 1880 (Modified). Meridian of Origin: 27°00' East of Greenwich. Latitude of Origin: Equator. Datum: New (1950) Arc.

United States Geological Survey. *Borehole Geophysical Methods*. Website:

<http://www.pah2o.er.usgs.gov/malvern/geophysics.html>

University of Massachusetts, Boston. Department Earth and Geographic Science. *Information paper on Infiltrometer tests*. Website:

<http://www.geog.umb.edu/wdripps/Fieldmethods/infiltration.doc>

van Dyk, G (1993). Department of Water Affairs Technical Report No. GH3813. *Geohydrological Investigation for SADF Pomfret. District Vryburg. Drainage Region D410*.

van Dyk, G. (1997). Letter to the Director General, Department of Public Works dated 01 April 1997. *Pomfret Watervoorsiening*.

WLPU Consultants (August 1983). *Munkumpu Project. Report on Development of Water Resources*.

Appendix A:

Geological Borehole Logs and Borehole Geophysical Data.

Characterisation of the Dolomitic Aquifer in the Copperbelt Province, Northern Zambia. MDC Borehole Logs

Hole Name :A3000

Segment Start Depth :0.00 Segment End Depth :70.00

Lithology\$		'Gamma Log\$'	'Single Point Resistance\$'	'Spontaneous Potential\$'	
Depth At	Strat Column	Description	Gamma	SPR	SP
	Soil	Overburden.			
-10	W-Limestone	Weathered limestone.			
-20					
-30	U-Limestone	Un-weathered limestone. Water level @ 32m.			
-40	Clay	Fracture or fault zone with much clay and weathered limestone. Cavity?			
-50	Limestone	Lost circulation. No samples.			
-60					
	U-Limestone	Un-weathered limestone.			

Hole Name :A12500

Segment Start Depth :0.00 Segment End Depth :30.00

	Lithology\$		'Gamma Log\$'	'Single Point Resistance\$'	'Spontaneous Potential\$'
Depth At	Strat Column	Description	Gamma	SPR	SP
	Soil	Overburden.			
	Schist	Un-weathered schist. Dry borehole.			
-5	Schist	Weathered schist.			
-10					
-15					
-20					
-25					

Characterisation of the Dolomitic Aquifer in the Copperbelt Province, Northern Zambia. MDC Borehole Logs

Hole Name :A20500

Segment Start Depth :0.00 Segment End Depth :48.00

	Lithology\$		'Gamma Log\$'	'Single Point Resistance\$'	'Spontaneous Potential\$'
Depth At	Strat Column	Description	Gamma	SPR	SP
-5	Soil	Overburden and decomposed material.			
-10					
-15					
-20					
-25	Limestone	Un-weathered limestone. Solution cavity @37m. Water strike.			
-30					
-35					
-40					
-45					

Characterisation of the Dolomitic Aquifer in the Copperbelt Province, Northern Zambia. MDC Borehole Logs

Hole Name :B6500

Segment Start Depth :0.00 Segment End Depth :51.30

	Lithology\$		'Gamma Log\$'	'Single Point Resistance\$'	'Spontaneous Potential\$'
Depth At	Strat Column	Description	Gamma	SPR	SP
	Soil	Overburden.			
-10	Schist	Weathered schist.			
-20					
-30	Schist	Un-weathered schist. Only minor water strikes intersected.			
-40					
-50					

Characterisation of the Dolomitic Aquifer in the Copperbelt Province, Northern Zambia.				MDC Borehole Logs		
Hole Name :B14000						
Segment Start Depth :0.00			Segment End Depth :70.00			
	Lithology\$		'Gamma Log\$'	'Single Point Resistance\$'	'Spontaneous Potential\$'	
Depth At	Strat Column	Description	Gamma	SPR	SP	
-10	Soil	Soil and weathered material.				
-20						
-30		Schist	Weathered schist.			
-40						
-50	Schist	Schist and limestone.				
-60	Schist	Weathered schist. Water level @ 51m.				

Scale 1:519.75052

09/24/04

14:12:53

Characterisation of the Dolomitic Aquifer in the Copperbelt Province, Northern Zambia. MDC Borehole Logs

Hole Name :C6000

Segment Start Depth :0.00 Segment End Depth :62.00

	Lithology\$		'Gamma Log\$'	'Single Point Resistance\$'	'Spontaneous Potential\$'
Depth At	Strat Column	Description	Gamma	SPR	SP
-10	Soil	Overburden.			
-20	Schist	Weathered schist			
-30	Schist	Un-weathered schist. Only minor water strikes intersected.			
-40					
-50					
-60					

Characterisation of the Dolomitic Aquifer in the Copperbelt Province, Northern Zambia. MDC Borehole Logs

Hole Name :C8000

Segment Start Depth :0.00 Segment End Depth :56.00

	Lithology\$		'Gamma Log\$'	'Single Point Resistance\$'	'Spontaneous Potential\$'
Depth At	Strat Column	Description	Gamma	SPR	SP
-10	Soil	Overburden.			
-20	Schist	Weathered schist.			
-30		Un-weathered schist. Only minor water strikes intersected.			
-40					
-50	Schist				

Characterisation of the Dolomitic Aquifer in the Copperbelt Province, Northern Zambia. MDC Borehole Logs

Hole Name :D3400

Segment Start Depth :0.00 Segment End Depth :32.00

	Lithology\$		'Gamma Log\$'	'Single Point Resistance\$'	'Spontaneous Potential\$'
Depth At	Strat Column	Description	Gamma	SPR	SP
-5	Soil	Overburden and decomposed material. Water level @ 17.2m.			
-10					
-15					
-20	W-Limestone	Weathered limestone.			
-25	U-Limestone	Un-weathered limestone.			
-30					

Characterisation of the Dolomitic Aquifer in the Copperbelt Province, Northern Zambia. MDC Borehole Logs

Hole Name :D4400

Segment Start Depth :0.00 Segment End Depth :38.20

Lithology\$		'Gamma Log\$'	'Single Point Resistance\$'	'Spontaneous Potential\$'	
Depth At	Strat Column	Description	Gamma	SPR	SP
-5	Soil	Overburden.			
-10					
-15	W-Limestone	Weathered limestone. Water level @ 16.5m.			
-20					
-25	Limestone	Lost circulation. Cavity @ 20-22m. No samples recovered.			
-30					
-35	U-Limestone	Un-weathered limestone.			

Characterisation of the Dolomitic Aquifer in the Copperbelt Province, Northern Zambia. MDC Borehole Logs

Hole Name :D7400

Segment Start Depth :0.00 Segment End Depth :45.00

	Lithology\$		'Gamma Log\$'	'Single Point Resistance\$'	'Spontaneous Potential\$'
Depth At	Strat Column	Description	Gamma	SPR	SP
-5	Soil	Overburden and decomposed material.			
-10					
-15	Limestone	Limestone. First water strike @ 22m. First solution cavity @ 33m - little water. Second solution cavity @ 40m - abundant water. Water level @ 16m.			
-20					
-25					
-30					
-35					
-40					

Characterisation of the Dolomitic Aquifer in the Copperbelt Province, Northern Zambia. MDC Borehole Logs

Hole Name :D7400Ob

Segment Start Depth :0.00 Segment End Depth :40.00

	Lithology\$		'Gamma Log\$'	'Single Point Resistance\$'	'Spontaneous Potential\$'
Depth At	Strat Column	Description	Gamma	SPR	SP
-5	Soil	Overburden.			
-10	U-Limestone				
-15					
-20					
-25		Un-weathered limestone. Water strike @ 20m. Water level @ 16.2m.			
-30					
-35					

Characterisation of the Dolomitic Aquifer in the Copperbelt Province, Northern Zambia. MDC Borehole Logs

Hole Name :D8400

Segment Start Depth :0.00 Segment End Depth :50.00

	Lithology\$		'Gamma Log\$'	'Single Point Resistance\$'	'Spontaneous Potential\$'
Depth At	Strat Column	Description	Gamma	SPR	SP
-10	Soil	Overburden.			
-20	U-Limestone				
-30		Un-weathered limestone. Water level @ 15.6m.			
-40					

Characterisation of the Dolomitic Aquifer in the Copperbelt Province, Northern Zambia. MDC Borehole Logs

Hole Name :E3000

Segment Start Depth :0.00 Segment End Depth :32.50

	Lithology\$		'Gamma Log\$'	'Single Point Resistance\$'	'Spontaneous Potential\$'
Depth At	Strat Column	Description	Gamma	SPR	SP
-5	Soil	Overburden.			
-10	Schist	Weathered schist.			
-15					
-20	Schist	Un-weathered schist.			
-25					
-30					

Characterisation of the Dolomitic Aquifer in the Copperbelt Province, Northern Zambia. MDC Borehole Logs

Hole Name :E3700

Segment Start Depth :0.00 Segment End Depth :68.30

	Lithology\$		'Gamma Log\$'	'Single Point Resistance\$'	'Spontaneous Potential\$'
Depth At	Strat Column	Description	Gamma	SPR	SP
-10	Soil	Laterite overburden.			
-20	W-Limestone	Weathered limestone.			
-30	Limestone	Limestone.			
-40	W-Limestone	Partly weathered limestone.			
-50	Limestone	Limestone. Some schist and phyllite @ 48m.			
-60	U-Limestone	Un-weathered limestone.			

Characterisation of the Dolomitic Aquifer in the Copperbelt Province, Northern Zambia. MDC Borehole Logs

Hole Name :E5000

Segment Start Depth :0.00 Segment End Depth :72.00

	Lithology\$		'Gamma Log\$'	'Single Point Resistance\$'	'Spontaneous Potential\$'
Depth At	Strat Column	Description	Gamma	SPR	SP
-10	Soil	Soil and weathered material. Small inflow of water @ 13.5 & 20.5m.			
-20					
-30	Limestone	Alternating weathered and un-weathered limestone. Solution cavity @ 50m.			
-40					
-50					
-60					
-70					

Characterisation of the Dolomitic Aquifer in the Copperbelt Province, Northern Zambia. MDC Borehole Logs

Hole Name :E5000

Segment Start Depth :0.00 Segment End Depth :72.00

	Lithology\$		'Gamma Log\$'	'Single Point Resistance\$'	'Spontaneous Potential\$'
Depth At	Strat Column	Description	Gamma	SPR	SP
-10	Soil	Soil and weathered material. Small inflow of water @ 13.5 & 20.5m.			
-20					
-30	Limestone	Alternating weathered and un-weathered limestone. Solution cavity @ 50m.			
-40					
-50					
-60					
-70					

Characterisation of the Dolomitic Aquifer in the Copperbelt Province, Northern Zambia. MDC Borehole Logs

Hole Name :F500

Segment Start Depth :0.00 Segment End Depth :56.00

	Lithology\$		'Gamma Log\$'	'Single Point Resistance\$'	'Spontaneous Potential\$'
Depth At	Strat Column	Description	Gamma	SPR	SP
	Soil	Overburden.			
-10 -20 -30 -40 -50	Limestone	Un-weathered limestone. Dry solution cavity @ 14-16m. Abundant small fractures 22-48m.			

Characterisation of the Dolomitic Aquifer in the Copperbelt Province, Northern Zambia.			MDC Borehole Logs		
Hole Name :F2000					
Segment Start Depth :0.00			Segment End Depth :79.00		
	Lithology\$		'Gamma Log\$'	'Single Point Resistance\$'	'Spontaneous Potential\$'
Depth At	Strat Column	Description	Gamma	SPR	SP
	Soil	Overburden.			
-10	W-Limestone	Weathered limestone.			
-20	U-Limestone	Un-weathered limestone. Cavernous & large fracture @ 24-26m. Water strike @ 22m. Water level @ 17m.			
-30					
-40					
-50	U-Limestone	Un-weathered limestone. Extensive fractures 26-50m. Large solution cavity @ 66-68m.			
-60					
-70					

Scale 1:586.575587

09/24/04

14:19:37

Hole Name :F2000Ob

Segment Start Depth :0.00 Segment End Depth :75.00

		Lithology\$	'Gamma Log\$'	'Single Point Resistance\$'	'Spontaneous Potential\$'
Depth At	Strat Column	Description	Gamma	SPR	SP
	Soil	Overburden.			
-10	W-Limestone	Weathered limestone.			
-20	Limestone	Un-weathered limestone. Solution cavities at 24 and 41m depth. Lost circulation from 23m to bottom. Water strike @ 22m. Water level @ 17m.			
-30					
-40					
-50					
-60					
-70					

Characterisation of the Dolomitic Aquifer in the Copperbelt Province, Northern Zambia. MDC Borehole Logs

Hole Name :F3000

Segment Start Depth :0.00 Segment End Depth :60.00

	Lithology\$		'Gamma Log\$'	'Single Point Resistance\$'	'Spontaneous Potential\$'
Depth At	Strat Column	Description	Gamma	SPR	SP
-10	Soil	Overburden.			
	W-Limestone	Weathered limestone.			
-20	Limestone	Un-weathered limestone. Fracture zone @ 50-60m. Lost circulation. Water strike @ 30m. Water level @ 24.5m.			
-30					
-40					
-50					

Characterisation of the Dolomitic Aquifer in the Copperbelt Province, Northern Zambia. MDC Borehole Logs

Hole Name :F8000

Segment Start Depth :0.00 Segment End Depth :80.00

	Lithology\$		'Gamma Log\$'	'Single Point Resistance\$'	'Spontaneous Potential\$'
Depth At	Strat Column	Description	Gamma	SPR	SP
-10	Soil	Red soil.			
-20	Schist	Brown grey and greenish weathered schist.			
-30					
-40					
-50	Schist	Weathered calcareous schist. Water level @ 51.3m. Only minor inflow of water.			
-60	Schist	Un-weathered calcareous schist.			
-70					

Characterisation of the Dolomitic Aquifer in the Copperbelt Province, Northern Zambia. MDC Borehole Logs

Hole Name :F12000

Segment Start Depth :0.00 Segment End Depth :48.00

	Lithology\$		'Gamma Log\$'	'Single Point Resistance\$'	'Spontaneous Potential\$'
Depth At	Strat Column	Description	Gamma	SPR	SP
-5	Soil	Overburden.			
-10	Schist	Weathered schist.			
-15	Schist				
-20	Schist				
-25	Schist	Un-weathered schist with some alternating limestone. Dry solution cavity @ 18-20m. Water level @ 31.3m.			
-30	Schist				
-35	Limestone	Alternating limestone and some schist. Transition zone.			
-40	Limestone				
-45	Limestone	Limestone.			

Characterisation of the Dolomitic Aquifer in the Copperbelt Province, Northern Zambia. MDC Borehole Logs

Hole Name :G12500

Segment Start Depth :0.00 Segment End Depth :41.60

	Lithology\$		'Gamma Log\$'	'Single Point Resistance\$'	'Spontaneous Potential\$'
Depth At	Strat Column	Description	Gamma	SPR	SP
-5	Soil	Overburden.			
-10	Schist	Weathered schist.			
-15					
-20	Schist	Un-weathered pyritic schist. Only minor water strikes intersected.			
-25					
-30					
-35					
-40					

Characterisation of the Dolomitic Aquifer in the Copperbelt Province, Northern Zambia. MDC Borehole Logs

Hole Name :F14500

Segment Start Depth :0.00 Segment End Depth :40.00

	Lithology\$		'Gamma Log\$'	'Single Point Resistance\$'	'Spontaneous Potential\$'
Depth At	Strat Column	Description	Gamma	SPR	SP
	Soil	Overburden.			
-5	Limestone	Limestone. Extensive fracturing @ 18-20m, with numerous smaller fractures 20-40m. Water strike @ 20m. Water level @ 12.4m.			
-10					
-15					
-20					
-25					
-30					
-35					

Characterisation of the Dolomitic Aquifer in the Copperbelt Province, Northern Zambia.			MDC Borehole Logs		
Hole Name :F14500Ob					
Segment Start Depth :0.00			Segment End Depth :50.00		
	Lithology\$		'Gamma Log\$'	'Single Point Resistance\$'	'Spontaneous Potential\$'
Depth At	Strat Column	Description	Gamma	SPR	SP
	Soil	Overburden.			
	W-Limestone	Weathered limestone.			
-10	U-Limestone	Un-weathered limestone. Water strike @ 19m. Water level @ 10m.			
-20	W-Limestone	Weathered limestone. Fractured 14-36m. Lost circulation. No drill samples recovered.			
-30	U-Limestone	Un-weathered limestone.			
-40	Limestone	Lost circulation. No samples.			

Scale 1:371.250371

09/24/04

14:19:28

Hole Name :G7500

Segment Start Depth :0.00 Segment End Depth :33.00

	Lithology\$		'Gamma Log\$'	'Single Point Resistance\$'	'Spontaneous Potential\$'
Depth At	Strat Column	Description	Gamma	SPR	SP
	Soil	Overburden.			
-5	Limestone	Limestone. Solution cavity @ 9-14m. Water strike.			
-10					
-15					
-20					
-25					
-30					

Characterisation of the Dolomitic Aquifer in the Copperbelt Province, Northern Zambia. MDC Borehole Logs

Hole Name :G16000

Segment Start Depth :0.00 Segment End Depth :40.00

	Lithology\$		'Gamma Log\$'	'Single Point Resistance\$'	'Spontaneous Potential\$'
Depth At	Strat Column	Description	Gamma	SPR	SP
-5	Soil	Overburden. Water level @ 9.1m.			
-10					
-15	W-Limestone	Weathered limestone.			
-20	U-Limestone	Un-weathered limestone.			
-25					
-30					
-35					

Characterisation of the Dolomitic Aquifer in the Copperbelt Province, Northern Zambia. MDC Borehole Logs

Hole Name :G18500(1)

Segment Start Depth :0.00 Segment End Depth :25.00

	Lithology\$		'Gamma Log\$'	'Single Point Resistance\$'	'Spontaneous Potential\$'
Depth At	Strat Column	Description	Gamma	SPR	SP
	Soil	Overburden.			
	Sand	Sandy material.			
-5	Schist	Weathered schist. Only minor water strikes intersected.			
-10					
-15	Schist	Un-weathered schist.			
-20					

Characterisation of the Dolomitic Aquifer in the Copperbelt Province, Northern Zambia. MDC Borehole Logs

Hole Name :G18500(1)

Segment Start Depth :0.00 Segment End Depth :25.00

	Lithology\$		'Gamma Log\$'	'Single Point Resistance\$'	'Spontaneous Potential\$'
Depth At	Strat Column	Description	Gamma	SPR	SP
	Soil	Overburden.			
	Sand	Sandy material.			
-5	Schist	Weathered schist. Only minor water strikes intersected.			
-10					
-15					
-20	Schist	Un-weathered schist.			

Characterisation of the Dolomitic Aquifer in the Copperbelt Province, Northern Zambia. MDC Borehole Logs

Hole Name :GCS1

Segment Start Depth :0.00 Segment End Depth :85.00

	Lithology\$		'Gamma Log\$'	'Single Point Resistance\$'	'Spontaneous Potential\$'
Depth At	Strat Column	Description	Gamma	SPR	SP
	Soil	Red-brown ferricreaceous laterite.			
-10	Sand	Very fine brown sand.			
-20	Limestone	Dark grey, baked crystalline limestone. Massive quartz present. Soft drilling 29-31m. Fractures 34-38m and 53-57m.			
-30					
-40	Limestone	Transition zone between limestone and schist.			
-50					
-60	Schist	Dark grey schist. Massive fluoride and some mica present.			
-70					
-80					

Characterisation of the Dolomitic Aquifer in the Copperbelt Province, Northern Zambia. MDC Borehole Logs

Hole Name :GCS2

Segment Start Depth :0.00 Segment End Depth :60.00

Lithology\$		'Gamma Log\$'	'Single Point Resistance\$'	'Spontaneous Potential\$'	
Depth At	Strat Column	Description	Gamma	SPR	SP
	Soil	Red brown weathered material and laterite. Some ferricrete.			
-10	Soil	Calcareous, weathered material.			
-20	Limestone	Decomposed brown limestone.			
-30	W-Limestone	Weathered dark grey limestone. Some white limestone and quartz. Water strike @ 43m. Less than 0.5l/s.			
-40	Clay	Hard white to pink clay. Soapy feel when wet.			
-50					

Hole Name :H4000

Segment Start Depth :0.00 Segment End Depth :58.00

	Lithology\$		'Gamma Log\$'	'Single Point Resistance\$'	'Spontaneous Potential\$'
Depth At	Strat Column	Description	Gamma	SPR	SP
	Soil	Overburden.			
-10	Schist	Weathered schist. Minor water strikes intersected.			
-20					
-30	Schist	Un-weathered schist.			
-40					
-50					

Characterisation of the Dolomitic Aquifer in the Copperbelt Province, Northern Zambia. MDC Borehole Logs

Hole Name :IN3A

Segment Start Depth :0.00 Segment End Depth :54.00

		Lithology\$	'Gamma Log\$'	'Single Point Resistance\$'	'Spontaneous Potential\$'
Depth At	Strat Column	Description	Gamma	SPR	SP
-10	Soil	Laterite overburden.			
-20	W-Limestone	Weathered limestone.			
-30	Limestone	Limestone. Lost circulation below 35m depth. Solution cavity @ 40m.			
-40					
-50					

Hole Name :IS2

Segment Start Depth :0.00 Segment End Depth :30.00

	Lithology\$		'Gamma Log\$'	'Single Point Resistance\$'	'Spontaneous Potential\$'
Depth At	Strat Column	Description	Gamma	SPR	SP
-5	Soil	Overburden. Water level @ 11.2m.			
-10					
-15	W-Limestone	Weathered limestone. Cavernous and fractured @ 13-17m.			
-20					
-25	Limestone	Schistose limestone.			

Hole Name :J1000

Segment Start Depth :0.00 Segment End Depth :54.00

	Lithology\$		'Gamma Log\$'	'Single Point Resistance\$'	'Spontaneous Potential\$'
Depth At	Strat Column	Description	Gamma	SPR	SP
	Soil	Overburden.			
-10	W-Limestone	Weathered limestone. Water level @ 7.3m.			
-20					
-30	Limestone	Lost circulation - no samples.			
-40					
-50	U-Limestone	Un-weathered limestone.			

Characterisation of the Dolomitic Aquifer in the Copperbelt Province, Northern Zambia. MDC Borehole Logs


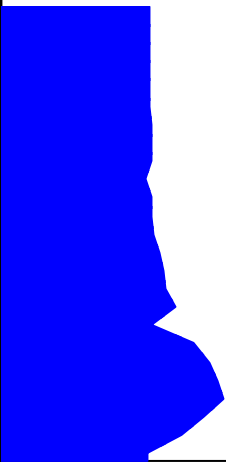

Hole Name :K1500

Segment Start Depth :0.00 Segment End Depth :53.50

	Lithology\$		'Gamma Log\$'	'Single Point Resistance\$'	'Spontaneous Potential\$'		
Depth At	Strat Column	Description	Gamma	SPR	SP		
-10	Soil	Soil and un-weathered material. Only minor inflow of water. Water level @ 26m.					
-20							
-30						Quartz	Massive quarts vein.
-40						Clay	Clay in fault or fracture zone.
-50	Limestone	Limestone.					

Hole Name :MDP1

Segment Start Depth :0.00 Segment End Depth :55.80

	Lithology\$		'Gamma Log\$'	'Single Point Resistance\$'	'Spontaneous Potential\$'
Depth At	Strat Column	Description	Gamma	SPR	SP
-10	Soil	Laterite overburden.			
-20	Silt	Brown decomposed material.			
	Silt	White material with schistose texture in a brown silt matrix.			
-30	Soil	Brown laterite and thoroughly weathered calcareous material.			
-40	Limestone	Strong, slightly weathered grey limestone and brown greenish brown and white thoroughly decomposed rock occurring as calcareous silt.			
-50	Schist	Un-weathered calcareous schist, thin bedded limestone and calcareous mudstone. Some pyrite present.			

Hole Name :MDP2

Segment Start Depth :0.00 Segment End Depth :70.00

	Lithology\$		'Gamma Log\$'	'Single Point Resistance\$'	'Spontaneous Potential\$'
Depth At	Strat Column	Description	Gamma	SPR	SP
	Soil	Yellowish brown laterite gravel and overburden.			
-10	Limestone	Sandy limestone.			
	Limestone	Slightly weathered, cream colored crystalline limestone. Fissures at 11 & 20m depth.			
-20	Limestone	Grey limestone with solution etching. Fissure @ 24m depth.			
	Sand	Fine brown calcareous sand.			
-30	Limestone	Grey limestone. Fissure @ 31m depth.			
	Limestone	Sandy limestone.			
-40	Limestone	Slightly weathered grey or brown crystalline limestone.			
	Limestone	Sandy limestone.			
	W-Limestone	Weathered limestone.			
-50	Limestone	Sandy limestone.			
-60	Limestone	Un-weathered grey, pink or white crystalline limestone.			

Characterisation of the Dolomitic Aquifer in the Copperbelt Province, Northern Zambia. MDC Borehole Logs

Hole Name :MDP3

Segment Start Depth :0.00 Segment End Depth :73.20

		Lithology\$	'Gamma Log\$'	'Single Point Resistance\$'	'Spontaneous Potential\$'
Depth At	Strat Column	Description	Gamma	SPR	SP
	Soil	Laterite overburden.			
-10	U-Limestone	Un-weathered crystalline limestone.			
-20	Limestone	Cream colored limestone.			
-30	U-Limestone	Un-weathered, massive crystalline limestone. Fissuring @ 48m.			
-40	U-Limestone	Un-weathered, massive crystalline limestone. Fissuring @ 48m.			
-50	Limestone	Fine grained, cream colored sandy limestone.			
-60	U-Limestone	Mostly un-weathered cream crystalline limestone. A few fragments indicate 1mm fissuring.			
-70	U-Limestone	Mostly un-weathered cream crystalline limestone. A few fragments indicate 1mm fissuring.			

Characterisation of the Dolomitic Aquifer in the Copperbelt Province, Northern Zambia.			MDC Borehole Logs		
Hole Name :MDP3Ab					
Segment Start Depth :0.00			Segment End Depth :68.30		
	Lithology\$		'Gamma Log\$'	'Single Point Resistance\$'	'Spontaneous Potential\$'
Depth At	Strat Column	Description	Gamma	SPR	SP
	Soil	Laterite overburden.			
-10	Limestone	Fine grained, cream colored sandy limestone.			
-20	U-Limestone	Un-weathered white limestone			
	U-Limestone	Un-weathered blueish-grey limestone. Fissuring @ 22m.			
-30	Limestone	Crystalline limestone. Decrease weathering with depth indicated by colour change from cream to white.			
-40	Limestone	Light yellow sandy limestone. At 53m evidence of open structured calcite deposition. Repeated at 62 and 64m depth. Fissuring at 52m.			
-50	Limestone				
-60	U-Limestone	Un-weathered light grey limestone.			

Scale 1:507.128007

09/24/04

14:27:02

Characterisation of the Dolomitic Aquifer in the Copperbelt Province, Northern Zambia. MDC Borehole Logs

Hole Name :MDP4



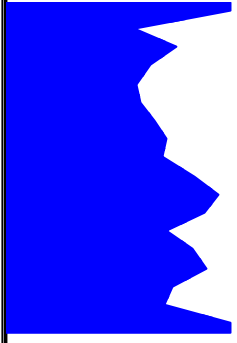
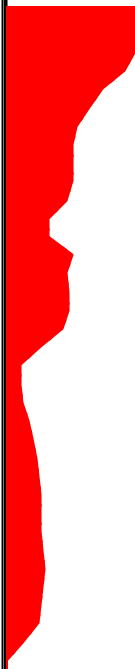
Segment Start Depth :0.00 Segment End Depth :93.30

	Lithology\$		'Gamma Log\$'	'Single Point Resistance\$'	'Spontaneous Potential\$'
Depth At	Strat Column	Description	Gamma	SPR	SP
	Soil	Laterite overburden.			
-10	Limestone	Light brown sandy limestone.			
-20					
-30					
-40					
-50					
-60					
-70					
-80	Limestone	Sample occurs as above. Some un-weathered grey mudstone occurs.			
-90					

Characterisation of the Dolomitic Aquifer in the Copperbelt Province, Northern Zambia. MDC Borehole Logs

Hole Name :MDP5

Segment Start Depth :0.00 Segment End Depth :55.40

Lithology\$		'Gamma Log\$'	'Single Point Resistance\$'	'Spontaneous Potential\$'	
Depth At	Strat Column	Description	Gamma	SPR	SP
	Soil	Laterite overburden.			
-10	U-Limestone	Un-weathered white limestone. Some weathered on fracture surfaces. More weathering below 15m.			
-20		Un-weathered light grey to white crystalline limestone. Occasional weathering.			
-30		Un-weathered crystalline limestone.			
-40	U-Limestone				
-50					


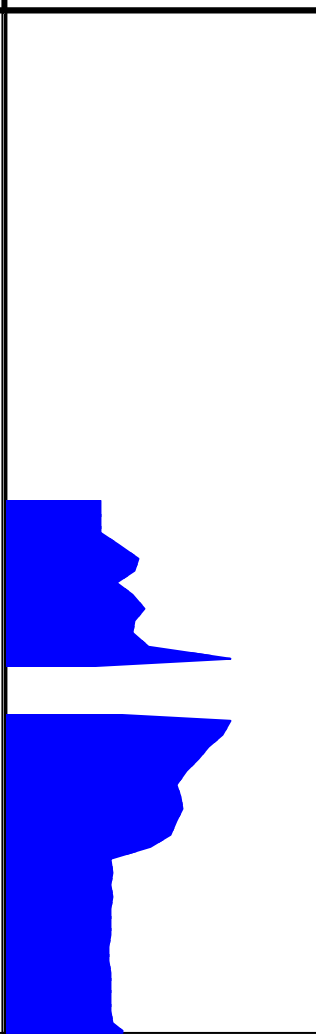
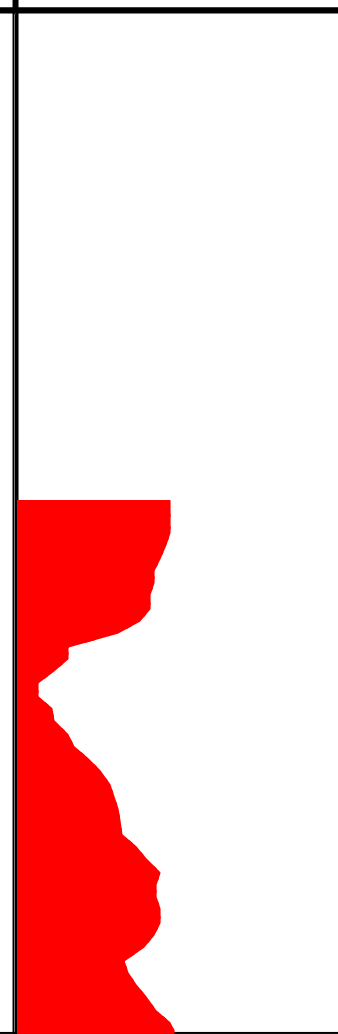
Hole Name :MDP6


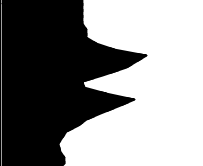


















Segment Start Depth :0.00 Segment End Depth :48.80

Lithology\$		'Gamma Log\$'	'Single Point Resistance\$'	'Spontaneous Potential\$'	
Depth At	Strat Column	Description	Gamma	SPR	SP
-5	Soil	Laterite overburden with some silt.	[Gamma Log Data]	[SPR Data]	[SP Data]
-10					
-15	Limestone	Greyish brown sandy limestone. Fissuring @ 22m.			
-20					
-25	U-Limestone	Un-weathered limestone.			
-30					
-35	Breccia	Fine, angular quartz gravel in a weakly cemented matrix of light brown calcareous silt. A breccia.			
-40					
-45	U-Limestone	Un-weathered dark grey limestone.			

Hole Name :MDP7

Segment Start Depth :0.00 Segment End Depth :40.60

Lithology\$		'Gamma Log\$'	'Single Point Resistance\$'	'Spontaneous Potential\$'	
Depth At	Strat Column	Description	Gamma	SPR	SP
	Soil	Laterite overburden.			
-5	Schist	Laterite and grey decomposed schist. Some quartz fragments.			
-10	Mudstone	Grey, weathered, fissile mudstone.			
-15	U-Limestone	Grey un-weathered limestone.			
-20	Schist	Finely laminated or fissile schist, calcareous mudstone and some limestone. Some calcite veining.			
-25	Mudstone	Un-weathered, fissile black mudstone with minor iron pyrites.			
-30	Limestone	Un-weathered, massive grey limestone. Some pyrite and calcite.			
-35					
-40					

Characterisation of the Dolomitic Aquifer in the Copperbelt Province, Northern Zambia.			MDC Borehole Logs		
Hole Name :MDP8					
Segment Start Depth :0.00			Segment End Depth :80.50		
Lithology\$			'Gamma Log\$'	'Single Point Resistance\$'	'Spontaneous Potential\$'
Depth At	Strat Column	Description	Gamma	SPR	SP
-10	Soil	Laterite overburden and quarts gravel.			
-20	Schist	Decomposed to un-weathered schist. Below 22m, the material display solution etching and open fissures.			
-30	Limestone	Grey limestone. Fissuring @ 29 and 31m depth.			
-40	Limestone	Generally un-weathered crystalline limestone. Some beds of un-weathered soft black mudstone occur below 42m depth.			
-50					
-60					
-70					
-80					

Scale 1:597.713098




09/24/04

14:27:50

Characterisation of the Dolomitic Aquifer in the Copperbelt Province, Northern Zambia. MDC Borehole Logs





Hole Name :MDP9

Segment Start Depth :0.00 Segment End Depth :75.00

	Lithology\$		'Gamma Log\$'	'Single Point Resistance\$'	'Spontaneous Potential\$'
Depth At	Strat Column	Description	Gamma	SPR	SP
	Soil	Laterite overburden.			
-10	Limestone	Light brown limestone.			
-20	Limestone	Light brown sandy limestone.			
-30					
-40					
-50					
-60					
-70					

Hole Name :MDP10

Segment Start Depth :0.00 Segment End Depth :60.40

Lithology\$		'Gamma Log\$'	'Single Point Resistance\$'	'Spontaneous Potential\$'	
Depth At	Strat Column	Description	Gamma	SPR	SP
	Soil	Laterite overburden.			
	Limestone	Thoroughly weathered, moderately strong changing to un-weathered white crystalline limestone with depth.			
-10	U-Limestone	White to pink strong, un-weathered limestone with some soft yellow, thoroughly weathered zones. Some grey thin bedded limestone below 20m.			
-20	Limestone	Cream limestone and some white un-weathered limestone.			
-30	Limestone	Cream limestone sand and fragments of white or brown un-weathered limestone. Open fissure @36m.			
-40	U-Limestone	Mainly un-weathered, white, pink or light brown limestone. Some light brown limestone sand.			
-50	U-Limestone	White to light brown un-weathered sandy crystalline limestone.			
-60					

Hole Name :MDP11

Segment Start Depth :0.00 Segment End Depth :87.00

	Lithology\$		'Gamma Log\$'	'Single Point Resistance\$'	'Spontaneous Potential\$'
Depth At	Strat Column	Description	Gamma	SPR	SP
-10	Soil	Laterite overburden.			
-20	Limestone	Strong, white limestone. Some thoroughly weathered. Weathering staining on fracture surfaces.			
-40	Limestone	Light yellowish brown or red limestone, some thoroughly weathered.			
-50	Limestone	Limestone fragments have solution etched surfaces, some thoroughly weathered.			
-60	U-Limestone	Un-weathered light yellowish brown, white or pink limestone. Fissures between 30-70m depth.			
-80	Limestone	Calcification of fracture zone.			
	U-Limestone	Un-weathered, light brown limestone.			

Hole Name :MDP12

Segment Start Depth :0.00 Segment End Depth :60.40

	Lithology\$		'Gamma Log\$'	'Single Point Resistance\$'	'Spontaneous Potential\$'
Depth At	Strat Column	Description	Gamma	SPR	SP
	Soil	Laterite overburden.	[REDACTED]		
-10	Sand	Light brown calcareous sand, a little black mudstone and some laterite.			
-20	Limestone	Strong, light grey, thin bedded limestone with some weathering staining on fracture surfaces.			
-30	Sand	Greenish brown quartz and calcareous sand.			
-40	U-Limestone	Un-weathered light grey, thin bedded limestone. Light brown silt and infilling white marl @ 49m. Soft drilling @ 35, 38 & 39m depth. Minor fissuring @ 49m depth.			
-50	U-Limestone	Un-weathered, blueish grey crystalline limestone with weathered fracture surfaces.			
-60					

Hole Name :MDP13

Segment Start Depth :0.00 Segment End Depth :60.20

		Lithology\$	'Gamma Log\$'	'Single Point Resistance\$'	'Spontaneous Potential\$'
Depth At	Strat Column	Description	Gamma	SPR	SP
	Soil	Laterite overburden.	[REDACTED]		
-10	Limestone	Light brown calcareous sand, some light grey, thin bedded limestone and mica.			
-20	Limestone				
-30	Limestone	Brown calcareous sand, light grey thin bedded limestone and some quartz, mica, heavily weathered phyllite and brown clay.			
-40	Limestone				[REDACTED]
-50	U-Limestone	Mostly un-weathered, grey argillaceous limestone with minor black mudstone, quartz and weathered mica.		[REDACTED]	[REDACTED]
-60	U-Limestone			[REDACTED]	[REDACTED]

Hole Name :MDP14

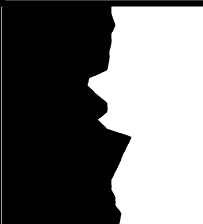





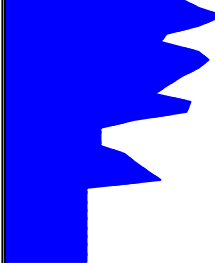

Segment Start Depth :0.00 Segment End Depth :60.40

	Lithology\$		'Gamma Log\$'	'Single Point Resistance\$'	'Spontaneous Potential\$'
Depth At	Strat Column	Description	Gamma	SPR	SP
	Soil	Laterite overburden.	[REDACTED]	[REDACTED]	[REDACTED]
-10	U-Limestone	Un-weathered limestone.			
-20	Limestone	Fine grained, cream colored sandy limestone.			
-30					
-40	U-Limestone	Un-weathered, thin bedded, blueish grey crystalline limestone.			
-50	Limestone	Fine grained, cream colored sandy limestone.			
-60					

Hole Name :MDP15

Segment Start Depth :0.00 Segment End Depth :55.80

Lithology\$		'Gamma Log\$'	'Single Point Resistance\$'	'Spontaneous Potential\$'	
Depth At	Strat Column	Description	Gamma	SPR	SP
	Soil	Laterite overburden.			
-10	Mudstone	Un-weathered, grey, calcareous mudstone.			
	Sand	Light grey sandy material.			
	Shale	Un-weathered, light grey shale.			
-20	Shale	Un-weathered, dark grey shale with a developing schistose texture and occasional iron pyrites.			
-30	Shale	Un-weathered grey shale. Metallic sulphides developed in fracture planes.			
-40	Shale	Un-weathered, light grey quartzite with some metallic sulphides.			
-50	Quartzite				

Characterisation of the Dolomitic Aquifer in the Copperbelt Province, Northern Zambia.				MDC Borehole Logs	
Hole Name :MDP16					
Segment Start Depth :0.00			Segment End Depth :55.40		
	Lithology\$		'Gamma Log\$'	'Single Point Resistance\$'	'Spontaneous Potential\$'
Depth At	Strat Column	Description	Gamma	SPR	SP
-10	Soil	Quartz, gravel and laterite overburden.			
-20	Schist	Generally highly weathered greenish brown mica schist with some muscovite veining. Some un-weathered zones.			
-30	Schist	Slightly weathered, becoming less weathered with depth, greenish grey mica schist. Some gravel sized fragments of free quarts.			
-40	Schist	Un-weathered grey calcareous mica schist. Calcite veining @ 49m depth.			
-50	Schist				

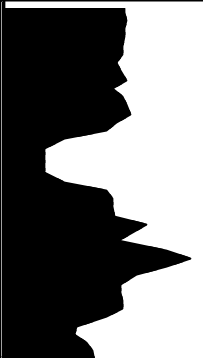
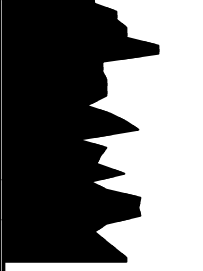
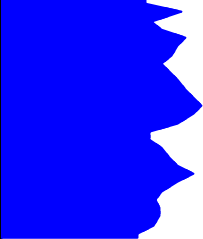

Scale 1:411.345411

09/24/04

14:25:13

Hole Name :MDP17

Segment Start Depth :0.00 Segment End Depth :60.10

	Lithology\$		'Gamma Log\$'	'Single Point Resistance\$'	'Spontaneous Potential\$'
Depth At	Strat Column	Description	Gamma	SPR	SP
-10	Soil	Laterite and quartz overburden.			
-20	Shale	Mixed weathered and un-weathered grey calcareous shale. Some iron pyrite, quartz and calcite veining present.			
-30		Weathered, non-calcareous shale.			
		Grey calcareous shale with some black mudstone.			
-40		Weathered, non-calcareous shale.			
		Un-weathered, massive dark grey shale with calcite veining.			
-50		Dark grey shale and limestone.			
-60		Light grey calcareous shale and dark grey mudstone. Some open calcite veining. Pyrite increase to 10% of sample by 60m depth.			

Hole Name :MDP18

Segment Start Depth :0.00 Segment End Depth :82.30

Lithology\$		'Gamma Log\$'	'Single Point Resistance\$'	'Spontaneous Potential\$'	
Depth At	Strat Column	Description	Gamma	SPR	SP
	Soil	Laterite overburden.			
-10	Limestone	Un-weathered grey or cream massive limestone.			
	Limestone	Grey, thin bedded limestone.			
-20	U-Limestone	Un-weathered grey or white limestone. Some calcareous sand and phyllite. Soft drilling.			
-30	Limestone	Cream colored, massive, strong crystalline limestone.			
-40	Limestone	Pink reddish brown changing to cream or light grey with depth limestone. Limestone is massive and strongly crystalline. Frequent marl and calcite infilling above 50m.			
-50	Limestone				
-60	U-Limestone	Un-weathered thin bedded, grey limestone.			
-70	U-Limestone	Un-weathered thin bedded, grey crystalline limestone. Some pyrite and occasional phyllitic bands or mica veining present.			
-80	U-Limestone				

Characterisation of the Dolomitic Aquifer in the Copperbelt Province, Northern Zambia. MDC Borehole Logs

Hole Name :MDP19

Segment Start Depth :0.00 Segment End Depth :72.50

Lithology\$		'Gamma Log\$'	'Single Point Resistance\$'	'Spontaneous Potential\$'	
Depth At	Strat Column	Description	Gamma	SPR	SP
-10	Soil	Laterite overburden.			
-20	Shale	Un-weathered greenish grey calcareous shale. Some mica and calcite veining present.			
	Sand	Lateritic, mica and quartz rich calcareous sand.			
-30	Limestone	Laterite and grey thin bedded limestone. Weathering on joint surfaces. Some calcite and occasional pyllite.			
	Limestone	Un-weathered white limestone			
-40	Sand	Fine grained brown calcareous sand.			
-50	U-Limestone	Un-weathered grey to white, crystalline thin bedded limestone. Some infilling, heavily weathered marl from 49-53m.			
-60	W-Limestone	Weathered limestone, with an un-weathered zone between 57-62m depth. Some mica and calcite present.			
-70					

Characterisation of the Dolomitic Aquifer in the Copperbelt Province, Northern Zambia. MDC Borehole Logs




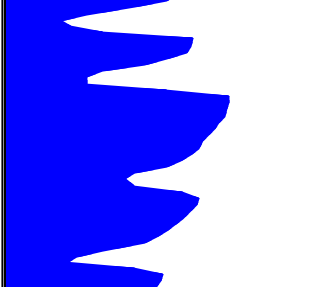

























Hole Name :MDP19A

Segment Start Depth :0.00 Segment End Depth :32.00

	Lithology\$		'Gamma Log\$'	'Single Point Resistance\$'	'Spontaneous Potential\$'
Depth At	Strat Column	Description	Gamma	SPR	SP
-5	Soil	Laterite overburden.			
-10					
-15	Limestone	Weathered grey limestone.			
-20	U-Limestone	Un-weathered grey shaley limestone.			
-25					
-30					

Hole Name :MDP20

Segment Start Depth :0.00 Segment End Depth :80.00

		Lithology\$	'Gamma Log\$'	'Single Point Resistance\$'	'Spontaneous Potential\$'
Depth At	Strat Column	Description	Gamma	SPR	SP
	Soil	Laterite overburden.			
-10	U-Limestone	Un-weathered limestone.			
-20	U-Limestone	Light grey crystalline limestone. Fissuring @ 15 and 28m depths.			
-30	U-Limestone				
-40	Limestone	Grey sandy limestone.			
-45	Limestone	Grey or brown crystalline limestone.			
-50	Limestone	Grey un-weathered limestone. Marl and mica present. Soft drilling.			
-55	Limestone				
-60	U-Limestone	Cream colored, sandy limestone.			
-65	U-Limestone	Un-weathered light brown limestone and calcite.			
-70	U-Limestone	Un-weathered, cream colored sandy limestone.			

Characterisation of the Dolomitic Aquifer in the Copperbelt Province, Northern Zambia. MDC Borehole Logs

Hole Name :MDP21A

Segment Start Depth :0.00 Segment End Depth :60.00

Lithology\$		'Gamma Log\$'	'Single Point Resistance\$'	'Spontaneous Potential\$'	
Depth At	Strat Column	Description	Gamma	SPR	SP
	Soil	Laterite overburden.	[REDACTED]		[REDACTED]
-10	U-Limestone	Un-weathered, greying brown limestone. Fissuring @ 15m.			
	Limestone	Brown, sandy limestone. Some mica and quartz present.			
-20	Limestone	Limestone. Fissuring @ 22m.			
	Limestone	Grey to white and pink limestone.			
-30	U-Limestone	Un-weathered, light brown limestone. Some mica and quartz present.			
	Limestone	Limestone with calcite banding.			
-40	U-Limestone	Un-weathered, cream colored limestone. Minor calcite and white marl infilling.			
-50	U-Limestone	Un-weathered crystalline limestone.			

Hole Name :MDP21B

Segment Start Depth :0.00 Segment End Depth :40.00

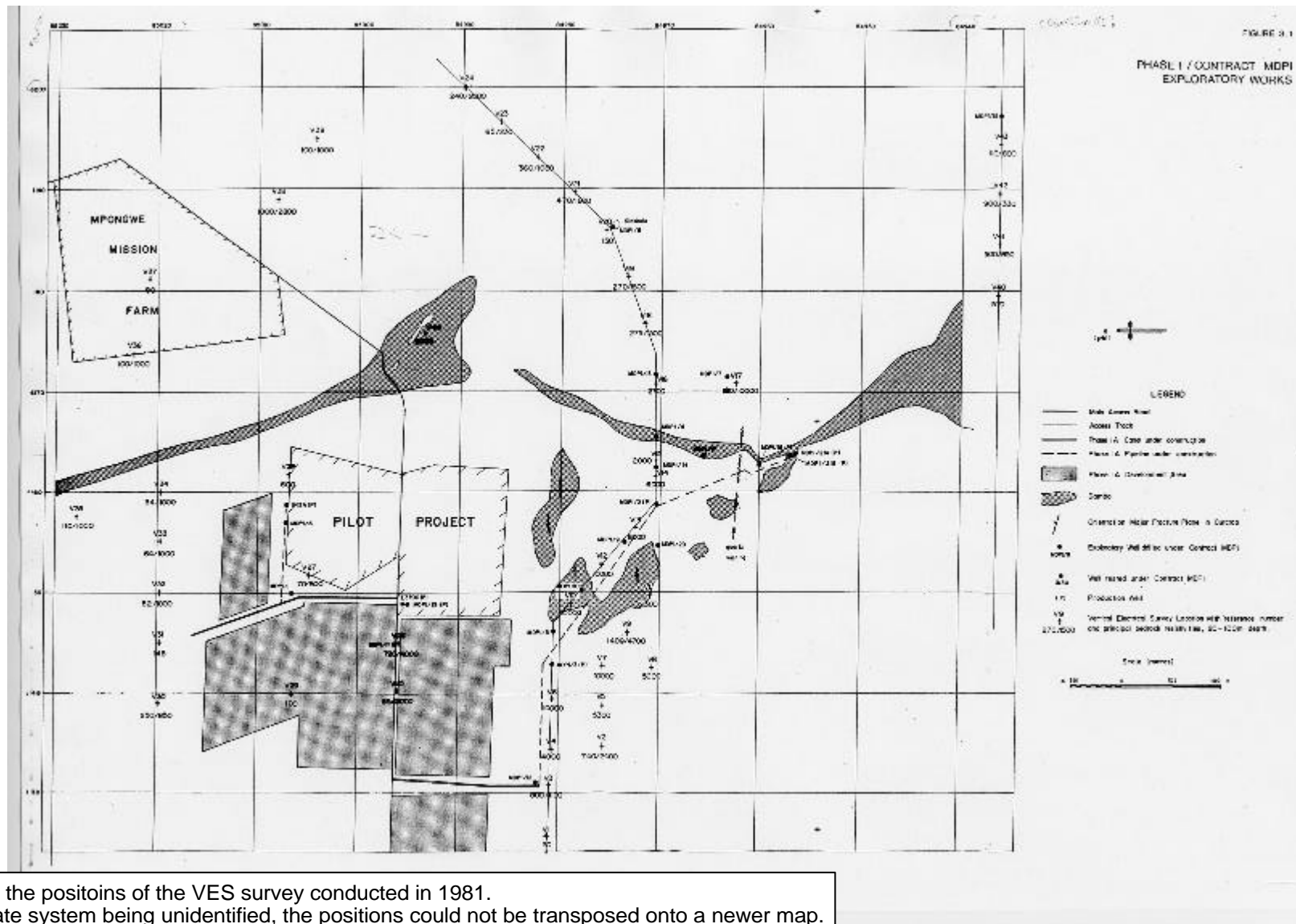
		Lithology\$	'Gamma Log\$'	'Single Point Resistance\$'	'Spontaneous Potential\$'
Depth At	Strat Column	Description	Gamma	SPR	SP
-5	Soil	Laterite overburden.			
-10	U-Limestone	Un-weathered crystalline limestone. Some weathering on fractures below 15m.			
-15	Limestone	Brown, sandy limestone. Some mica and quartz present.			
-20	Limestone	Limestone. Solution cavity @ 20m.			
-25	U-Limestone	Un-weathered limestone.			
-25	Limestone	Brown, sandy limestone. Some mica and quartz present.			
-30	U-Limestone	Un-weathered limestone. Fissuring from 20m down.			
-35	U-Limestone				

Appendix B:

Surface Geophysical Investigation of 1982:

VES Results

1982 VES Survey Postions



The Figure indicate the positioins of the VES survey conducted in 1981. Due to the coordinate system being unidentified, the positions could not be transposed onto a newer map. A copy was made of the original map as shown in the Macdonald report (1982).

Station V1.

Wenner Spacing a (m)	Resistance R (ohm)	Resistivity p (ohm.m)
7	10.9	481
10	4.77	300
15	2.19	206
25	0.505	79
60	0.0814	30.7
90	0.0657	37.2
130	0.0672	54.9

Station V2

Wenner Spacing a (m)	Resistance R (ohm)	Resistivity p (ohm.m)
5	39.4	1238
7	32.7	1438
10	25.9	1627
15	13.9	1310
25	6.43	1010
40	4.36	1096
60	3.30	1244
90	2.51	1419
130	2.18	1781
200	1.84	2312

Station V3

Wenner Spacing a (m)	Resistance R (ohm)	Resistivity p (ohm.m)
10	22.2	1394
20	10.3	1294
35	4.2	1037
60	3.28	1236
100	2.24	1407
150	1.68	1583
200	1.50	1885

Station V4

Wenner Spacing a (m)	Resistance R (ohm)	Resistivity p (ohm.m)
5	45.9	1442
7	31.3	1337
10	23.1	1451
14	13.9	1223
20	12.0	1508
28	9.54	1678
40	7.27	1827
56	6.00	2111
80	4.60	2312
110	3.86	2668
150	3.28	3091
200	2.73	3431

Station V5

Wenner Spacing a (m)	Resistance R (ohm)	Resistivity p (ohm.m)
5	23.8	748
7	14.8	650
10	10.0	628
15	6.69	630
25	6.46	1014
40	5.63	1414
60	5.23	1971
90	4.29	2426
130	3.73	3046
200	2.85	3581

Station V6

Wenner Spacing a (m)	Resistance R (ohm)	Resistivity p (ohm.m)
20	10.6	1132
40	8.13	2043
70	6.92	3043
100	5.61	3524
140	4.90	4310
200	3.80	4775

Station V7

Wenner Spacing a (m)	Resistance R (ohm)	Resistivity p (ohm.m)
5	71.2	2237
10	28.4	1784
20	16.0	2011
35	13.5	2969
60	10.0	3770
90	8.94	5055
140	7.2	6791
200	5.84	7339

Station V8

Wenner Spacing a (m)	Resistance R (ohm)	Resistivity p (ohm.m)
5	44.6	4101
10	13.	873
20	7.13	896
35	5.64	1240
60	4.93	1859
90	4.44	2511
140	3.94	3466
200	3.10	3896

Station V9A

Wenner Spacing a (m)	Resistance R (ohm)	Resistivity p (ohm.m)
7	17.4	768
10	12.8	802
15	9.50	895
25	8.73	1371
40	8.81	2214
60	7.27	2741
90	5.42	3065
130	4.99	4076
200	5.17	6497

Station V9B

Wenner Spacing a (m)	Resistance R (ohm)	Resistivity p (ohm.m)
32	9.27	1864
50	8.39	2636
64	7.06	2839
75	6.67	3143
90	5.52	3121
110	5.05	3490

Station V10

Wenner Spacing a (m)	Resistance R (ohm)	Resistivity p (ohm.m)
20	6.38	801
40	6.00	1508
70	6.34	2788
100	6.18	3883
140	4.83	4249
200	4.70	5906

Station V11

Wenner Spacing a (m)	Resistance R (ohm)	Resistivity p (ohm.m)
7	11.9	523
10	10.5	660
15	9.29	875
25	7.93	1246
40	6.67	1676
60	5.27	1989
90	4.17	2356
130	3.73	3047
200	3.84	4825

Station V12

Wenner Spacing a (m)	Resistance R (ohm)	Resistivity p (ohm.m)
20	3.46	435
40	3.46	870
70	4.80	2111
100	4.62	2902
140	4.33	3808
200	3.40	4272

Station V13

Wenner Spacing a (m)	Resistance R (ohm)	Resistivity p (ohm.m)
20	4.40	553
40	4.27	1073
70	4.62	2031
100	4.16	2614
130	3.53	2883
160	3.30	3318
200	2.94	3695

Station V14

Wenner Spacing a (m)	Resistance R (ohm)	Resistivity p (ohm.m)
20	5.77	725
40	3.25	817
70	3.20	1407
100	3.05	1916
140	2.40	2111

Station V15

Wenner Spacing a (m)	Resistance R (ohm)	Resistivity p (ohm.m)
20	4.96	623
40	4.40	1106
70	3.30	1451
100	2.96	1860
130	1.93	1576
170	1.75	1869
200	1.39	1746

Station V16

Wenner Spacing a (m)	Resistance R (ohm)	Resistivity p (ohm.m)
20	4.05	509
40	3.67	922
70	2.79	1227
100	2.43	1527
130	2.27	1854
170	1.85	1976
200	2.48	3116

Station B17

Wenner Spacing a (m)	Resistance R (ohm)	Resistivity p (ohm.m)
20	0.889	118
40	0.556	140
70	0.564	248
100	0.622	391
140	0.551	485
200	0.413	519

Station V18

Wenner Spacing a (m)	Resistance R (ohm)	Resistivity p (ohm.m)
7	9.23	406.0
10	4.43	278.3
15	3.33	313.8
25	2.46	386.4
40	2.11	530.3
60	2.00	754.0
90	1.74	983.9
130	1.60	1307
200	1.11	1395

Station V19

Wenner Spacing a (m)	Resistance R (ohm)	Resistivity p (ohm.m)
7	10.1	444.2
10	5.41	340.0
15	3.20	301.6
25	2.42	381.1
40	1.68	422.2
60	1.72	648.4
90	1.44	814.3
130	1.04	849.5
200	0.899	1130

Station V20

Wenner Spacing a (m)	Resistance R (ohm)	Resistivity p (ohm.m)
20	1.700	214
40	0.456	115
70	0.361	159
100	0.276	173
140	0.434	382
200	0.290	364

Station V21

Wenner Spacing a (m)	Resistance R (ohm)	Resistivity p (ohm.m)
5	56.8	1784
7	37.0	1627
10	20.1	1263
15	8.55	806
25	3.82	600
40	1.93	485
60	0.881	332
90	0.815	164
130	0.704	575
200	0.575	723

Station V22

Wenner Spacing a (m)	Resistance R (ohm)	Resistivity p (ohm.m)
5	15.4	484
7	8.83	388
10	6.16	387
15	4.02	379
25	2.52	396
40	2.27	570
60	1.79	675
90	1.38	780
130	1.09	890
200	0.713	896

Station V23

Wenner Spacing a (m)	Resistance R (ohm)	Resistivity p (ohm.m)
5	17.5	550
7	12.2	536
10	6.10	383
15	1.56	147
25	0.416	65.3
40	0.295	74.1
60	0.313	118
90	0.272	154
130	0.193	158
200	0.184	231

Station V24

Wenner Spacing a (m)	Resistance R (ohm)	Resistivity p (ohm.m)
5	18.2	571
7	9.27	408
10	4.13	259
15	2.81	265
25	1.38	217
40	1.05	264
60	1.29	486
90	1.27	718
130	1.15	939
200	0.89	1118

Station V25

Wenner Spacing a (m)	Resistance R (ohm)	Resistivity p (ohm.m)
5	24.7	776
10	9.86	619
20	1.89	237
35	0.600	132
60	0.308	116
90	0.241	136
140	0.254	223
200	0.182	229

Station V26A

Wenner Spacing a (m)	Resistance R (ohm)	Resistivity p (ohm.m)
5	16.3	512
10	12.5	785
20	5.98	751
35	5.38	1183
60	4.32	1629
90	3.44	1945
140	2.36	2075
200	1.22	1533

Station V26B

Wenner Spacing a (m)	Resistance R (ohm)	Resistivity p (ohm.m)
7	19.3	849
13	9.23	754
16	7.44	748
25	6.04	949
75	4.12	1941
115	3.12	2254
170	2.08	2222

Station V27

Wenner Spacing a (m)	Resistance R (ohm)	Resistivity p (ohm.m)
7	4.25	187
10	3.00	188
15	1.84	173
25	0.674	106
40	0.415	104
60	0.413	156
90	0.291	165
130	0.267	218
200	0.246	309

Station V28

Wenner Spacing a (m)	Resistance R (ohm)	Resistivity p (ohm.m)
5	1.85	58.1
10	0.872	54.8
20	0.634	79.7
35	0.634	139
60	0.482	182
90	0.334	189
140	0.256	229
200	0.260	327

Station V29A

Wenner Spacing a (m)	Resistance R (ohm)	Resistivity p (ohm.m)
5	40.8	1282
7	26.3	1157
10	19.3	1213
15	13.3	1253
25	3.52	553
40	0.935	235
60	0.585	220
90	0.402	227
130	0.313	256

Station V29B

Wenner Spacing a (m)	Resistance R (ohm)	Resistivity p (ohm.m)
5	45.5	1429
7	29.2	1284
10	17.8	1100
15	8.25	778
25	4.98	782
40	1.44	362
60	0.577	218
90	0.362	205
130	0.317	259
200	0.302	380

Station V30

Wenner Spacing a (m)	Resistance R (ohm)	Resistivity p (ohm.m)
5	48.4	1520
7	32.8	1442
10	29.0	1822
15	16.0	1508
25	5.15	809
40	1.89	475
60	1.22	460
90	0.927	524
130	0.692	565
200	0.503	632

Station V31

Wenner Spacing a (m)	Resistance R (ohm)	Resistivity p (ohm.m)
5	51.0	1621
10	19.0	1194
20	7.80	980
35	2.13	468
60	0.615	232
90	0.295	167
140	0.333	300
200	0.343	431

Station V32

Wenner Spacing a (m)	Resistance R (ohm)	Resistivity p (ohm.m)
5	12.9	405
10	5.85	368
20	1.39	175
35	0.475	104
60	0.300	113
90	0.344	194
140	0.340	299
200	0.288	262

Station V33

Wenner Spacing a (m)	Resistance R (ohm)	Resistivity p (ohm.m)
5	10.3	324
10	2.99	188
20	0.744	93.5
35	0.308	67.7
60	0.254	95.7
90	0.250	141
140	0.245	215
200	0.250	314

Station V34

Wenner Spacing a (m)	Resistance R (ohm)	Resistivity p (ohm.m)
7	5.89	259
10	1.35	84.8
15	0.502	47.3
25	0.244	38.3
40	0.173	43.5
60	0.168	63.3
90	0.137	77.5
130	0.143	117
200	0.133	167

Station V35

Wenner Spacing a (m)	Resistance R (ohm)	Resistivity p (ohm.m)
5	12.8	402
7	6.29	277
10	3.11	195
15	1.45	137
25	0.851	134
40	0.828	208
60	0.602	227
90	0.356	201
130	0.383	313
200	0.325	408

Station V36

Wenner Spacing a (m)	Resistance R (ohm)	Resistivity p (ohm.m)
5	43.0	1351
7	25.3	1113
10	10.5	600
15	2.04	192
25	0.937	147
40	0.630	158
60	0.510	192
90	0.476	269
130	0.415	339
200	0.297	373

Station V37

Wenner Spacing a (m)	Resistance R (ohm)	Resistivity p (ohm.m)
5	25.0	785
7	13.7	603
10	7.88	495
15	3.82	360
25	1.85	291
40	0.469	118
60	0.250	94.2
90	0.247	140
130	0.230	188
200	0.136	171

Station V38

Wenner Spacing a (m)	Resistance R (ohm)	Resistivity p (ohm.m)
5	48.3	1517
7	30.5	1341
10	15.7	986
15	11.6	1093
25	6.54	1027
40	4.44	1116
60	3.78	1425
90	2.84	1606
130	2.43	1985
200	1.77	2224

Station V39

Wenner Spacing a (m)	Resistance R (ohm)	Resistivity p (ohm.m)
5	22.2	697
7	11.3	497
10	5.06	318
15	1.87	176
25	1.49	234
40	0.720	181
60	0.446	168
90	0.607	343
130	0.957	782
200	0.751	944

Station V40

Wenner Spacing a (m)	Resistance R (ohm)	Resistivity p (ohm.m)
5	3.95	124
7	2.19	96.3
10	1.72	108
15	1.60	151
25	1.35	212
40	1.17	294
60	0.940	354
90	0.619	350
130	0.516	421
200	0.464	583

Station V41

Wenner Spacing a (m)	Resistance R (ohm)	Resistivity p (ohm.m)
5	21.0	659
7	3.87	170
10	3.18	200
15	2.38	224
25	2.04	320
40	2.04	513
60	1.43	539
90	1.06	599
130	0.857	700
200	0.582	731

Station V42

Wenner Spacing a (m)	Resistance R (ohm)	Resistivity p (ohm.m)
5	3.05	95.8
7	1.87	82.2
10	1.60	100
15	1.68	158
25	1.66	261
40	1.35	339
60	1.10	414
90	0.949	536
130	0.612	500
200	0.355	446

Station V43

Wenner Spacing a (m)	Resistance R (ohm)	Resistivity p (ohm.m)
5	11.7	368
7	4.93	217
10	2.17	136
15	1.40	132
25	1.11	174
40	1.03	259
60	0.888	335
90	0.673	381
130	0.522	426
200	0.393	494

Station V44

Wenner Spacing a (m)	Resistance R (ohm)	Resistivity p (ohm.m)
20	76.0	9550
40	34.5	8070
70	12.9	5673
100	9.93	6245
140	5.86	5154

Appendix C:

Surface Geophysical Investigations of 2004:

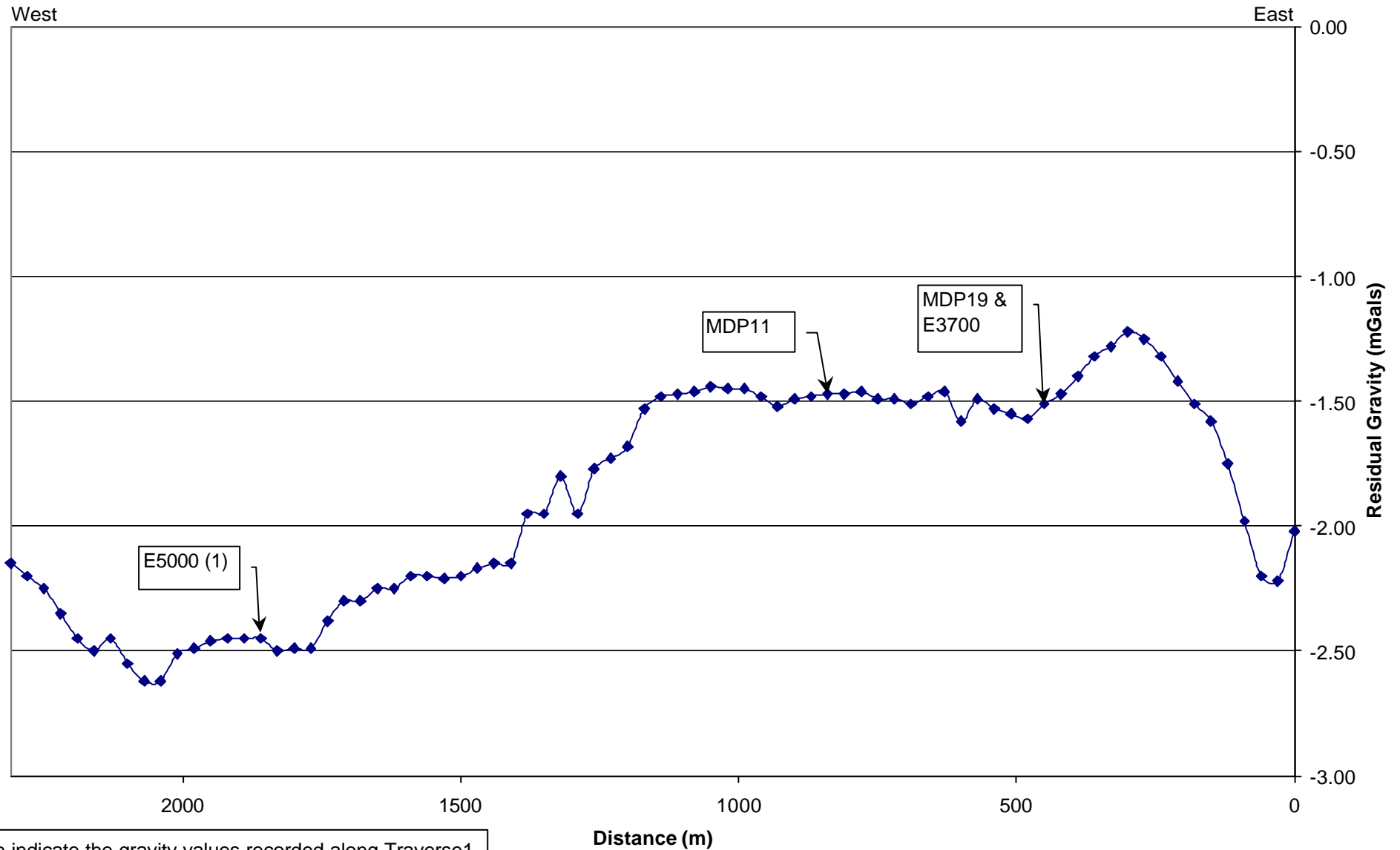
Gravity, EM and Magnetometer Results

TRAVERSE 1 DATA

STATION	DISTANCE (m)	GRAVITY (milligal)	STATION	DISTANCE (m)	GRAVITY (milligal)
101	0	-2.02	140	1170	-1.53
102	30	-2.22	141	1200	-1.68
103	60	-2.20	142	1230	-1.73
104	90	-1.98	143	1260	-1.77
105	120	-1.75	144	1290	-1.95
106	150	-1.58	145	1320	-1.80
107	180	-1.51	146	1350	-1.95
108	210	-1.42	147	1380	-1.95
109	240	-1.32	148	1410	-2.15
110	270	-1.25	149	1440	-2.15
111	300	-1.22	150	1470	-2.17
112	330	-1.28	151	1500	-2.20
113	360	-1.32	152	1530	-2.21
114	390	-1.40	153	1560	-2.20
115	420	-1.47	154	1590	-2.20
116	450	-1.51	155	1620	-2.25
117	480	-1.57	156	1650	-2.25
118	510	-1.55	157	1680	-2.30
119	540	-1.53	158	1710	-2.30
120	570	-1.49	159	1740	-2.38
121	600	-1.58	160	1770	-2.49
122	630	-1.46	161	1800	-2.49
123	660	-1.48	162	1830	-2.50
124	690	-1.51	163	1860	-2.45
125	720	-1.49	164	1890	-2.45
126	750	-1.49	165	1920	-2.45
127	780	-1.46	166	1950	-2.46
128	810	-1.47	167	1980	-2.49
129	840	-1.47	168	2010	-2.51
130	870	-1.48	169	2040	-2.62
131	900	-1.49	170	2070	-2.62
132	930	-1.52	171	2100	-2.55
133	960	-1.48	172	2130	-2.45
134	990	-1.45	173	2160	-2.50
135	1020	-1.45	174	2190	-2.45
136	1050	-1.44	175	2220	-2.35
137	1080	-1.46	176	2250	-2.25
138	1110	-1.47	177	2280	-2.20
139	1140	-1.48	178	2310	-2.15

FIGURE C1

Gravity Survey - Traverse 1



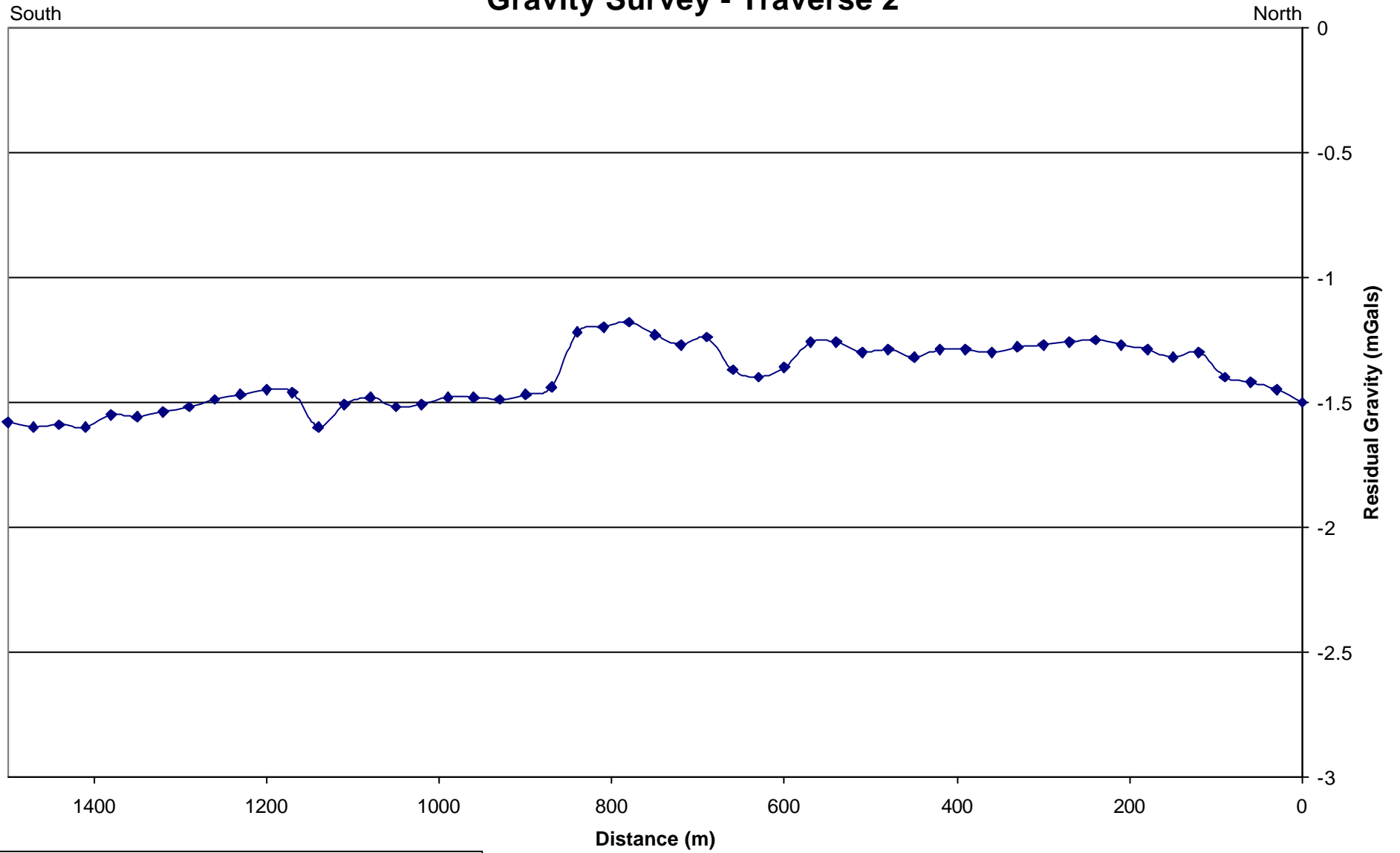
The graph indicate the gravity values recorded along Traverse1.
The existing boreholes along this traverse are shown.

TRAVERSE 2 DATA

STATION	DISTANCE (m)	GRAVITY (milligal)	STATION	DISTANCE (m)	GRAVITY (milligal)
200	0	-1.5	226	780	-1.18
201	30	-1.45	227	810	-1.2
202	60	-1.42	228	840	-1.22
203	90	-1.4	229	870	-1.44
204	120	-1.3	230	900	-1.47
205	150	-1.32	231	930	-1.49
206	180	-1.29	232	960	-1.48
207	210	-1.27	233	990	-1.48
208	240	-1.25	234	1020	-1.51
209	270	-1.26	235	1050	-1.52
210	300	-1.27	236	1080	-1.48
211	330	-1.28	237	1110	-1.51
212	360	-1.3	238	1140	-1.6
213	390	-1.29	239	1170	-1.46
214	420	-1.29	240	1200	-1.45
215	450	-1.32	241	1230	-1.47
216	480	-1.29	242	1260	-1.49
217	510	-1.3	243	1290	-1.52
218	540	-1.26	244	1320	-1.54
219	570	-1.26	245	1350	-1.56
220	600	-1.36	246	1380	-1.55
221	630	-1.4	247	1410	-1.6
222	660	-1.37	248	1440	-1.59
223	690	-1.24	249	1470	-1.6
224	720	-1.27	250	1500	-1.58
225	750	-1.23			

FIGURE C2

Gravity Survey - Traverse 2



The graph indicate the gravity values recorded along Traverse 2

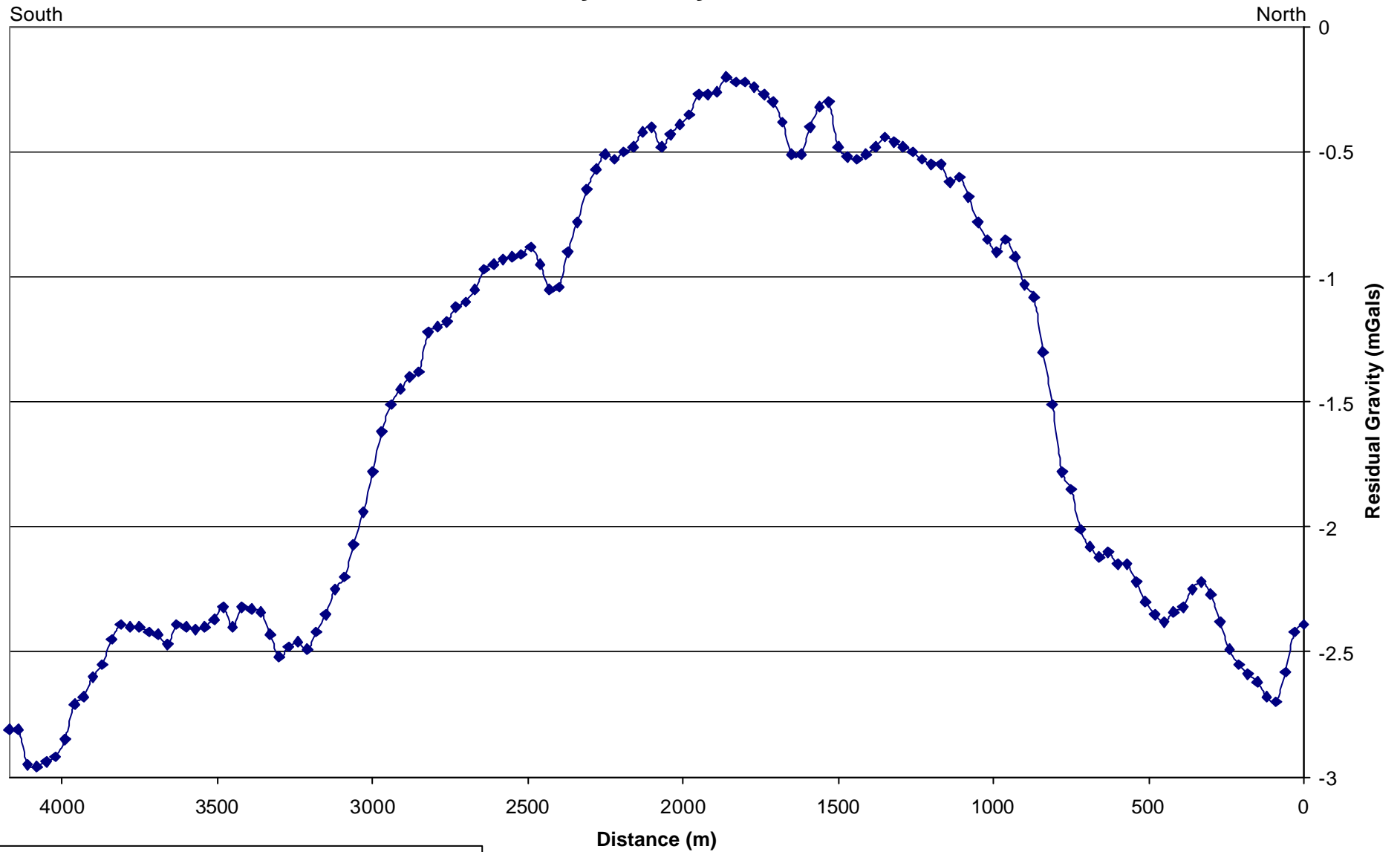
TRAVERSE 3 DATA

STATION	DISTANCE (m)	GRAVITY (milligal)	STATION	DISTANCE (m)	GRAVITY (milligal)
300	0	-2.39	345	1350	-0.44
301	30	-2.42	346	1380	-0.48
302	60	-2.58	347	1410	-0.51
303	90	-2.7	348	1440	-0.53
304	120	-2.68	349	1470	-0.52
305	150	-2.62	350	1500	-0.48
306	180	-2.59	351	1530	-0.3
307	210	-2.55	352	1560	-0.32
308	240	-2.49	353	1590	-0.4
309	270	-2.38	354	1620	-0.51
310	300	-2.27	355	1650	-0.51
311	330	-2.22	356	1680	-0.38
312	360	-2.25	357	1710	-0.3
313	390	-2.32	358	1740	-0.27
314	420	-2.34	359	1770	-0.24
315	450	-2.38	360	1800	-0.22
316	480	-2.35	361	1830	-0.22
317	510	-2.3	362	1860	-0.2
318	540	-2.22	363	1890	-0.26
319	570	-2.15	364	1920	-0.27
320	600	-2.15	365	1950	-0.27
321	630	-2.1	366	1980	-0.35
322	660	-2.12	367	2010	-0.39
323	690	-2.08	368	2040	-0.43
324	720	-2.01	369	2070	-0.48
325	750	-1.85	370	2100	-0.4
326	780	-1.78	371	2130	-0.42
327	810	-1.51	372	2160	-0.48
328	840	-1.3	373	2190	-0.5
329	870	-1.08	374	2220	-0.53
330	900	-1.03	375	2250	-0.51
331	930	-0.92	376	2280	-0.57
332	960	-0.85	377	2310	-0.65
333	990	-0.9	378	2340	-0.78
334	1020	-0.85	379	2370	-0.9
335	1050	-0.78	380	2400	-1.04
336	1080	-0.68	381	2430	-1.05
337	1110	-0.6	382	2460	-0.95
338	1140	-0.62	383	2490	-0.88
339	1170	-0.55	384	2520	-0.91
340	1200	-0.55	385	2550	-0.92
341	1230	-0.53	386	2580	-0.93
342	1260	-0.5	387	2610	-0.95
343	1290	-0.48	388	2640	-0.97
344	1320	-0.46	389	2670	-1.05

STATION	DISTANCE (m)	GRAVITY (milligal)	STATION	DISTANCE (m)	GRAVITY (milligal)
390	2700	-1.1	415	3450	-2.4
391	2730	-1.12	416	3480	-2.32
392	2760	-1.18	417	3510	-2.37
393	2790	-1.2	418	3540	-2.4
394	2820	-1.22	419	3570	-2.41
395	2850	-1.38	420	3600	-2.4
396	2880	-1.4	421	3630	-2.39
397	2910	-1.45	422	3660	-2.47
398	2940	-1.51	423	3690	-2.43
399	2970	-1.62	424	3720	-2.42
400	3000	-1.78	425	3750	-2.4
401	3030	-1.94	426	3780	-2.4
402	3060	-2.07	427	3810	-2.39
403	3090	-2.2	428	3840	-2.45
404	3120	-2.25	429	3870	-2.55
405	3150	-2.35	430	3900	-2.6
406	3180	-2.42	431	3930	-2.68
407	3210	-2.49	432	3960	-2.71
408	3240	-2.46	433	3990	-2.85
409	3270	-2.48	434	4020	-2.92
410	3300	-2.52	435	4050	-2.94
411	3330	-2.43	436	4080	-2.96
412	3360	-2.34	437	4110	-2.95
413	3390	-2.33	438	4140	-2.81
414	3420	-2.32	439	4170	-2.81

FIGURE C3

Gravity Survey - Traverse 3



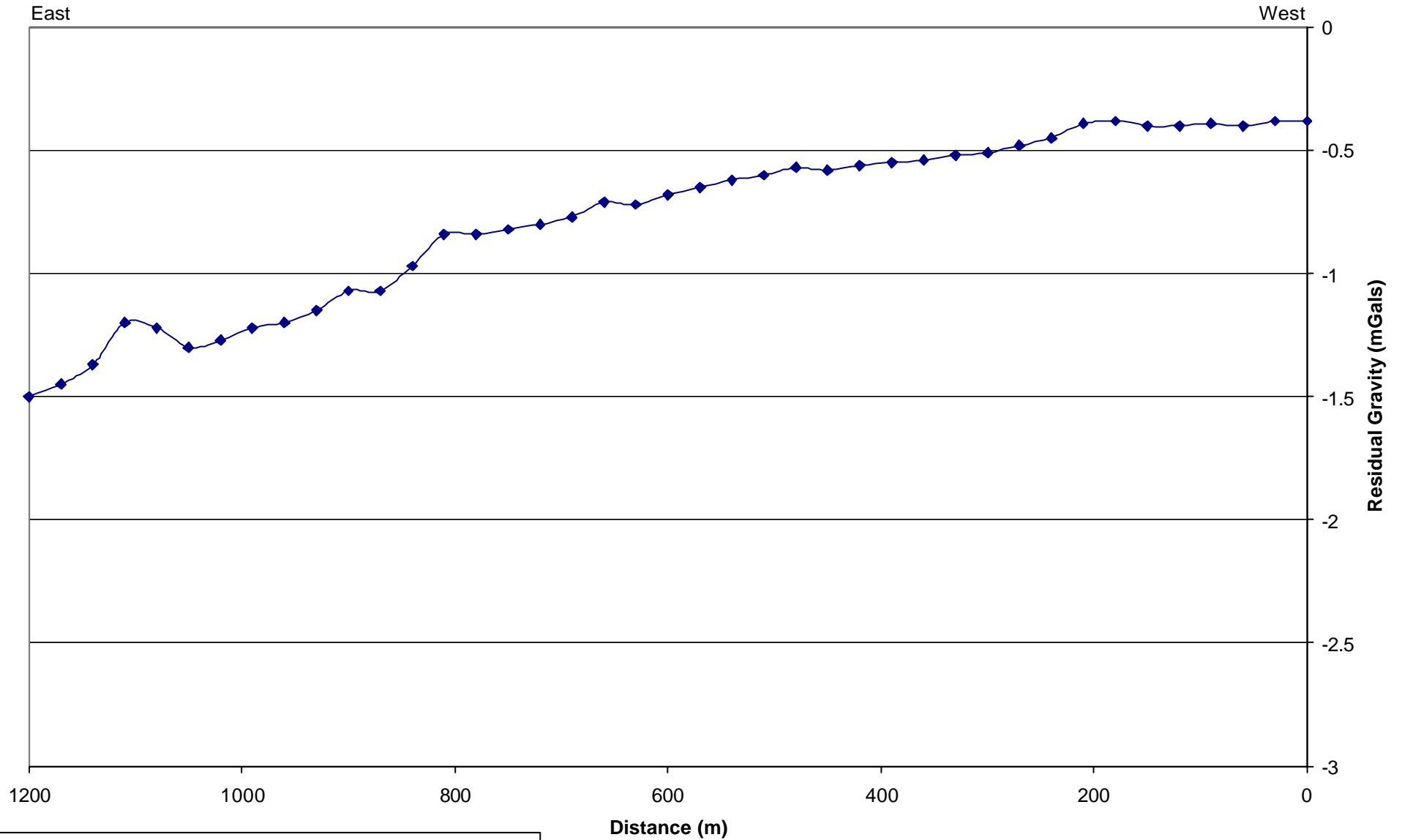
The graph indicate the gravity values recorded along Traverse 3

TRAVERSE 4 DATA

STATION	DISTANCE (m)	GRAVITY (milligal)
400	0	-0.38
401	30	-0.38
402	60	-0.4
403	90	-0.39
404	120	-0.4
405	150	-0.4
406	180	-0.38
407	210	-0.39
408	240	-0.45
409	270	-0.48
410	300	-0.51
411	330	-0.52
412	360	-0.54
413	390	-0.55
414	420	-0.56
415	450	-0.58
416	480	-0.57
417	510	-0.6
418	540	-0.62
419	570	-0.65
420	600	-0.68
421	630	-0.72
422	660	-0.71
423	690	-0.77
424	720	-0.8
425	750	-0.82
426	780	-0.84
427	810	-0.84
428	840	-0.97
429	870	-1.07
430	900	-1.07
431	930	-1.15
432	960	-1.2
433	990	-1.22
434	1020	-1.27
435	1050	-1.3
436	1080	-1.22
437	1110	-1.2
438	1140	-1.37
439	1170	-1.45
440	1200	-1.5

FIGURE C4

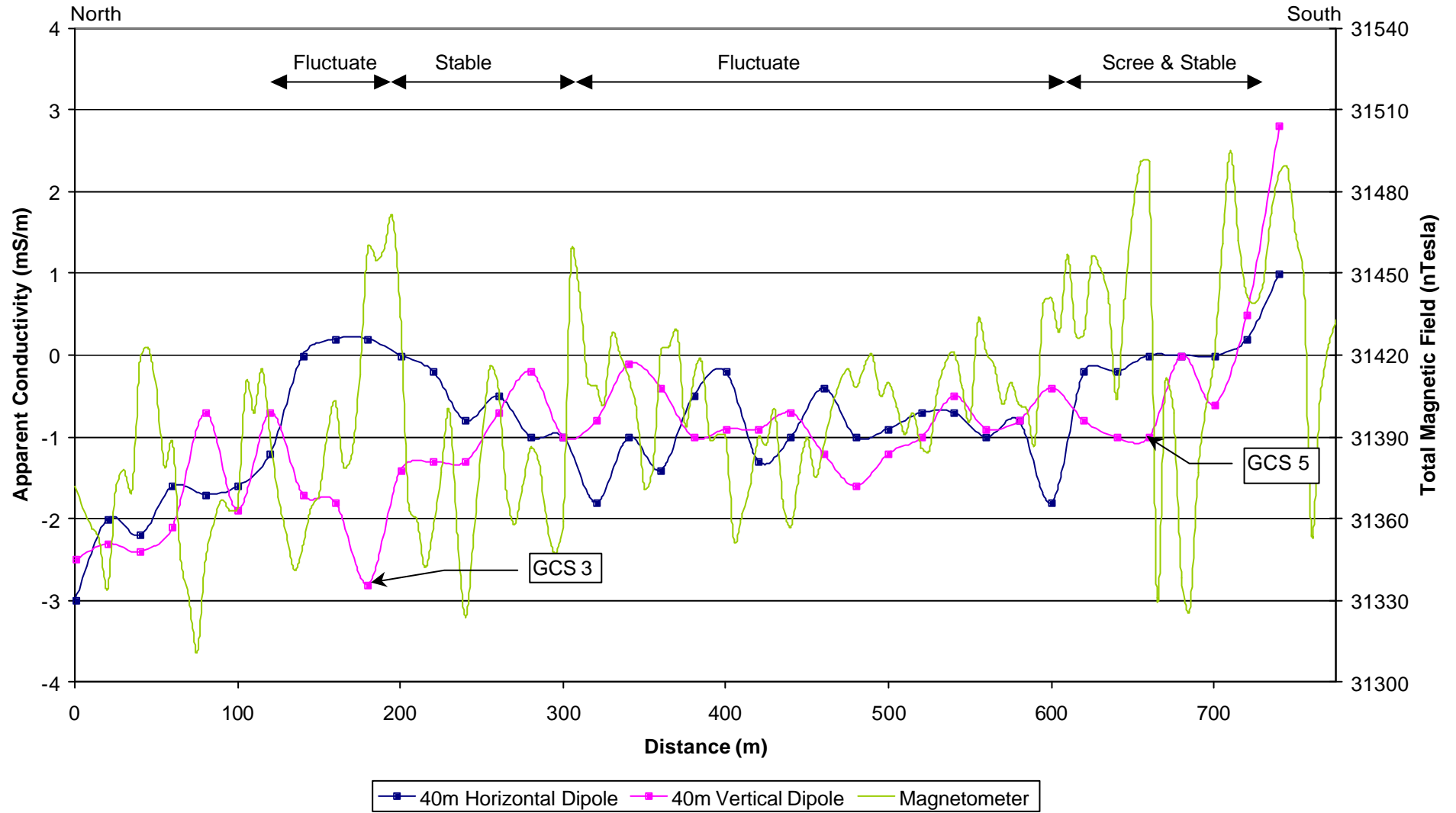
Gravity Survey - Traverse 4



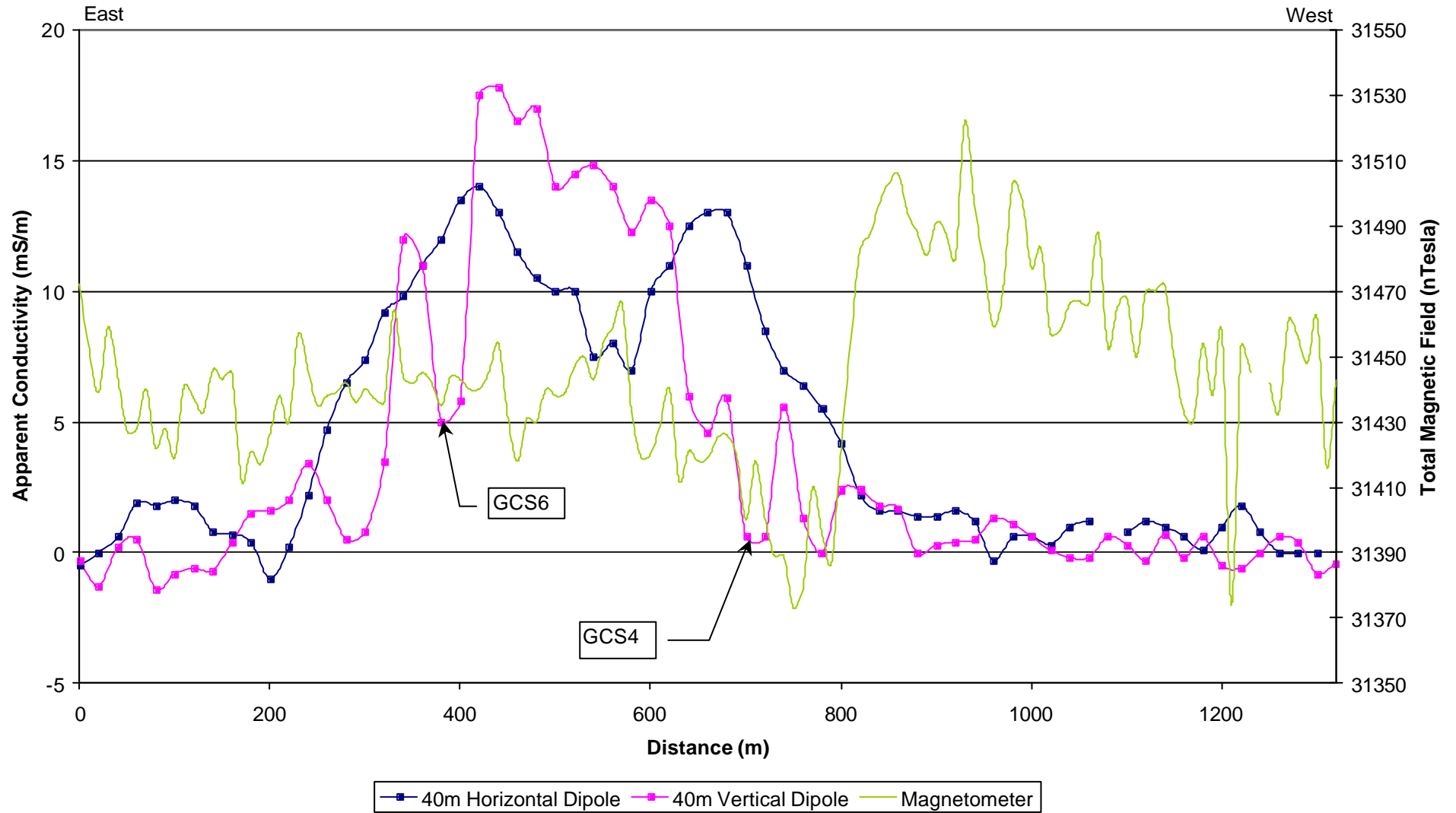
The graph indicate the gravity values recorded along Traverse 4

FIGURE C5 TO C10

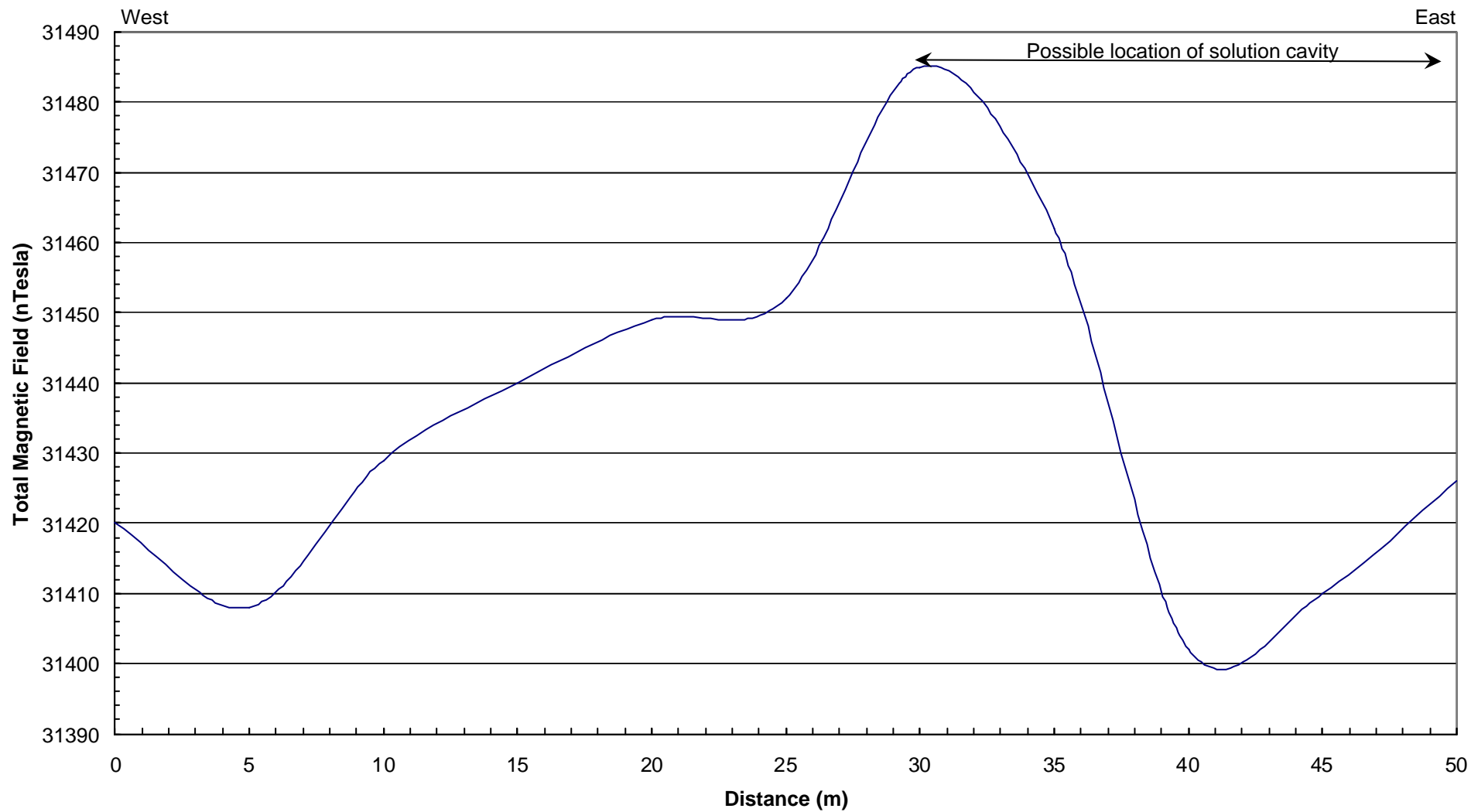
Traverse Turnbull



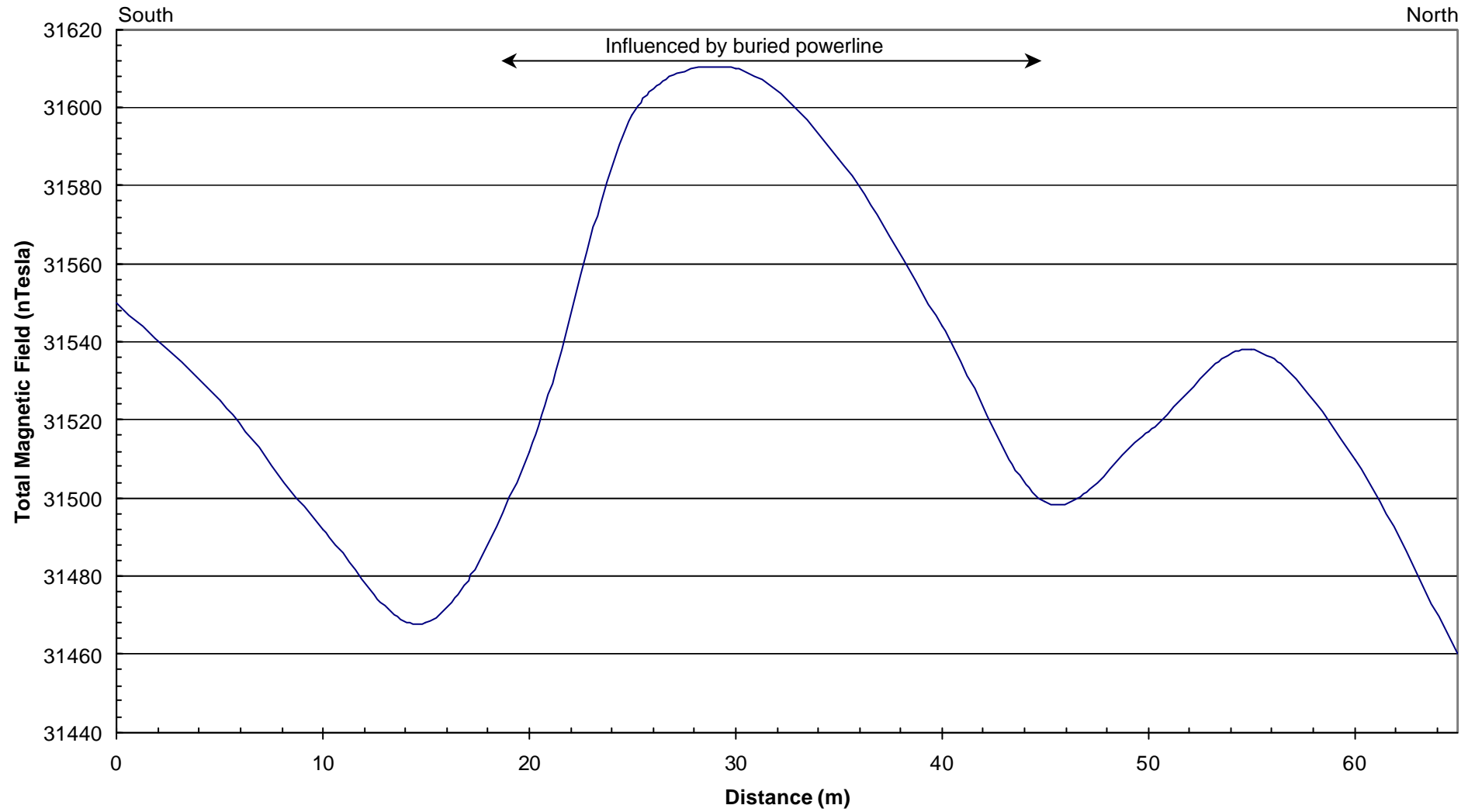
Traverse Turnbull Cross



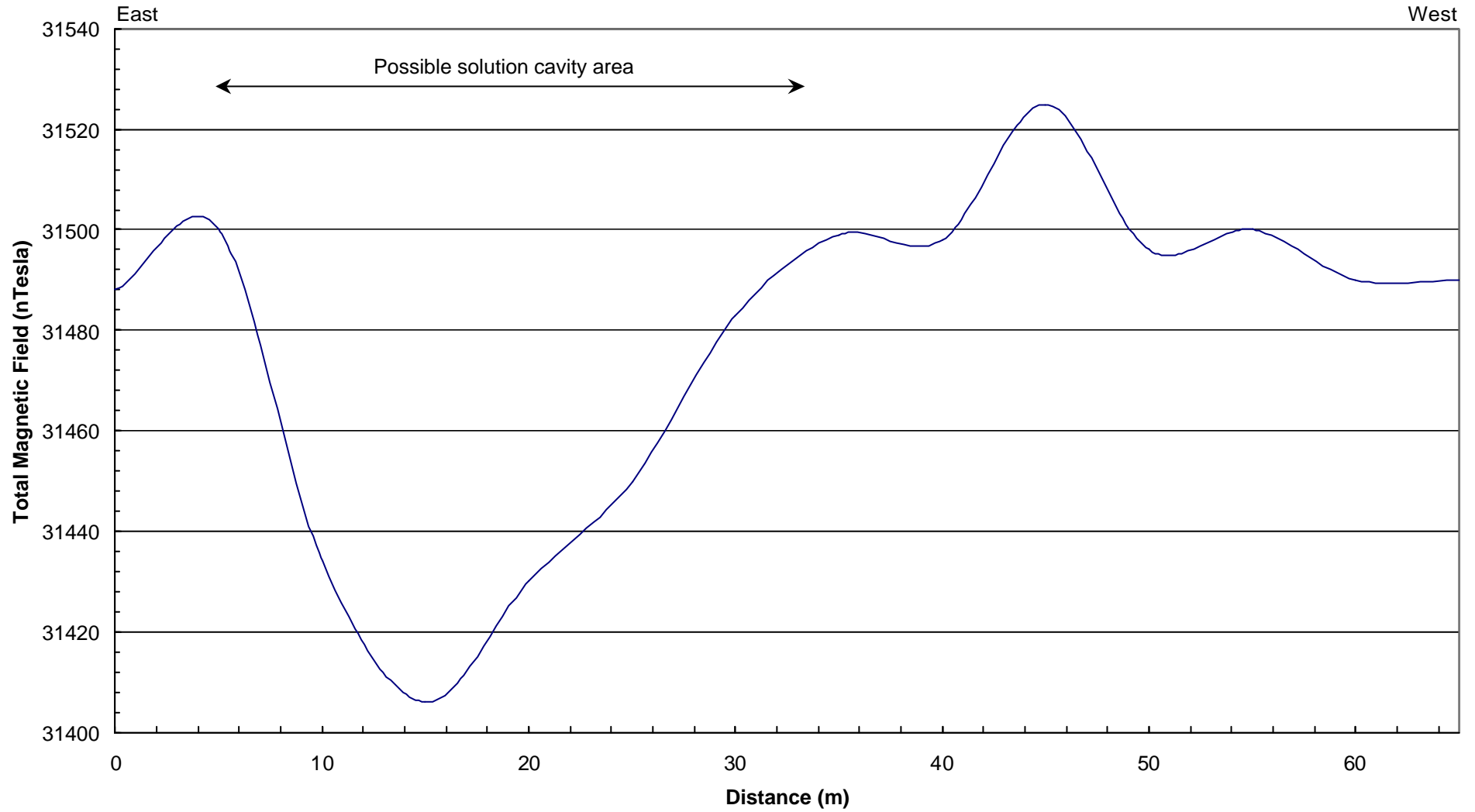
Archibald Traverse 1



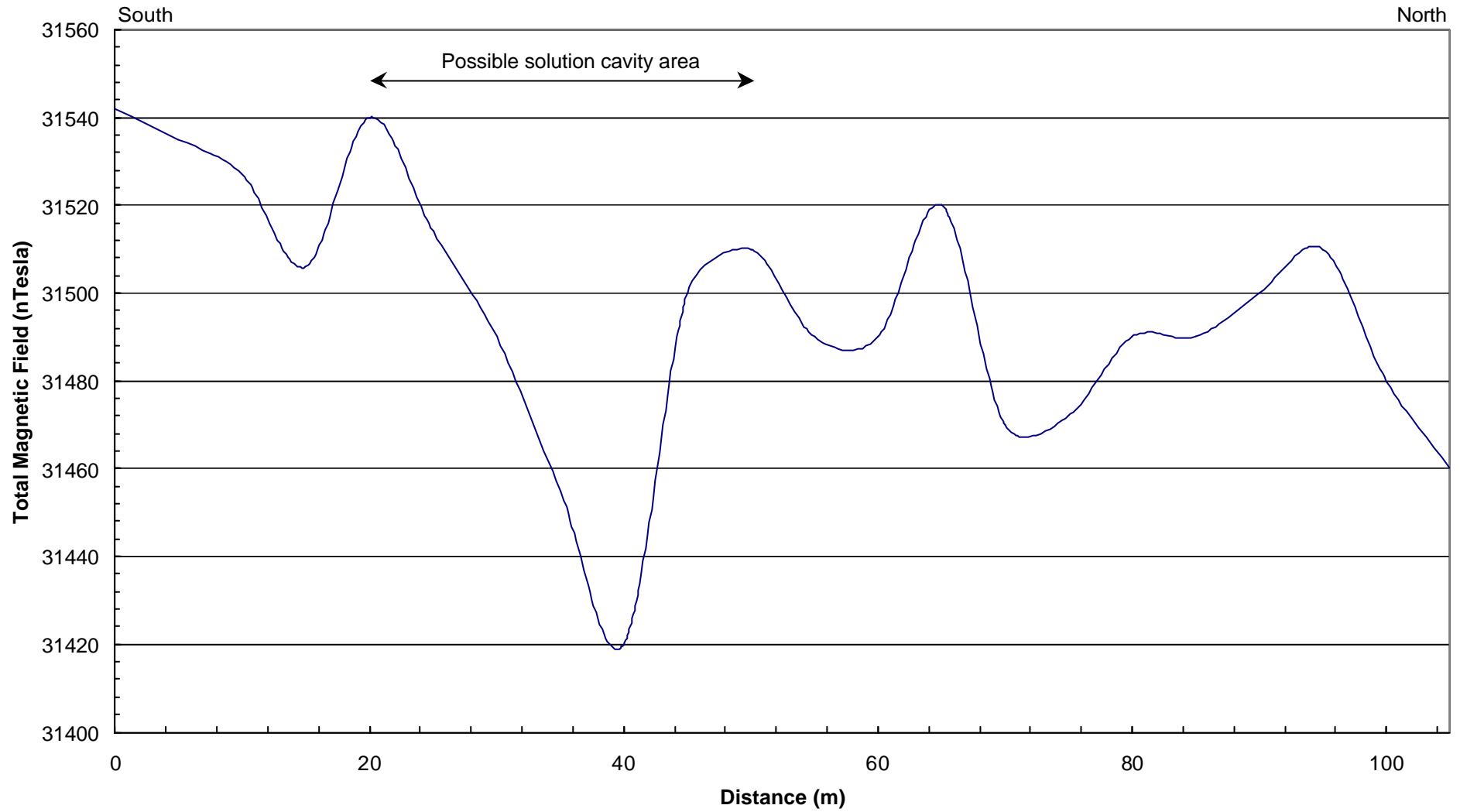
Archibald Traverse 2



Archibald Traverse 3



Archibald Traverse 4





Appendix D:

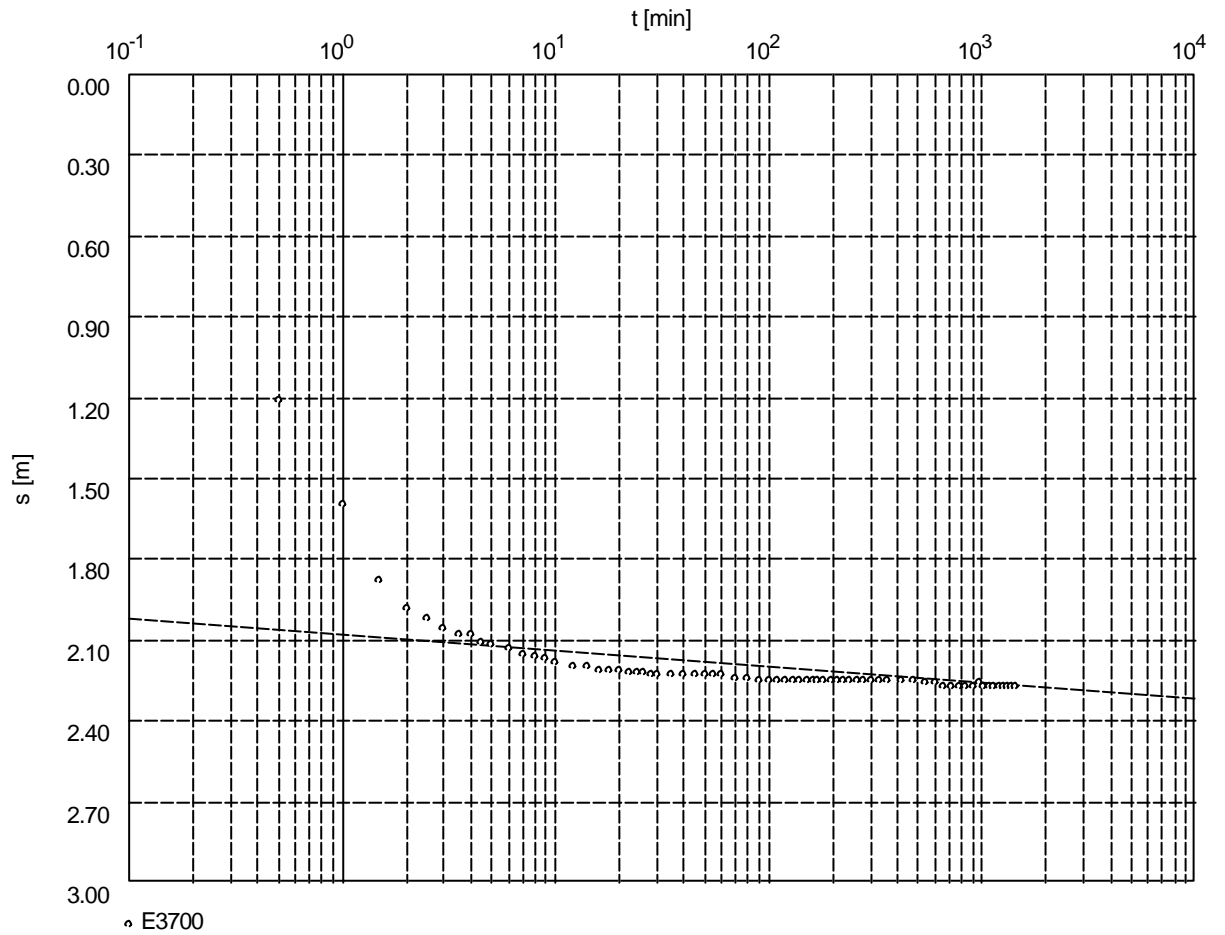
Aquifer Test Data and Borehole Sustainable Yield Calculations for 2004.

Pumping Test No. 1

Test conducted on: 2004/03/05

E3700

Discharge 25.10 l/s



Transmissivity [m²/min]: 4.58×10^0

Storativity: 0.00×10^0

Waterloo Hydrogeologic

180 Columbia St. W.

Waterloo, Ontario, Canada

ph.(519)746-1798

Pumping test analysis
Time-Drawdown-method after
COOPER & JACOB
Confined aquifer

Page 2

Project: Zambia Hydrogeological Inv.

Evaluated by: MP

Date: 04.06.2004

Pumping Test No. 1

Test conducted on: 2004/03/05

E3700

E3700

Discharge 25.10 l/s

Distance from the pumping well 0.080 m

Static water level: 18.020 m below datum

	Pumping test duration	Water level	Drawdown	
	[min]	[m]	[m]	
1	0.50	19.230	1.210	
2	1.00	19.620	1.600	
3	1.50	19.900	1.880	
4	2.00	20.000	1.980	
5	2.50	20.040	2.020	
6	3.00	20.080	2.060	
7	3.50	20.100	2.080	
8	4.00	20.100	2.080	
9	4.50	20.130	2.110	
10	5.00	20.140	2.120	
11	6.00	20.150	2.130	
12	7.00	20.170	2.150	
13	8.00	20.180	2.160	
14	9.00	20.190	2.170	
15	10.00	20.200	2.180	
16	12.00	20.220	2.200	
17	14.00	20.220	2.200	
18	16.00	20.230	2.210	
19	18.00	20.230	2.210	
20	20.00	20.230	2.210	
21	22.00	20.240	2.220	
22	24.00	20.240	2.220	
23	26.00	20.240	2.220	
24	28.00	20.250	2.230	
25	30.00	20.250	2.230	
26	35.00	20.250	2.230	
27	40.00	20.250	2.230	
28	45.00	20.250	2.230	
29	50.00	20.250	2.230	
30	55.00	20.250	2.230	
31	60.00	20.250	2.230	
32	70.00	20.260	2.240	
33	80.00	20.260	2.240	
34	90.00	20.270	2.250	
35	100.00	20.270	2.250	
36	110.00	20.270	2.250	
37	120.00	20.270	2.250	
38	130.00	20.270	2.250	
39	140.00	20.270	2.250	
40	150.00	20.270	2.250	
41	160.00	20.270	2.250	
42	170.00	20.270	2.250	
43	180.00	20.270	2.250	
44	195.00	20.270	2.250	
45	210.00	20.270	2.250	
46	225.00	20.270	2.250	
47	240.00	20.270	2.250	
48	260.00	20.270	2.250	
49	280.00	20.270	2.250	
50	300.00	20.270	2.250	

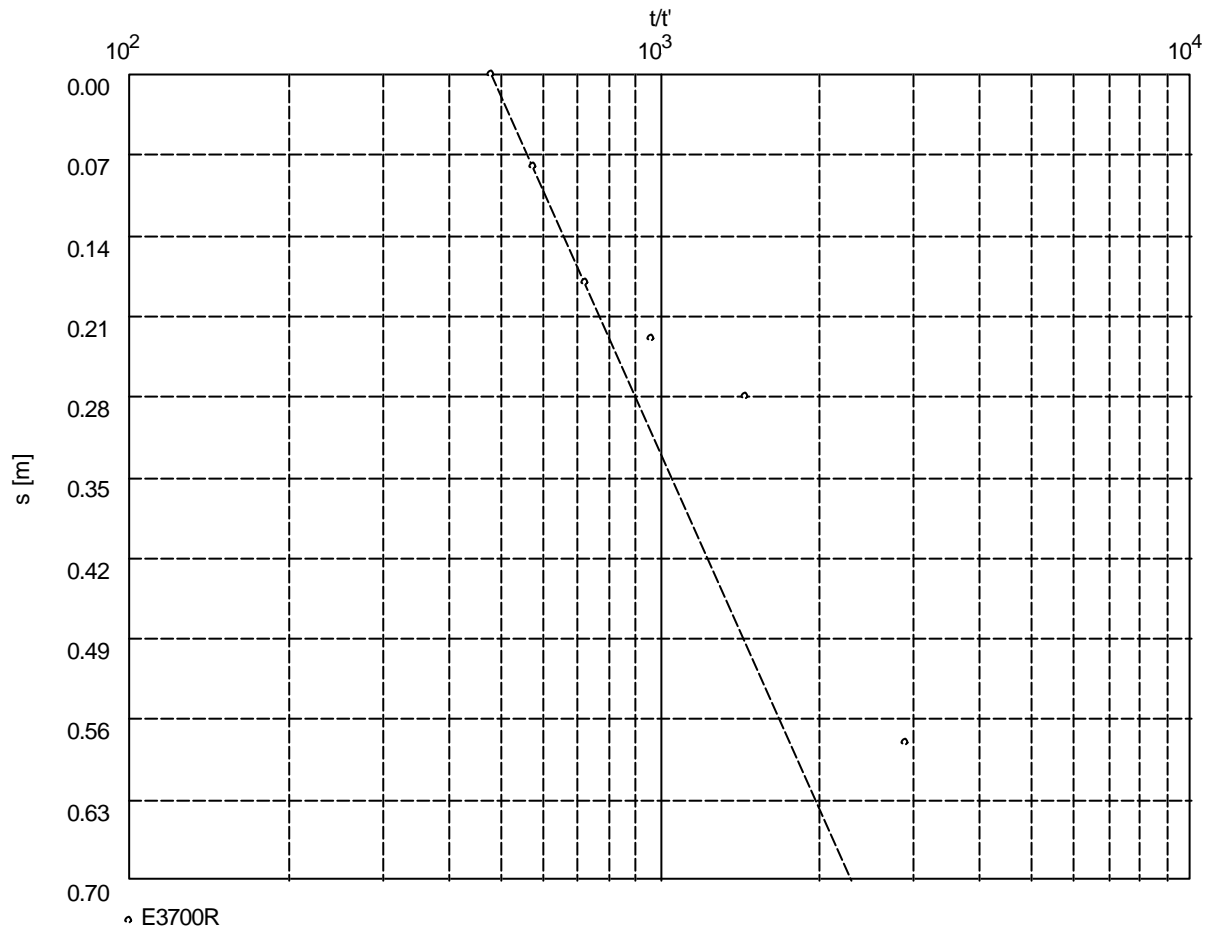
Pumping Test No. 1

Test conducted on: 2004/03/05

E3700R

Discharge 25.10 l/s

Pumping test duration: 1440.00 min



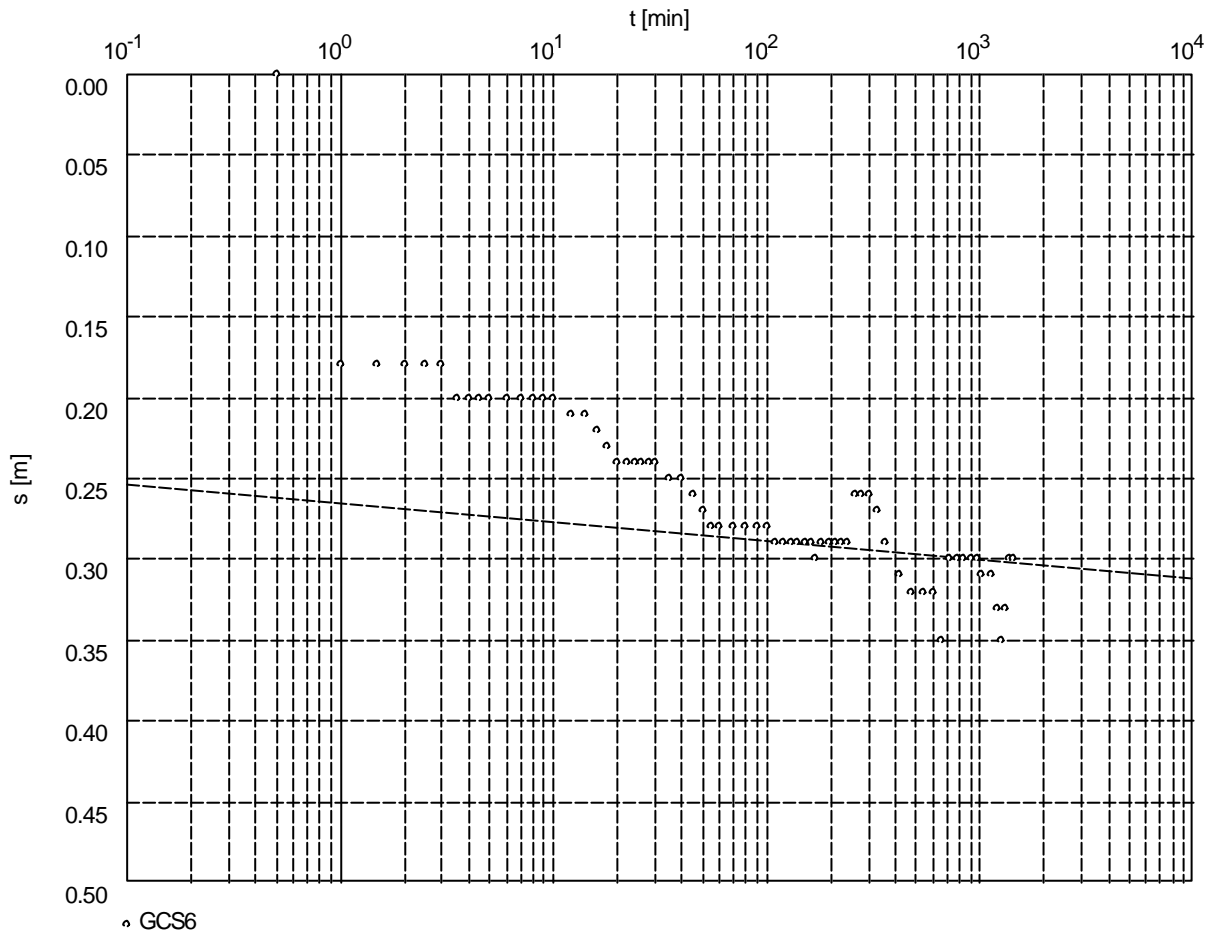
Transmissivity [m²/min]: 2.65×10^{-1}

Pumping Test No. 1

Test conducted on: 06/06/2004

GCS6

Discharge 25.00 l/s



Transmissivity [m²/min]: 2.35×10^1

Storativity: 1.06×10^{-19}

Waterloo Hydrogeologic

180 Columbia St. W.

Waterloo, Ontario, Canada

ph.(519)746-1798

Pumping test analysis
Time-Drawdown-method after
COOPER & JACOB
Confined aquifer

Page 2

Project: Zambia Hydrogeological Inv.

Evaluated by: MP

Date: 01.07.2004

Pumping Test No. 1

Test conducted on: 06/06/2004

GCS6

GCS6

Discharge 25.00 l/s

Distance from the pumping well 0.100 m

Static water level: 27.600 m below datum

	Pumping test duration	Water level	Drawdown	
	[min]	[m]	[m]	
1	0.50	27.600	0.000	
2	1.00	27.780	0.180	
3	1.50	27.780	0.180	
4	2.00	27.780	0.180	
5	2.50	27.780	0.180	
6	3.00	27.780	0.180	
7	3.50	27.800	0.200	
8	4.00	27.800	0.200	
9	4.50	27.800	0.200	
10	5.00	27.800	0.200	
11	6.00	27.800	0.200	
12	7.00	27.800	0.200	
13	8.00	27.800	0.200	
14	9.00	27.800	0.200	
15	10.00	27.800	0.200	
16	12.00	27.810	0.210	
17	14.00	27.810	0.210	
18	16.00	27.820	0.220	
19	18.00	27.830	0.230	
20	20.00	27.840	0.240	
21	22.00	27.840	0.240	
22	24.00	27.840	0.240	
23	26.00	27.840	0.240	
24	28.00	27.840	0.240	
25	30.00	27.840	0.240	
26	35.00	27.850	0.250	
27	40.00	27.850	0.250	
28	45.00	27.860	0.260	
29	50.00	27.870	0.270	
30	55.00	27.880	0.280	
31	60.00	27.880	0.280	
32	70.00	27.880	0.280	
33	80.00	27.880	0.280	
34	90.00	27.880	0.280	
35	100.00	27.880	0.280	
36	110.00	27.890	0.290	
37	120.00	27.890	0.290	
38	130.00	27.890	0.290	
39	140.00	27.890	0.290	
40	150.00	27.890	0.290	
41	160.00	27.890	0.290	
42	170.00	27.900	0.300	
43	180.00	27.890	0.290	
44	195.00	27.890	0.290	
45	210.00	27.890	0.290	
46	225.00	27.890	0.290	
47	240.00	27.890	0.290	
48	260.00	27.860	0.260	
49	280.00	27.860	0.260	
50	300.00	27.860	0.260	

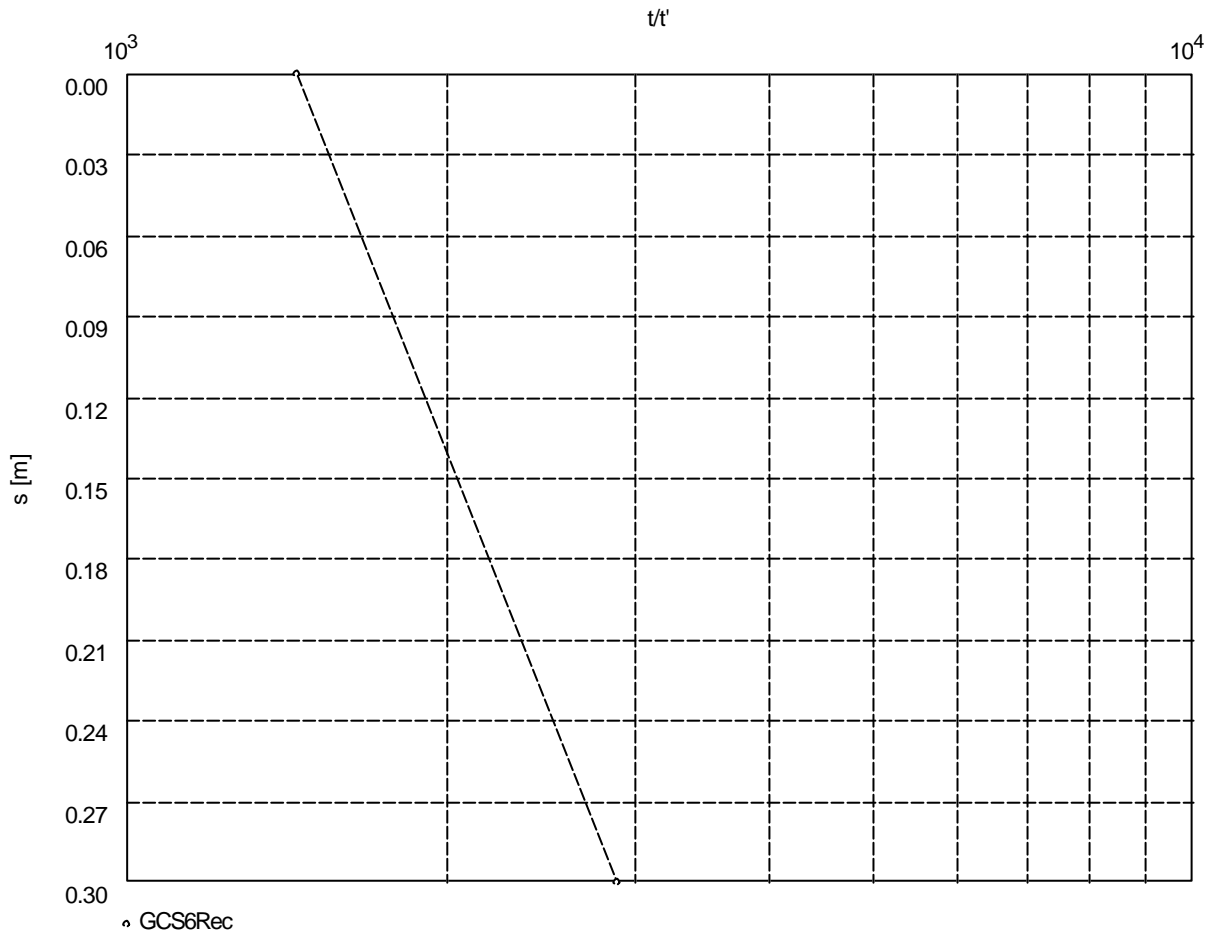
Pumping Test No. 1

Test conducted on: 06/06/2004

GCS6Rec

Discharge 25.00 l/s

Pumping test duration: 1440.00 min



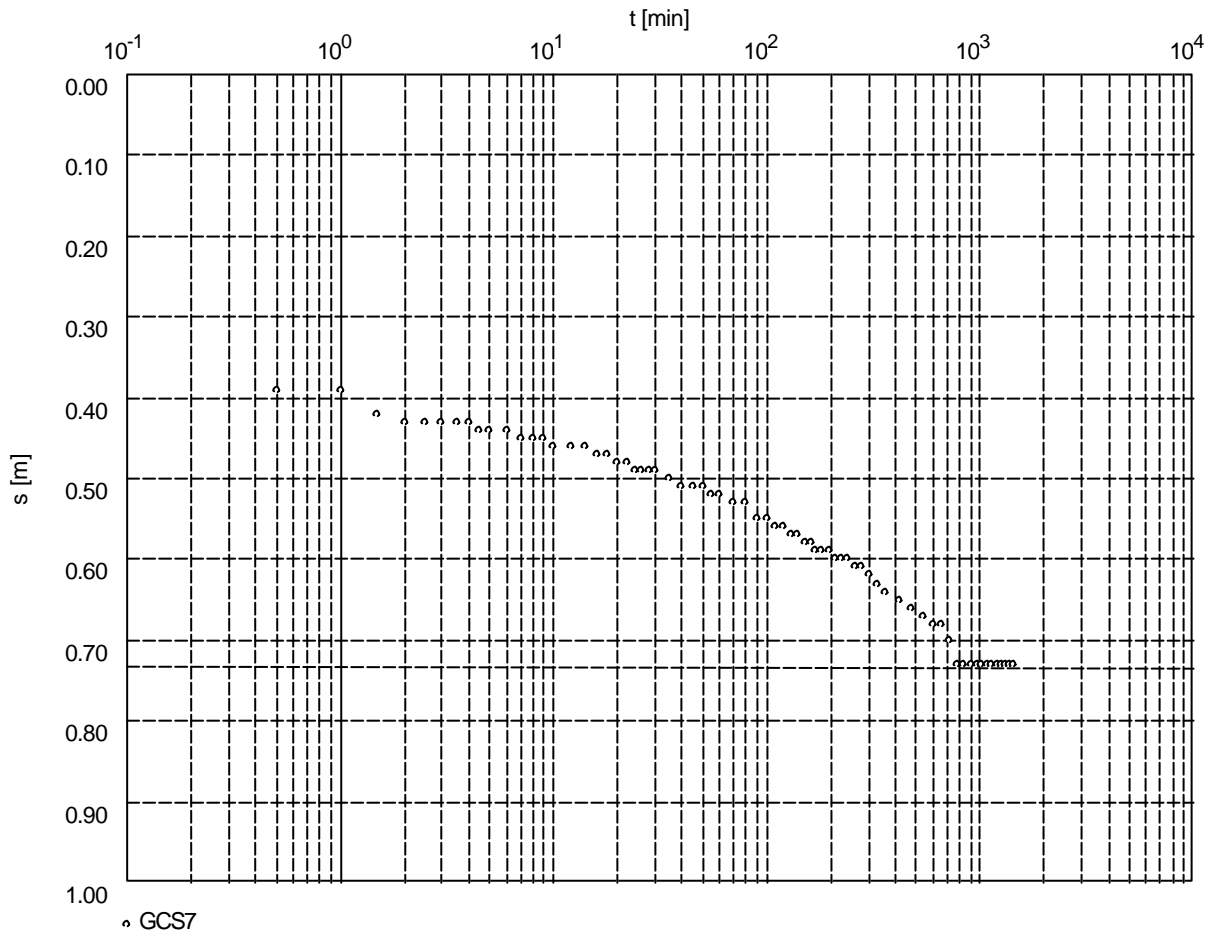
Transmissivity [m²/min]: 2.75×10^{-1}

Pumping Test No. 1

Test conducted on: 11/06/2004

GCS7

Discharge 25.00 l/s



Transmissivity [m²/min]: 7.42×10^2

Storativity: 0.00×10^0

Waterloo Hydrogeologic

180 Columbia St. W.

Waterloo, Ontario, Canada

ph.(519)746-1798

Pumping test analysis
Time-Drawdown-method after
COOPER & JACOB
Confined aquifer

Page 2

Project: Zambia Hydrogeological Inv.

Evaluated by: MP

Date: 01.07.2004

Pumping Test No. 1

Test conducted on: 11/06/2004

GCS7

GCS7

Discharge 25.00 l/s

Distance from the pumping well 0.100 m

Static water level: 34.290 m below datum

	Pumping test duration	Water level	Drawdown	
	[min]	[m]	[m]	
2	0.50	34.680	0.390	
3	1.00	34.680	0.390	
4	1.50	34.710	0.420	
5	2.00	34.720	0.430	
6	2.50	34.720	0.430	
7	3.00	34.720	0.430	
8	3.50	34.720	0.430	
9	4.00	34.720	0.430	
10	4.50	34.730	0.440	
11	5.00	34.730	0.440	
12	6.00	34.730	0.440	
13	7.00	34.740	0.450	
14	8.00	34.740	0.450	
15	9.00	34.740	0.450	
16	10.00	34.750	0.460	
17	12.00	34.750	0.460	
18	14.00	34.750	0.460	
19	16.00	34.760	0.470	
20	18.00	34.760	0.470	
21	20.00	34.770	0.480	
22	22.00	34.770	0.480	
23	24.00	34.780	0.490	
24	26.00	34.780	0.490	
25	28.00	34.780	0.490	
26	30.00	34.780	0.490	
27	35.00	34.790	0.500	
28	40.00	34.800	0.510	
29	45.00	34.800	0.510	
30	50.00	34.800	0.510	
31	55.00	34.810	0.520	
32	60.00	34.810	0.520	
33	70.00	34.820	0.530	
34	80.00	34.820	0.530	
35	90.00	34.840	0.550	
36	100.00	34.840	0.550	
37	110.00	34.850	0.560	
38	120.00	34.850	0.560	
39	130.00	34.860	0.570	
40	140.00	34.860	0.570	
41	150.00	34.870	0.580	
42	160.00	34.870	0.580	
43	170.00	34.880	0.590	
44	180.00	34.880	0.590	
45	195.00	34.880	0.590	
46	210.00	34.890	0.600	
47	225.00	34.890	0.600	
48	240.00	34.890	0.600	
49	260.00	34.900	0.610	
50	280.00	34.900	0.610	

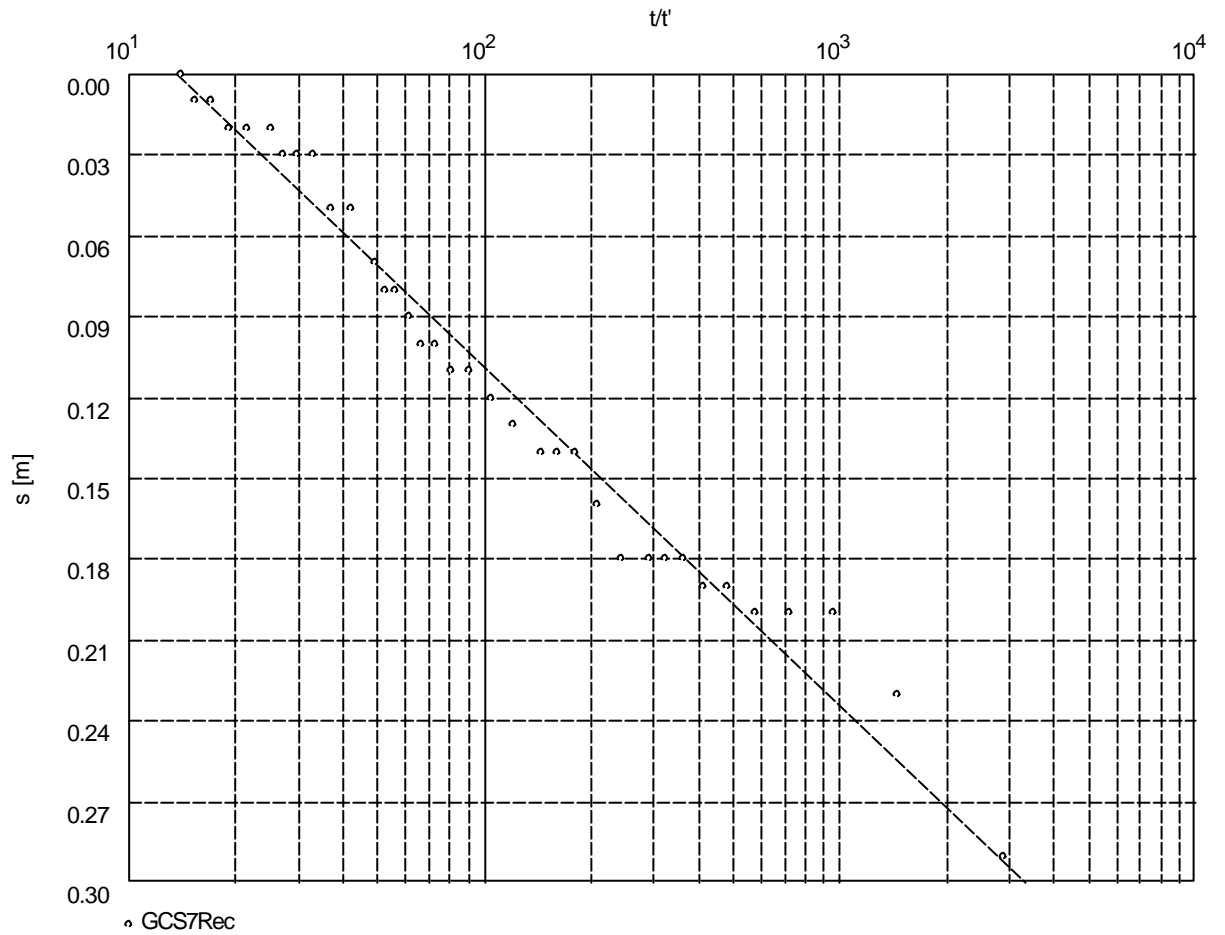
Pumping Test No. 1

Test conducted on: 11/06/2004

GCS7Rec

Discharge 25.00 l/s

Pumping test duration: 1440.00 min



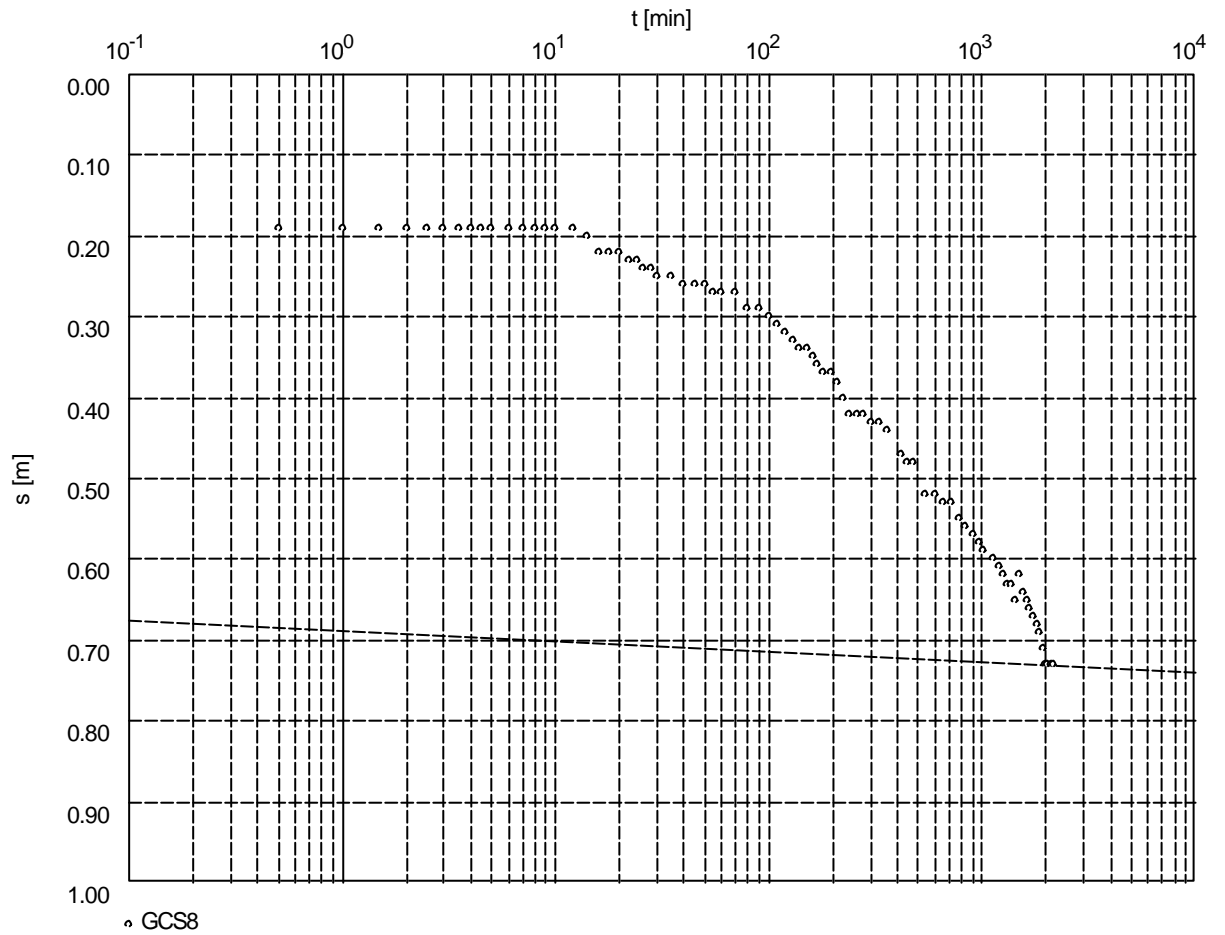
Transmissivity [m^2/min]: 2.18×10^0

Pumping Test No. 1

Test conducted on: 01/06/2004

GCS8

Discharge 25.00 l/s



Transmissivity [m²/min]: 2.05 x 10¹

Storativity: 0.00 x 10⁰

Waterloo Hydrogeologic

180 Columbia St. W.

Waterloo, Ontario, Canada

ph.(519)746-1798

Pumping test analysis
Time-Drawdown-method after
COOPER & JACOB
Confined aquifer

Page 2

Project: Zambia Hydrogeological Inv.

Evaluated by: MP

Date: 01.07.2004

Pumping Test No. 1

Test conducted on: 01/06/2004

GCS8

GCS8

Discharge 25.00 l/s

Distance from the pumping well 0.100 m

Static water level: 33.260 m below datum

	Pumping test duration	Water level	Drawdown	
	[min]	[m]	[m]	
1	0.50	33.450	0.190	
2	1.00	33.450	0.190	
3	1.50	33.450	0.190	
4	2.00	33.450	0.190	
5	2.50	33.450	0.190	
6	3.00	33.450	0.190	
7	3.50	33.450	0.190	
8	4.00	33.450	0.190	
9	4.50	33.450	0.190	
10	5.00	33.450	0.190	
11	6.00	33.450	0.190	
12	7.00	33.450	0.190	
13	8.00	33.450	0.190	
14	9.00	33.450	0.190	
15	10.00	33.450	0.190	
16	12.00	33.450	0.190	
17	14.00	33.460	0.200	
18	16.00	33.480	0.220	
19	18.00	33.480	0.220	
20	20.00	33.480	0.220	
21	22.00	33.490	0.230	
22	24.00	33.490	0.230	
23	26.00	33.500	0.240	
24	28.00	33.500	0.240	
25	30.00	33.510	0.250	
26	35.00	33.510	0.250	
27	40.00	33.520	0.260	
28	45.00	33.520	0.260	
29	50.00	33.520	0.260	
30	55.00	33.530	0.270	
31	60.00	33.530	0.270	
32	70.00	33.530	0.270	
33	80.00	33.550	0.290	
34	90.00	33.550	0.290	
35	100.00	33.560	0.300	
36	110.00	33.570	0.310	
37	120.00	33.580	0.320	
38	130.00	33.590	0.330	
39	140.00	33.600	0.340	
40	150.00	33.600	0.340	
41	160.00	33.610	0.350	
42	170.00	33.620	0.360	
43	180.00	33.630	0.370	
44	195.00	33.630	0.370	
45	210.00	33.640	0.380	
46	225.00	33.660	0.400	
47	240.00	33.680	0.420	
48	260.00	33.680	0.420	
49	280.00	33.680	0.420	
50	300.00	33.690	0.430	

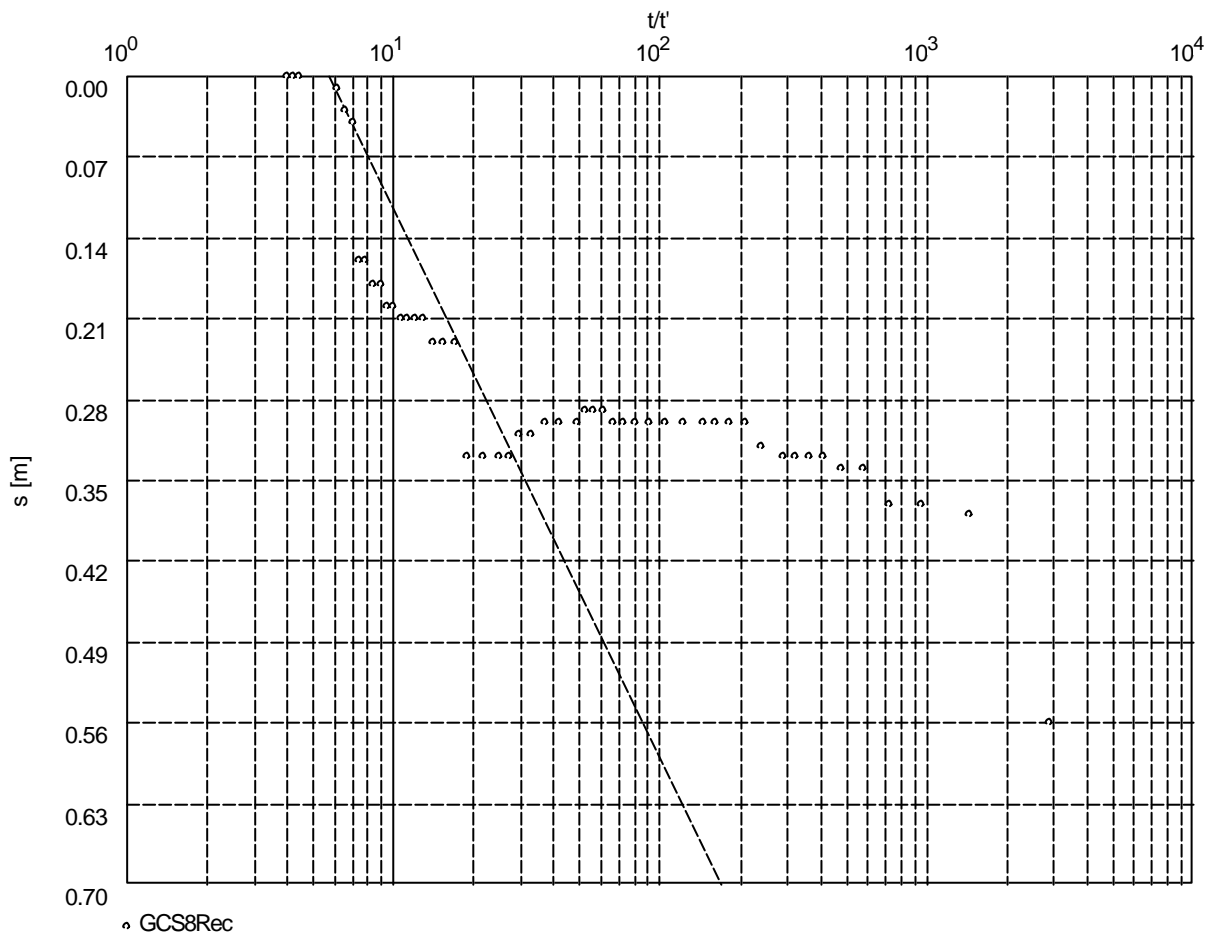
Pumping Test No. 1

Test conducted on: 01/06/2004

GCS8Rec

Discharge 25.00 l/s

Pumping test duration: 1440.00 min



Transmissivity [m²/min]: 5.75×10^{-1}

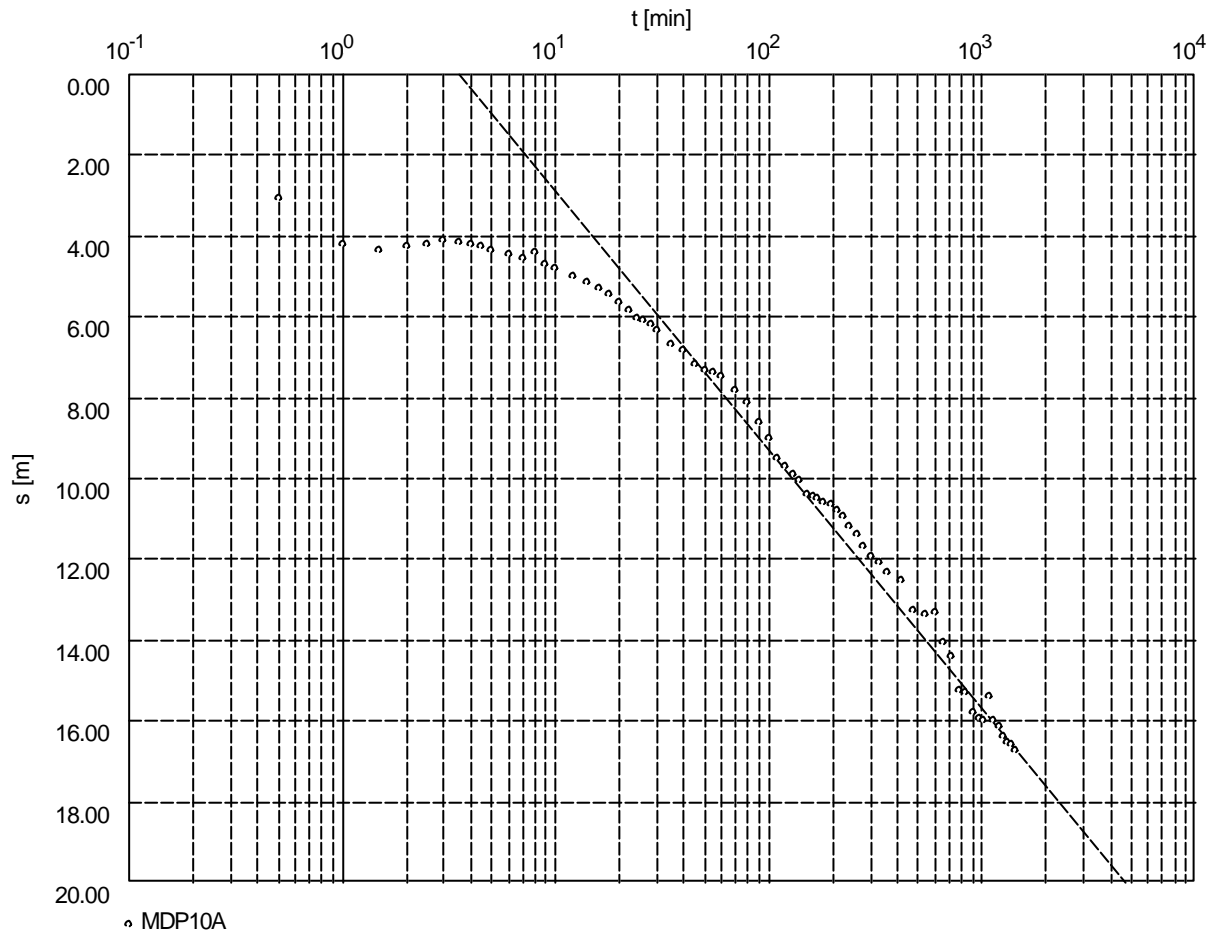
Waterloo Hydrogeologic 180 Columbia St. W. Waterloo, Ontario, Canada ph.(519)746-1798		Pumping test analysis Recovery method after THEIS & JACOB Confined aquifer		Page 2	
				Project: Zambia Hydrogeological Inv.	
				Evaluated by: MP	Date: 01.07.2004
Pumping Test No. 1			Test conducted on: 01/06/2004		
GCS8Rec			GCS8Rec		
Discharge 25.00 l/s					
Static water level: 33.260 m below datum			Pumping test duration: 1440.00 min		
	Time from end of pumping [min]	Water level [m]	Residual drawdown [m]		
1	0.50	33.820	0.560		
2	1.00	33.640	0.380		
3	1.50	33.630	0.370		
4	2.00	33.630	0.370		
5	2.50	33.600	0.340		
6	3.00	33.600	0.340		
7	3.50	33.590	0.330		
8	4.00	33.590	0.330		
9	4.50	33.590	0.330		
10	5.00	33.590	0.330		
11	6.00	33.580	0.320		
12	7.00	33.560	0.300		
13	8.00	33.560	0.300		
14	9.00	33.560	0.300		
15	10.00	33.560	0.300		
16	12.00	33.560	0.300		
17	14.00	33.560	0.300		
18	16.00	33.560	0.300		
19	18.00	33.560	0.300		
20	20.00	33.560	0.300		
21	22.00	33.560	0.300		
22	24.00	33.550	0.290		
23	26.00	33.550	0.290		
24	28.00	33.550	0.290		
25	30.00	33.560	0.300		
26	35.00	33.560	0.300		
27	40.00	33.560	0.300		
28	45.00	33.570	0.310		
29	50.00	33.570	0.310		
30	55.00	33.590	0.330		
31	60.00	33.590	0.330		
32	70.00	33.590	0.330		
33	80.00	33.590	0.330		
34	90.00	33.490	0.230		
35	100.00	33.490	0.230		
36	110.00	33.490	0.230		
37	120.00	33.470	0.210		
38	130.00	33.470	0.210		
39	140.00	33.470	0.210		
40	150.00	33.470	0.210		
41	160.00	33.460	0.200		
42	170.00	33.460	0.200		
43	180.00	33.440	0.180		
44	195.00	33.440	0.180		
45	210.00	33.420	0.160		
46	225.00	33.420	0.160		
47	240.00	33.300	0.040		
48	260.00	33.290	0.030		
49	280.00	33.270	0.010		
50	300.00	33.250	-0.010		

Pumping Test No. 1

Test conducted on: 29/05/2004

MDP10A

Discharge 10.50 l/s



Transmissivity [m²/min]: 1.80×10^{-2}

Storativity: 1.42×10^{-1}

Waterloo Hydrogeologic

180 Columbia St. W.

Waterloo, Ontario, Canada

ph.(519)746-1798

Pumping test analysis
Time-Drawdown-method after
COOPER & JACOB
Confined aquifer

Page 2

Project: Zambia Hydrogeological Inv.

Evaluated by: MP

Date: 01.07.2004

Pumping Test No. 1

Test conducted on: 29/05/2004

MDP10A

MDP10A

Discharge 10.50 l/s

Distance from the pumping well 0.100 m

Static water level: 12.310 m below datum

	Pumping test duration	Water level	Drawdown	
	[min]	[m]	[m]	
1	0.50	15.360	3.050	
2	1.00	16.510	4.200	
3	1.50	16.670	4.360	
4	2.00	16.570	4.260	
5	2.50	16.530	4.220	
6	3.00	16.420	4.110	
7	3.50	16.470	4.160	
8	4.00	16.530	4.220	
9	4.50	16.590	4.280	
10	5.00	16.650	4.340	
11	6.00	16.760	4.450	
12	7.00	16.850	4.540	
13	8.00	16.740	4.430	
14	9.00	17.000	4.690	
15	10.00	17.090	4.780	
16	12.00	17.300	4.990	
17	14.00	17.470	5.160	
18	16.00	17.600	5.290	
19	18.00	17.780	5.470	
20	20.00	17.950	5.640	
21	22.00	18.170	5.860	
22	24.00	18.330	6.020	
23	26.00	18.420	6.110	
24	28.00	18.520	6.210	
25	30.00	18.650	6.340	
26	35.00	18.990	6.680	
27	40.00	19.160	6.850	
28	45.00	19.470	7.160	
29	50.00	19.650	7.340	
30	55.00	19.690	7.380	
31	60.00	19.780	7.470	
32	70.00	20.140	7.830	
33	80.00	20.420	8.110	
34	90.00	20.910	8.600	
35	100.00	21.340	9.030	
36	110.00	21.810	9.500	
37	120.00	22.020	9.710	
38	130.00	22.200	9.890	
39	140.00	22.340	10.030	
40	150.00	22.700	10.390	
41	160.00	22.780	10.470	
42	170.00	22.800	10.490	
43	180.00	22.880	10.570	
44	195.00	22.960	10.650	
45	210.00	23.100	10.790	
46	225.00	23.240	10.930	
47	240.00	23.480	11.170	
48	260.00	23.680	11.370	
49	280.00	24.000	11.690	
50	300.00	24.230	11.920	

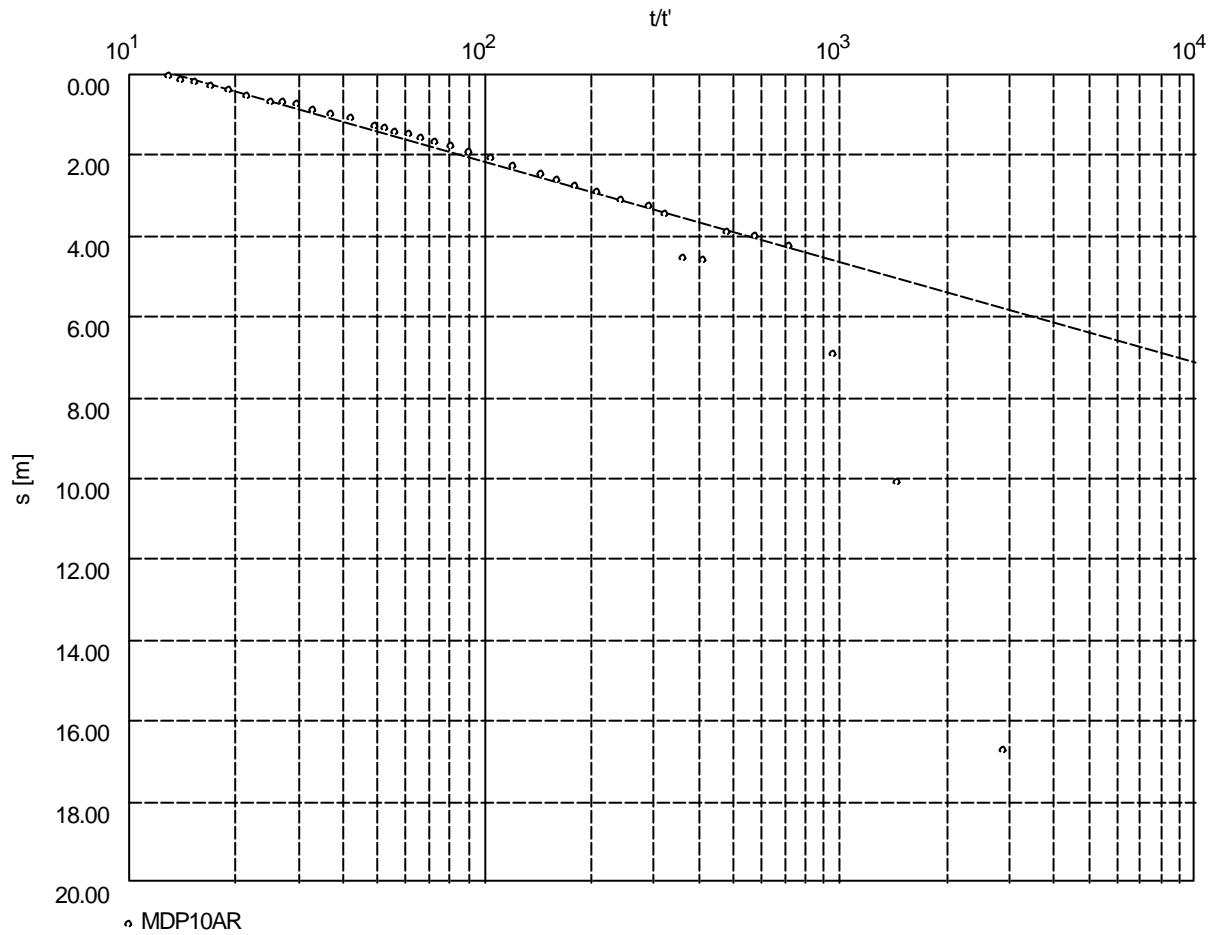
Pumping Test No. 1

Test conducted on: 29/05/2004

MDP10AR

Discharge 10.50 l/s

Pumping test duration: 1440.00 min



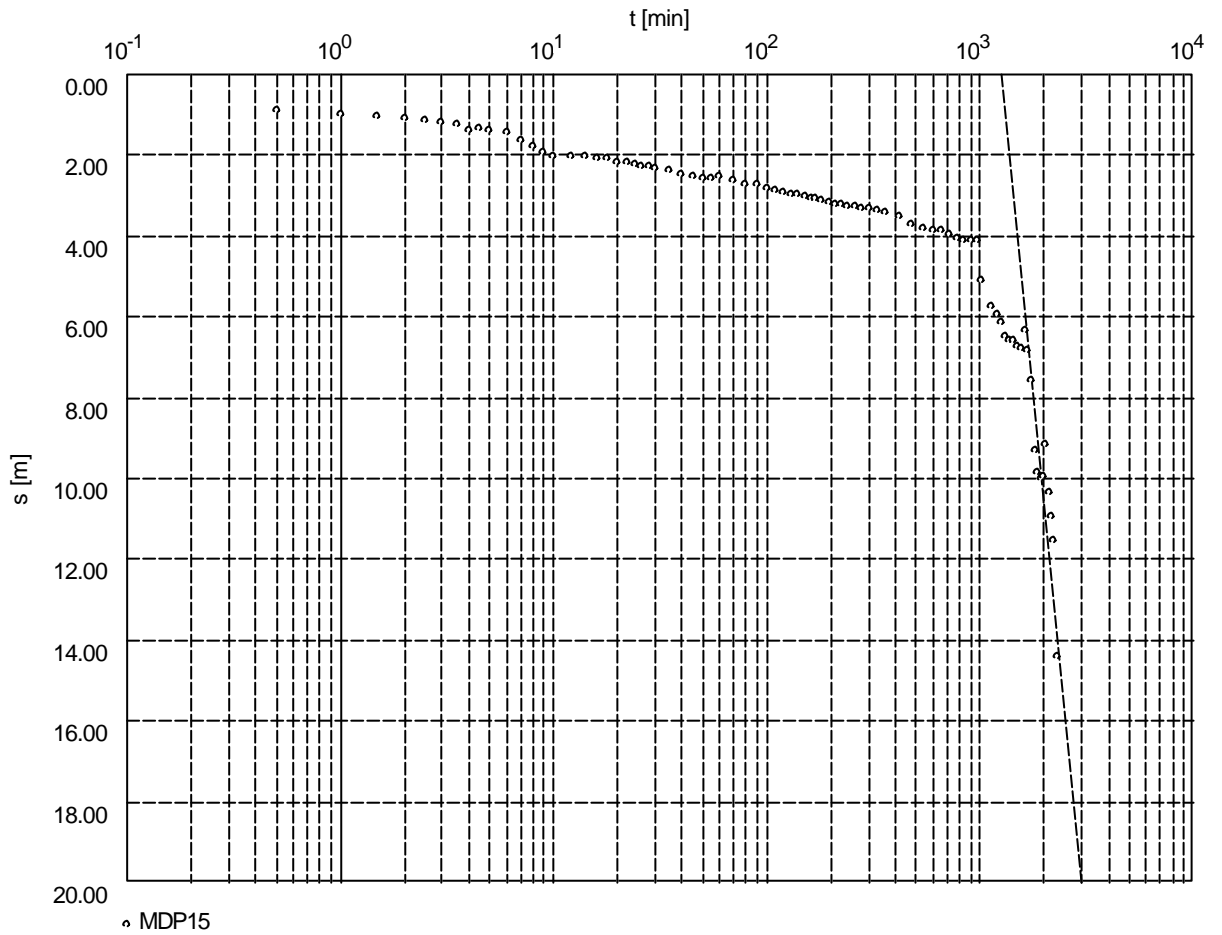
Transmissivity [m²/min]: 4.63×10^{-2}

Pumping Test No. 1

Test conducted on: 2004/04/24

MDP15

Discharge 17.10 l/s



Transmissivity [m²/min]: 3.50×10^{-3}

Storativity: 1.55×10^{-3}

Waterloo Hydrogeologic

180 Columbia St. W.

Waterloo, Ontario, Canada

ph.(519)746-1798

Pumping test analysis
Time-Drawdown-method after
COOPER & JACOB
Confined aquifer

Page 2

Project: Zambia Hydrogeological Inv

Evaluated by: MP

Date: 04.06.2004

Pumping Test No. 1

Test conducted on: 2004/04/24

MDP15

MDP15

Discharge 17.10 l/s

Distance from the pumping well 0.080 m

Static water level: 10.900 m below datum

	Pumping test duration	Water level	Drawdown	
	[min]	[m]	[m]	
1	0.50	11.790	0.890	
2	1.00	11.880	0.980	
3	1.50	11.950	1.050	
4	2.00	12.000	1.100	
5	2.50	12.060	1.160	
6	3.00	12.100	1.200	
7	3.50	12.160	1.260	
8	4.00	12.290	1.390	
9	4.50	12.260	1.360	
10	5.00	12.300	1.400	
11	6.00	12.350	1.450	
12	7.00	12.520	1.620	
13	8.00	12.700	1.800	
14	9.00	12.830	1.930	
15	10.00	12.940	2.040	
16	12.00	12.910	2.010	
17	14.00	12.930	2.030	
18	16.00	12.960	2.060	
19	18.00	13.000	2.100	
20	20.00	13.070	2.170	
21	22.00	13.100	2.200	
22	24.00	13.130	2.230	
23	26.00	13.180	2.280	
24	28.00	13.200	2.300	
25	30.00	13.230	2.330	
26	35.00	13.300	2.400	
27	40.00	13.370	2.470	
28	45.00	13.420	2.520	
29	50.00	13.470	2.570	
30	55.00	13.450	2.550	
31	60.00	13.420	2.520	
32	70.00	13.500	2.600	
33	80.00	13.600	2.700	
34	90.00	13.640	2.740	
35	100.00	13.730	2.830	
36	110.00	13.760	2.860	
37	120.00	13.810	2.910	
38	130.00	13.850	2.950	
39	140.00	13.880	2.980	
40	150.00	13.920	3.020	
41	160.00	13.950	3.050	
42	170.00	13.980	3.080	
43	180.00	14.020	3.120	
44	195.00	14.060	3.160	
45	210.00	14.100	3.200	
46	225.00	14.130	3.230	
47	240.00	14.160	3.260	
48	260.00	14.180	3.280	
49	280.00	14.200	3.300	
50	300.00	14.230	3.330	

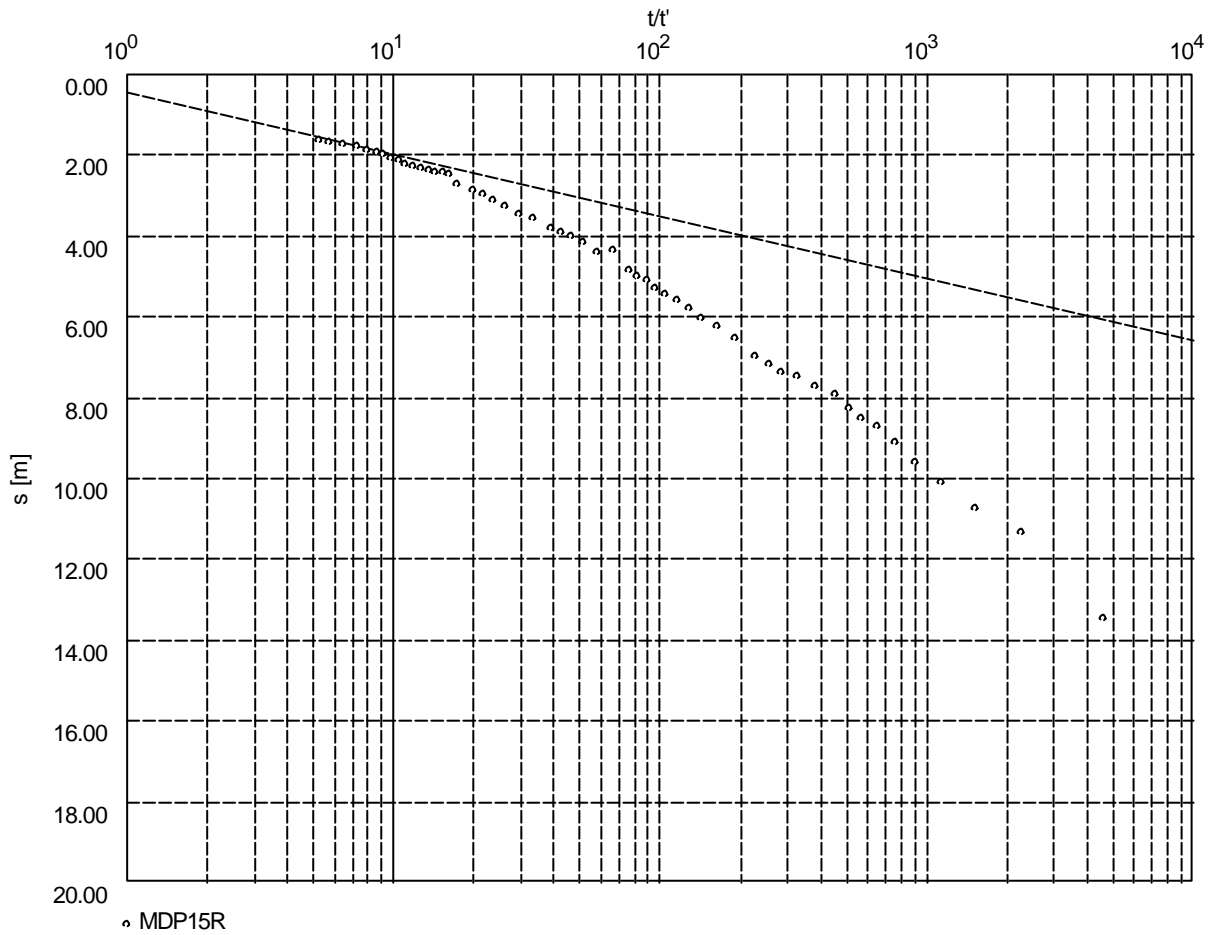
Pumping Test No. 1

Test conducted on: 2004/04/24

MDP15R

Discharge 17.10 l/s

Pumping test duration: 2280.00 min



Transmissivity [m²/min]: 1.23×10^{-1}

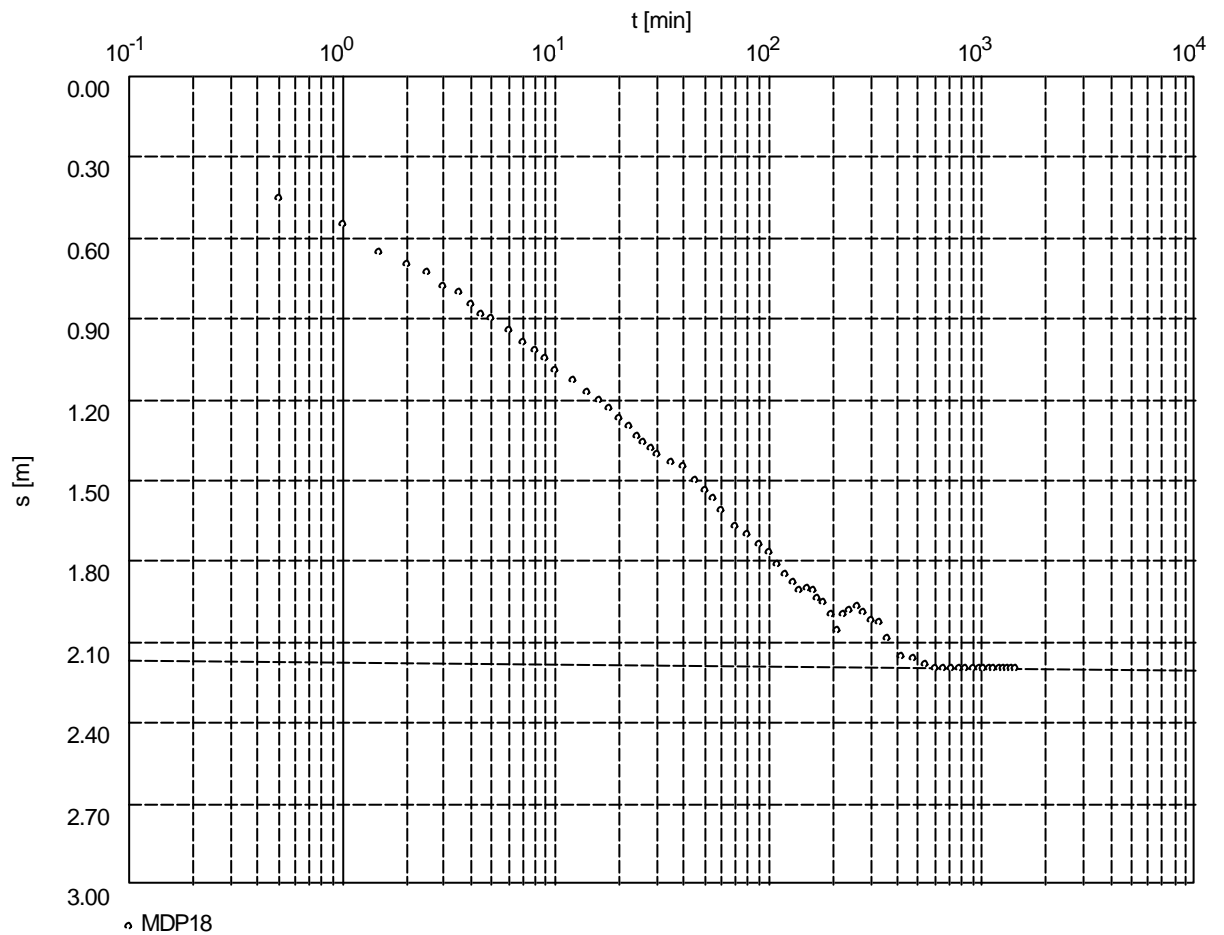
Waterloo Hydrogeologic 180 Columbia St. W. Waterloo, Ontario, Canada ph.(519)746-1798		Pumping test analysis Recovery method after THEIS & JACOB Confined aquifer		Page 2	
				Project: Zambia Hydrogeological Inv	
				Evaluated by: MP	Date: 04.06.2004
Pumping Test No. 1			Test conducted on: 2004/04/24		
MDP15R			MDP15R		
Discharge 17.10 l/s					
Static water level: 10.900 m below datum			Pumping test duration: 2280.00 min		
	Time from end of pumping [min]	Water level [m]	Residual drawdown [m]		
1	0.50	24.360	13.460		
2	1.00	22.250	11.350		
3	1.50	21.650	10.750		
4	2.00	21.000	10.100		
5	2.50	20.490	9.590		
6	3.00	20.000	9.100		
7	3.50	19.600	8.700		
8	4.00	19.400	8.500		
9	4.50	19.190	8.290		
10	5.00	18.840	7.940		
11	6.00	18.600	7.700		
12	7.00	18.400	7.500		
13	8.00	18.300	7.400		
14	9.00	18.100	7.200		
15	10.00	17.900	7.000		
16	12.00	17.450	6.550		
17	14.00	17.160	6.260		
18	16.00	16.920	6.020		
19	18.00	16.690	5.790		
20	20.00	16.500	5.600		
21	22.00	16.360	5.460		
22	24.00	16.200	5.300		
23	26.00	16.010	5.110		
24	28.00	15.900	5.000		
25	30.00	15.770	4.870		
26	35.00	15.260	4.360		
27	40.00	15.300	4.400		
28	45.00	15.070	4.170		
29	50.00	14.910	4.010		
30	55.00	14.830	3.930		
31	60.00	14.730	3.830		
32	70.00	14.450	3.550		
33	80.00	14.350	3.450		
34	90.00	14.180	3.280		
35	100.00	14.030	3.130		
36	110.00	13.870	2.970		
37	120.00	13.750	2.850		
38	140.00	13.620	2.720		
39	150.00	13.390	2.490		
40	160.00	13.350	2.450		
41	170.00	13.330	2.430		
42	180.00	13.280	2.380		
43	195.00	13.250	2.350		
44	210.00	13.180	2.280		
45	225.00	13.110	2.210		
46	240.00	13.030	2.130		
47	260.00	12.970	2.070		
48	280.00	12.900	2.000		
49	300.00	12.810	1.910		
50	330.00	12.790	1.890		

Pumping Test No. 1

Test conducted on: 2004/05/01

MDP 18

Discharge 25.00 l/s



Transmissivity [m²/min]: 3.46×10^1

Storativity: 0.00×10^0

Waterloo Hydrogeologic

180 Columbia St. W.

Waterloo, Ontario, Canada

ph.(519)746-1798

Pumping test analysis
Time-Drawdown-method after
COOPER & JACOB
Confined aquifer

Page 2

Project: Zambia Hydrogeological Inv

Evaluated by: MP

Date: 04.06.2004

Pumping Test No. 1

Test conducted on: 2004/05/01

MDP 18

MDP18

Discharge 25.00 l/s

Distance from the pumping well 0.080 m

Static water level: 13.000 m below datum

	Pumping test duration	Water level	Drawdown	
	[min]	[m]	[m]	
1	0.50	13.450	0.450	
2	1.00	13.550	0.550	
3	1.50	13.650	0.650	
4	2.00	13.700	0.700	
5	2.50	13.730	0.730	
6	3.00	13.780	0.780	
7	3.50	13.800	0.800	
8	4.00	13.850	0.850	
9	4.50	13.880	0.880	
10	5.00	13.900	0.900	
11	6.00	13.940	0.940	
12	7.00	13.990	0.990	
13	8.00	14.020	1.020	
14	9.00	14.050	1.050	
15	10.00	14.090	1.090	
16	12.00	14.130	1.130	
17	14.00	14.170	1.170	
18	16.00	14.200	1.200	
19	18.00	14.230	1.230	
20	20.00	14.270	1.270	
21	22.00	14.300	1.300	
22	24.00	14.340	1.340	
23	26.00	14.360	1.360	
24	28.00	14.380	1.380	
25	30.00	14.400	1.400	
26	35.00	14.430	1.430	
27	40.00	14.450	1.450	
28	45.00	14.500	1.500	
29	50.00	14.540	1.540	
30	55.00	14.570	1.570	
31	60.00	14.610	1.610	
32	70.00	14.670	1.670	
33	80.00	14.700	1.700	
34	90.00	14.740	1.740	
35	100.00	14.770	1.770	
36	110.00	14.810	1.810	
37	120.00	14.850	1.850	
38	130.00	14.880	1.880	
39	140.00	14.910	1.910	
40	150.00	14.900	1.900	
41	160.00	14.910	1.910	
42	170.00	14.940	1.940	
43	180.00	14.950	1.950	
44	195.00	15.000	2.000	
45	210.00	15.060	2.060	
46	225.00	15.000	2.000	
47	240.00	14.980	1.980	
48	260.00	14.970	1.970	
49	280.00	14.990	1.990	
50	300.00	15.020	2.020	

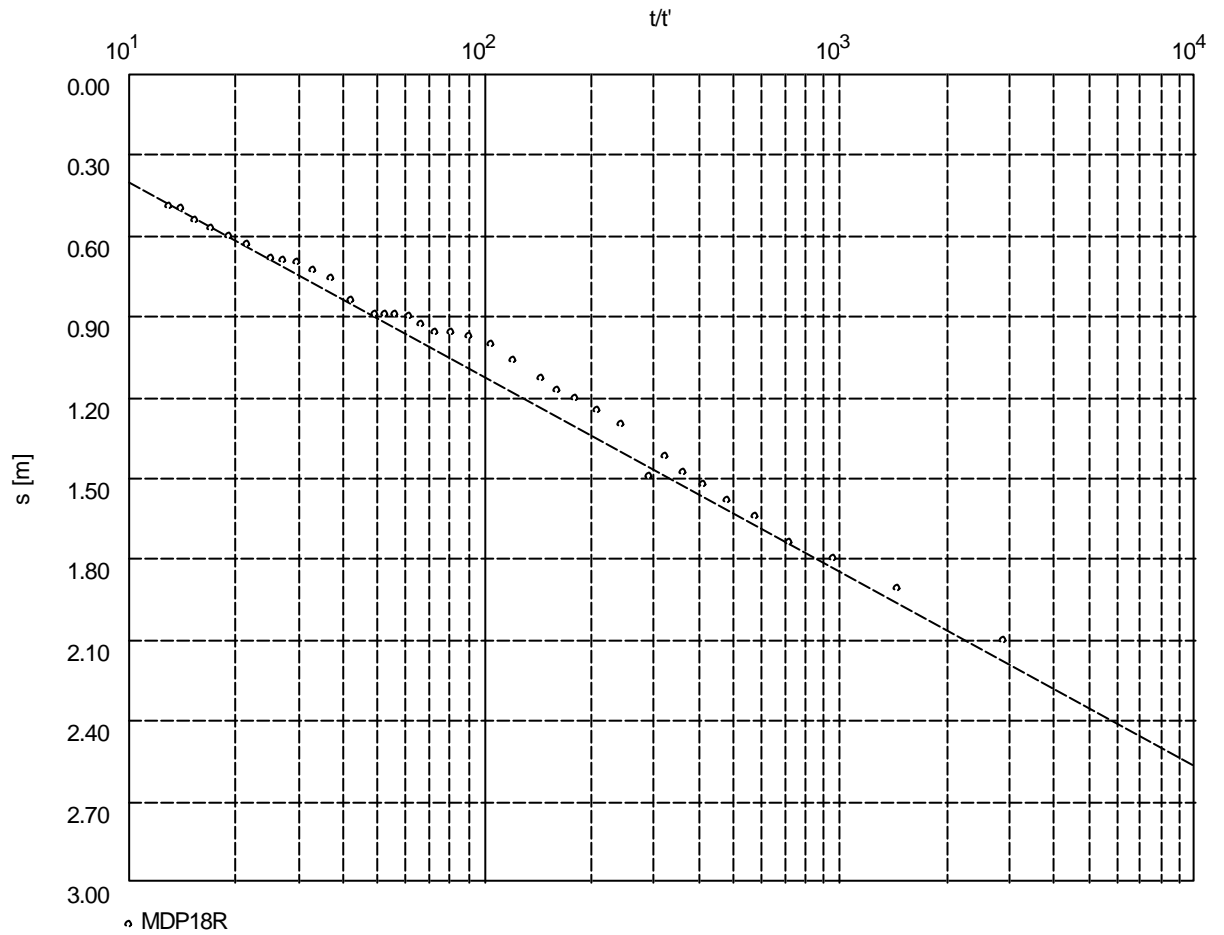
Pumping Test No. 1

Test conducted on: 01/05/2004

MDP18R

Discharge 25.00 l/s

Pumping test duration: 1440.00 min



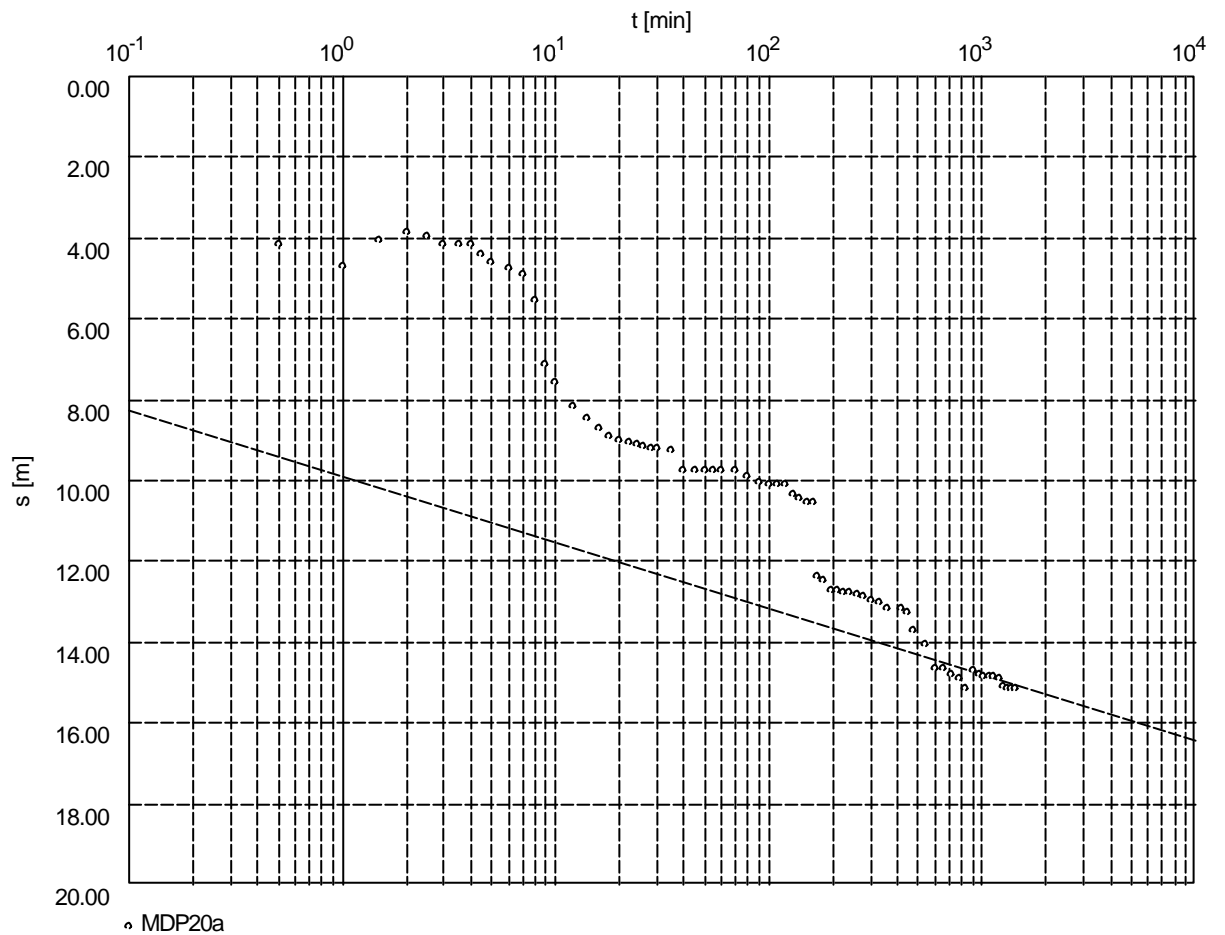
Transmissivity [m²/min]: 3.80×10^{-1}

Pumping Test No. 1

Test conducted on: 09/06/2004

MDP20a

Discharge 13.00 l/s



Transmissivity [m²/min]: 8.72×10^{-2}

Storativity: 1.78×10^{-5}

Waterloo Hydrogeologic

180 Columbia St. W.

Waterloo, Ontario, Canada

ph.(519)746-1798

Pumping test analysis
Time-Drawdown-method after
COOPER & JACOB
Confined aquifer

Page 2

Project: Zambia Hydrogeological Inv.

Evaluated by: MP

Date: 01.07.2004

Pumping Test No. 1

Test conducted on: 09/06/2004

MDP20a

MDP20a

Discharge 13.00 l/s

Distance from the pumping well 0.100 m

Static water level: 12.530 m below datum

	Pumping test duration	Water level	Drawdown	
	[min]	[m]	[m]	
1	0.50	16.680	4.150	
2	1.00	17.240	4.710	
3	1.50	16.590	4.060	
4	2.00	16.400	3.870	
5	2.50	16.480	3.950	
6	3.00	16.690	4.160	
7	3.50	16.680	4.150	
8	4.00	16.690	4.160	
9	4.50	16.950	4.420	
10	5.00	17.120	4.590	
11	6.00	17.290	4.760	
12	7.00	17.450	4.920	
13	8.00	18.080	5.550	
14	9.00	19.670	7.140	
15	10.00	20.090	7.560	
16	12.00	20.680	8.150	
17	14.00	21.000	8.470	
18	16.00	21.250	8.720	
19	18.00	21.430	8.900	
20	20.00	21.530	9.000	
21	22.00	21.580	9.050	
22	24.00	21.630	9.100	
23	26.00	21.710	9.180	
24	28.00	21.730	9.200	
25	30.00	21.750	9.220	
26	35.00	21.810	9.280	
27	40.00	22.280	9.750	
28	45.00	22.290	9.760	
29	50.00	22.290	9.760	
30	55.00	22.280	9.750	
31	60.00	22.280	9.750	
32	70.00	22.280	9.750	
33	80.00	22.450	9.920	
34	90.00	22.600	10.070	
35	100.00	22.620	10.090	
36	110.00	22.640	10.110	
37	120.00	22.650	10.120	
38	130.00	22.880	10.350	
39	140.00	22.970	10.440	
40	150.00	23.050	10.520	
41	160.00	23.050	10.520	
42	170.00	24.930	12.400	
43	180.00	25.000	12.470	
44	195.00	25.260	12.730	
45	210.00	25.270	12.740	
46	225.00	25.300	12.770	
47	240.00	25.320	12.790	
48	260.00	25.360	12.830	
49	280.00	25.400	12.870	
50	300.00	25.490	12.960	

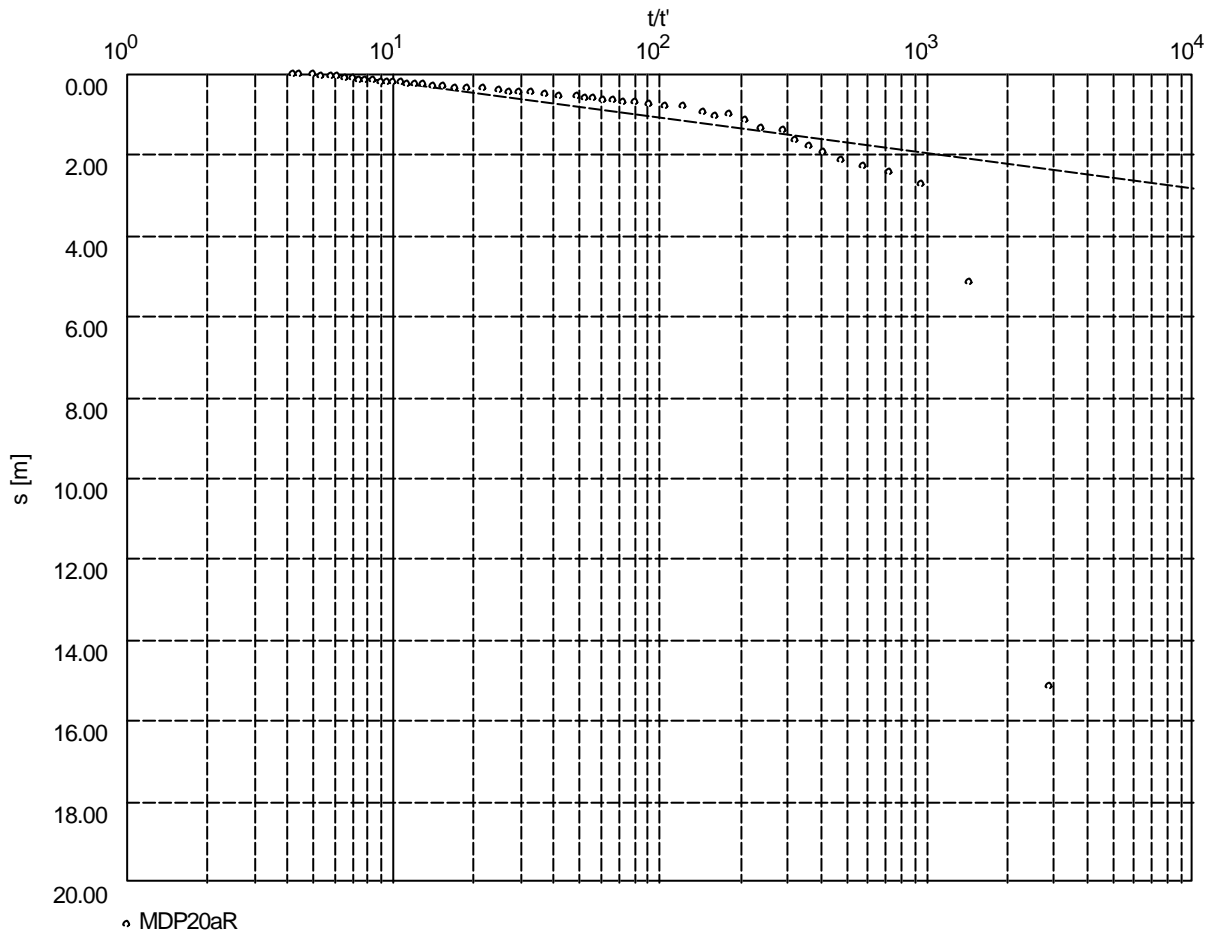
Pumping Test No. 1

Test conducted on: 09/06/2004

MDP20aR

Discharge 13.00 l/s

Pumping test duration: 1440.00 min



Transmissivity [m²/min]: 1.63×10^{-1}

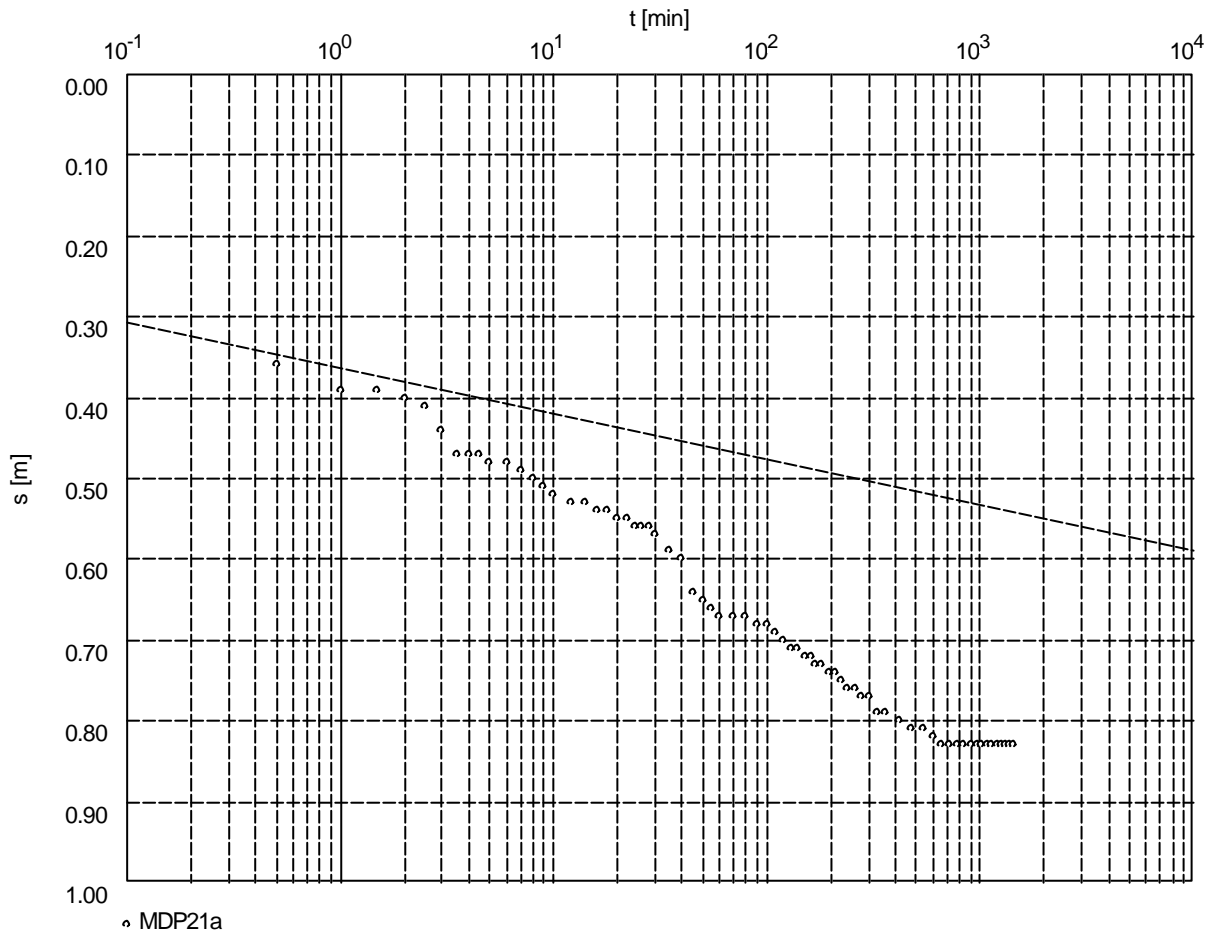
Waterloo Hydrogeologic 180 Columbia St. W. Waterloo, Ontario, Canada ph.(519)746-1798		Pumping test analysis Recovery method after THEIS & JACOB Confined aquifer		Page 2	
				Project: Zambia Hydrogeological Inv.	
				Evaluated by: MP	Date: 01.07.2004
Pumping Test No. 1			Test conducted on: 09/06/2004		
MDP20aR			MDP20aR		
Discharge 13.00 l/s					
Static water level: 12.530 m below datum			Pumping test duration: 1440.00 min		
	Time from end of pumping [min]	Water level [m]	Residual drawdown [m]		
1	0.50	27.660	15.130		
2	1.00	17.660	5.130		
3	1.50	15.230	2.700		
4	2.00	14.960	2.430		
5	2.50	14.820	2.290		
6	3.00	14.660	2.130		
7	3.50	14.460	1.930		
8	4.00	14.290	1.760		
9	4.50	14.150	1.620		
10	5.00	13.920	1.390		
11	6.00	13.850	1.320		
12	7.00	13.650	1.120		
13	8.00	13.500	0.970		
14	9.00	13.550	1.020		
15	10.00	13.480	0.950		
16	12.00	13.340	0.810		
17	14.00	13.300	0.770		
18	16.00	13.260	0.730		
19	18.00	13.230	0.700		
20	20.00	13.200	0.670		
21	22.00	13.180	0.650		
22	24.00	13.160	0.630		
23	26.00	13.120	0.590		
24	28.00	13.100	0.570		
25	30.00	13.090	0.560		
26	35.00	13.060	0.530		
27	40.00	13.030	0.500		
28	45.00	13.000	0.470		
29	50.00	12.990	0.460		
30	55.00	12.980	0.450		
31	60.00	12.950	0.420		
32	70.00	12.900	0.370		
33	80.00	12.880	0.350		
34	90.00	12.860	0.330		
35	100.00	12.850	0.320		
36	110.00	12.810	0.280		
37	120.00	12.800	0.270		
38	130.00	12.790	0.260		
39	140.00	12.760	0.230		
40	150.00	12.740	0.210		
41	160.00	12.720	0.190		
42	170.00	12.710	0.180		
43	180.00	12.710	0.180		
44	195.00	12.700	0.170		
45	210.00	12.690	0.160		
46	225.00	12.660	0.130		
47	240.00	12.640	0.110		
48	260.00	12.620	0.090		
49	280.00	12.600	0.070		
50	300.00	12.580	0.050		

Pumping Test No. 1

Test conducted on: 27/04/2004

MDP21b

Discharge 25.60 l/s



Transmissivity [m²/min]: 5.00×10^0

Storativity: 5.94×10^{-4}

Waterloo Hydrogeologic

180 Columbia St. W.

Waterloo, Ontario, Canada

ph.(519)746-1798

Pumping test analysis
Time-Drawdown-method after
COOPER & JACOB
Confined aquifer

Page 2

Project: Zambia Hydrogeological Inv

Evaluated by: MP

Date: 04.06.2004

Pumping Test No. 1

Test conducted on: 27/04/2004

MDP21b

MDP21a

Discharge 25.60 l/s

Distance from the pumping well 0.080 m

Static water level: 14.360 m below datum

	Pumping test duration	Water level	Drawdown	
	[min]	[m]	[m]	
1	0.50	14.720	0.360	
2	1.00	14.750	0.390	
3	1.50	14.750	0.390	
4	2.00	14.760	0.400	
5	2.50	14.770	0.410	
6	3.00	14.800	0.440	
7	3.50	14.830	0.470	
8	4.00	14.830	0.470	
9	4.50	14.830	0.470	
10	5.00	14.840	0.480	
11	6.00	14.840	0.480	
12	7.00	14.850	0.490	
13	8.00	14.860	0.500	
14	9.00	14.870	0.510	
15	10.00	14.880	0.520	
16	12.00	14.890	0.530	
17	14.00	14.890	0.530	
18	16.00	14.900	0.540	
19	18.00	14.900	0.540	
20	20.00	14.910	0.550	
21	22.00	14.910	0.550	
22	24.00	14.920	0.560	
23	26.00	14.920	0.560	
24	28.00	14.920	0.560	
25	30.00	14.930	0.570	
26	35.00	14.950	0.590	
27	40.00	14.960	0.600	
28	45.00	15.000	0.640	
29	50.00	15.010	0.650	
30	55.00	15.020	0.660	
31	60.00	15.030	0.670	
32	70.00	15.030	0.670	
33	80.00	15.030	0.670	
34	90.00	15.040	0.680	
35	100.00	15.040	0.680	
36	110.00	15.050	0.690	
37	120.00	15.060	0.700	
38	130.00	15.070	0.710	
39	140.00	15.070	0.710	
40	150.00	15.080	0.720	
41	160.00	15.080	0.720	
42	170.00	15.090	0.730	
43	180.00	15.090	0.730	
44	195.00	15.100	0.740	
45	210.00	15.100	0.740	
46	225.00	15.110	0.750	
47	240.00	15.120	0.760	
48	260.00	15.120	0.760	
49	280.00	15.130	0.770	
50	300.00	15.130	0.770	

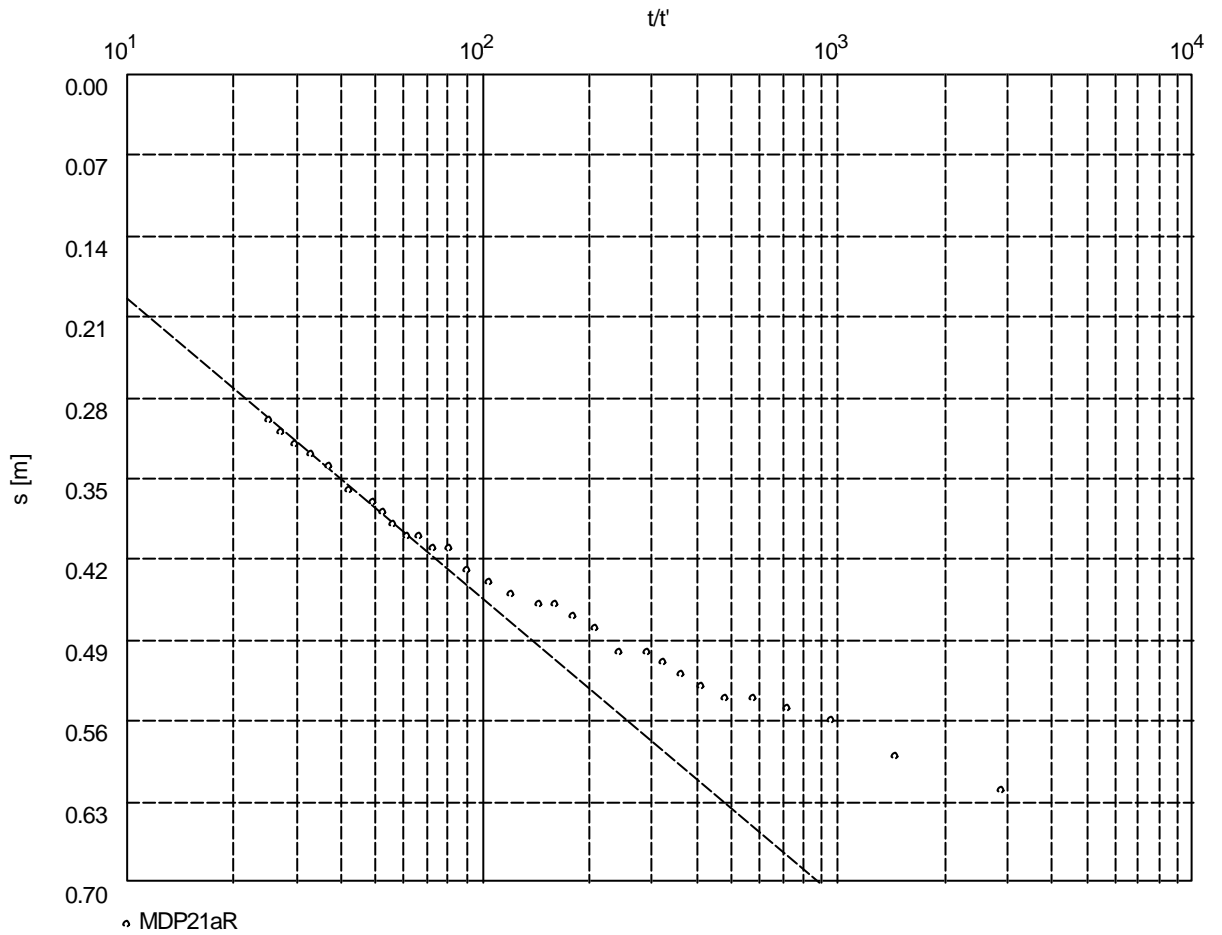
Pumping Test No. 1

Test conducted on: 24/04/2004

MDP21aR

Discharge 25.60 l/s

Pumping test duration: 1440.00 min



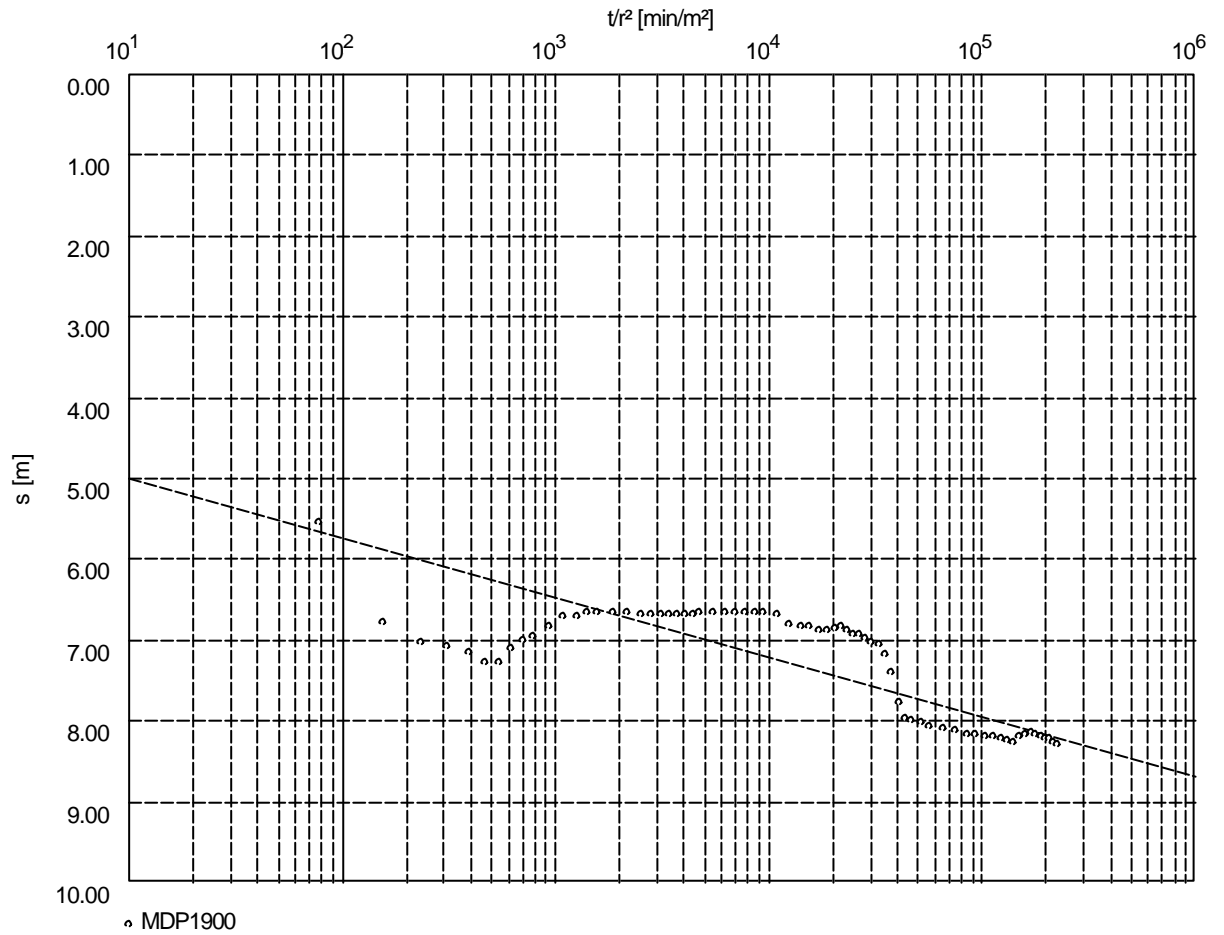
Transmissivity [m²/min]: 1.08×10^0

Pumping Test No. 1

Test conducted on: 2004/05/05

MDP 1900

Discharge 14.20 l/s



Transmissivity [m²/min]: 2.11×10^{-1}

Storativity: 8.19×10^{-7}

Waterloo Hydrogeologic

180 Columbia St. W.

Waterloo, Ontario, Canada

ph.(519)746-1798

Pumping test analysis
Distance-Time-Drawdown-method
after COOPER & JACOB
Confined aquifer

Page 2

Project: Zambia Hydrogeological Inv

Evaluated by: MP

Date: 04.06.2004

Pumping Test No. 1

Test conducted on: 2004/05/05

MDP 1900

MDP1900

Discharge 14.20 l/s

Distance from the pumping well 0.080 m

Static water level: 18.500 m below datum

	Pumping test duration	Water level	Drawdown	
	[min]	[m]	[m]	
1	0.50	24.040	5.540	
2	1.00	25.280	6.780	
3	1.50	25.530	7.030	
4	2.00	25.590	7.090	
5	2.50	25.650	7.150	
6	3.00	25.770	7.270	
7	3.50	25.780	7.280	
8	4.00	25.600	7.100	
9	4.50	25.500	7.000	
10	5.00	25.450	6.950	
11	6.00	25.330	6.830	
12	7.00	25.200	6.700	
13	8.00	25.220	6.720	
14	9.00	25.160	6.660	
15	10.00	25.150	6.650	
16	12.00	25.170	6.670	
17	14.00	25.170	6.670	
18	16.00	25.180	6.680	
19	18.00	25.180	6.680	
20	20.00	25.180	6.680	
21	22.00	25.190	6.690	
22	24.00	25.190	6.690	
23	26.00	25.190	6.690	
24	28.00	25.190	6.690	
25	30.00	25.170	6.670	
26	35.00	25.170	6.670	
27	40.00	25.170	6.670	
28	45.00	25.170	6.670	
29	50.00	25.170	6.670	
30	55.00	25.150	6.650	
31	60.00	25.150	6.650	
32	70.00	25.190	6.690	
33	80.00	25.300	6.800	
34	90.00	25.320	6.820	
35	100.00	25.340	6.840	
36	110.00	25.380	6.880	
37	120.00	25.370	6.870	
38	130.00	25.360	6.860	
39	140.00	25.340	6.840	
40	150.00	25.390	6.890	
41	160.00	25.420	6.920	
42	170.00	25.440	6.940	
43	180.00	25.480	6.980	
44	195.00	25.520	7.020	
45	210.00	25.560	7.060	
46	225.00	25.680	7.180	
47	240.00	25.890	7.390	
48	260.00	26.260	7.760	
49	280.00	26.480	7.980	
50	300.00	26.500	8.000	

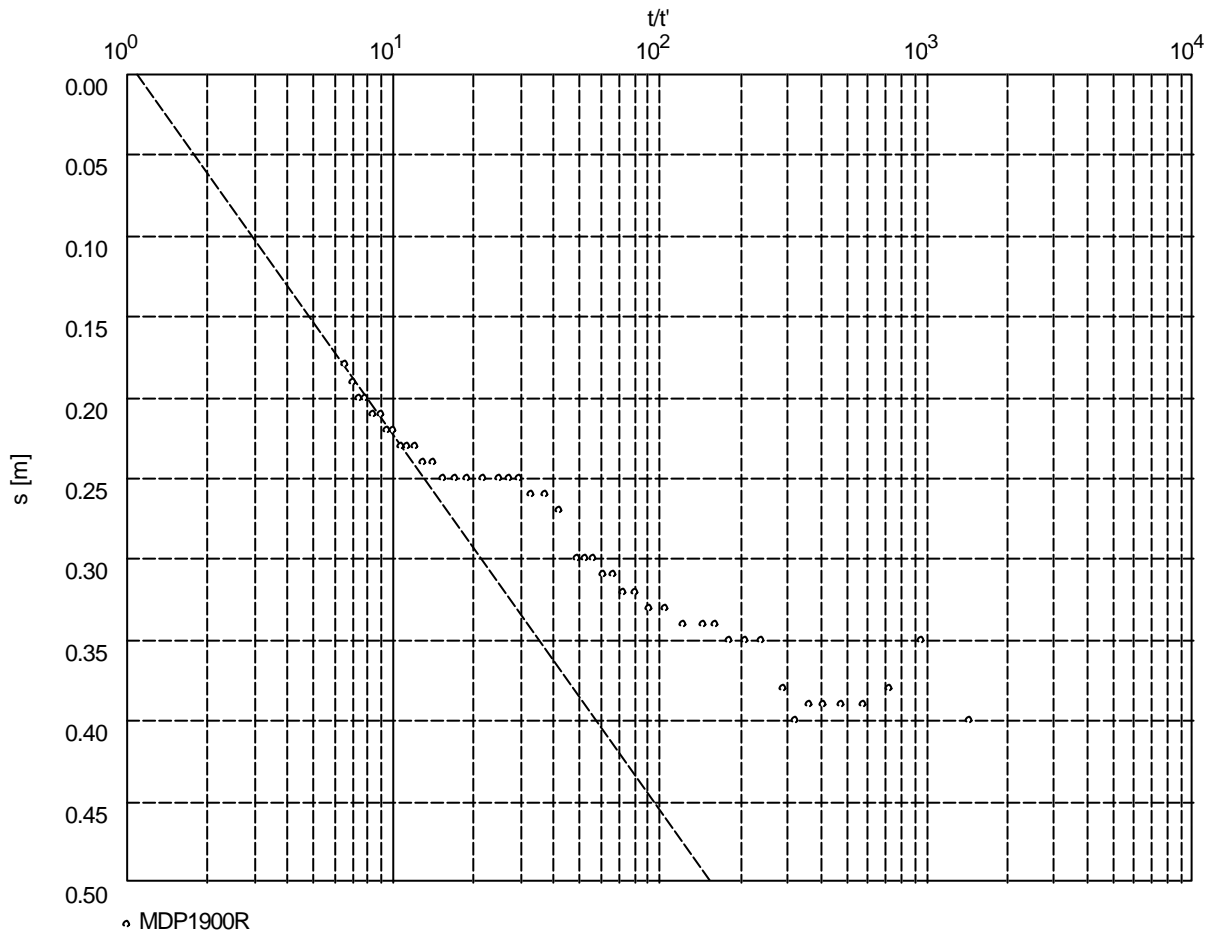
Pumping Test No. 1

Test conducted on: 2004/05/05

MDP1900R

Discharge 14.20 l/s

Pumping test duration: 1440.00 min



Transmissivity [m²/min]: 6.73×10^{-1}

Waterloo Hydrogeologic 180 Columbia St. W. Waterloo, Ontario, Canada ph.(519)746-1798		Pumping test analysis Recovery method after THEIS & JACOB Confined aquifer		Page 2	
				Project: Zambia Hydrogeological Inv	
				Evaluated by: MP	Date: 04.06.2004
Pumping Test No. 1			Test conducted on: 2004/05/05		
MDP1900R			MDP1900R		
Discharge 14.20 l/s					
Static water level: 18.500 m below datum			Pumping test duration: 1440.00 min		
	Time from end of pumping [min]	Water level [m]	Residual drawdown [m]		
1	1.00	18.900	0.400		
2	1.50	18.850	0.350		
3	2.00	18.880	0.380		
4	2.50	18.890	0.390		
5	3.00	18.890	0.390		
6	3.50	18.890	0.390		
7	4.00	18.890	0.390		
8	4.50	18.900	0.400		
9	5.00	18.880	0.380		
10	6.00	18.850	0.350		
11	7.00	18.850	0.350		
12	8.00	18.850	0.350		
13	9.00	18.840	0.340		
14	10.00	18.840	0.340		
15	12.00	18.840	0.340		
16	14.00	18.830	0.330		
17	16.00	18.830	0.330		
18	18.00	18.820	0.320		
19	20.00	18.820	0.320		
20	22.00	18.810	0.310		
21	24.00	18.810	0.310		
22	26.00	18.800	0.300		
23	28.00	18.800	0.300		
24	30.00	18.800	0.300		
25	35.00	18.770	0.270		
26	40.00	18.760	0.260		
27	45.00	18.760	0.260		
28	50.00	18.750	0.250		
29	55.00	18.750	0.250		
30	60.00	18.750	0.250		
31	70.00	18.750	0.250		
32	80.00	18.750	0.250		
33	90.00	18.750	0.250		
34	100.00	18.750	0.250		
35	110.00	18.740	0.240		
36	120.00	18.740	0.240		
37	130.00	18.730	0.230		
38	140.00	18.730	0.230		
39	150.00	18.730	0.230		
40	160.00	18.720	0.220		
41	170.00	18.720	0.220		
42	180.00	18.710	0.210		
43	195.00	18.710	0.210		
44	210.00	18.700	0.200		
45	225.00	18.700	0.200		
46	240.00	18.690	0.190		
47	260.00	18.680	0.180		

Summary.

External factors that influence the aquifer characteristics of, and sustainable yield from, the dolomitic aquifer include topography, rainfall, surface drainage, evapotranspiration, plant growth, geology, and soils.

The topography is gently undulating with a gradient of between 1:400 and 1:800. The low topographical gradients inhibit surface run-off and promote high recharge rates.

The annual rainfall will provide the volume of water present in the catchment area that is available for potential recharge to the aquifer. The average rainfall is 1 115mm/annum.

Water that leaves the hydrological system of the study area as surface run-off impacts on the volume of water available for recharge to the aquifer in the area. Despite the high rainfall volume and high rainfall intensity only one perennial surface run-off structure exists in the study area. The Kafue River is on average 10 to 20m wide and 3m deep. Only one non-perennial surface run-off feature exists. This feature feeds into the Ipumbu Dam.

The volume of water that evaporates from the soil and vegetation before it can reach the underlying aquifer will impact on the volume of water that can be abstracted from the aquifer without negatively impacting on the volume of water in storage in the aquifer. Very little evaporation data is available for the study area. Comparing the calculated potential total evaporation volume with the measured net evaporation and annual rainfall indicates a discrepancy between the evaporation and rainfall data. The rainfall data is considered to be accurate, and based on perceived inaccuracy of the evaporation data, it is recommended that the evaporation data not be used in water balance calculations.

The natural plant growth influences the evapotranspiration and in some cases the surface run-off characteristics. *Brachystegia* Miombo woodlands cover the study area with areas of widespread grass cover between the trees.

The main aquifer consists of Upper Roan Formation limestone and dolomite. The main joint set (160° strike direction) controls the strike direction of the solution cavities in the area. Schist and quartzite of the Lower Roan Formation border the limestone and dolomite. Extensive fracturing in the dolomite is found in the geological logs of the high yielding boreholes drilled in the area.

The soil in the study area displays infiltration rates higher than the observed rainfall intensity. Combined with the low topographical gradients that retard run-off the high infiltration rate leads to high recharge percentages.

The aquifer hydraulic characteristics were determined during the investigation. It is considered that Lake Nampamba forms part of an extensive, well-connected solution cavity network. No compartmentalisation of the dolomite is evident. Three prominent karstic features (Lake Nampamba, Lake Kashiba and the “Chibili Pavement”) occur in the area. Both Lake Nampamba and Lake Kashiba are sinkholes in the dolomite.

The author has no scientific evidence to conclude that the solution cavity network stretches as far as the Kafue River. However, analysis of the water level, abstraction and

water level data does confirm that Lake Nampamba in the east and the dambo areas in the west that feed Ipumbu dam are interconnected.

The groundwater displays a calcium-magnesium dominant character, as is expected from a dolomitic aquifer. Plotting the chemistry data on a trilinear (Piper) diagram indicates that the groundwater recently recharged. This corresponds to the theory of high recharge due to the relatively high rainfall, flat topography, and high soil infiltration rate.

Depth to groundwater varies on a seasonal basis due to fluctuations in rainfall and thus recharge, and abstraction volumes. The groundwater level shows an immediate response to recharge, but does indicate a one to two month delay between maximum rainfall and peak groundwater level.

A total of 65 boreholes were drilled in the study area between 1978 and 2004. Preliminary aquifer tests were performed on 38 boreholes, and 14 boreholes were identified as high yielding boreholes. Constant rate aquifer tests were performed on these boreholes. The aquifer test data was analysed to obtain the aquifer transmissivity. The aquifer transmissivity ranges between 1 and 6 900m²/day. This wide range is expected in karstic aquifers where the high transmissivity is associated with solution cavities and fractured areas. The low transmissivities are associated with the fine crystalline, competent, unweathered rock. Sustainable yields from the borehole calculated from the aquifer test data range between 5 and 100l/s (432 and 8 640m³/day).

Recharge calculations were performed using the Chloride, SVF, Equal Volume and CRD methods. The chloride method is used only as an indication of the recharge percentage. The SVF, Equal Volume, and CRD methods calculated recharge as 25% of the annual rainfall.

Aquifer storativity is calculated using the SVF and CRD methods at 0.02 (2%).

The total volume of water that can be abstracted from the combined eastern and western aquifers is calculated to be 136Mm³/annum. The current and proposed future annual abstraction volumes are 25.3Mm³ and 44.42Mm³ respectively. This indicates that the combined eastern and western aquifers are capable of sustaining the abstraction volumes.

A numerical model was constructed to evaluate the assumptions made, and correlates the calculated values of the manual calculations. The model was initially constructed in steady state without taking the abstraction from the aquifer into account.

Once the model was successfully calibrated, the abstraction volumes were incorporated into the numerical model and the model was further calibrated against time series observed rainfall, groundwater levels and abstraction volumes by comparing the groundwater levels with time against those calculated using the numerical model.

Once the model was calibrated, the model was applied to evaluate the sustainability of the current and proposed abstraction programs. The numerical model confirms that the combined eastern and western aquifers are capable of sustaining the abstraction programs.

Opsomming.

Die eksterne faktore wat die eienskappe en volhoubare onttrekking van die dolomitiese akwifereer in die Koperbelt Provinsie beïnvloed sluit in topografie, reënval, oppervlak afloop, evapotranspirasie, plantergroei, geologie en grond.

Die topografie is golwend met 'n gradiënt van tussen 1:400 en 1:800. Die lae gradiënt beperk oppervlak afloop van water en bevorder insypeling van water in die grond in.

Die jaarlikse reënval voorsien die hoeveelheid water wat beskikbaar is in die opvang gebied vir potensiële aanvulling tot die akwifereer. Die gemiddelde jaarlikse reënval word bereken as 1 115mm/jaar.

Die volume water wat die sisteem verlaat as oppervlak afloop beïnvloed die volume water wat beskikbaar sal wees vir aanvulling tot die akwifereer. Ten spyte van die hoë reënval volumes en reënval intensiteit bestaan daar slegs een standhoudende rivier in die omgewing. Die Kafuerivier is gemiddeld 10 tot 20m breed en 3m diep. Slegs een nie-standhoudende rivier bestaan in die gebied.

Die hoeveelheid water wat verdamp van die plantegroei en grond voordat dit die onderliggende akwifereer kan bereik, sal die volume water wat volhoubaar onttrek kan word beïnvloed. Baie min evaporasie data is beskikbaar vir die studie area. 'n Vergelyking tussen die berekende potensiële totale evaporasie, netto evaporasie en reënval dui op onakkuraatheid van sommige van die data. Die reënval data word beskou as relatief akkuraat en gebaseer op die oënskynlike onbetroubaarheid van die evaporasie data word dit aanbeveel dat die evaporasie data nie gebruik word in water balans berekeninge nie.

Die natuurlike plantegroei sal die evapotranspirasie en in sommige gevalle die oppervlak afloop eienskappe beïnvloed. *Brachystegia Miombo* woude kom voor in die studie gebied, met wydverspreide grasvelde tussen in.

Die hoof akwifereer bestaan uit die Boonste Roan Formasie dolomiet en kalksteen. Die hoof naatstelsel strek in die rigting 160° en beheer ook die strekking van die ondergrondse oplossings holtes. Skis en kwartsiet van die Laer Roan Formasie grens aan die dolomiet en kalksteen. Goed ontwikkelde krake en nate word gevind in die geologiese profiele van die hoë lewering boorgate.

Die grond in die studie area besit infiltrasie eienskappe wat hoër is as die reënval intensiteit van die area. Gekombineerd met die lae topografiese gradiënt gee die grond se infiltrasie tempo aanleiding tot hoë grondwater aanvullings waardes vir die akwifereer.

Die hidroliese eienskappe van die akwifereer is bepaal tydens die studie. Lake Nampamba maak deel uit van 'n wye, goed ontwikkelde netwerk van oplossings holtes in die dolomiet. Daar is geen bewys van kompartementalisasie van die dolomiet nie. Beide Lake Nampamba en Lake Kashiba is sinkgate wat in die dolomiet ontwikkel het.

Die skrywer het geen wetenskaplike bewys gevind dat die oplossings netwerk tot by die Kafuerivier strek nie. Analise van reënval, grondwater vlakke en grondwater onttrekking volumes dui egter daarop dat die dolomitiese akwifereer in die ooste geassosieer met

Lake Nampamba, en die dambo areas in die weste wat Ipumbu Dam voed, hidrolies verbind is.

Die grondwater het 'n kalsium – magnesium dominante karakter, soos verwag in 'n dolomitiese area. 'n Piper diagram plot dui op onlangse aanvulling tot die akwifere. Dit stem ooreen met die teorie van hoë aanvulling tot die akwifere as gevolg van relatiewe hoë reënval, plat topografie en hoë grond infiltrasie tempos.

Die diepte tot die grondwater vlak varieër op 'n seisoenale basis as gevolg van fluktuasies in reënval, en dus aanvulling tot die akwifere, en onttrekkings volumes. Die grondwater vlakke toon 'n onmiddellike reaksie op reënval en aanvulling tot die akwifere, maar 'n een tot twee maande tussenpose tussen maksimum reënval en maksimum grondwater vlakke.

'n Totaal van 65 boorgate is tussen 1978 en 2004 in die area geboor. Voorlopige akwifere toetse is op 38 van die boorgate uitgevoer en 14 boorgate is geïdentifiseer wat moontlik hoë lewering gate kon wees. Konstante abstraksie tempo toetse is op hierdie 14 boorgate uitgevoer. Die pomp toets data is ontleed om die transmissiwiteit van die akwifere te bepaal.

Die akwifere transmissiwiteit varieër tussen 1 en 6 900m²/dag. Hierdie wye reeks is te verwagte in karst areas waar die hoë transmissiwiteite geassosieer word met die oplossings holtes of naatsones. Die lae transmissiwiteite word geassosieer met die fyn kristallyne, soliede, onverweerde gesteentes. Volhoubare lewerings van die boorgate varieer tussen 5 en 100l/sek (432 en 8 640m³/dag).

Aanvulling persentasie berekeninge is uitgevoer gebaseer op die chloried-, SVF-, gelyke volume- en CRD-metodes. Die chloried-metode is slegs as 'n aanduiding van die ordegrootte van die aanvullings persentasie gebruik. Die SVF-, gelyke volume- en CRD-metodes dui aan dat 25% van die reënval uiteindelik die grondwater aanvul.

Die akwifere storing is bereken as 0.02 deur die SVF en CRD metodes toe te pas.

Die totale volume water wat gesamentlik uit die oostelike en westelike akwifere onttrek kan word is bereken as 136Mm³/jaar. Die huidige en voorgestelde toekomstige onttrekking beloop onderskeidelik 25.3Mm³/jaar en 44.42Mm³/jaar. Die gesamentlike oostelike en westelike akwifere kan dus die onttrekkings volumes te onderhou.

'n Numeriese model is opgestel om die aannames wat gebruik is te evalueer en met die berekeninge soos bespreek in hoofstukke 2 en 3 te korreleer. Die model is aanvanklik opgestel sonder om die onttrekking vanuit die akwifere in ag te neem.

Na suksesvolle kalibrasie van die aanvanklike model, is abstraksie geïnkorporeer en die model is verder gekalibreer. Tyd reeks reënval, grondwater vlak en onttrekking data is gebruik om die vlak van kalibrasie van die model te meet deur die geobserveerde grondwater vlakke met tyd te vergelyk met dit wat bereken is deur die numeriese model.

Na die finale kalibrasie van die model is die model toegepas deur die volhoubaarheid van die huidige en toekomstige onttrekkings volumes te evalueer. Die numeriese model bevestig dat die gekombineerde oostelike en westelike akwifere in staat is om die onttrekkings programme te onderhou.